# Astronomical relevance of materials from Earth and Space: A laboratory study

A thesis submitted to Cardiff University for the degree of Doctor of Philosophy by

Kani Mustafa Rauf BSc. UMI Number: U585403

#### All rights reserved

#### INFORMATION TO ALL USERS

The quality of this reproduction is dependent upon the quality of the copy submitted.

In the unlikely event that the author did not send a complete manuscript and there are missing pages, these will be noted. Also, if material had to be removed, a note will indicate the deletion.



#### UMI U585403

Published by ProQuest LLC 2013. Copyright in the Dissertation held by the Author.

Microform Edition © ProQuest LLC.

All rights reserved. This work is protected against unauthorized copying under Title 17, United States Code.



ProQuest LLC 789 East Eisenhower Parkway P.O. Box 1346 Ann Arbor, MI 48106-1346

#### **SUMMARY**

The present study used scanning and transmission electron microscopy, energy dispersive analysis of X-rays (EDAX) and spectroscopy (FTIR, UV-Visible and fluorescence) to examine terrestrial materials of possible astronomical significance (Oedogonium sp., Enteromopha intestinalis, Pelvetia canaliculata, Fucus vesiculosus, Bacillus cereus, Staphyllococcus aureus, poppy seed, chlorophylls 'a' and 'b', Panicum maximum, anthracite, bituminous coal, naphthalene), the Tagish lake and Carancas meteorites, a Kerala red rain sample and stratospheric air particles collected at altitudes of 38-41 km. The study was designed to determine if any of the terrestrial samples could be proposed as an effective model for the interpretation of astronomical spectroscopic observations. The study also set out to search for evidence to shed light on the origin of these meteorites, red rain and stratospheric air particles.

The spectra of all the terrestrial samples (including the meteorites) exhibited absorptions in the Mid-IR region, similar to astronomical features displayed by a variety of galactic sources. Algae (*Odeogonium sp.*) in particular produced the largest number of absorption peaks, most of which matched those of the astronomical emission spectra of PPNe and also the UIBs. Based on these observations, algae could be defended as a biological model for the interpretation of UIBs and PPNe, and a potential candidate for interstellar material. Coal and semi anthracite, that can be regarded as steps in the degradation of biomaterial, preserve the UIB-PPNe spectral features to varying degrees. The results are consistent with the panspermia theory of Hoyle and Wickramasinghe.

UV-Visible studies were also conducted on all these materials. The main absorption feature was one close to 217.5 nm (2175 Å). The normalized (averaged) spectrum of the whole sequence of biological materials and their degradation products absorption feature at 217.5 nm (2175 Å) further support the contention that aromatic molecules in biological materials are responsible for the interstellar absorption feature centred at 217.5 nm.

The X-ray microanalysis data together with the infrared spectrum and ultrastructural information on the Tagish Lake and Carancas meteorites confirm the presence of nano sized particles, but their biological provenance remains indeterminate.

In the concluding chapters of the thesis I report results of investigations of a similar kind conducted on aerosols collected at height of 41 km in the stratosphere. A variety of microstructures were identified within these particles, some with probable biological provenance. The red rain of Kerala is also investigated; unidentified algal-type cells were discovered, but their origin remains uncertain and controversial.

#### **CONTENTS**

	Page
Title	i
Summary	ii
Contents	iv
Declaration	xi
Acknowledgements	xii
CHAPTER 1: General Introduction	
1.1. The Solar System	2
1.1.1. The Sun	2
1.1.2. The Solar Nebula	3
1.1.2.1. Terrestrial Planets	3
1.1.2.2. Giant Planets	5
1.1.2.3. Satellites	8
1.1.2.4. Comets	10
1.1.2.5. Asteroids	11
1.1.2.6. Meteorites	11
1.2. Major Elements in the Solar System	12
1.3. Evidence of Early Life on Earth	12
1.4. Survival of Organisms in Extreme Environments	14
1.5. Delivery of Extraterrestrial Materials to Earth	16
1.5.1. Minerals	16
1.5.1.1. Comets	16
1.5.1.2. Meteorites	17
1.5.2. Organic Matter	18
1.5.2.1. Interstellar Dust	18
1.5.2.2. Meteorites	21
1.5.2.3. Cometary Dust	24
1.5.2.4. Stratospheric Particles	25
1.6. Hypotheses of Panspermia	27
1.7. Interstellar Dust Models	29

1.7.1. Interstellar Spectral Observations	29
1.7.2. Proposed Models	31
1.7.3. Carriers of Interstellar bands	33
1.8. Aims and Objectives of study	35
CHAPTER 2: General Materials and Methods	
2.1. Materials	39
2.1.1. Major Laboratory Instruments	39
2.1.1.1. KBr Die Assembly	39
2.1.1.2. Fourier Transform Infrared Spectrometer	40
2.1.1.3. Ultraviolet-Visible Absorption Spectrometer	40
2.1.1.4. Microscopes and Ancillary Equipment	41
2.1.1.4.1. Light Microscope	41
2.1.1.4.2. Transmission Electron Microscope	41
2.1.1.4.3. Scanning Electron Microscope	42
2.1.1.4.4. Environmental Scanning Electron Microscope	42
2.1.1.4.5. Energy Dispersive Analyser of X-rays (EDAX)	43
2.1.2. Chemicals	43
2.1.2.1. KBr for Infrared Spectroscopy	43
2.1.2.2. Cyclohexane for Ultraviolet –Visible Spectrophotometry	44
2.1.2.3. Chemicals for Electron Microscopy	44
2.2. Methods	46
2.2.1. Infrared Spectroscopy	46
2.2.1.1. Principles of Infrared Spectroscopy	46
2.2.1.2. Sample preparation for FTIR	48
2.2.2. Ultraviolet-Visible (UV-Vis) Absorption Spectroscopy	49
2.2.2.1. Principles of UV-Vis Absorption Spectroscopy	50
2.2.2.2. Sample preparation for UV-Visible Spectroscopy	51
2.2.3. Fluorescence Spectroscopy	51
2.2.3.1. Principles of Fluorescence Spectroscopy	51
2.2.3.2. Sample preparation for Fluoresecence Spectroscopy	52
2.2.4. Microscopy Methods	52
2.2.4.1. Principles of Microscopy	52

2.2.4.2. Sample preparation for Light Microscopy (LM)	53
2.2.4.3. Sample preparation for Transmission Electron Microscopy (TEM	() 53
2.2.4.4. Sample preparation for Scanning Electron Microscopy (SEM)	54
2.2.5. Energy Dispersive Analysis of X-Rays (EDAX)	55
2.2.5.1. Principles of EDAX	55
2.2.5.2. Protocols for the preparation of samples for EDAX	56
CHAPTER 3: Comparison of Infrared Spectra of Biological Models	with those
of Astronomical Sources	
3.1. Summary	58
3.2. Introduction	58
3.2.1. Space observatories	58
3.2.2. Astronomical observations	59
3.2.3. Organic models for studying interstellar grains	60
3.2.4. Aim and objectives of the study	62
3.3. Materials and Methods	62
3.3.1. Materials	62
3.3.2. Methods of sample preparation for FTIR analysis	62
3.4. Results	63
3.4.1. Infrared (IR) spectra of Algae	63
3.4.2. Infrared (IR) spectrum of Bacillus cereus	65
3.4.3. Infrared (IR) spectrum of Staphylococcus aureus	66
3.4.4. Infrared (IR) spectrum of Poppy seeds	67
3.4.5. Infrared (IR) spectra of Chlorophyll 'a' and 'b'	68
3.4.6. Infrared (IR) spectra of Seaweed	69
3.4.7. Infrared (IR) spectrum of Grass (Panicum maximum)	70

3.5. Discussion

74

# CHAPTER 4: Interpretaion of Laboratory Models as Possible Analogues of Carriers for the Unidentified Infrared Bands and Protoplanetary Nebulae

4.1. Summary	80
4.2. Introduction	80
4.2.1. Coal	81
4.2.2. Aim of the study	82
4.3. Materials and Methods	83
4.4. Results	84
4.4.1. Infrared absorption of Graphite	84
4.4.2. Infrared absorption of Anthracite	85
4.4.3. Infrared absorption of Bituminous Coal	86
4.4.4. Infrared absorption of Naphthalene	88
4.5. Discussion	91

# CHAPTER 5: A Proposed Ensemble of Degraded and Non-Degraded Biomaterials as a Carrier of the 217.5 nm (2175 Å) Interstellar Extinction Feature

5.1. Summary	96
5.2. Introduction	96
5.2.1. Interstellar dust and its extinction curve	96
5.2.2. The extinction curve feature and its carrier	98
5.2.3. Dust models	99
5.2.4. Aim of the study	100
5.3. Materials and Methods	100
5.3.1. Materials	100
5.3.2. Methods of sample mounting and preparation	101
5.4. Results	101
5.5. Discussion	106

#### CHAPTER 6: Microstructure and Elemental Composition of the Tagish Lake Meteorite and its Astrobiological Implications

6.1. Summary	110
6.2. Introduction	110
6.2.1. Types of meteorites	112
6.2.2. Relationships between meteorites and asteroids	113
6.2.3. Tagish lake meteorite	113
6.2.4. Aim of the study	114
6.3. Materials and Methods	114
6.4. Results	115
6.4.1. Electron Microscopy	115
6.4.2. X-ray nanoprobe analysis	120
6.4.3. FTIR	123
6.5. Discussion	123

# CHAPTER 7: The Carancas Meteorite: A study by Electron Microscopy, Energy Dispersive X-Ray Microanalysis and Fourier Transform Infrared Spectroscopy

7.1. Summary	128
7.2. Introduction	129
7.2.1. Aim of the study	130
7.3. Materials and Methods	130
7.3.1. Scanning Electron Microscopy	130
7.3.2. Transmission Electron Microscopy	131
7.3.3. EDAX Analysis	131
7.3.4. FTIR Spectroscopy	131
7.4. Results	132
7.4.1. Scanning Electron Microscopy	132
7.4.2. Transmission Electron Microscopy	132
7.4.3. X-ray nanoprobe analysis	136
7.4.4. FTIR	138
7.5. Discussion	138

#### **CHAPTER 8:** Astrobiological Aspects of Kerala Red Rain

8.1. Summary	143
8.2. Introduction	143
8.2.1. Brief historical of red rain	143
8.2.2. Controversial aspects of Kerala red rain	144
8.2.3. Aim of the study	146
8.3. Materials and Methods	146
8.3.1. Electron Microscopy	146
8.3.2. FTIR Spectroscopy	147
8.3.3. UV-Visible Spectrophotometry	147
8.3.4. Fluorescence Spectroscopy	148
8.3.5. Energy Dispersive Analysis of X-rays (EDAX)	148
8.4. Results	148
8.4.1. Structural Analysis	148
8.4.1.1. Light Microscopy	148
8.4.1.2. Electron Microscopy	149
8.4.2. UV-Vis Spectrophotometry	155
8.4.3. FTIR Spectroscopy	156
8.4.4. Fluorescence Spectroscopy	158
8.4.5. EDAX	159
8.5. Discussion	161
CHAPTER 9: Study of Putative Microfossils in Space D	ust from the
Stratosphere by Scanning Electron Microscopy and UV-	Vis Spectroscopy
9.1. Summary	167
9.2. Introduction	167
9.2.1. The Earths' Atmosphere	167
9.2.2. Aerosols	169
9.2.3. Interplanetary Dust Particles (IDPs)	169
9.2.4. Microorganisms in space	170
9.2.5. Aim of the study	171

9.3. Materials and Methods	171
9.3.1. Collection of stratospheric air samples	171
9.3.2. Scanning Electron Microscopy	172
9.3.3. UV- Visible Spectrophotometry	172
9.4. Results	173
9.4.1. Scanning Electron Microscopy of stratospheric air samples	173
9.4.2. UV-Vis Spectroscopy of stratospheric air samples	180
9.5. Discussion	180
CHAPTER 10: Concluding Remarks	185
References	188
APPENDIX	230

#### **ACKNOWLEDGEMENTS**

First of all, I should very much like to express my profound gratitude to the following persons whom I dearly respect:

- Prof. Chandra Wickramasinghe at the Cardiff Centre for Astrobiology for giving me an opportunity to study for a PhD degree, for supervising my research projects, and for his invaluable advice and guidance.
- Dr Anthony Hann at the Cardiff School of Biosciences for providing me with a bench space in his laboratory for sample preparation, and for allowing me whenever I need to gain access to Biosciences Electron Microscopy Unit. I am deeply indebted to him for giving me constructive criticism, confidence to take my own initiatives, technical advice and all his support throughout the period of my study.
- Drs Shirwan Al-Mufti and Max Wallis at the Cardiff Centre for Astrobiology for their encouragement and helpful advice.
- Prof. Godfrey Louis at Mahatma Gandhi University in Kerala, and Dr.
   Barry DiGregorio for providing me with samples of red rain and the Carancas meteorite, respectively.
- Mr Guy Pitt at Cardiff School of Biosciences for giving me access to the image scanning facilities in his laboratory.

I also take this opportunity to thank Dr Norimune Miyake and Mr Rajkumar Gangappa at the Cardiff Centre for Astrobiology for their friendship and helping hand.

Last but not least, special thanks go to Dawan, my beloved husband and best friend for always being there for me, and my parents to whom I am most grateful for giving me heartfelt encouragement and warmest support in times of need.

## **CHAPTER 1**

### **General Introduction**

#### 1.1. The Solar System

The embryonic Solar System consisted of the Sun and Solar Nebula within which comets, asteroids and other planets were formed. The events leading to the formation of the Solar System are well documented. As generally agreed, the Solar System formed about 4.56 billion years ago from a collapsed dense interstellar dust as a result of the Big Bang (Tscharnuter and Boss, 1993; Whittet, 1996; Irvine, 1996; Gaffey, 1997; Wright, 2004).

#### 1.1.1. The Sun

The Universe was generally perceived as a hot fireball after the Big Bang. Its space was densely packed with elementary particles and as a result, no light could travel anywhere. After about several hundred thousand years, the temperature in the Universe dropped to about the same as that of the surface of the Sun. This was the time when particles joined to form atoms and as a result, light travelled around unimpeded and shone through the Universe (Wright, 2004).

The Universe took more than one billion years to evolve into a network of galaxies and stars (Whittet, 1996). As generally understood, the birth of the Sun was preceded by a series of events: (i) a cloud of gases on the very edge of the Milky Way was drifting, slowly shrinking and spinning; (ii) this cloud (or nebula) gradually contracted to form a disc that heated up; (iii) once the temperature reached a few thousands degrees, the nebula began to separate into clouds of variable density; and (iv) the scorching centre continued to heat up until eventually the Sun was born. As described by McBride (2004), the Sun is a huge ball of gas, composed mainly of helium and hydrogen although other elements are also present in smaller amounts. Furthermore, Wright (2004) described that the Sun is rather a complex and 'active' star with a radius of 695,500 km, a mass of 1.99x10<sup>30</sup> kg and a distance of about 149.6 million km from Earth. Its surface (also known as the photosphere) is 547 km thick with temperatures ranging from 5,500 K to 6,000 K. It has dark spots called 'sunspots' which are very active. Above the photosphere the temperature is around 4,000 K and above that, the temperature rises to 27,800 K; this region is called chromosphere and

is made up of hot gases in violent motion displaying fountains of flaming gases. Immediately below the photosphere, is the convection zone which is 96,560 km thick, and its temperature can reach up to  $2x10^6$  K. The radiation zone is directly below convection zone. Nuclear reactions release energy from the Sun with temperature at its core reaching  $15.6x10^6$  K (Wright, 2004).

#### 1.1.2. The Solar Nebula

It is widely believed that the solar nebula from which the sun formed was a flattened revolving disc of gas and dust which gradually cooled down. As the temperature continued to decrease, the gas quickly condensed into particles of rock, metal and ice. These particles collided with each other inside the spinning disc, and as a result stuck together, forming larger particles which rapidly fused into rocks and then boulders. After about 100 million years, a set of planets in stable orbits were eventually formed around the Sun (McBride, 2004).

Of all these planets shown in Fig. 1.1 in order of increasing distance from the Sun, those known as terrestrial planets are Mercury, Venus, Earth and Mars; they are 'small' bodies and located closer to the Sun. The other larger planets are situated farther from the Sun; these are called 'giant' planets which include: Jupiter, Saturn, Uranus and Neptune. Pluto (not normally classed as a planet) is the smallest of all, and is positioned furthest away from the Sun. Some physical characteristics of each of these objects are shown in Table 1.1.

#### 1.1.2.1. Terrestrial Planets

#### Mercury

Within the Solar System as shown in Figure 1, the planet Mercury is the closest body to the Sun with a radius of 2440 km; it is therefore very hot, and its surface facing the Sun can reach up to 743 K, but its shaded part is very cold with a temperature of about 83 K (McBride, 2004). The surface of the planet Mercury is covered with linear

features and impact craters which are caused by continuous bombardment of asteroids and comets (McBride and Gilmore, 2004)..

#### Venus

With a radius of 6052 km, this planet appears featureless because of its thick atmosphere. According to McBride and Gilmore (2004), the atmosphere is mostly (97 % by volume) carbon dioxide, and its surface atmospheric pressure is almost a hundred times that on Earth with a temperature reaching around 673 K. This high temperature is thought to be caused by the greenhouse effect of CO<sub>2</sub> (McBride, 2004). The surface structure of Venus is covered with old lava flows in many places, but there are less impact craters as compared to the surface of Mercury. It is possible that the clouds of Venus harbour microbial life (Wickramasinghe and Wickramasinghe, 2008).

#### Earth

The planet Earth has a radius of 6371 km. The surface of the Earth is covered with landscape surrounded by oceans and ice-capped frozen poles. Its surface temperature varies from hot in the Equator to cold at the polar regions. On average, the temperature is around 15 °C (McBride, 2004). Because of the circulation of hot and cold air over the planet, evaporation of water is minimal, thus maintaining the existence of life. Unlike the atmosphere of Venus, that of the Earth is composed of nitrogen (78 %) and oxygen (21 %) with traces of other gases such as carbon dioxide (Wright, 2004). Life of all sorts abound in the Earth's biosphere that extends from depths of several kilometers to heights of over 40 km in the atmosphere.

#### Mars

The planet Mars has a radius of 3390 km with an atmosphere composed mainly of carbon dioxide (95 %) (McBride, 2004). The surface of Mars shows a large canyon system (called Valles Marineris), huge old volcanoes and lava flows. The canyon has a long fracture about 4000 km across. In general, the surface appears dry and is

covered with large boulders embedded in dust and soil. A debate continues as to whether or not Mars harbours or harboured present or past life.

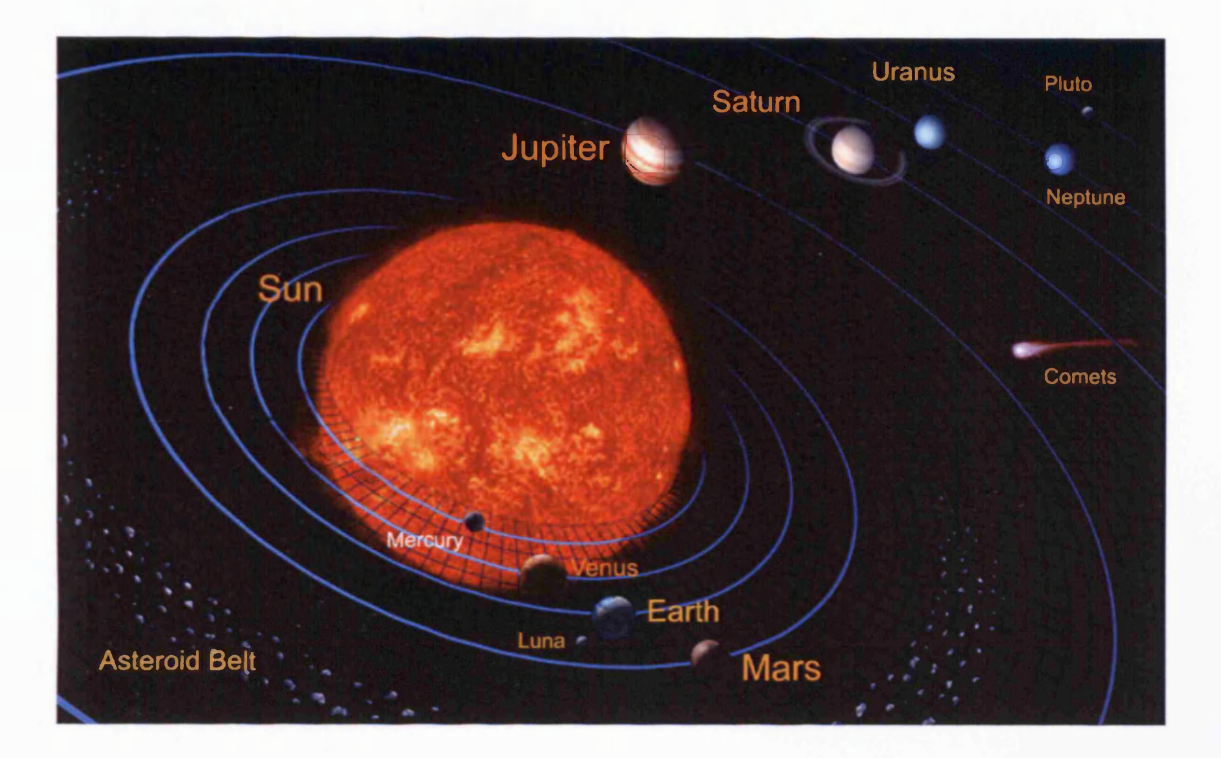


Fig.1.1: Solar System showing the position of its planets in relation to the Sun.

#### 1.1.2.2. Giant Planets

#### Jupiter

This is the largest planet of all planets with a radius of 69,910 km. The atmosphere is composed of hydrogen (90 %) and helium (10 %), with traces of methane, ammonia and water vapour (Lewis, 1995). The surface of Jupiter shows a pattern of alternate dark and light bands parallel to the equator, called belts and zones respectively. The temperature in the dark belts increases and that in the light zones decreases. This creates atmospheric motion. The most striking feature is a large region about 20,000 km across (called the Great Red Spot); this is a circulating atmospheric feature (or giant storm) with an anticlockwise rotation (Moore, 2004).

#### Saturn

With a radius of 58,230 km Saturn is the second largest planet in the solar system. The image taken by the Voyager reveals that the planet has rings around it. These rings showing distinctive gaps between them form a prominent flat disc orbiting in parallel to the equator of the planet; they are made up of icy, reflective particles and boulders with sizes ranging from a centimetre to a few metres (McBride, 2004).

#### • Uranus

This planet with a radius of 25,360 km has a featureless atmosphere. Its atmosphere consists of hydrogen, helium and methane (Moore, 2004). The image seen through the Hubble Space Telescope shows rings around the planet (McBride, 2004).

#### Neptune

Discovered in 1846 by astronomers, Johann Galle and Heinrich D'Arrest, the planet Neptune has a radius of 24,620 km, and is therefore slightly smaller than Uranus. The image of Neptune taken by Voyager 2 shows a spectacular 'Great Dark Spot' (McBride and Gilmore, 2004).

#### Pluto

With a radius of only 1137 km, Pluto is small as compared to other planets as mentioned above. It is located in the outermost region of the Solar System. Pluto was discovered in 1930 by astronomer Clyde Tombaugh, and it did not attract interest until its satellite, Charon, was discovered in 1978. The Hubble Space Telescope shows Pluto and Charon orbiting each other by synchronous rotation at a distance of about 19,400 km; both bodies are thought to have formed in the Kuiper Belt region beyond the planet Neptune (McBride, 2004). Since 2006 the International Astronomical Union (IAU) has declared Pluto as a dwarf planet or planetoid instead of a fully fledged planet.

Table 1.1: Characteristics of planets (information taken from Cox, 2000; McBride and Gilmore, 2004)

Planet	Atmospheric composition	Radius (km)	Mass (/Earth)	Density (10 <sup>3</sup> kgm <sup>-3</sup> )	Surface temp. (T/K)	Distance from the Sun (km)	Albedo
Mercury	O <sub>2</sub> , Na, H <sub>2</sub> , He, K	2440	0.055	5.43	443	57,909,175	0.10
Venus	CO <sub>2</sub> , N <sub>2</sub> , SO <sub>2</sub> , H <sub>2</sub> O, Ar, H <sub>2</sub> , CO	6052	0.815	5.20	733	108,208,93	0.77
Earth	N <sub>2</sub> , O <sub>2</sub> , H <sub>2</sub> O, Ar, CO <sub>2</sub> , Ne	6371	1	5.51	288	149,597,89	0.30
Mars	CO <sub>2</sub> , N <sub>2</sub> , Ar, O <sub>2</sub> , CO, H <sub>2</sub> O	3390	0.107	3.93	223	227,936,64	0.25
Jupiter	H <sub>2</sub> ,He,CH <sub>4</sub> , NH <sub>3</sub> ,H <sub>2</sub> O, H <sub>2</sub> S, C <sub>2</sub> H <sub>6</sub> , C <sub>2</sub> H <sub>2</sub> ,PH <sub>3</sub> , CO, GeH <sub>4</sub>	69910	318	1.33	165	778,412,02	0.34
Saturne	H <sub>2</sub> ,He,CH <sub>4</sub> , NH <sub>3</sub> ,H <sub>2</sub> O, H <sub>2</sub> S, C <sub>2</sub> H <sub>6</sub> , C <sub>2</sub> H <sub>2</sub> , PH <sub>3</sub> , CO, GeH <sub>4</sub>	58230	95.2	0.69	134	1,426,725,4	0.34
Uranus	H <sub>2</sub> ,He,CH <sub>4</sub> , C <sub>2</sub> H <sub>2</sub>	25360	14.4	1.32	76	2,870,972,2	0.30
Neptune	H <sub>2</sub> ,He,CH <sub>4</sub> , C <sub>2</sub> H <sub>6</sub> , C <sub>2</sub> H <sub>2</sub>	24620	17.1	1.64	72	4,498,252,9	0.29
Pluto	N <sub>2</sub> ,CH <sub>4</sub> ,CO <sub>2</sub>	1137	0.002	2.1	40	5,906,380,0	0.6
	Mercury  Venus  Earth  Mars  Jupiter  Saturne  Uranus  Neptune	Mercury  O <sub>2</sub> , Na, H <sub>2</sub> , He, K  Venus  CO <sub>2</sub> , N <sub>2</sub> , SO <sub>2</sub> , H <sub>2</sub> O, Ar, H <sub>2</sub> , CO  Earth  N <sub>2</sub> , O <sub>2</sub> , H <sub>2</sub> O, Ar, CO <sub>2</sub> , Ne  Mars  CO <sub>2</sub> , N <sub>2</sub> , Ar, O <sub>2</sub> , CO, H <sub>2</sub> O  Jupiter  H <sub>2</sub> ,He,CH <sub>4</sub> , NH <sub>3</sub> ,H <sub>2</sub> O, H <sub>2</sub> S, C <sub>2</sub> H <sub>6</sub> , C <sub>2</sub> H <sub>2</sub> ,PH <sub>3</sub> , CO, GeH <sub>4</sub> Saturne  H <sub>2</sub> ,He,CH <sub>4</sub> , NH <sub>3</sub> ,H <sub>2</sub> O, H <sub>2</sub> S, C <sub>2</sub> H <sub>6</sub> , C <sub>2</sub> H <sub>2</sub> , PH <sub>3</sub> , CO, GeH <sub>4</sub> Uranus  H <sub>2</sub> ,He,CH <sub>4</sub> , C <sub>2</sub> H <sub>2</sub>	Mercury  O <sub>2</sub> , Na, H <sub>2</sub> , He, K  2440  Venus  CO <sub>2</sub> , N <sub>2</sub> , SO <sub>2</sub> , H <sub>2</sub> O, Ar, H <sub>2</sub> , CO  6052  Earth  N <sub>2</sub> , O <sub>2</sub> , H <sub>2</sub> O, Ar, CO <sub>2</sub> , Ne  6371  Mars  CO <sub>2</sub> , N <sub>2</sub> , Ar, O <sub>2</sub> , CO, H <sub>2</sub> O  3390  Jupiter  H <sub>2</sub> ,He,CH <sub>4</sub> , NH <sub>3</sub> ,H <sub>2</sub> O, H <sub>2</sub> S, C <sub>2</sub> H <sub>6</sub> , C <sub>2</sub> H <sub>2</sub> ,PH <sub>3</sub> , CO, GeH <sub>4</sub> Saturne  H <sub>2</sub> ,He,CH <sub>4</sub> , NH <sub>3</sub> ,H <sub>2</sub> O, H <sub>2</sub> S, C <sub>2</sub> H <sub>6</sub> , C <sub>2</sub> H <sub>2</sub> , PH <sub>3</sub> , CO, GeH <sub>4</sub> Uranus  H <sub>2</sub> ,He,CH <sub>4</sub> , C <sub>2</sub> H <sub>2</sub> 25360  Neptune  H <sub>2</sub> ,He,CH <sub>4</sub> , C <sub>2</sub> H <sub>6</sub> , C <sub>2</sub> H <sub>2</sub> 24620	Mercury         O2. Na, H2, He, K         2440         0.055           Venus         CO2, N2, SO2, H2O, Ar, H2, CO         6052         0.815           Earth         N2, O2, H2O, Ar, CO2, Ne         6371         1           Mars         CO2, N2, Ar, O2, CO, H2O         3390         0.107           Jupiter         H2,He,CH4, NH3,H2O, H2S, C2H6, C2H2,PH3, CO, GeH4         69910         318           Saturne         H2,He,CH4, NH3,H2O, H2S, C2H6, C2H2, PH3, CO, GeH4         58230         95.2           Uranus         H2,He,CH4, C2H2         25360         14.4           Neptune         H2,He,CH4, C2H6, C2H2         24620         17.1	Mercury         O <sub>2</sub> , Na, H <sub>2</sub> , He, K         2440         0.055         5.43           Venus         CO <sub>2</sub> , N <sub>2</sub> , SO <sub>2</sub> , H <sub>2</sub> O, Ar, H <sub>2</sub> , CO         6052         0.815         5.20           Earth         N <sub>2</sub> , O <sub>2</sub> , H <sub>2</sub> O, Ar, CO <sub>2</sub> , Ne         6371         1         5.51           Mars         CO <sub>2</sub> , N <sub>2</sub> , Ar, O <sub>2</sub> , CO, H <sub>2</sub> O         3390         0.107         3.93           Jupiter         H <sub>2</sub> ,He,CH <sub>4</sub> , NH <sub>3</sub> ,H <sub>2</sub> O, H <sub>2</sub> S, C <sub>2</sub> H <sub>6</sub> , C <sub>2</sub> H <sub>2</sub> ,PH <sub>3</sub> , CO, GeH <sub>4</sub> 69910         318         1.33           Saturne         H <sub>2</sub> ,He,CH <sub>4</sub> , NH <sub>3</sub> ,H <sub>2</sub> O, H <sub>2</sub> S, C <sub>2</sub> H <sub>6</sub> , C <sub>2</sub> H <sub>2</sub> , PH <sub>3</sub> , CO, GeH <sub>4</sub> 58230         95.2         0.69           Uranus         H <sub>2</sub> ,He,CH <sub>4</sub> , C <sub>2</sub> H <sub>2</sub> 25360         14.4         1.32           Neptune         H <sub>2</sub> ,He,CH <sub>4</sub> , C <sub>2</sub> H <sub>6</sub> , C <sub>2</sub> H <sub>2</sub> 24620         17.1         1.64	Mercury         O <sub>2</sub> , Na, H <sub>2</sub> , He, K         2440         0.055         5.43         443           Venus         CO <sub>2</sub> , N <sub>2</sub> , SO <sub>2</sub> , H <sub>2</sub> O, Ar, H <sub>2</sub> , CO         6052         0.815         5.20         733           Earth         N <sub>2</sub> , O <sub>2</sub> , H <sub>2</sub> O, Ar, CO <sub>2</sub> , Ne         6371         1         5.51         288           Mars         CO <sub>2</sub> , N <sub>2</sub> , Ar, O <sub>2</sub> , CO, H <sub>2</sub> O         3390         0.107         3.93         223           Jupiter         H <sub>2</sub> ,He,CH <sub>4</sub> , NH <sub>3</sub> ,H <sub>2</sub> O, H <sub>2</sub> S, C <sub>2</sub> H <sub>6</sub> , C <sub>2</sub> H <sub>2</sub> ,PH <sub>3</sub> , CO, GeH <sub>4</sub> 69910         318         1.33         165           Satume         H <sub>2</sub> ,He,CH <sub>4</sub> , NH <sub>3</sub> ,H <sub>2</sub> O, H <sub>2</sub> S, C <sub>2</sub> H <sub>6</sub> , C <sub>2</sub> H <sub>2</sub> , PH <sub>3</sub> , CO, GeH <sub>4</sub> 95.2         0.69         134           Uranus         H <sub>2</sub> ,He,CH <sub>4</sub> , C <sub>2</sub> H <sub>2</sub> 25360         14.4         1.32         76           Neptune         H <sub>2</sub> ,He,CH <sub>4</sub> , C <sub>2</sub> H <sub>6</sub> , C <sub>2</sub> H <sub>2</sub> 24620         17.1         1.64         72	Mercury         O <sub>2</sub> , Na, H <sub>2</sub> , He, K         2440         0.055         5.43         443         57,909,175           Venus         CO <sub>2</sub> , N <sub>2</sub> , SO <sub>2</sub> , H <sub>2</sub> O, Ar, H <sub>2</sub> , CO         6052         0.815         5.20         733         108,208,93           Earth         N <sub>2</sub> , O <sub>2</sub> , H <sub>2</sub> O, Ar, CO <sub>2</sub> , Ne         6371         1         5.51         288         149,597,89           Mars         CO <sub>2</sub> , N <sub>2</sub> , Ar, O <sub>2</sub> , CO, H <sub>2</sub> O         3390         0.107         3.93         223         227,936,64           Jupiter         H <sub>2</sub> ,He,CH <sub>4</sub> , NH <sub>3</sub> ,H <sub>2</sub> O, H <sub>2</sub> S, C <sub>3</sub> H <sub>6</sub> , C <sub>2</sub> H <sub>2</sub> , PH <sub>3</sub> , CO, GeH <sub>4</sub> 69910         318         1.33         165         778,412,02           Saturne         H <sub>2</sub> ,He,CH <sub>4</sub> , NH <sub>3</sub> ,H <sub>2</sub> O, H <sub>2</sub> S, C <sub>3</sub> H <sub>6</sub> , C <sub>2</sub> H <sub>2</sub> , PH <sub>3</sub> , CO, GeH <sub>4</sub> 95.2         0.69         134         1,426,725,4           Uranus         H <sub>2</sub> ,He,CH <sub>4</sub> , C <sub>3</sub> H <sub>2</sub> 25360         14.4         1.32         76         2,870,972,2           Neptune         H <sub>2</sub> ,He,CH <sub>4</sub> , C <sub>3</sub> H <sub>2</sub> , C <sub>2</sub> H <sub>2</sub> 24620         17.1         1.64         72         4,498,252,9

#### 1.1.2.3. Satellites

The Solar System contains numerous satellites of various sizes, some of which are described below:

- The Moon: The images taken by the spacecraft, Galileo and Apollo 16, show the Moon having two distinctive regions: a bright highland area covered with numerous impact craters and a darker, less cratered region.
- Phobos and Deimos: These are the satellites of Mars which have an irregular shape. The size of Phobos is 26km x 18km with large and small impact craters. On the other hand, Deimos with the size of 16km x 10km, has fewer impact craters (McBride, 2004).
- Io, Europa, Ganymede and Callisto: These are four principal satellites of Jupiter amongst many. They are called Gallilean satellites because they were first observed by Galileo Galilei. The image taken by the Gallileo spacecraft shows that with a radius of 1821 km Io has a pizza-like appearance with large volcanic activity extending about 250 km across. On the other hand, Europa with a radius of 1565 km has an icy surface covered with cracks but shows no obvious impact craters. With a radius of 2634 km, Ganymede is the largest satellite in the Solar System but contains less mass than the planet Mercury. Callisto is the outermost satellite with a radius of 2403 km. Both, Ganymede and Callisto are icy bodies and heavily cratered; their surfaces are more ancient than those of Io and Europa (McBride, 2004).
- **Titan:** Amongst all the satellites of Saturn, Titan is the largest; it has a radius of 2575 km, a surface temperature of around 90 K and an atmospheric pressure about 1.5 times that of Earth (McBride, 2004). Although this satellite appears featureless, it is of great interest to astrobiologists because of its massive atmosphere, its richness in organic matter and a possible prebiotic chemistry of relevance to astrobiology (Lewis, 1995). According to Lewis (1995), these organics are protected by the thick atmosphere of Titan from harmful UV radiation. The Titan's atmosphere is composed of nitrogen (N<sub>2</sub>), methane (CH<sub>4</sub>), hydrogen (H<sub>2</sub>), argon (Ar) and low density

hydrocarbons (HCN, C<sub>2</sub>H<sub>2</sub> and C<sub>2</sub>H<sub>4</sub>) (Somogyi et al., 2005). It is now clear from the infrared interferometer spectrometer (IRIS) obervations conducted by instruments aboard Voyager 1 and Voyager 2 that the atmosphere of Titan is dominated by nitrogen and methane. Methane accounts only for several percent of the total atmospheric pressure. The hydrogen abundance in Titan is about 0.2% and nitrogen makes up almost all the rest (Lewis, 1995).

Methane and nitrogen are supplied with energy from solar ultraviolet radiation and energetic particles in Saturn's magnetosphere (Waite et al., 2007). This solar energy provides favourable conditions for the formation of complex organic materials including unsaturated hydrocarbon species (Yung et al., 1984; Yelle et al., 2006) and in particular hydrocarbon–nitrile compounds with masses reaching up to 100 daltons (Waite et al., 2005). It has been suggested that such organic chemical process as occured in the early Earth's atmosphere before the build-up of oxygen about 2.2 x10<sup>9</sup> years ago (Pavlov et al., 2003).

The lower atmosphere of Titan is reported to contain aerosols which are formed from simple molecules, such as methane (CH<sub>4</sub>) and nitrogen (N<sub>2</sub>) (Lewis, 1995). One of these aerosols is known as Tholin, and it forms the organic feedstock for a complex chemistry at the surface level (Somogyi et al., 2005). However, Waite et al., (2007) showed evidence of tholin formation at the upper atmosphere (950-11500 km) of Titan. Furthermore, based on the Ion Neutral Mass Spectrometer (INMS) observations in the Cassini spacecraft, Waite et al. (2007) confirmed that the formation of tholin was accompanied by the presence of negatively charged molecules of massive molecular weight (~8000 daltons), and suggested that these negative ions may play an important role in the formation of tholin. The possibility of an active biology on Titan, rather than prebiology cannot be excluded.

#### 1.1.2.4. Comets

These are small bodies, often seen from Earth as objects with a bright head, a coma, and a long faint tail (McBride, 2004). The tail includes of dust particles that reflect sunlight. The comets are known to be responsible for causing impact craters found on the surfaces of Earth as well as other planetary objects. Comets are divided into two types based on the period of their orbit. The comets that complete their orbit in 200 or less years are known as short period comets, whereas those taking more than 200 years to orbit the Sun are long period comets. The former have less elliptical orbits and are made up of the leftover bits that were never incorporated into a planet during planet formation. It is widely accepted that the official names for the identification of periodic comets should begin with "P" or a number followed by "P". Whilst the names begin with a "C" should be assigned for the non-periodic comets, those beginning with a "D" are used to identify those comets that have been lost or disappeared. The effects of collisions between comets and planets and the evolution of these orbits are both active areas of research. Other research interests are associated with the photochemistry and plasma physics of comet tails. Studies on the composition of the vapour from the nucleus using spectroscopy have provided evidence for the abundance of both silicaceous dust and mixed ices and organics in fresh comets prior to alteration by the sun. The presence of organic polymers in comet dust was first investigated by Vanysek and Wickramasinghe (1975).

One of the most famous and extensively studied is comet P/Halley; its image released by the European Space Agency shows its body as a dark irregular object about 15x7 km in size. This body emitted large amounts of dust and gas produced from sublimating ices (mainly water, ammonia,  $CO_2$ , CO) when it comes close to the Sun. The dust spectrum obtained by Allen and Wickramasinghe (1981) was found to be closely similar to that of bacteria in the 2-4  $\mu$ m infrared spectral region (Hoyle and Wickramasinghe, 1985).

#### **1.1.2.5.** Asteroids

These bodies are abundant in the Solar System. More than one hundred thousand asteroids have been discovered, and most of these have orbits that form the Asteroid belt (McBride, 2004). The asteroids are in fact fragments of small planetary bodies that never stuck together to form a single large body because Jupiter's gravitational effects tend to continuously break up larger aggregates. There are about 2000 asteroids that are known to have orbits coming near to the orbit of the Earth, and these are called Near Earth Asteorids or NEAs (McBride, 2004). About 400 of them are now called 'Potentially Hazardous Asteroids (PHAs). The Earth has been occasionally hit by such an asteroid.

Asteroids have variable sizes; the largest is Ceres with a diameter of 913 km and it was discovered in 1801 (McBride, 2004). Their elemental composition is also variable depending on the thermal, physical and chemical processing. Asteroids are classified according to their reflectance spectrum (or albedo) such as C (carbonaceous with an albedo of 0.03-0.07), E (mineral magnesium silicate with an albedo of 0.25-0.60), M (metallic with an albedo of 0.10-0.18) and S- types (stone with an albedo of 0.10-0.22).

#### 1.1.2.6. Meteorites

These are pieces of extraterrestrial objects, mostly from fragmented asteroids, that fall to Earth after having survived impact with the atmosphere. In general, the meteorite fragments appear as solid rocks. Depending on their elemental composition, the meteorites are classified as iron-meteorite (mainly metal iron), stony-meteorites (silicate minerals) or stony iron-meteorites (mixture of iron and silicates). Stony meteorites most frequently fall to Earth, and most of them are chondrites containing globules of silicate minerals (known as chondrules) (Wright, 2004). Meteorites are thought to constitute a major means of delivery of extraterrestrial material onto Earth, and the relevant detailed information is described in section 1.5 of this Chapter.

#### 1.2. Major Elements in the Solar System

The major biogenic elements found in the Solar System include carbon, nitrogen, sulphur and phosphorus (Lewis, 1995). In fact, the Sun and materials in the outer solar system have more than 10,000 times the carbon content of the bulk of Earth (McKay, 1991). This carbon in the form of organic molecules together with liquid water may play a role in extraterrestrial life (Pace, 2001). It has also been suggested that extraterrestrial life may use other solvents such as liquid methane, liquid nitrogen, hydrocarbon and the element silicon (Pace, 2001; Bains, 2004). These major and other minor elements form the complex feedstock for life to evolve on Earth.

#### 1.3. Evidence of Early Life on Earth

Our planet contains ingredients that are needed to support life. Water is an absolute requirement of life and the other elements include carbon, hydrogen, oxygen, nitrogen and minerals such as S, P, Na, K, Mg, Ca, Mn, Fe, Cu and Zn, all of which form the chemical elements for life to evolve (McKay, 1991). For these chemical elements to form molecules and to react, an energy source is also needed. In general, the vast majority of life forms on Earth get their energy from sunlight. Most primitive plants obtain energy by absorbing ultraviolet light from the Sun and this process is known as photosynthesis. As we know, humans and other animals get their energy by consuming plants, or other animals. Ultimately all animals rely on energy from the Sun to live. However, only until recently, it was thought that life couldn't exist in a place that was shaded from sunlight. Scientists have recently discovered organisms that live deep beneath the ocean. These organisms absorb energy directly from chemicals in the water around them. Liquid water or possibly an ocean existed at the surface of the Earth as early as 4.3 billions years ago (Javaux, 2006). This is confirmed by the discovery of ancient zircons (minerals formed in water) that were dated at that time (Mojzsis et al., 1996). In the early Archean period, the Earth was rich in liquid water (Javaux, 2006).

Carbon, hydrogen, nitrogen, oxygen and other elements that make our bodies and other living creatures, were synthesised billions years ago in the interiors of stars

(Burbidge et al., 1957), and in the case of hydrogen, in the Big Bang itself (Trimble, 1997). A good understanding of the origin and evolution of life on Earth is useful for the search for past or present extraterrestrial life. It is generally agreed that the Earth formed by coagulation and accretion of planetary dust (Tscharnuter and Boss, 1993; Harper, 1996; Gaffey, 1997). Following its initial accretion, the Earth was hot and could not have supported water at its surface. Comet impacts brought water to form oceans on the surface, and evaporation of water produced a primitive atmosphere (Oró, 1961). The stage was set for the emergence of life.

Although liquid water, chemical elements and energy are considered to be necessary for life to emerge, the environmental conditions for early life to evolve are not yet understood. Furthermore, as we know, life has tremendously affected the landscapes and atmospheres of the Earth about 3.5 billions years ago (Schopf, 1992; 1993). Searching for early life on the Earth is difficult since most of its signatures were erased by geological processes such as fossilisation and metamorphism (Javaux, 2006). Fortunately, some places on continents have sedimentary rocks that are still preserved, and have been found to contain traces of early life. Microfossils, stromatolites, and isotopes of sedimentary carbon and sulphur found on Earth were recorded to be dated before 2.5 billions years during the Archean time; these materials show the presence of microorganisms and that their metabolism was developed in the same way as those of many recent terrestrial microbes (Brocks et al., 2003). Thus, the presence of biosignatures on Earth have made the detection of past and present life possible.

The direct evidence of earliest life on Earth is shown by the presence of the oldest fossils, which dated about 3.5 billions years (Schopf, 1992; 1993). The samples contained primitive cyanobacteria that presumably went through evolution a few hundred million years earlier before reaching the stage of complexity found in the samples (Whittet, 1996). The indirect evidence of early life is obtained from the geological record at about 3.83-4 billion years ago. The presence of free oxygen in the atmosphere is confirmed by the discovery of sedimentary rocks in the ocean floor, that consists of alternating, layers of iron-rich and iron-poor (Schopf, 1992). According to Kasting (1997), the formation of such rock shows that the atmosphere is weakly aerobic and that the primary source of atmospheric oxygen is photosynthesis.

#### 1.4. Survival of Organisms in Extreme Environments

One of the main aims of astrobiologists is to find evidence for signs of life in space. Trent (2000) has suggested that to approach this goal, it would be useful to have a good knowledge of the physical and chemical factors that limit life on the Earth, and perhaps most importantly the underlying biophysical characteristics of life that set these limits.

In nature, some terrestrial organisms are more resistant than others to living conditions that a human being would consider extreme. Those organisms that thrive beyond these limits are referred to as extremophiles. According to Rothschild and Mancinelli (2001), the extreme environments where this group of organisms are found, can be of various forms such as physical, geochemical or biological.

It is fortunate from the astrobiological point of view that the continuous exploration of Earth for signs of early life has led to the discovery of a variety of unexpected microbial habitats. Bacteria, archaea and other primitive living creatures have been found to thrive in most habitats, especially in extreme habitats (Trent, 2000). Some microbes of the family known as barophiles or piezophiles survive and even thrive in cold, deep-sea environments where temperatures are between 2-4 °C and pressure up to 1100 bars (Yayanos, 1995). Members of psychrophiles grow in the Siberian permafrost where the tremperature is below -20 °C (Mazur, 1980).

There have been reports of another extreme case where bacteria are present either in hot water with temperatures reaching a few degrees above 100 °C or cultured at 105 °C (Trent, 2000). Those organisms that thrive at temperatures above 80 °C are called hyperthermophiles, and these include prokaryotic organisms that are found in environments with temperatures higher than 75 °C above which microbial diversity sharply decreases (Brock, 1978).

The frequently asked question is how these organisms can survive and in most cases thrive under such extreme conditions. As pointed out by Trent (2000), the extremophiles are equipped with biochemical and molecular adaptations that allow

them to thrive under such extreme environments. As Trent (2000) also indicated, some of these adaptations may involve changes in biomolecules (eg. lipids, nucleic acids and proteins), and regulation of compounds (eg. organic solutes, salts and proteins), which stabilise both the macromolecules and cellular organisation.

Liquid water is also important either as a reactant or product for most metabolic processes (Franks, 1985). However, water freezes at low temperatures by nucleation, resulting in ice crystal formation and freezing of intracellular water. In this context, temperature creates a series of challenges: from one extreme structural devastation by ice crystals, and to the other denaturation of biomolecules by excessive heat (Rothschild and Mancinelli, 2001). From the biochemical point of view, temperatures reaching 100 °C normally denature the essential biomolecule such as proteins and nucleic acids, and increase the fluidity of the membranes to lethal levels.

The story of the red rain event that took place on the 25<sup>th</sup> of July, 2001 in Kerala (India), has recently prompted detailed studies. Louis and Kumar (2003) reported that the microorganisms in the red rain samples could grow in extreme environmental conditions (300 °C). Furthermore, their spectroflurometric study confirmed that these microorganisms had proteins but no visible DNA in their cells. The above findings have attracted interest amongst astrobiologists in the search for the origin of these microorganisms. It is acknowledged that all known living systems of terrestrial origin can not survive at 100 °C, let alone 300 °C, because under this temperature their metabolic activities completely shut down. There are however a number of reports indicating that some microorganisms isolated from the ocean hydrothermal vent systems and deep-sea oil wells are able to grow even at 121 °C, such as Pyrolobus fumarii (Blochl et al., 1997), and a microbe known as Strain 121 (Kashefi and Lovley, 2003). The fact that these hyperthermophilic microorganisms can thrive in such high temperature is explained by their ability to evolve either by altering their metabolism or genetic make-up. Grogan (1998) claimed that these microroganisms are equipped with a DNA repair system against thermal denaturing process.

Despite the experimental reports produced by Louis and Kumar (2003 and 2006), the origin of the red rain particles still remains unclear. As suggested by Louis and Kumar (2006), the particles may be of cometary origin fitting a panspermia hypothesis which

proposes that the Earth was seeded in the past, and is still being seeded, with microorganisms from outerspace. This theory has recently been confirmed by the results of isotopic analysis of Murchison meteorite, which has shown that the organic compounds found in the samples are not terrestrial (Martins et al., 2008).

#### 1.5. Delivery of Extraterrestrial Materials to Earth

#### 1.5.1. Minerals

#### 1.5.1.1. Comets

Many comets such as those of Oort cloud and Jupiter family contain crystalline silicates that were formed in the early solar nebula at temperature T >1000 K (Crovisier et al., 2000; Harker, 2004; Reach, 2004; Hanner and Bradley, 2005). A number of other comets have also been reported to contain both amorphous and crystalline silicate grains. One of the comets reported to contain chondritic porous interplanetary dust particles or CP IDPs is comet 81P/Wild 2 (Ishii et al., 2008). The dust particles were collected by the Stardust spacecraft which passed through the dusty coma. The analysis of the samples has shown that they contain silicates (namely olivines and pyroxenes) and refractory minerals such as melilite, anorthite, corundum, osbomite and roedderite (Zolensly et al., 2006). These minerals are believed to originate in the inner nebula (Ishii et al., 2008). According to Joswiak et al. (2007), these refractory minerals are all related to calcium-aluminium inclusions and also to chondrule fragments. It has also been reported that the dust ejected into the coma from the nucleus of comet 9P/Tempel 1 after an impact, was a mixture of amorphous and crystalline grains. The presence of clay particles in this comet was inferred from infrared spectroscopy (Wickramasinghe et al., 2010). The infrared observations with the MICHELLE imaging spectrograph on the 8-m Fredrick C. Gillettte (Gemini-N) telescope on Mouna Kea, Hawaii, showed that the amorphous grains appear slightly porous and are composed mainly of amorphous pyroxene and amorphous olivine whereas the crystalline grains contain magnesium rich crystalline olivine (Harker et al., 2005). The observation of Comet Hale-Bopp (C/1995 O1) with the Infrared Space Observatory (ISO) revealed the presence of silicates composed of magnesium-rich

crystalline olive in addition to volatile elements such as water, carbon monoxide and carbon dioxide (Crovisier et al., 1997).

Interplanetary dust particles collected in the stratosphere also show fragile microstructures with an abundance of carbon and Mg-rich silicates (Bradley et al., 1999). These objects are also found within the matrices of chondritic porous of the IDPs or embedded in amorphous carbonaceous material (Bradley, 1994). These grains are similar to those of astronomical 'amorphous' silicate grains that are widespread throughout interstellar and circumstellar space (Martin, 1995).

#### **1.5.1.2.** Meteorites

Minerals are also present in abundance in meteorites found on Earth. The two main silicates in CP IDPs that are believed to be unique to the class of meteorite materials include: amorphous silicates known as GEMS (glass with embedded metal and sulfides) and a whisker (elongated silicate crystal) of the crystalline silicate enstatite (Bradley, 2003). These GEMS show a spectral match (10 µm wavebands) to astronomical amorphous silicates, one of the constituents that form the fundamental building blocks from which the solar system is thought to have formed (Bradley et al., 1999; Messenger, 2003).

Some minerals such as melilite, spinel and perovskite are also found in small refractory inclusions in a few meteorites such as phylosilicates which are distinguished by their layered (mica-like) structure and high water content (Lewis, 1995). These phylosilicates are found only in the very volatile-rich carbonaceous chondrites and in association with organic matter, sulphur, sulfates, carbonated, magnetite, and other oxidised and volatile-rich materials (Lewis, 1995).

#### 1.5.2. Organic Matter

#### 1.5.2.1. Interstellar Dust

The nature of interstellar dust has been extensively reviewed over recent years. The most highly debated topics are related to: (i) whether the interstellar particles can survive the processes associated with the origin of our Solar System; (ii) whether these particles contain complex organic molecules; and (iii) whether some of which are delivered to Earth by comets and asteroids, and subsequently play a role in the origin of life on Earth.

The Universe is thought to have originated nearly 13.7 billion years ago (Irvine, 1996). Throughout much of the age of the Universe, interstellar dust has existed in space. Evidence for the presence of organics in interstellar dust is compelling. As we learn more about the nature of comets and asteroids, support is also growing for the view that interstellar material survived the origin of the solar system. A number of investigations have indicated that the interstellar particles contain complex organic molecules (Wickramasinghe, 1974; Hoyle et al., 1978; Hoyle and Wickramasinghe, 1980a; Hollenbach and Thronson, 1987; Irvine, 1996; Trimble, 1991 and 1997). In the interstellar medium of our Milky Way Galaxy, most of the material is in the form of interstellar clouds where organic particles are abundant (Hoyle et al., 1978; Hoyle and Wickramasinghe, 1980a; Henkel et al., 1991). These clouds consist of two types: diffuse and dense interstellar media (Irvine, 1996). Omont (1991) and Whittet (1992) reported that some of the dust grains in the diffuse clouds are predominantly formed in the expelled envelopes of cool, evolved red giant stars. Most of these grains are subjected to various planetary processes which may destroy them. Fortunately, a significant amount of the grains in the diffuse clouds escaped these processes. In this diffuse region, ultraviolet photons photolyse most molecules and diatomic species were for the first time clearly identified (Irvine, 1996).

The presence of complex organic molecules in galactic material has been extensively studied following the early work by Wickramasinghe (1974). Wickramasinghe and Allen (1980) detected a 3.4 µm absorption feature in IRS 7 source using the 3.9m

Anglo-Australian Telescope and an infrared photometer-spectrometer. They have shown that the ratio of the absorption coefficient of grains at 3.4  $\mu$ m to the extinction coefficient at  $\lambda_v \sim 5500$  Å is within the range  $\sim 0.003$ -0.006 and that the data is consistent with all the grains in the interstellar medium containing a polymer based on the H<sub>2</sub>CO molecule. They have further suggested that this 3.4  $\mu$ m feature is a CH stretching band and that it is not confined to either diffuse or dense clouds, but rather to the general interstellar medium. Based on this data and the observations of Duley and Williams (1979), Wickramasinghe and Allen (1980) concluded that the mass fraction of interstellar grains is predominantly rich in carbon in the form of organic molecules.

Organic substances are known to possess a characteristic band resulting from CH stretching centred at 3.3-3.5 µm wavelengths (Silverstein et al., 1974). Some have argued that the 3.4 µm band is associated with the organic molecules in the form of gas rather than grains (Duley and Williams, 1979). However, this argument seems to exclude the fact that the gaseous molecules are volatile, and thus can not survive in the harsh interstellar environment. The positive detection of organic molecules from the infrared spectra has provided a new insight into the story of the interstellar grains. In earlier studies, Wickramasinghe (1974) found that a paraformaldehyde grain of 0.3  $\mu$ m radius had a CH band centered at 3.4  $\mu$ m and a ratio of  $k_{3.4\mu}$  / $k_{5500}$   $\lambda$ = 0.006. He further claimed that these data were consistent with the astronomical observations and matched with the value reported for IRS 7. Polysaccharides, cellulose, amylase and αglucans have also been analysed spectroscopically in relation to interstellar dust properties. For polysaccharides, the position of the 3.4 µm band centre varies slightly from one type to another (Hoyle and Wickramasinghe, 1977) whereas that of cellulose is centred at 3.45 µm (Hoyle et al., 1978), and that of glucans is 3.41 µm (Michell and Scurfield, 1970).

Attempts to characterise the specific nature of dust particles spectroscopically have proved quite difficult since their infrared spectra show only the functional groups rather than specific large organic molecules (Irvine, 1996). The interstellar grains show absorptions in the 3-10 µm waveband which are attributed to aromatic and aliphatic groups (Whittet, 1992; Sandford, 1996). Polycyclic aromatic hydrocarbons (PAHs) are reported to produce infrared bands in 2-14 µm region but some

investigators have argued that this emission may be due to either free molecules or amorphous carbon grains that have been hydrogenated (Tielens, 1993). PAHs are observed in a number of cosmic environments such as vicinity of evolved stars, carbonaceous meteorites, interplanetary dust particles and Martian rocks (Roche et al., 1996; McKay et al., 1996). According to Witt (1999), the 3.4 µm feature is the infrared interstellar absorption which is attributed to CH stretch transition in aliphatic hydrocarbon materials.

The spectra of distant stars show broad absorption features with widths ranging from 0.1 to 3 nm but with invariable wavelengths and profiles (Irvine, 1996). These diffuse interstellar bands (DIBs) (200 of these features) are observed in the optical and near infrared spectra of the stars (Herbig, 1995; Irvine, 1996).

Studies on Interplanatery dust particles (IDPs) have provided some insight into the origin of the early solar system. Much of what astrobiologists have known about IDPs comes from their ultraviolet (UV) spectra. Earlier observations reported the presence of a conspicuous peak centered near 2200 Å in the extinction curves of starlight (Stecher, 1965; Savage, 1975; Nandy et al., 1975). Furthermore, quantitative analyses of the ultraviolet extinction of starlight demonstrated that all extinction curves had an approximately linear relationship with respect to  $1/\lambda$  between  $\lambda$  =0.33  $\mu$ m and  $\lambda$  =1  $\mu$ m, a narrow peak between 4.5  $\mu$ m<sup>-1</sup> and 4.7  $\mu$ m<sup>-1</sup>, and a flat minimum at 5.5  $\mu$ m<sup>-1</sup> (Al Mufti, 1985). Wickramasinghe and Guillaume (1965) originally proposed that this feature was attributed to graphite grains from carbon stars. According to Draine (1989), one of the features seen in the diffuse interstellar medium (ISM) is the 2175 Å UV extinction peak which is attributed to the absorption by small grains of carbonaceous, and is most likely of graphitic nature.

According to Hoyle and Wickramasinghe (1962 and 1969) and Stecher and Donn (1965), the 217.5 nm extinction bump is attributable to small spheres of graphite. However, Hoyle and Wickramasinghe, (1977) later proposed the alternative molecular explanation of the 217.5 nm absorption; they argued that the requirement of graphite which has a planar lattice structure to be in the form of small spheres in interstellar medium, appears scarcely relevant, and instead suggested the involvement of aromatic organic molecules. Furthermore, photo-reflective measurements of anthracite produce

a feature close to 217.5 nm, suggesting that this feature probably arises from a complex carbonaceous compound (Kwok, 2009).

Recently, Bradley et al. (2005) have also detected a 5.7 electron volt (2175 Å) feature in interstellar grains embedded within IDPs and pointed out that this was the strongest visible-ultraviolet spectral signature of dust in the interstellar medium. The interstellar medium has previously been reported to be rich in carbonaceous matter and amorphous silicates (Steel and Duley, 1987; Draine, 1989; Sandford, 1996). According to Floss and Stadermann (2004) and Messenger (2000), the carbonaceous matter is a mixture of organic and inorganic carbon and some of the organic materials have nonsolar isotopic compositions comparable to those found in interstellar molecular clouds. Bradley et al. (2005) have suggested that both organic compounds and amorphous silicates in IDPs may be carriers of the 2175 Å feature.

#### 1.5.2.2. Meteorites

During the formation and evolution of planets, most materials from the early Solar System have been continuously processed and consequently became less primitive. However, there are some regions of the Solar System that have escaped the planetary processes such as asteroid belt where small objects have not been subjected to the transformation after the birth of the Solar System (McBride, 2004). Due to gravitational force of some planets like Jupiter, the asteroids close by are likely to be involved in some form of collisions and as a result, fragmented into rocks which are then propelled into the orbit of the Earth and subsequently fall down to its surface under its gravitational pull.

These rocks are meteorites and thousands have been collected throughout the world and subsequently studied in various laboratories. The Earth has been continuously bombarded by meteorites since its initial accretion several hundreds millions years ago. However, their sources were rarely reported in the very early years. It was not until 1959 when the fall of a meteorite was spectacularly captured by cameras at Priram, near Prague, Czech Republic that their points of entry were recorded and reported (Ceplecha, 1977; Llorca, 2004). Since then, the orbits of other meteorites have also been identified such as Lost City in Oklahoma (1970), Innisfail in Alberta

(1977), Peekskill in New York (1992), Moravia in Czech Republic (2000) and Neuschwanstein in Austria (2002). The meteorites collected on Earth are considered to be parts of asteroids or extinct comets. Due to the gravitational force of Jupiter, asteroids could never be assembled into a planet in the early stages of planetary formation and their total mass is less than that of the Moon (Llorca, 2004). No light is produced by asteroids but the reflection of sunlight from their surfaces produces spectra which can be used to compare with those obtained from the analysis of meteorites in the laboratories. The largest asteroid is Ceres and has been classified as Type C of which the surface contains water-bearing clays and organic materials (Buseck and Hua, 1993).

In the past, meteorite falls were not well understood and frequently thought to be the result of divine phenomena or acts of God. Nowadays, there are expeditions designed to collect meteorites either in hot and cold deserts and also dust particles in space. Space missions have also been regularly undertaken to collect samples from the planetary system. The main aim of these expeditions is to provide new opportunities for scientific advancement in the area of astrobiology. Certain types of meteorites such as the ones found in Murchison, Australia in 1969, have been reported to contain a large amount of organic materials such as: hydrocarbons, alcohols, aldehydes, ketones, carboxylic acids, amino acids, amines, amides, heterocycles, phosphonic acids, sulfonic acids, sugar-related compounds and other poorly defined highmolecular weight macromolecules (Sephton, 2005). Analysis of isotopic ratios  $(C^{12}/C^{13})$  of organic compounds found in the Murchison meteorite confirms that these molecules are of non-terrestrial origin and that the relevant molecules identified include uracil, an RNA nucleobase and xanthine (Martins et al., 2008). The organic matter was found to be localised within the inorganic matrix of the chondrites which also contained traces of water (Llorca, 2004). It has been suggested that this organicinorganic combination may play a role in the formation of complex organic matter in the early Solar System. Since many of these compounds are also present in terrestrial living systems, it may be possible that extraterrestrial organic matter was involved in the origin of life on Earth. Proof that the cosmos delivers some exogenous organic molecules onto the surface of the Earth, is provided by analysis of carbonaceous meteorites. In addition to the Murchison meteorite, the chemical analysis was also

carried out on the others such as Cold Bokkeveld (South Africa, 1838), Orgueil (France, 1864), Murray (USA, 1950) and Allende (Mexico, 1969).

About 85% of the meteorites collected are chondrites with an overall elemental composition similar to the Sun (Sephton, 2005). This evidence supports the view that the chondrites were formed during or shortly after the birth of the Sun. Since the Sun contains more than 99% of the mass of the whole planetary system and that the elemental composition of the solar system is equivalent to the chemistry of the sun, the close similarity between the elemental composition of the sun and carbonaceous chondrites suggests that unlike all the rocks on Earth, this type of meteorites has not encountered extensive chemical alteration. Of all the chondrites observed, it is the carbonaceous chondrites that belong to the most primitive meteorites. This observation seems to indicate that studies on carbonaceous chondrites could provide some new insights into the origin of life on Earth.

A new type of carbonaceous chondrite has recently been found in the meteorite which was collected in the frozen lake, called Tagish Lake in Canada (Llorca, 2004). This chondrite is related to a primitive meteorite rich in organic compounds with 3.6 % carbon in weight (Brown et al., 2000; Llorca, 2004). According to McSween (1989), the meteorite-carbonaceous chondrites are grouped into seven main types as shown in Table 1.3. Most carbonaceous chondrites are older than 4.5 billions year and are representative of primitive meteorites; they contain water (up to 10% of their weight) and carbon (more than 3% of their weight) (Cronin et al., 1988).

Table 1.3: Classification of carbonaceous chondrites (taken from Llorca, 2004; McSween, 1989).

Туре	Prototype	Year
CI	Ivuna (Tanzania)	1938
СМ	Mighei (Ukraine)	1889
CV	Vigarano (Italy)	1910
СО	Ornans (France)	1868
CR	Ranazzo (Italy)	1824
CK	Karoonda (Australia)	1930
СН	ALH85085 (Antartica)	1985

#### 1.5.2.3. Cometary Dust

The sources of interplanetary dust particles (IDPs) include asteroids, comets, planetary rings, and interstellar space. Comets are composed of ices, gases and dust, and they are considered to be the most important sources of IDPs. The comets near perihelion inject several thousands kilograms of dust per second with sizes ranging from 1 to 100 µm (Llorca, 2005). Halleys's comet released about 3,000 kg of dust per second into the interplanetary medium (McDonnell et al., 1986).

A proportion of cometary IDPs is expected to vaporise under radiation of the Sun but the remainder blown out of the Solar System as a result of the radiation pressure that exceeds gravity (Llorca, 2005). These IDPs enter the Earth's atmostphere at high velocities in excess of about 11 km/s but decelerate when coming down to an altitude of 80 km before reaching the stratosphere (Sandford, 1987). The samples collected in the stratosphere have been found to contain extraterrestrial materials which include organic molecules and microorganisms amongst many other compounds such as minerals and gases (Schramm et al., 1989). The organic matter is rich in C,H,O and N elements and the average carbon content of IDPs has been found to be 10-12 % (Schramm et al., 1989; Thomas et al., 1993) which is about 2.5-3 times the carbon in the primitive meterorites (Llorca, 2005). However, the precise nature of the organic component in comets remains unknown.

Furthermore, it is interesting to note that the comet Halley shows a mixture of bright and dark materials and that the bright area contains ices whereas the dark part consists of mineral and organic components (Huebner, 1990) and most of which are aromatic and aliphatic hydrocarbons (Llorca, 2004). The comet Pholus contains a complex of carbon compounds as shown by its spectra (Cruikshank et al., 1998), red colour (Llorca, 2005) and the presence of hydrocarbons along with H<sub>2</sub>O ice on the surface (Llorca, 2005). Allamandola et al. (1988) and McDonald et al. (1996) reported that laboratory irradiation of ice similar to comet produced a number of organic compounds. As they observed, the formation of complex organic molecules took place as soon as the ices were warmed up and this organic complex included alcohols, amides, amines, ketones and nitriles.

According to Oro et al. (1992), the fall of meteorites, comets and interplanetary dust into the Earth's atmosphere is about 10<sup>5</sup> kg/day. Some of the organic material in this dust can survive temperature up to 577 °C for 1 second and an IDP particle is subjected to the temperature around -173 °C only a few seconds on entering the Earth's atmosphere (Chyba et al., 1990). The Earth was seeded with more than 10<sup>12</sup> kg of IDPs in the form of fine dust during the first 0.5 millions years (Delsemme, 1984; Oro et al., 1992).

#### 1.5.2.4. Stratospheric Particles

Dust swirled about in space for millions years and contaminated planetary objects. The Earth's atmosphere is thought by some to have been contaminated with cometary materials and other space debris. A proportion of dust particles are expected to melt and evaporate, but the rest should fall gently to Earth under gravity over time.

A number of papers reported that in addition to dust particles, microorganisms were also found in the samples collected from stratosphere (Wainwright et al., 2003; Wickramasinghe, 2004b). The findings have prompted a series of questions which remain to be answered such as: (i) Do microorganisms exist in the stratosphere? (ii) Can they survive at high altitude and (iii) Are they extra-terrestrial? To answer these questions, a team of scientists in India worked in collaboration with those in the United Kingdom on a project to collect stratospheric samples at different altitudes, 20-

41 km, using balloon-borne sterile "cryosamplers" (Wainwright et al., 2003; Wickramasinghe, 2004b).

Their preliminary study confirmed the presence of viable bacteria in air samples collected at an altitude as high as 41km. Furthermore, Wainwright et al. (2003) identified a fungus (*Engyodontium album*) and two types of bacteria (*Bacillus simplex* and *Staphylococcus pasteuri*) in one of the samples collected at this altitude. As reported by these scientists, the isolated organisms were very similar to known terrestrial species. However, they noted that there were remarkable differences in their properties, thus possibly pointing to a different origin.

The state of Kerala in India received red rain over several months from 25<sup>th</sup> July in 2001 (Louis and Kumar, 2003). This phenomenon was treated as an extraordinary event since the coloured rain water fell in various places spreading over hundreds of kilometres within a state and contained several tons of particles. Most of these particles appeared red. There were some cases where the rain also showed yellow colouration. Much attention has since been focussed as to the sources of these particles and the question is asked as to whether such a quantity of particles can be transported upward to reach the altitude of the rain clouds. Sampath et al. (2001) claimed that the red rain particles were fungal spores from trees.

As proposed by Satyanarayana et al. (2004) desert storm activity in the West Asian countries may be the contributory factor. It has been even suggested that the red rain could have been a splash of blood cells caused by a meteor hitting a flock of bats while flying in the sky (Reed, 2006) or even fungal spores (Sampath et al., 2001). However, based on the results of their investigation, Louis and Kumar (2006) proposed that the red particles might be the fragments of a cometary meteor. The UV absorption spectra of the non-diluted red rain reveal two significant peaks, a major at 505 nm and a minor at 600 nm whereas the UV-visible absorption spectra of the diluted rain water show a strong peak at 200 nm (Louis and Kumar, 2006). This absorption feature at 200 nm is close to that of the interstellar extinction at 217.5 nm. So far, there has been no additional reports to support these findings.

# 1.6. Hypotheses of Panspermia

The theory of panspermia posits that living organisms can exist and develop in the Universe where the environment is favourable (Thomson, 1871). This theory suggests that life exists, first in an extraterrestrial place and subsequently migrates to Earth where it developes. A more clearly defined theory of Panspermia was introduced by Arrhenius (1908) who proposed the following: that germs would have ejected from planets outside the solar system and would have been scattered in the galaxy where carried by the radiation pressure of stars, they would finally have encountered and infected our planet.

The theories of panspermia were born during the 19<sup>th</sup> century, but its meaning has only changed in the middle of the last century (Raulin-Cerceau et al., 1998). A variation of Arrhenius theory was presented in the 1950s by Otto Struve who suggested that life may be carried from planet to planet by intelligent intervention (Raulin-Cerceau, 1998). This proposal was followed in subsequent years by other hypotheses, one of which speculated that life arose on Earth because some extraterrestrial organisms were deliberately transmitted to Earth by intelligent beings on another (extra-solar) planet in order to develop life on Earth (Crick and Orgel, 1973). Hoyle and Wickramasinghe (1979) proposed a more convincing idea that bacteria carried by comets came from space and seeded the Earth.

The modern concept of panspermia associates the origin of life on Earth with organic materials (including seeds and microorganisms) in space, and has been described by many contemporary researchers including Hoyle and Wickramasinghe (1991), and Rothschild and Mancinelli (2001). The organic compounds found in the Murchison meteorite have been shown to be of non-terrestrial origin (Martins et al., 2008), and the discovery suggests that they may come from outer space.

The suggested mechanisms for panspermia include radiation pressure (Arrhenius, 1903; Hoyle and Wickramasinghe, 1991), lithopanspermia or microorganisms transported in rocks (Melosh, 1988) and directed panspermia from an intelligent

source in space to seed Earth (Crick and Orgel, 1973), or from Earth to seed other solar planet (Mautner, 1997).

Cockell (2008) has posed the question of whether planets and the solar system are bio-geographical islands or whether they can exchange biological materials. We know that on Earth, microorganisms can be dispersed from one region of a continent to another and they can also be dispersed from one continent to another. So far, no evidence has been provided that this kind of regional distribution occurred between planets within the Solar System. As Cockell (2001) has suggested, for an organism to be transferred from one planet to another, it must survive several dispersal filters in the following order:

- (i) the ejection of organisms from a planetary surface (as a result of an asteroid or comet collision) involves extreme physical forces (acceleration, shock and high temperatures), which the organisms must first survive.
- (ii) following the transit through the atmosphere, the organisms must survive the interplanetary transport or interstellar transfer, during which they are subjected to extreme environments such as long-time dessication, low temperatures and stellar radiation.
- (iii) organisms must also survive on entering the atmosphere of the host planet and be able to thrive under the new physical and chemical conditions offered by the host planet .

A lingering question is whether life-forms do really exist in planets beyond Earth or whether it is worth considering the possibility of panspermia (the transport of life from one planet to another). Since the theory of panspermia was proposed, it has been the highly debated issue. After many decades of scientific studies about extraterrestrial life, the question still remains unanswered today of how the first living creatures came to existence. Interplanetary transfer of material is well documented, as evidenced by images taken by spacecraft and meteorites of Martian origin found on Earth. However, claim that these meteorites carry evidence of extraterrestrial microorganisms or even viable dormant life-forms, is hotly disputed.

Critics of panspermia have argued that living organisms cannot survive long in space due to extreme environmental conditions. The critics argue that most damage to living microorganisms exposed to space is due to UV radiation. Dose et al. (1995) reported that the organism (*Deinococcus radiodurans*) did not survive 7 months in space and its DNA had extensive breakage. Furthermore, Nicholson et al. (2000) pointed out that *Bacillus subtilis* spores in a monolayer are killed within minutes of being exposed to the UV radiation.

The counter-argument to the above critics has been presented in recent years by a series of space experiments and calculations (Wickramasinghe et al., 2010). The findings suggest that terrestrial organisms could withstand UV radiation in space if they are protected by a thin layer of carbon. Nicholson et al., (2000) reported that *Bacillus subtilis* spores in a multilayer or mixed with glucose, can survive for years in space and that this evidence was provided by the Long Duration Exposure Facility and BioPan space experiments. Moreover, Mancinelli and Klovstad (2000) also confirmed that *Bacillus subtilis* spores in a monolayer shielded by a dust layer of 10 µm thick, can survive for weeks and probably years when exposed to a simulated martian UV-radiation flux.

#### 1.7. Interstellar Dust Models

# 1.7.1. Interstellar Spectral Observations

Interstellar dust is now known to play an important role in astronomy (Wickramasinghe, 1967). In galaxies, the dust absorbs energy from starlight. This energy is re-radiated at infrared (IR) and far-infrared (FIR) wavelengths. Spectroscopic absorption features allow the identification of specific components of grains, some of which features are observed in the diffuse interstellar medium (ISM). The Unidentified Infrared Bands UIBs are the prominent features in the diffuse ISM (Onaka et al., 1996) and their principal emission is centered at 3.3, 6.2, 7.7, 8.6 and 11.3 μm wavelengths (Hennings et al., 1998; Ehrenfreund et al., 2002; Reynaud et al., 2001; Cataldo et al., 2004). Other spectral observations include the infrared interstellar absorption bands at 9.7 μm and 18 μm with the Si-O stretch and Si-O-Si

bending modes in amorphous silicates and the attribution of the infrared interstellar absorption feature at  $3.4 \mu m$  to CH stretch transition in aliphatic hydrocarbon solids (Witt, 1999).

An interstellar absorption band centred at 217.5 nm (2175 Å) with a half-width at full maximum of ~ 25 nm (250 Å) in the range of UV-visible wavelengths was also discovered in the spectra of most reddened stars (Stecher, 1965; Wickramasinghe, 1967; Fitzpatrick and Massa, 1990; Bradley, 2005). This feature was first detected by the Aerobee rocket observations (Stecher, 1965; Wang et al., 2004), and later observed by the International Ultraviolet Explorer (IUE) satellite (Stecher, 1969). Several studies have demonstrated that the 217.5 nm extinction feature is associated with the presence of biomaterials in space such as microroganisms (Hoyle et al., 1985; Yahushita et al., 1986), polycyclic aromatic hydrocarbons, PAHs (Duley and Seahra, 1999; Muthumaraippan et al., 2008), coal (Papoular et al., 1996; Li and Greenberg, 2003), quenched carbon composite (Li and Greenberg, 2003) and hydrogenated amorphous carbon (Mennella et al., 1996). However, the exact carrier responsible for this feature is still controversial.

Interstellar Emission Features have also been detected in the interstellar gains in the form of Extended Red Emission (ERE). The intense ERE was detected in the diffuse ISM of the Milky Way Galaxy (Gordon et al., 1998; Szomoru and Guhathakurta, 1998a), in the reflection nebulae (eg. the Red Rectangle) (Schmidt et al., 1980), in planetary nebulae and in external galaxies (Szomoru and Guhathakurta, 1998a; Gordon et al., 1998). The ERE consists of an emission extending from 550 nm to 900 nm with a peak near 660 nm. The analysis of spectral properties of dust allows the determination of the composition of dust, size distribution of particles, the intrinsic luminosity of stars and the total mass of dust (Draine and Li, 2007). For laboratory study of interstellar grains, dust models with acceptable properties should be generated. The search for such models has progressed significantly in the last decade. A comprehensive model for interstellar grains should provide detailed information on the following characteristics that are fully consistent with those of interstellar environments: composition, size distribution, optical properties, physical structure and shape, extinction, scattering, polarization and emission properties, spectroscopic absorption and emission features, and the abundances of refractory elements in the

interstellar medium (ISM) and their observed depletion patterns (Hoyle and Wickramasinghe, 1990; Witt, 1999).

#### 1.7.2. Proposed Models

A number of terrestrial models have been proposed in early studies to mimic extraterrestrial objects, some of which are briefly described as follows:

#### • The Silicate-Graphite Model

Hoyle and Wickramasinghe (1969) first proposed a grain model involving a mixture of graphite and silicate grains. The same model was developed further by Mathis et al. (1977) and Draine and Lee (1984). This model consists of two separate types of spherical particles, graphite and silicate. The two species form in two different types of basic chemical environments. In one case, all available C atoms make CO, and the available excess O-atoms form silicates and metal oxides. In the other case, all O-atoms make up CO and the free C-atoms form graphite and carbonaceous molecules. Attempts have been made by Draine and Lee (1984) and Draine and Anderson (1985) to refine the silicate graphite model. These include adoption of better optical constants for 'astronomical silicates' and 'astronomical graphites' to provide a better fit to the interstellar curve. However, since there is no terrestrial material that matches the requirements for either, this procedure is arbitrary and highly suspect (Hoyle and Wickramasinghe, 1990). Ad hoc adjustments also add a population of nanoparticles ranging from 0.3 nm to 5 nm to ensure that the near IR-continum emissions as well as that of UIBs are included.

#### • Silicate Core-Carbonaceous Mantle Model

A model known as Core-Mantle Model has been proposed by Wickramasinghe (1967) and Greenberg and his colleagues (Greenberg and Hong, 1974; Hong and Greenburg, 1980; Li and Greenberg, 1997). This model is based on the concept that the bulk of the carbonaceous material in the ISM is in the form of an organic refractory residue, which formed a mantle on the surface of silicate grains. This model was later

modified to include polycyclic aromatic hydrocarbon, PAH, known as the silicate-graphite-PAH model (Siebenmorgen and Krugel, 1992; Li and Draine, 2001b; Weingartner and Draine, 2001a).

The model thus includes large core-mantle grains containing most of the mass, small grains of carbonaceous graphite having the 2175 Å feature, and a population of PAH molecules that give rise to the far -UV extinction and is also the source for the emission of UIBs. Although this model can be made to match the infrared spectrum of dust emission, it also has the following drawbacks: (i) the population of small carbonaceous grains is poorly characterised; and (ii) it shows no polarisation in the 3.4 µm C-H aliphatic hydrocarbon feature on the sight line of sources, where the 9.7 µm Si-O silicate band is reported to be polarised (Adamson et al., 1999; Li and Greenberg, 2002; Chiar et al., 2006).

#### The composite model

This model was originally proposed by Mathis and Whiffen, (1989). It considers the dust to be low density aggregates of small silicate and carbonaceous particles (Mathis, 1996; Zubko et al., 2004). This model either produces a FIR emission that is too flat (Draine, 1994) or emits too much the FIR (Dwek, 1997) as compared to astronomical data.

#### • The Post-IRAS Model

Desert et al. (1990) proposed a dust model which takes into account three populations of grains of different sizes: big grains (110-15 nm), small (15-1.2 nm) and PAHs (1.2-0.4 nm). Witt (1999) claimed that although this model correctly predicts the UIB emission, it may be insufficient to explain the observations of interstellar polarisation and near-IR scattering. It is also inconsistent with the population of interstellar grains found within the solar system.

#### • Organic- Biological Model

Hoyle and Wickramasinghe (1982) have established an organic model for the interpretation of interstellar extinction, which consists of three main components: graphite spheres (20 nm radius), small dielectric spheres (40 nm radius) and hollow dielectric cylinders (0.66 nm diameter). Based on the analysis of the interstellar extinction, they further proposed that the dielectric grains are mainly composed of organic material. On the other hand, Jabir et al. (1983) have proposed a three component grain model made up of bacterial grains in the form of long hollow needles, graphite spheres (20 nm radius) and dielectric spheres (40 nm radius). This model is found to correlate well with the observed features of interstellar dust.

Al-Mufti (1985) reported that the organic and biological models which include microorganisms such as *E. coli*, diatoms, yeast, and blue-green algae were found to produce infrared spectra that could match the astronomical observations over a wide range of wavelengths regardless of size and shape. He further confirmed that a good agreement was obtained between the spectra of a mixed culture of diatoms and the emission spectra of the Trapezium Nebula.

#### 1.7.3. Carriers of Interstellar Bands

#### • Polycyclic Aromatic Hydrocarbons (PAHs)

PAHs are important constituents of the interstellar medium (ISM), and show absorption features in stellar spectra. They have been proposed as the possible carriers of the diffuse interstellar bands (DIBs) and hundreds of other absorption bands in the optical and near–infrared spectra of stars reddened by interstellar material (Crawford et al., 1985; Puget and Leger, 1989).

PAHs are also the postulated carriers of the mid-infrared emission features observed in the interstellar medium (Puget and Leger, 1989; Allamandola et al., 1985, 1989), and of a diffuse IR emission detected at high Galactic latitude (Watson et al., 2005; Hildebrandt et al., 2007). Furthermore, PAHs are considered good candidates for

carriers of the unidentified Infrared bands (UIBs) because of their spectroscopic properties and their stability against photodissociation in strong UV fields (Le Page et al., 1999). PAH exhibit particularly strong absorption in the UV (Witt, 1999).

#### Naphthalene

Naphthalene is generally thought to be the simplest PAH; it has been detected in meteorites (Watson et al., 2005), and has been reported to exhibit a UV spectral feature centred at 2175 Å (Beegle et al., 1997). Iglesias-Groth et al. (2008) performed high resolution optical spectroscopy of Cernis 52 (BD+31640), a reddened star located in a region of the Perseus molecular cloud; they have recorded a spectrum between 3800 Å and 10000 Å, which display features within the range of 5800-6800 Å. These features are thought to be of interstellar origin, with wavelengths and strengths consistent with those of naphthalene. On the basis of these observations, Iglesias-Groth et al. (2008) suggested that the simplest PAHs molecules are the carriers of diffuse interstellar bands and diffuse IR emission in particular.

#### Anthracite

According to Popular et al. (1993), coal can be used as a model for carbonaceous interstellar grains; they found that anthracite produced a feature that matches the interstellar extinction at 2175 Å. Coal is known to consist essentially of three abundant elements, C, H and O (1:0.5:0.02 atomic concentrations), and provides a class of natural models for the interstellar dust. Its main insoluble organic constituent, termed kerogen, exhibits all unidentified infrared bands (UIBs). The major elements, H, O and C, form hydrocarbon functional groups that are responsible for the vibration bands that mimic the UIBs. The study carried out by Popular et al. (1993) has demonstrated that coal is the carrier of  $\pi$  –resonance associated with the UV 2175 Å absorption band. As suggested by Cataldo et al. (2004), coal can be an interesting model for the carrier of the UIBs.

# 1.8. Aims and Objectives of Study

As suggested by Javaux (2006), astrobiology involves multidisciplinary fields of study, namely astronomy, astrophysics, biochemistry, chemistry, geology, microbiology, molecular biology, ecology of extremophiles, palaeontology, and space exploration. The explosion in the 20<sup>th</sup> century of research interests in such diverse areas has brought to light some questions and consolidated some hypotheses of panspermia. However, some basic issues still remain unresolved, such as whether life is an extension of complex organic chemical evolution or whether there is a discontinuity, for instance from chemical to biological, in the type of evolution.

The discovery of many organic molecules in interstellar and planetary environments has at least provided some proof of a universal organic or biological chemistry. Examples of such chemistry in the early solar system have been found in the carbonaceous meteorites. Their organic material is composed of biogenic elements such as carbon, hydrogen, nitrogen and oxygen, and these elements have a long cosmic history (Pizzarello, 2006). The complex organic molecules found in astrophysical sources were probably formed in diverse environments from gas and dust of the interstellar clouds to small solar system bodies (Wood and Chang, 1985). Since the last century, much information about the organic chemistry of the Universe has been obtained from the analyses of extraterrestrial materials, space missions and astronomical observations. As pointed out by Wickramasinghe (2010) a large fraction of the molecules found in interstellar clouds may represent degradation products of biology, rather than as steps towards biology. The former possibility links up with the theory of panspermia (Hoyle and Wickramasinghe, 2000).

The focal point of the present study involves laboratory analyses of samples collected from various locations on Earth and at high altitudes. The aim of the laboratory work is to search for bio-signatures (if any) in these samples, which may have a bearing on the origin of life on Earth or to its transport from elsewhere.

The specific aims and objectives of the investigation are as follows:

- To analyse the following biological materials by Fourier transform infrared spectroscopy: algae (*Oedogonium sp.*), two bacteria (*B. cereus*, *S. aoureus*), poppy seed, biological pigments (chlorophyll a & b), three species of seaweed (*Enteromopha intestinalis*, *Pelvetia canaliculata* and *Fucus vesiculosus*) and grass (*Panicum maximum*). The result of the analysis will be compared with those astronomical observations reported in earlier studies. The comparison may reveal some characteristics of the biological materials having a significant number of spectral features that match those of astronomical objects. The findings may form a basis for proposing the potential choice for the study of interstellar medium (Chapter 3).
- To determine the infrared absorption spectra of graphite, anthracite, bituminous coal and naphthalene by FTIR. The resulting spectra will be analysed to see if they show any correlation with those astronomical observations, in particular UIBs and PPNe (Chapter 4).
- To determine by UV-Vis spectroscopy whether any of the following laboratory models produces a feature that perfectly fits the interstellar extinction observation of 217.5 nm (2175Å). The result could give an insight into the absorption properties and hence into the nature of their degradation from the astrobiological perspective (Chapter 5).
- To investigate whether there are traces of organic materials and or microfossils in two meteorites (Tagish Lake, Chapter 6 and Canrancas, Chapter 7) using electron microscopy, X-ray nanoprobe analysis and infrared spectroscopy.
- To examine the astrobiological aspects of a Kerala red rain sample supplied by Prof. Godfrey Louis (Kerala, India) using electron microscopy, X-ray nanoprobe analysis and FTIR, fluorescence and UV-Vis spectroscopy (Chapter 8).
- To identify the nature of aerosols in stratospheric air samples collected from a balloon flight at altitudes between 38 and 41 km. This study is intended to confirm

whether the samples are organic in nature and or there is any presence of microorganisms (Chapter 9).

The results obtained from this investigation would provide evidence to support the theory of panspermia, which proposes that life is a cosmic phenomenon, and that life on earth comes from a vast cosmic environment (Hoyle and Wickramasinghe, 2000).

# **CHAPTER 2**

# **General Materials and Methods**

## 2.1. Materials

The important instruments and materials used in the present study are described in this chapter. Details of other specific materials are appropriately given in the subsequent chapters of this thesis.

# 2.1.1. Major Laboratory Instruments

#### 2.1.1.1. KBr Die Assembly

This assembly unit is supplied by SPECAC Ltd., Kent, UK. Its use is to embed a sample of interest into dried KBr powder under a high vacuum and a pressure of about 10 tons cm<sup>-2</sup> to form a light-transmitted thin disc for use in conjunction with an infrared spectrometer.



Fig.2.1: KBr die assembly. (1) Hydraulic press consisting of a chamber (a) where sample is placed, a pressure lever (b) and a pressure gauge (c). (2) Grinding and blending mill for crushing sample. (3) Evaccuable pellet Dies where the sample is sandwiched between the two metal discs.

#### 2.1.1.2. Fourier Transform Infrared Spectrometer

The present study uses a Fourier Transform Infrared Spectrometer (JASCO Model FT/IR-660 Plus series) to analyse KBr embedded samples. This spectrometer is designed to allow the IR light to be guided through an interferometer. The FTIR spectrometer allows multiple samples to be measured and averaged together, thus resulting in an improvement in sensitivity. Due to this advantage, almost all infrared spectrometers used nowadays are FTIR instruments.

The model is supplied by JASCO Ltd. with the following specifications:

- Measurement of wavenumber range: 7800 to 350 cm<sup>-1</sup>
- Resolution: 0.5, 1, 2, 4, 8, 16 cm<sup>-1</sup>
- Optical system: Single beam
- Sample chamber: 200mm (W) x 260mm (D) x 185mm (H)
- Sample chamber light path:

Centre focus, light axis 70mm high 28° incident

Michelson interferometer

- Light source: Ceramic. [Optional] Halogen lamp, water-cooled mercury light source.
- Signal to noise ratio: 25,000:1 (4cm<sup>-1</sup> at near 2,200cm<sup>-1</sup>)
- Gain switching: Auto.

#### 2.1.1.3. Ultraviolet-Visible Absorption Spectrometer

The basic parts of this instrument include a light source, a sample holder, a diffraction grating or monochromator and a detector. The radiation source (300-2500 nm) is a filament made of tungsten, a deuterium arc lamp light emitting diodes (LED) and Xenon Arc Lamps for the visible wavelengths. The detector is a photodiode which is used with monochromators to filter the light. The diffraction gratings are used to collect light of different wavelengths on different pixels. The model of UV–Vis absorption spectrometer used in the present study is JASCO V-570 UV/VIS/NIR spectrophotometer with the following specifications:

- Optical system: Double beam system with single monochromator
   UV/VIS region: 1200 lines/mm plane grating.
- Resolution: 0.5 nm (UV/VIS region)
- Light source: Deuterium lamp: 190 to 350 nm
   Halogen lamp: 300 to 2500 nm
- Wavelength accuracy: ±1.5nm
- Spectral band width: 0.4, 0.8, 2, 4, 8, 20, 40 nm
   L8, L20 and L40 nm (with half slit height).

#### 2.1.1.4. Microscopes and Ancillary Equipment

The following microscopes and ancillary equipment are used.

#### 2.1.1.4.1. Light Microscope

The light microscope used in the present study is Olympus BH2 fitted with four objective lenses (10x, 20x, 40x, 100x) and 10x eyepiece.

#### 2.1.1.4.2. Transmission Electron Microscope

The transmission electron microscope used in the present study is Philips TEM 208 (FEI Co. Ltd, The Netherlands). This is a basic high contrast electron microscope that can be operated at a maximum accelerating voltage of 100 kV and at a maximum magnification of 180,000 x. The imaging system is fitted with a series of magnetic coils that function as lenses (2 condensers for electron beam focusing and illumination, 1 twin objective for image formation and 2 projectors for image magnification). The electron images are viewed on a fluorescent screen and photographed on Kodak 4489 cut film. The present study used an accelerating voltage of 80 kV and magnifications ranging from 5,000x to 50,000x.

#### 2.1.1.4.3. Scanning Electron Microscope

The present investigation used a Philips XL 20 SEM (FEI Co. Ltd, The Netherlands) to examine the surface structure of samples of interest. It can be operated at different accelerating voltages (5-30 kV) and with magnifications ranging from 20 x to 200 000 x. This SEM is fitted with a series of magnetic condenser lenses and a pair of deflecting coils. These coils focus the electron beam to a small spot of about 0.4 nm to 5 nm, which is scanned in a raster fashion over the sample surface. A detector collects secondary electrons that are emitted by inelastic scattering as a result of the interaction between the incident electrons and sample. These secondary signals are electronically filtered by an amplifier to produce a 3D-image of the sample. The image is then digitally captured on a high resolution cathode ray tube, and displayed on a computer monitor screen. The image can be either stored on the SEM hard drive and a zip drive for future scanning on a CD or memory stick or photographed directly onto a roll film for further processing. This SEM requires that biological samples must be fixed in aldehydes, dehydrated and gold coated prior to examination.

#### 2.1.1.4.4. Environmental Scanning Electron Microscope

The environmental scanning electron microscope used in the present study, is Philips ESEM-30XL- FEG (FEI Co. Ltd., The Netherlands). It allows samples to be observed in low-vacuum and high humidity. The system is fitted with apertures that can limit pressure under differential pumping. This design allows the vacuum to be separated around the gun and lenses from the sample chamber. The ESEM is especially useful for routine examination of unfixed and uncoated biological samples. This has several advantages over a conventional SEM since coating may conceal small features on the surface of the sample and therefore reduce the image resolution. Unlike the conventional SEM, the ESEM allows X-ray microanalysis be performed on uncoated non-conductive specimens. In brief, the ESEM is a new innovation in scanning microscopy since it is specifically designed to study wet and fresh samples without prior specimen preparation or gold coating. Samples can also be examined in water vapour or other gasses such as CO<sub>2</sub> or N<sub>2</sub> at near atmospheric pressures.

#### 2.1.1.4.5. Energy Dispersive Analyser of X-rays (EDAX)

The EDAX systems used in the present study include: EDAX/Genesis fitted into Philips CM12 transmission electron microscope and Oxford INCA Energy EDS into ESEM -3-XL 30 FEI scanning electron microscope. These analytical systems are used specifically for the identification and quantitative analysis of chemical elements; both of them consist of four primary components: beam source, X-ray detector, pulse processor and analyser.

#### 2.1.2. Chemicals

All chemicals used in this study were purchased from Sigma-Aldrich Ltd., unless otherwise stated.

#### 2.1.2.1. KBr for Infrared Spectroscopy

Potassium bromide (KBr) is available as a white crystalline powder. It is an ionic salt readily soluble in water. The physico-chemical properties of KBr are summarised in Table 2.1.

Table 2.1: Pysico-chemical properties of KBr

Chemical formular	KBr
Molar mass	119.01 g/mol
Appearance	white solid
Density	2.75g/cm <sup>3</sup>
Melting point	734 °C
Boiling point	1435 °C
Solubility	53.5 g/100 ml (0 °C) in water

#### 2.1.2.2. Cyclohexane for Ultraviolet -Visible Spectrophotometry

Cyclohexane  $(C_6H_{12})$  is a colorless nonpolar solvent with a mild, sweet odor resembling that of chloroform or benzene. The use of a non-polar solvent eliminates the effect of wavelength-shifts. Due to its unique chemical and conformational properties, cyclohexane is also used in laboratories as a standard for biochemical analysis.

Table 2.2: Physico-chemical properties of cyclohexane

Chemical formula	$C_6H_{12}$
Molar Mass	84.16 g/mol
Appearance	colorless clear liquid
Density	0.779 g/cm <sup>3</sup>
Melting point	6.47 °C
Boiling point	80.7 °C
Solubility	Insoluble in water

#### 2.1.2.3. Chemicals for Electron Microscopy

All chemicals used for electron microscopy in the present study are obtained from Agar Scientific Ltd. (Stansted, Essex, UK).

#### Glutaraldehyde (C<sub>5</sub>H<sub>8</sub>O<sub>2</sub>)

Glutaraldehyde has a strong and irritable odor. Commercially supplied in liquid form, it has been used for sterilisation of medical and dental equipment as well as for industrial water treatment. Glutaraldehyde is also used in biochemistry as an amine-reactive homo-bifunctional crosslinker. It was later found to be an effective primary fixative in biological electron microscopy applications since it proved to have the ability to cross-link cellular proteins, hence preserving fine structure of cell membranes. The chemical properties of glutaraldehyde are summarised in Table 2.3.

Table 2.3: Physico-chemical properties of glutaraldehyde

Chemical formula	$C_5H_8O_2$
Molar mass	100.12 g/mol
Appearance	Clear liquid
Density	1.06 g/mL
Melting point	-14 °C (259 K, 7 °F)
Boiling point	187 °C( 460 K, 369 °F)
Solubility	Miscible in water

#### • Osmium tetroxide (OsO<sub>4</sub>)

Osmium tetroxide is a crystalline solid with light yellow-brown colouration. Its vapour is highly toxic and has a characteristic acrid odor. In solution, osmium tetroxide appears clear, but can turn yellow or brown when osmium dioxide (OsO<sub>2</sub>) impurities are present. In electron micoscopy, OsO<sub>4</sub> is widely used as a post-fixative after glutaraldehyde fixation. It is used to fix lipids as well as to stain cell membranes.

Table 2.4: Physico-chemical properties of osmium tetroxide

Chemical formula	$O_8O_4$
Molar mass	254.23 g/mol
Appearance	clear or pale yellow translucent solid
Density	4.9 g/cm³ (solid)
Melting point	40.25 °C
Boiling point	130 °C

#### 2.2. Methods

# 2.2.1. Infrared Spectroscopy

# 2.2.1.1. Principles of Infrared Spectroscopy

Infrared (IR) spectroscopy is an important tool in organic chemistry. It measures different types of inter-atomic bond vibrations at different frequencies. The energy at which a typical molecule absorbs infrared radiation is shown in Fig. 2.2. The IR absorption is represented in the form of a spectrum with wavelength ( $\lambda$ ) or wavenumber ( $\nu$ ) as the x-axis and percent transmittance or absorption intensity as the y-axis. The wave-numbers can be converted into wavelengths by using the equation,  $\nu=1/\lambda$ . By definition, the wave numbers (cm<sup>-1</sup>) represent the number of waves per unit length; they are proportional to frequencies and also the energy of IR absorption. On the other hand, the wavelengths ( $\mu$ m) are inversely proportional to frequencies and their relevant energy. The IR absorption spectra show types of bonds that are present in the sample. The data also provide information on the structure and identity of compound and its purity. An IR spectrum can be considered either as a property of the molecule as a whole or as a composite of individual absorptions from various components of the molecule.

The IR spectra of organic compounds have two different characteristics: the vibration modes with single bonds, and those of a functional group (with multiple bonds). This distinction divides the spectrum into two regions. The first region is above 1500cm<sup>-1</sup> where the majority of absorptions are caused by stretching mode of multiple bonds (C=C, C=C, C=O, C=N, C=N). The second is below 1500 cm<sup>-1</sup> where absorptions are caused by C-X single bond stretching modes as well as other vibration mode. Since absorptions that are due to CH stretches, are also found around 3000 cm<sup>-1</sup> (as shown in Table 2.6), these distinctions are therefore not always absolute.

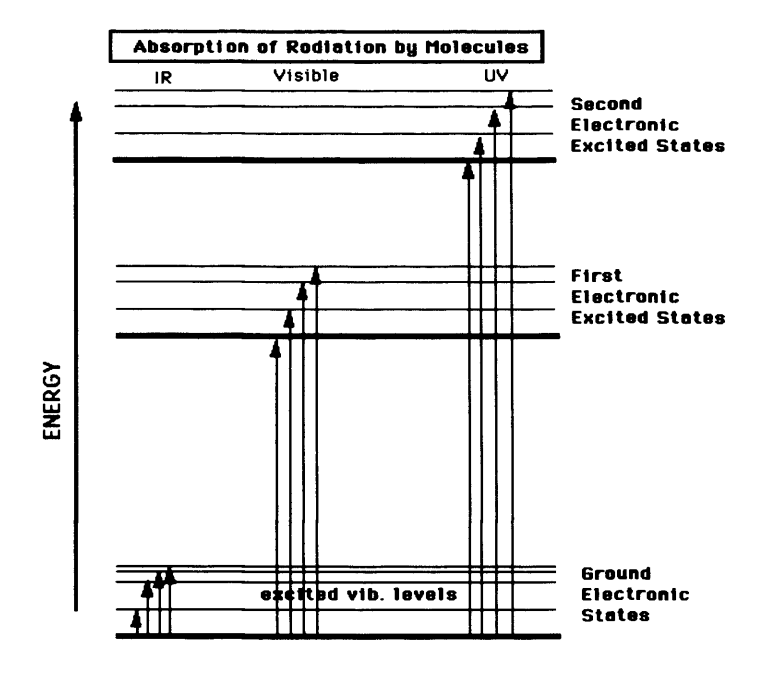


Fig. 2.2: Absorption of radiation by molecules (adapted from Housecroft and Constable, 2002). Most molecules are in the ground state whereas a small number of molecules are in the higher states. In IR spectroscopy, the IR radiation excites the molecule from the ground state to the first excited quantum state. The motion in a particular group can cause vibration in a molecule. However, not every vibration within a molecule causes an absorption band in the infrared region.

Table 2.6: Approximate ranges of stretching frequencies of O-H, N-H, S-H and C-H bonds (taken from Housecroft and Constable, 2002)

Group	Typical frequency ranges of absorption
	bands (cm <sup>-1</sup> )
О-Н	3600-3200 (broadened by hydrogen
	bonding)
N-H	3500-3300
S-H	2600-2350 (weak absorption)
C-H (sp <sup>3</sup> carbon)	2950-2850
C-H (sp² carbon)	3100-3010
C-H (sp carbon)	≈3300

#### 2.2.1.2. Sample preparation for FTIR

In order to run the FITR spectrometer, the sample must be embedded in a KBr disc according to the following protocol:

- 1. Transfer sample (approx. 0.5 mg) and dried KBr powder (approx. 20 mg of spectroscopic grade purity) into an agate mortar.
- 2. Grind the mixture in the mortar using an agate pestle until a fine powder is obtained.
- 3. Transfer the mixture into a small grinding and blending mill (SPECAmill <sup>TM</sup>, Kent, UK).
- 4. Allow the mixture to vibrate in the mill vigorously with 3 spheres inside the sample capsule for 10 mins.
- 5. Dry the sample in a high vaccum unit (Edward 360, Stansted, UK) for 3-4 hours.
- 6. Transfer the ground mixture into the Evacuable Pellet Dies (SPECAC Ltd, Kent, UK). This is done carefully in such a way that the sample is sandwiched between the polished faces of the two die disc (13mm diameter).
- 7. Carefully insert the plunger.
- 8. Transfer the die assembly into a hydraulic press.
- 9. Connect to a High Vacuum pump.
- 10. Gradually increase pressure up to 10 tons cm<sup>-2</sup>.
- 11. Slowly release the pressure after several seconds.
- 12. Carefully release the vacuum pressure.

- 13. Remove the die from the press.
- 14. Carefully dismantle the die to retrieve the sample.
- 15. Transfer the KBr disk to a spectrometer disk holder without touching the faces of the disk.

# 2.2.2. Ultraviolet-Visible (UV-Vis) Absorption Spectroscopy

#### 2.2.2.1. Principles of UV-Vis Absorption Spectroscopy

UV light is detected below the range visible to the human eye. It can be divided into four distinct spectral regions: Vacuum UV (100 to 200 nm), UV-C (200 to 280 nm), UV-B (280 to 315 nm), and UV-A (315 to 400 nm). It is noteworthy that the UV-C spectrum (200 to 280 nm) is the most harmful range of wavelengths for microorganisms. The UV/Vis spectrophotometer measures the intensity (I) of the transmitted light that passes through a sample, and compares it with that of incident light ( $I_0$ ). The transmittance (T) is the ratio of transmitted intensity (I) to the incident intensity ( $I_0$ ), and is expressed as percentage (%T). The UV-Visible absorption (A) is equal to  $-\log$  (%T/100). An absorption spectrum shows a number of absorption bands which correspond to structural groups within the molecule. The absorbance (A) is proportional to the path length (b), and the concentration (c) according to the following Beer's Law:  $A = \varepsilon bc$ , where ( $\varepsilon$ ) is a constant of proportionality.

Electrons of an atom become excited as a result of energy absorption. In a molecule, the atoms interact with each other by rotational and vibrational transitions. There are three types of electronic transitions: transitions involving  $\pi$ ,  $\sigma$ , and n electrons, transitions involving charge-transfer electrons, and transitions involving d and d electrons. The present study is concerned with the first type of transitions since it is related to organic molecules. These transitions are briefly described as follows:

#### Transitions involving $\pi$ , $\sigma$ , and n electrons

#### $\sigma \rightarrow \sigma^*$ Transitions

An electron in a bonding  $\sigma$  orbital can be excited to the anti-bonding orbital. This transition requires high energy. However, the spectra of typical UV-Vis (190 - 800 nm) does not show this transition ( $\sigma \to \sigma^*$ ) which is below this range.

#### $n \to \sigma^*$ Transitions

A non-bonding electron in 'n' orbital is excited to the anti-bonding orbital which requires less energy than  $\sigma \to \sigma^*$  transitions. It can be triggered by light of which the wavelength is between 150 - 250 nm.

#### $n \to \pi^*$ and $\pi \to \pi^*$ Transitions

An electron in a non-bonding orbital 'n' is excited to the corresponding anti-bonding orbital  $\pi^*$ . In the case of  $\pi \to \pi^*$  transitions, these are formed by the excitation of an electron from a bonding  $\pi$  orbital to the anti-bonding  $\pi^*$  orbital. The absorption peaks for these transitions can be generated within the spectral range of 200-700 nm. Therefore, absorption spectroscopy of organic compounds is mostly based on these transitions.

Furthermore, solvent also has an effect on the spectrum. By increasing the polarity of the solvent, the peaks shift to shorter wavelengths (blue shift) from the  $n \to \pi^*$  transitions. On the other hand, decreasing the solvent polarity often causes the peaks to shift to longer wavelengths (red shift) from  $\pi \to \pi^*$  transitions.

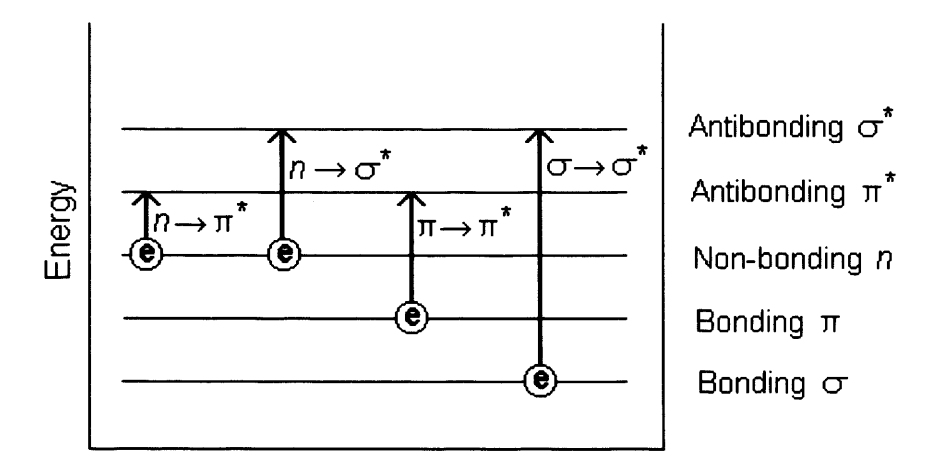


Fig. 2.3: Diagram showing possible electronic transitions of  $\pi$ ,  $\sigma$ , and n electrons

#### 2.2.2.2. Sample preparation for UV-Visible Spectroscopy

For use with UV-VIS spectroscopy, samples were dissolved in a solvent such as cyclohexane.

The sample (65 mg) was mixed with an appropriate solvent (500  $\mu$ l), agitated for a few minutes and allowed to stand still on the bench for 5 min to allow the sedimentation to settle. Clear solution (100  $\mu$ l) was carefully pipetted out from the top and placed in a test tube containing the solvent (3.5 ml). The tube was briefly agitated and transferred into a spectrophotometer (JASCO V-570 UV/VIS/NIR spectrophotometer).

# 2.2.3. Fluorescence Spectroscopy

#### 2.2.3.1. Principles of Fluorescence Spectroscopy

Fluorescence spectroscopy is commonly used in biochemistry and molecular biophysics. It involves transitions from the excited state to the ground state. At room temperature, the lowest level of vibration in the ground electronic state is occupied by most molecules. When energy is absorbed, these molecules are elevated to an excited state, and a series of absorption bands are produced. After reaching one of the high levels of the excited state, the molecule loses its energy through collision and then falls to the lowest level of the excited state. The molecules further lose their energy

until they reach the lowest level of vibration in the first excited state from which they can return to any of the levels of the ground state. This event leads to the emission of energy in the form of fluorescence.

#### 2.2.3.2. Sample Preparation for Fluorescence Spectroscopy

The method of preparation is exactly the same procedure as described in 2.2.2.2.

# 2.2.4. Microscopy Methods

# 2.2.4.1. Principles of Microscopy

Light microscope is used to examine an object of interest. Its optical components consist of a light bulb and a series of glass lenses that have the ability to illuminate the object and magnify its image. These lenses include a condenser, objectives of different magnifications and an eye piece of fixed magnification. Microscopes of today are now equipped with a digital camera to record images which are shown directly on a computer screen without the need for expensive eye-pieces. There are several types of light microscopes namely, brightfield, phase contrast, fluorescence, confocal scanning and polarization.

The resolving power of light microscope is limited by the physics of light to 1000 x magnification and 0.2 micrometer resolution. These limitations have prompted the development of an electron microscope. Transmission Electron Microscope (TEM) was first developed in 1931 to respond to this challenge. Scanning electron microscope (SEM) was first used in 1942. The Electron Microscope is one of the most advanced imaging instruments that use an accelerating voltage of high electron beam to resolve image of a very fine object to nanometer scales. The following information can be obtained from electron microscopy examination:

- The surface features of an object or topography and its texture
- The shape and size of the object or morphology
- The elements and compounds that make up the object or composition

An electron microscope operates very much like a light microscope except that the former is composed of magnetic coils that function as lenses. The light in the electron microscope is produced by a tungsten filament and focused into a narrow monochromatic beam by electromagnetism that is accelerated toward the specimen through metal apertures using a positive electrical potential. The sample-electron interactions produce electron signals which are then elastically transmitted in the case of transmission electron microscope (TEM) or back-scattered in the case of scanning electron microscope (SEM). Details of imaging and recording are described in the above sections: 2.1.1.4.1, 2.1.1.4.2 and 2.1.1.4.3.

#### 2.2.4.2. Sample preparation for Light Microscopy (LM)

Sample of interest is attached onto a microscope slide with a drop of either glycerol or balsam gum and protected with a coverslip. Subsequent microsopical observations were conducted using one of the appropriate light microscopes as described above in Section 2.1.1.4.

#### 2.2.4.3. Sample preparation for Transmission Electron Microscopy (TEM)

- 1. Fix samples for 1hr in glutaraldehyde (2.5 % in 0.1 M phosphate buffer, pH7.4).
- 2. Wash with 2 changes of 0.1 M phosphate buffer (2 x 10 min).
- 3. Post fix in 1 % osmium tetroxide for 1 hr at room temperature.
- 4. Dehydrate in a graded series of ethanol concentrations:

30%10min
50%10min
70%10min
80%10min
90%10min
100% RT 10min

- 6. Infiltrate overnight in a mixture (1:1v/v) of araldite (CY212) and propylene oxide.
- 7. Embed for 2 days at 60 °C in pure araldite.
- 8. Cut into 90 nm thick sections with a diamond knife using a Reichert E ultracut microtome (Reichert –Jung, Austria).
- 9. Collect thin sections on pioloform coated copper grids.
- 10. Counter-stain with 2 % uranyl acetate and Reynolds lead citrate.
- 11. Carry out observations using a Philips transmission electron microscope as described above in Section 2.1.1.4.

#### 2.2.4.4. Sample preparation for Scanning Electron Microscopy (SEM)

The samples are prepared using the same method as described above for TEM with some modifications. Following the complete dehydration in 100 % ethanol the samples are transferred into a critical point dryer (Samdri 780 CPD, Maryland, USA) and dried for 2 hrs under high vacuum (90 bars) using liquid CO<sub>2</sub>.

The CPD dried samples are mounted on metal stubs, coated with a thin layer of pure gold using a gold puttering coater (Emscope Sputter Coater, Model, Kent, UK) and examined using a scanning electron microscope as described above in Section 2.1.1.4.

# 2.2.5. Energy Dispersive Analysis of X-Rays (EDAX)

#### 2.2.5.1. Principles of EDAX

The EDAX system can be fitted into a transmission (TEM) or scanning (SEM) electron microscope. These electron microscopes are equipped with a cathode and magnetic lenses which allow a beam of electrons to be focused on the sample. The electron beam irradiates the sample, and as a result the photons are scattered elastically in TEM or inelastically in SEM. These photons are collected by a detector nearby and the signals are amplified by a pulse processor and converted into X-ray energy. The processor passes the information onto a computerised analyser for spectral display on a monitor screen and for data analysis.

As a type of spectroscopy, the system analyses X-rays which are produced by the interaction between electron radiation and sample. Its analytical capabilities are based on the fundamental principles that: (i) each element has a unique atomic structure; (ii) the X-rays are emitted from a specimen as a result of an electron beam being focused onto the sample; and its characteristic X-rays and energies can be specifically identified. The following events take place during X-ray excitation. In the absence of radiation, an atom in the sample rests in the ground or unexcited state and electrons in electron shells remain attached to the nucleus. When the incident electron beam hits the sample, it excites an electron in an inner shell of the atom, and the affected electron is ejected from the shell, thus leaving a hole. An electron from an outer, higher-energy shell then comes to fill the hole. This event leads to the emission of an X-ray photon.

Since the energy of the emitted X-rays is determined by the difference in energy between the two shells and the atomic structure of the element from which they are emitted, the elemental composition of the specimen and X-ray energy can be measured using an energy dispersive spectrometer. During the analysis, the electron beam should be focused onto the area of interest and the following parameters maintain constant throughout: electron beam size, accelerating voltage and analysis time.

#### 2.2.5.2. Protocols for the preparation of samples for EDAX

The following protocols are used in the present study:

- Red rain cells
- 1. Place sample on 0.4 µm millipore filter in plastic capsule.
- 2. Allow to air dry overnight.
- 3. Attach the millipore filter to metal stub with double-sided sticky tape.
- 4. Analyse sample using the Philips ESEM -XL30 fitted with an EDAX system.
- Meteorites
- 1. Embed several fragments of meteorite samples in LR White resin.
- 2. Polymerise the resin in gelatin capsule at 55 °C for 48 hours.
- 3. Cut the resin block into 90-100 µm sections.
- 4. Mount the sections on a pioloform-coated copper grid.
- 5. Analyse the samples using a Philips CM12 fitted with an EDAX Genesis system.

# **CHAPTER 3**

# Comparison of Infrared Spectra of Biological Models with those of Astronomical Sources

# 3.1. Summary

The present study sets out to determine whether biological materials of terrestrial origin can produce characteristic absorptions matching those of astronomical objects. The materials selected for analysis by Fourier Transform Infrared spectroscopy include: algae (*Oedogonium sp.*), two bacteria (*Bacillus cereus* and *Staphylococcus aureus*), poppy seed, two biological pigments (chlorophylls 'a' and 'b'), three species of seaweed (*Enteromopha intestinalis*, *Pelvetia canaliculata* and *Fucus vesiculosus*) and grass (*Panicum maximum*).

The results obtained from the analyses confirm that some of these biological models produce a series of infrared (IR) features, many of which match those of PPNe and UIBs. Algae in particular produces the largest number of absorption peaks, most of which match those of the emission spectra of PPNe and UIBs. Furthermore, the infrared waveband of algae displays a pattern resembling the Spitzer telescope emission spectra of galactic sources depicting PAH emissions as compiled by Smith et al. (2007) and shown in Fig 3.9. This evidence suggests that algae could be reasonably proposed as a biological model for the spectral interpretation of UIBs and PPNe as well as a potential candidate for the study of interstellar medium.

# 3.2. Introduction

# 3.2.1. Space observatories

Space observatories such as Spitzer, IRAS, ISO, AKARI and the Herschel Space Observatory have been placed in outer space for observations of distant planets, galaxies, and other outer space objects. The Infrared Astronomical Satellite or IRAS is the first observatory in space to perform an infrared survey of the entire sky. Launched in January 25, 1983 on a joint mission between NASA (USA), NIVR (the Netherlands) and SERC (UK), the project lasted ten months. The other space telescope is the Infrared Space Observatory or ISO which is developed by the European Space Agency (ESA), in cooperation with the Institute of Space and Astronomical Science (Japan) or ISAS (as part of JAXA) and NASA. The ISO was

established to study infrared light at wavelengths from 2.5 to 240  $\mu$ m, and was launched on 17 November 1995 from the ELA-2 launch pad at the Guiana Space Centre near Kourou (French Guiana). This satellite contained four instruments for imaging and photometry as well as for spectroscopy from 2.5 to 196.8  $\mu$ m. Furthermore, the Spitzer Space Telescope, formerly the Space Infrared Telescope Facility or SIRTF, is the fourth of NASA's Great Observatories. This is an infrared space observatory and its satellite contains three instruments for imaging and photometry from 3 to 180  $\mu$ m, for spectroscopy from 5 to 40  $\mu$ m, and spectrophotometry from 5 to 100  $\mu$ m.

The AKARI was launched on 21 February, 2006 by M-V rocket into Earth sunsynchronous orbit under the name of ASTRO-F. This infrared astronomy satellite was designed by the Japanese Aerospace Exploration Agency in cooperation with the institutes of Europe and Korea. Its mission is to survey the entire sky in near, midand far-infrared, through a 68.5 cm aperture telescope. A consortium of European scientists launched the Herschel Space Observatory mission from Kourou (French Guiana) under the auspices of the European Space Agency (ESA) on the 16th of April 2009.

#### 3.2.2. Astronomical observations

Many astronomical sources show a feature centred at ~3.4 μm (Willner et al., 1979), and have been considered as an ideal choice for studying the properties of interstellar dust (Allen and Wickramasinghe, 1981). The unidentified infrared bands (UIBs) were first detected in 1973 in the spectra of Galactic planetary nebulae by Gillett et al. (1973). Since then, the UIBs have been proposed to belong to a family of emission bands observed in the diffuse Galactic emission (Ristorcelli et al., 1994; Tanaka et al., 1996; Onaka et al., 1996; Mattila et al., 1996), in various celestial objects such as reflection nebulae and H II regions (Tokunaga, 1997), in cirrus clouds (Lemke et al., 1998; Onaka, 2000), and in external galaxies (e.g. Helou et al., 2000; Reach et al., 2000). The original sources of these features were thought to be PAHs (Leger and Puget, 1984; Allamandola et al., 1985).

The main components of the unidentified infrared bands are centered at 3.3, 6.2, 7.7, 8.6, and 11.3 µm. According to Allamandola et al. (1989), each unidentified infrared band is related to different atomic bonds and vibration modes. For example, the 3.3 µm band is attributed to an in-plane stretching mode of C-H whereas the 6.2 µm band to a stretching mode of C-C. The 7.7 µm band is associated with a bending of vibration modes of C-C while that of the 8.6 µm attributed to an in-plane bending mode of C-H, and the 11.3 µm band to an out-of-plane bending mode of C-H.

Astronomical sources also include proto-planetary nebulae (PPNe). The infrared spectra of PPNe's appear similar to that of UIBs; they have all the features of UIBs (3.3, 6.2, 7.7, 8.6, and 11.3  $\mu$ m). However, detailed observations of the PPNe spectra in common reveal that the PPNe have additional features that are usually not detected in UIBs, and that these additional features are centered at 3.4, 6.9, 7.2, 12.2 and 13.3  $\mu$ m (Hrivnak et al., 2000, Cataldo et al., 2002; Cataldo and Keheyan, 2003).

# 3.2.3. Organic models for studying interstellar grains

According to the theory of panspermia, early life on Earth may have come from elsewhere in the galaxy. Over the past decade, evidence has been presented to support this view. The first ever detected polyatomic molecule in the interstellar medium is formaldehyde (Snyder et al., 1969). Formaldehyde (H<sub>2</sub>CO) is the most abundant molecular species after H<sub>2</sub>, H<sub>2</sub>O and CO, and makes up the essential components of polysaccharides with an empirical formula  $(H_2CO)_n$  where n is = 3 or > 3 (Al Mufti, 1985). The most common and stable polysaccharide is cellulose with n=6. Al Mufti (1985) argued that cellulose is an ideal model for studying the properties of interstellar grain for two reasons. Firstly, it is the most abundant organic compound on Earth. Secondly, it is able to survive at high temperatures. According to Shafizadeh (1971), the cellulose of wood has been shown to be stable up to 350 °C. Cellulose is also an ancient molecule in eukaryotic organisms; therefore, it serves as an important signature of early life on Earth. Another important molecule in plants is chlorophyll. It remains to be seen whether these major components can be proposed as models for the study of carriers of unidentified infrared bands (UIBs) and emission spectrum of protoplanetary nebulae (PPNe).

Cellulose is the most dominant polysaccharide of the cell walls in algae which represent one of the most ancient class of organisms on Earth. Algae belong to a diverse group of organisms that vary widely in size, shape, colour and habitat. The types of algae in marine environments, also known as seaweed, which can be found abundantly in the British Isles, include *Enteromorpha intestinalis* (green seaweed), *Pelvetia canaliculata* (brown seaweed) and *Fucus vesiculosus* (brown seaweed).

Chlorophylls are found in all plants, algae, and cyanobacteria. According to Gross (1991), chlorophylls are the greenish pigments that are responsible for photosynthesis, which is the fundamental process of life that converts light energy into chemical energy. The pigments absorb light and this absorption causes excitation of electrons from their ground state to an excited state because the pigments contain a porphyrin ring which is a stable molecule around which electrons are free to migrate. Since the electrons move freely, the ring is capable of gaining or losing electrons easily to provide energised electrons to other molecules. This is the fundamental process by which chlorophyll captures the energy of sunlight.

Microorganisms found on Earth about 1.2 to 1.5 billion years ago, are also responsible for cellulose hydrolysis, especially in the rumens of cattle, and also known to have the ability to recycle organic matter in the environment. Cyanobacteria in particular are the important source of free oxygen in the early atmosphere. Some microorganisms live on the surface of Earth either close to freezing temperature or in the polar caps and in permafrost such as psychrophilic and psychrotophic archaea, bacteria and algae. Freeze-dried microorganisms lying dormant for 10-20 million years in permafrost and in the depth of Lake Vostok, have been recovered and cultured in the laboratory (Wickramasinghe, 2004). Outside the solar system, microorganisms become exposed to near-vacuum conditions in interstellar clouds, desiccated, and subjected to temperatures typically in the range of -240 to -260 °C. They remain in such conditions until the environments become favourable in newly formed comets or on planetary surfaces where they can replicate. Some authors have proposed that microbial life on Earth originate from the outer-space via comets (Hoyle and Wickramasinghe, 2000)

## 3.2.4. Aim and objective of the study

The current work analysed biological materials by Fourier Transform Infrared spectroscopy (FTIR). The objective was to compare their infrared spectra with those of interstellar emission bands, especially the protoplanetary nebulae (PPNe) and unidentified infrared bands (UIBs). The aim was to ascertain whether those materials could be used as models for studying the properties of interstellar grains.

### 3.3. Materials and Methods

#### 3.3.1. Materials

The following materials were used in the present study:

- Oedogonium sp. (a species of the fresh water green algae) collected from Roath Park, Cardiff.
- Bacillus cereus (Gram-positive spore foming bacterium) donated by Dr. V.
   Grays, Cardiff School of Biosciences
- Staphylococcus aureus (Gram-positive bacterium) donated by Dr. V. Grays,
   Cardiff School of Biosciences
- Poppy seed, donated by Dr M. Wallis, Cardiff Centre for Astrobiology
- Chlorophylls 'a' and 'b', obtained from Sigma Ltd.
- Enteromopha intestinalis (green seaweed), collected from Barry Island, Cardiff.
- Pelvetia canaliculata (brown seaweed), collected from Barry Island, Cardiff
- Fucus vesiculosus (brown seaweed), collected from Barry Island, Cardiff
- Grass (*Panicum maximum*) of Santa Cruz Island of the Galapagos, donated by Professor C. Wickramasinghe, Cardiff Centre for Astrobiology.

## 3.3.2. Methods of sample preparation for FTIR analysis

Algae and all seaweed specimens used in this study were transferred into a large plastic container filled with 2 litres of de-ionised water. The samples together with

some impurities were left in the container containing de-ionised water on the bench for about 15 minutes to allow large particles and clumps to sink to the bottom of the container. The samples were then washed in 6 -8 changes of de-ionised water and dried in a vacuum dryer for 4 days.

All samples were subjected to vigorous grinding and embedded in KBr according to the protocol as described in Chapter 2. The method is briefly described as follows: (1) sample (0.5 mg) was mixed with KBr powder (20 mg), carefully ground and placed in a die-set assembly; the KBr was pressed with a pressure of about 10 tons cm<sup>-2</sup> using a KBr dye assembly. The resulting KBr disc was then transferred onto a holder and analysed in the infrared spectrometer (JASCO Model FT/IR 660 Plus series). Five discs were prepared for each sample and taken for analysis. The data were averaged and the resulting spectra presented.

#### 3.4. Results

#### 3.4.1. Infrared (IR) spectra of Algae

All algae samples were treated at different temperatures (100, 120, 140, 165, and 250 °C) in an oven. The oven was pre-heated to the appropriate temperatures before use. Prior to temperature treatments, algae specimens (0.5 mg) were transferred into a glass tube with an overall diameter of 2.0 cm, which was then sealed under vacuum to remove air.

Fig.3.1a shows infrared spectra of all algae samples treated at different temperatures. All spectra display a waveband stretching from 2.5 µm to 25 µm with absorption peaks centred at the wavelengths as shown in Table 3.1 It is also interesting to note that the pattern of IR waveband of algae treated at RT is similar to those produced by the samples treated at higher temperatures. However, it is noteworthy that the KBr discs became less transparent as the temperatures increased.

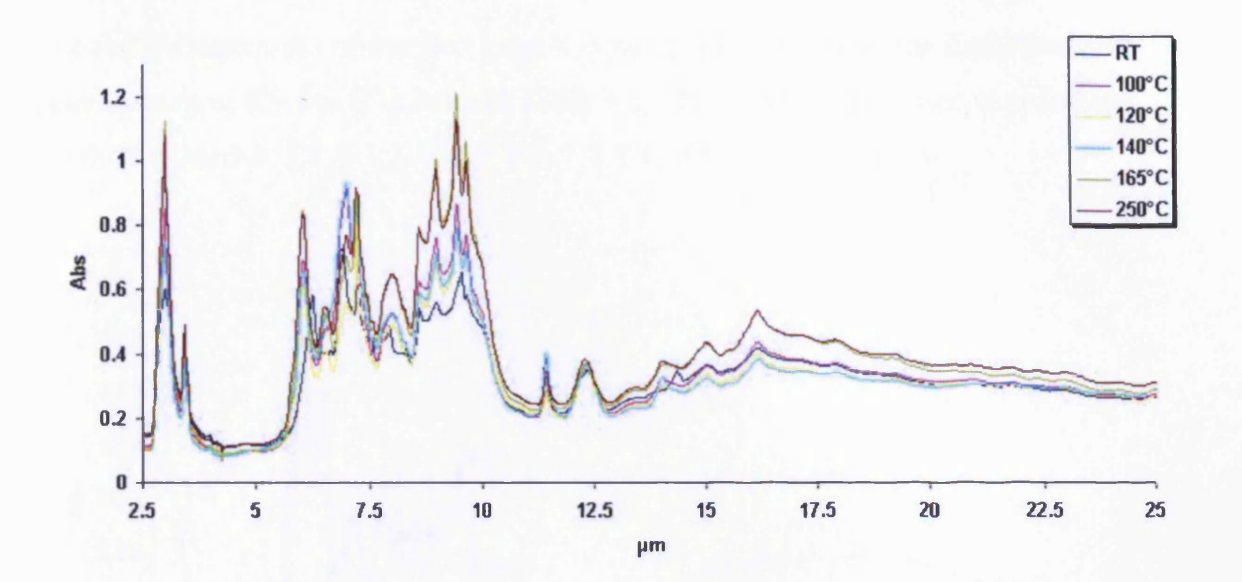


Fig.3.1.a: Overlayed FTIR spectra of algae treated at different temperatures showing a waveband stretching from 2.5 to 25  $\mu$ m. All the treated samples show the same pattern of absorptions.

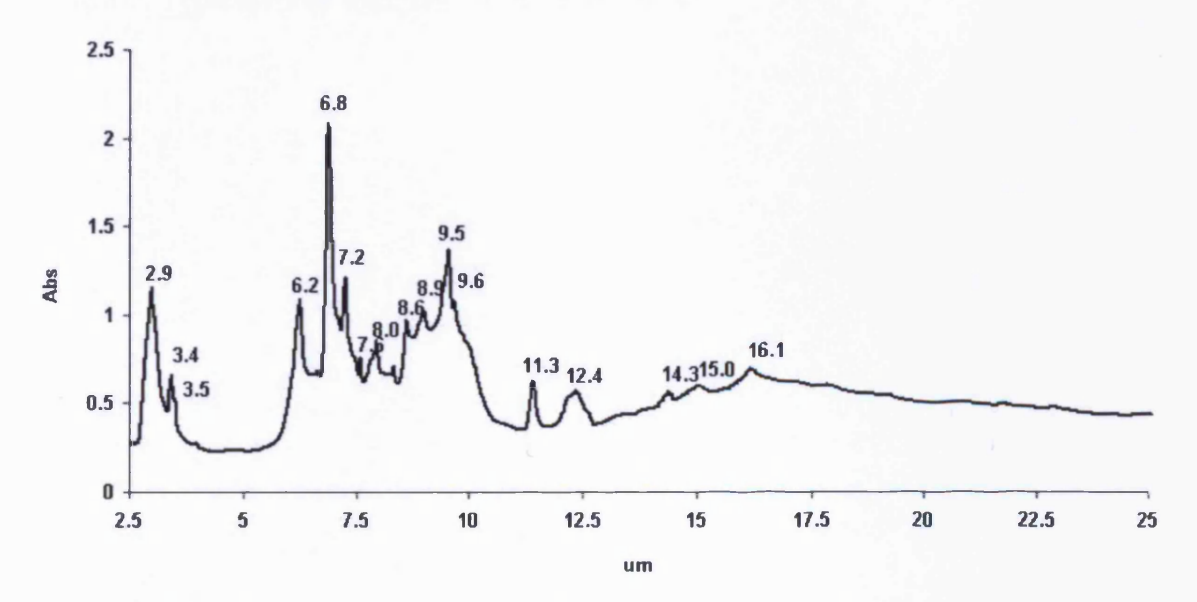


Fig.3.1.b: Typical FTIR spectrum of algae treated at room temperature showing a series of typical features centered at 2.9, 3.3, 3.5, 6.2, 6.8, 7.2, 7.6, 8.0, 8.6, 8.9, 9.5, 9.6, 11.3, 12.4, 14.3 15.0 and 16.1  $\mu$ m.

# 3.4.2. Infrared (IR) spectrum of Bacillus cereus

The infrared spectrum of *Bacillus cereus* shows a waveband with the first absorption peak starting at 2.9  $\mu$ m (Fig.3.2 and Table 3.2). The other major absorption features are detected at 3.4, 5.8, 6.1, 6.4, 6.9, 7.2, 7.7, 8.1, 8.5, 9.5 and 10.2  $\mu$ m.

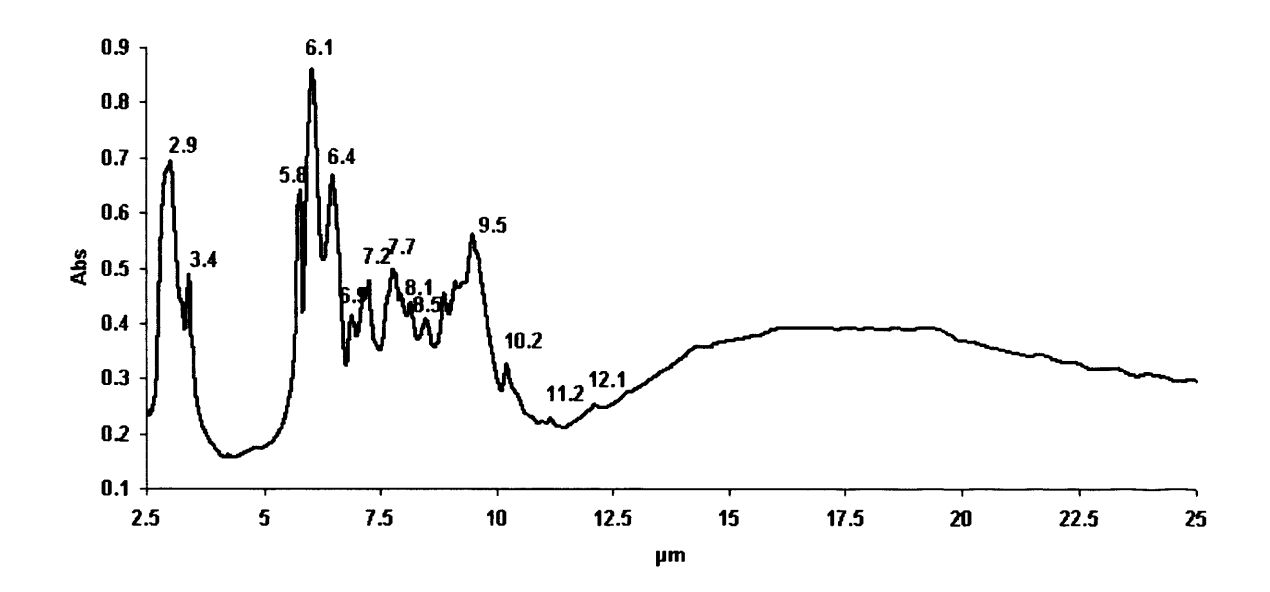


Fig.3.2: Typical FTIR spectrum of Bacillus cereus.

# 3.4.3. Infrared (IR) spectrum of Staphylococcus aureus

Staphylococcus aureus produces an infrared absorption band stretching from 2.5 to 25  $\mu$ m with detectable peaks centered at 2.9, 3.4, 6.1, 6.4, 6.9, 7.2, 7.6, 8.0, 8.6, 9.6, 11.3 and 12.0  $\mu$ m (Fig.3.3 and Table 3.2).

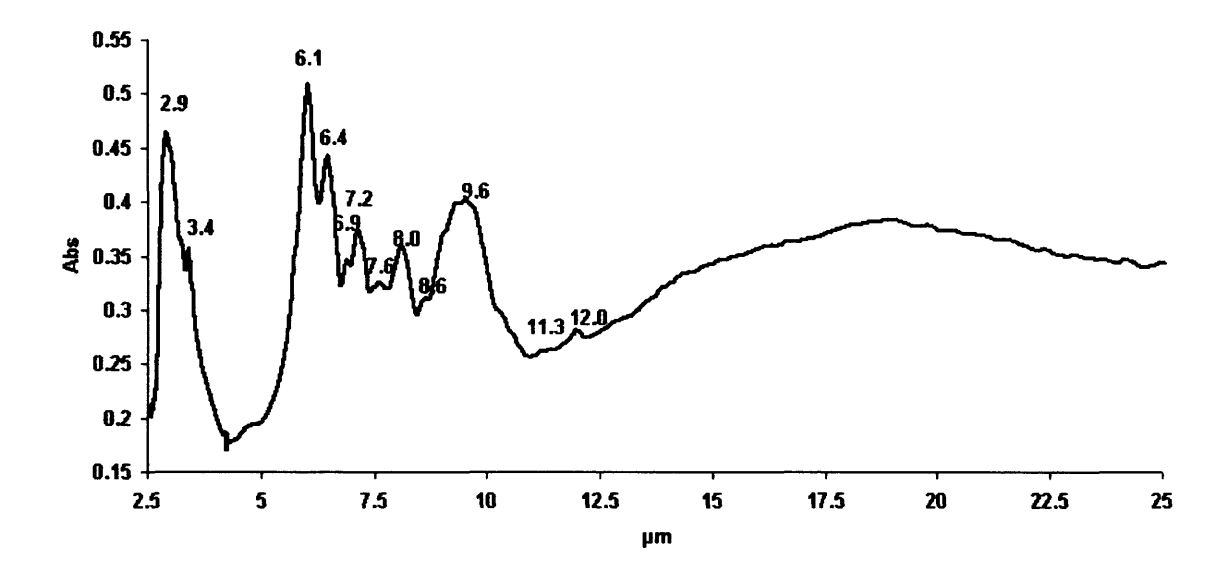


Fig.3.3: Typical Infrared spectrum of *Staphylococcus aureus* showing a waveband stretching from 2.5 to 25  $\mu m$ .

# 3.4.4. Infrared (IR) spectrum of Poppy seeds

Poppy seeds produce a waveband with detectable absorption peaks centered at 2.9, 3.3, 3.4, 5.7, 6.1, 6.4, 6.8, 7.2, 8, 8.6, 9.1 and 13.7  $\mu$ m (Fig.3.4 and Table 3.2).

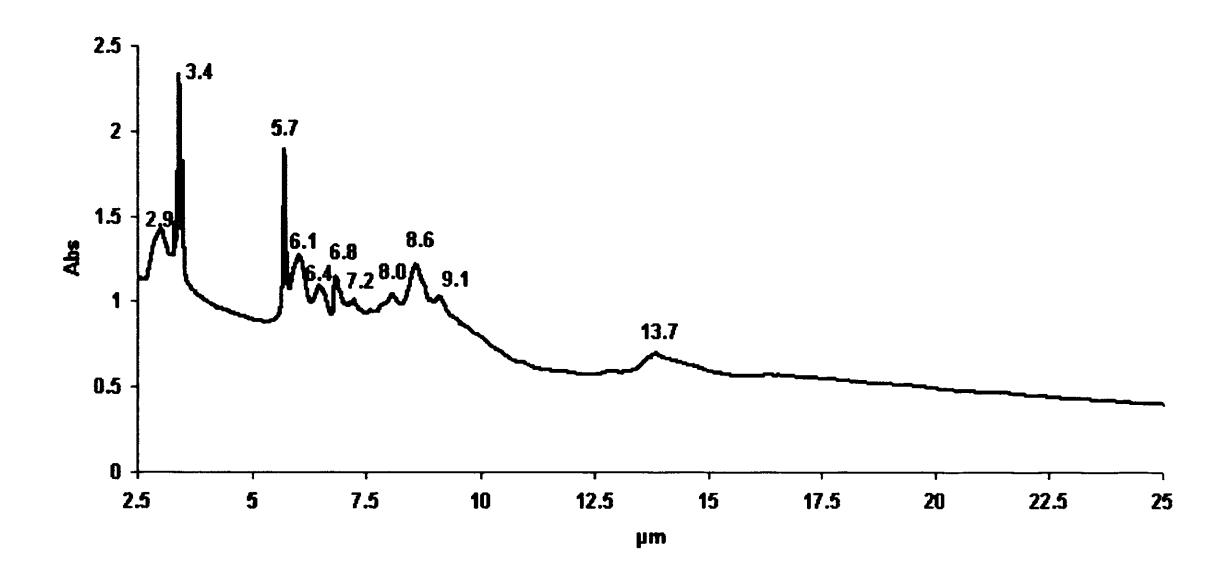


Fig.3.4: Typical Infrared spectrum of poppy seeds.

# 3.4.5. Infrared (IR) spectra of Chloropyll 'a' and 'b'

Chlorophyll 'a' exhibits a long wavelength range containing a series of major peaks centered at 2.9, 3.3, 3.4, 3.5, 5.7, 6.1, 6.5, 6.8, 7.2, 7.4, 7.7, 8.8, 9.6, 11.3, 12.5 and 13.4  $\mu$ m (Fig.3.5 and Table 3.2). Chlorophyll 'b' also shows the same number of peaks of absorption as well as two additional features centered at 8.3 and 8.6  $\mu$ m (Table 3.2).

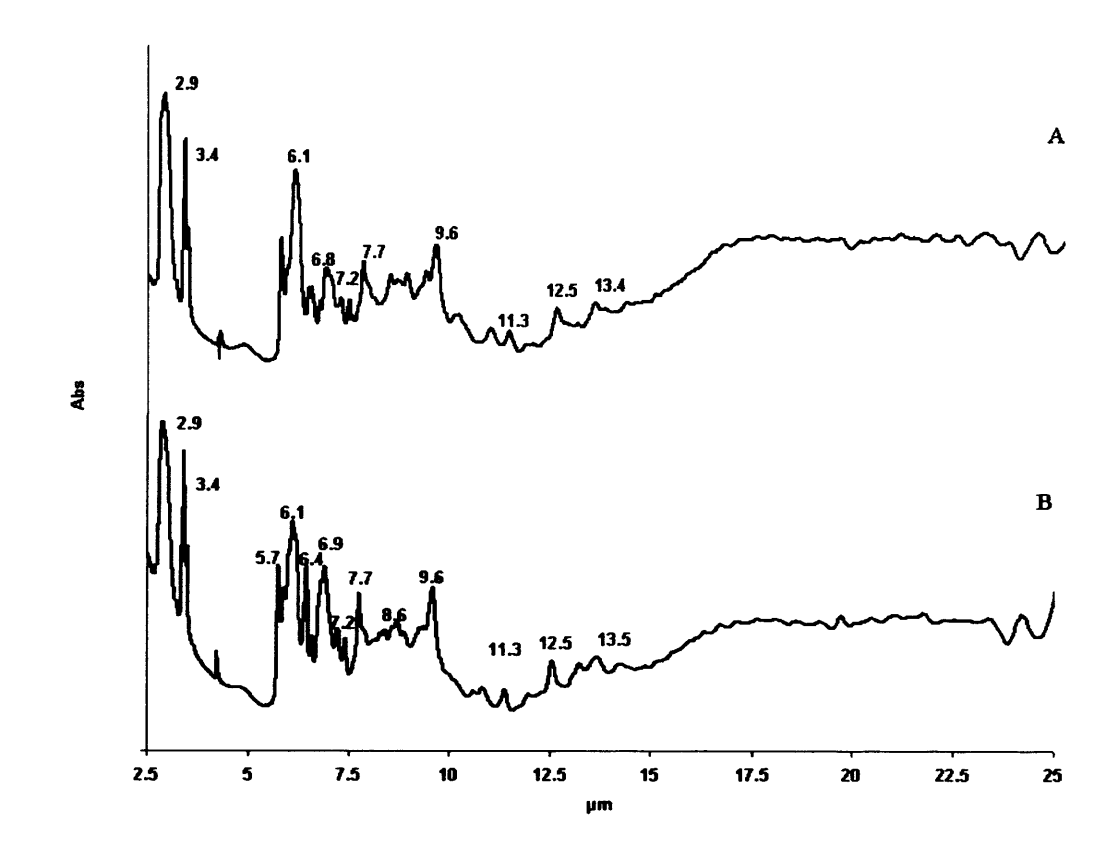


Fig.3.5: Typical FTIR spectra of chlorophyll 'a' (A) and FTIR spectra of chlorophyll 'b' (B).

#### 3.4.6. Infrared (IR) spectra of Seaweed

Typical FTIR spectra of three species of seaweed display a similar pattern of waveband with the same features centered at 2.9, 3.4, 6.9, 8.6 and 9.6 μm (Fig 3.6). Two species of brown seaweed (*Pelvetia canaliculata* and *Fucus vesiculosus*) show additional peaks which are located at 6.2, 7.8, 11.3, 12.2 and 16.1 μm (Figs. 3.6A and 3.6B; Table 3.2). These latter peaks are not detected in the green seaweed (*Enteromopha intestinalis*) (Fig. 3.6C; Table 3.2). However, the spectrum of *Enteromopha intestinalis* displays three peaks at 6.4, 7.2 and 11.8 μm that are not found in the brown seaweed species (Table 3.2).

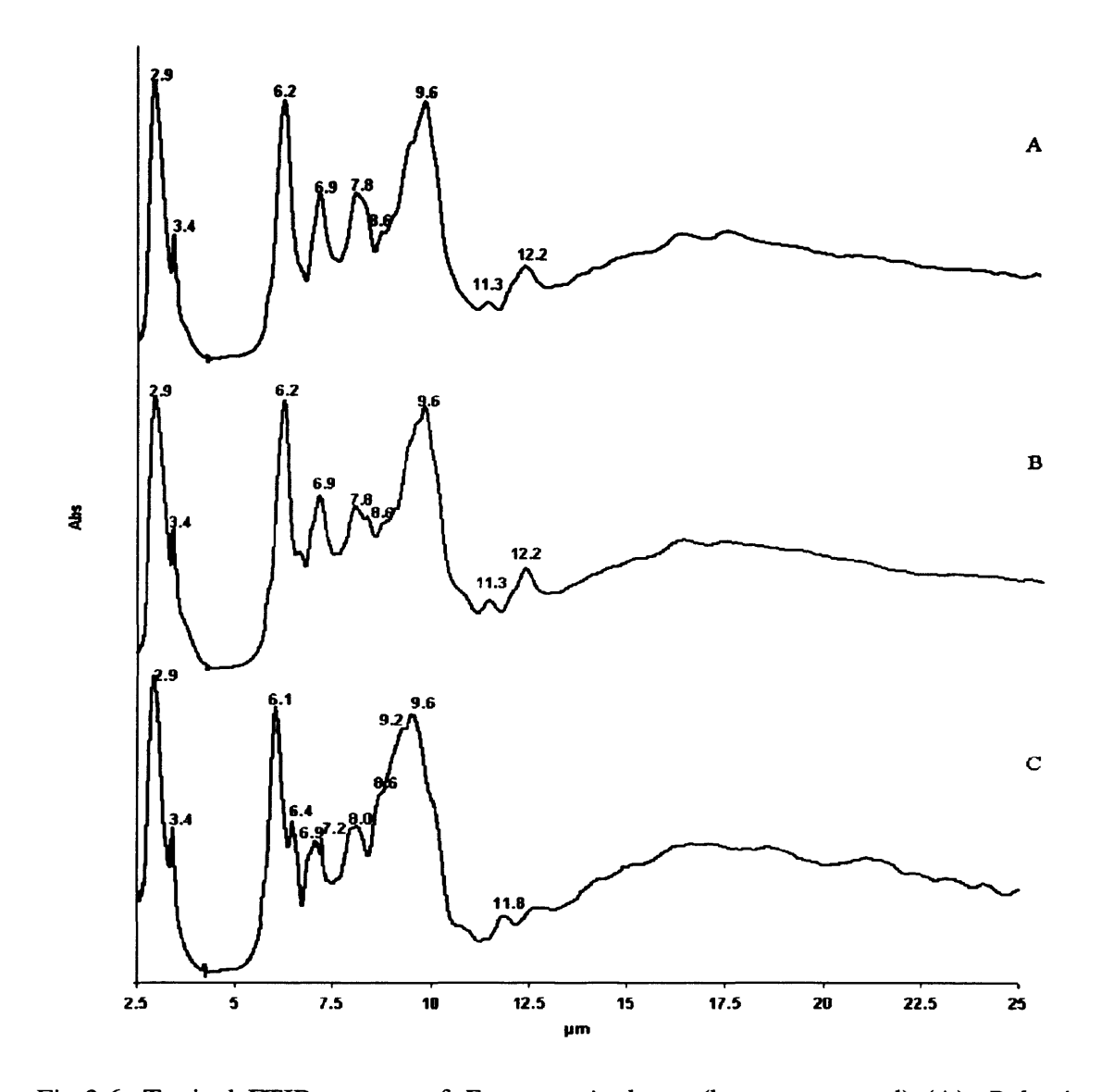


Fig.3.6: Typical FTIR spectra of *Fucus vesiculosus* (brown seaweed) (A), *Pelvetia canaliculata* (brown seaweed) (B) and *Enteromopha intestinalis* (green seaweed) (C).

# 3.4.7. Infrared (IR) spectrum of Grass (Panicum maximum)

The following spectrum shows prominent peaks centered at 2.9, 3.4, 6.1, 7.6, 9.3 12.8 and 19.3  $\mu m$  and minor features at 6.9, 7.2, 8.0 and 12.0  $\mu m$ .

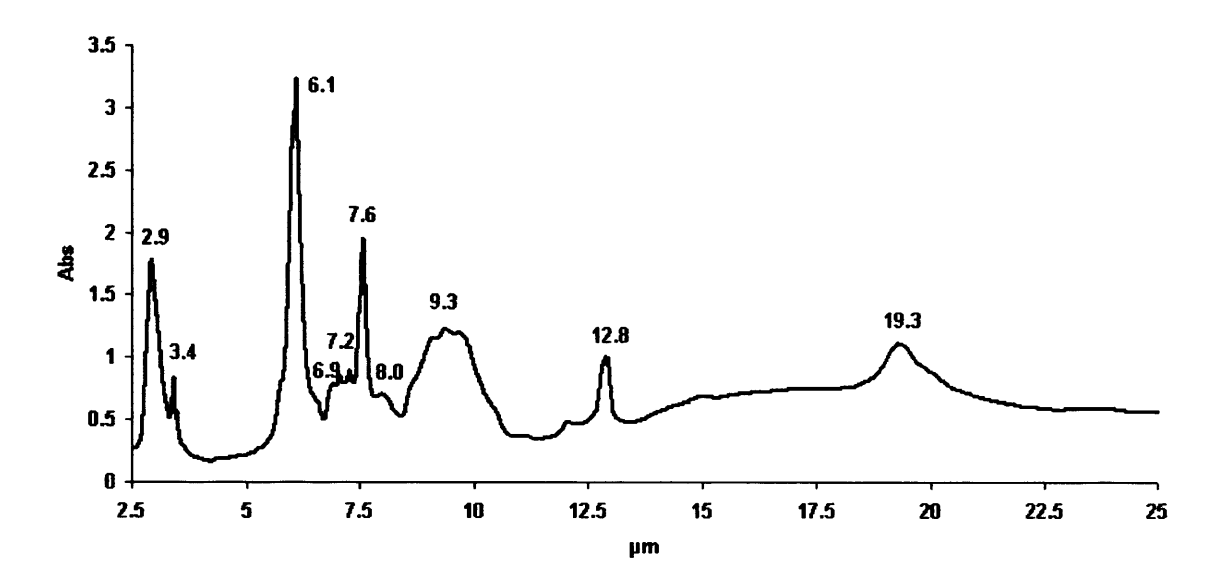


Fig.3.7: Infrared spectrum of grass (Panicum maximum)

Table 3.1: IR absorption wavelengths  $(\mu m)$  of algae samples treated at different temperatures.

Algae RT	Algae 100°C	Algae 120°C	Algae 140°C	Algae 165°C	Algae 250°C
(µm)	(µm)	(μm)	(μ <b>m</b> )	(μm)	(μ <b>m</b> )
2.98	2.98	2.98	2.98	2.98	2.98
3.3	-	-	-	-	-
3.4	3.4	3.4	3.4	3.4	3.4
3.5	3.5	3.5	3.5	3.5	3.5
6.2	6.2	6.2	6.2	6.2	6.2
-	-	6.5	6.5	6.5	_
6.89	6.9	-	6.9	-	-
-	_	7	-	7	7
7.2	7.2	7.2	7.2	7.2	7.2
7.6	-	-	-	-	-
8	8	8	8	8	8
8.6	8.6	8.6	8.6	8.6	8.6
8.9	8.9	8.9	8.9	8.9	8.9
9.5	9.4	9.4	9.4	9.4	9.4
9.6	9.6	9.6	9.6	9.6	9.6
11.3	11.3	11.3	11.3	11.3	11.3
12.4	12.1	12.1	12.05	12.1	12.5
14.3	14.03	14.05	14.05	14.07	14.05
15	15	15	15	15	15
16.1	16.1	16.1	16.1	16.1	16.1

Notes: The following features of algae are consistently displayed by all treated samples: 2.98, 3.4, 3.5, 6.2, 7.2, 8.0, 8.6, 8.9, 9.4, 9.6, 11.3, 15.0 and 16.1 µm. The features at 3.4, 6.2, 7.2, 8.0 and 8.6 µm have been reported to be expressed by the carriers of PPNe emission bands (Hrivnak et al., 2000; Cataldo et al., 2002 and Cataldo and Keheyan, 2003). The feature at 11.3 µm expressed by all algae samples is also one of the major components of the unidentified bands, UIBs (Henning et al., 1998; Ehrenfreud et al., 2000; Hrivnak et al., 2000; Cataldo et al., 2002 and Cataldo and Keheyan, 2003). These observations seem to suggest that algal emission spectra show a good match with those of astronomical sources, in particular the UIBs and PPNe.

Table 3.2: IR absorption wavelengths ( $\mu m$ ) of Experimental Models

Algae	Grass	Bacillus	Staphylococcus	Chlorophyll	Chlorophyll	Pelvetia	Fucus	Enteromopha	Poppy
		cereus	aureus	a	b	canaliculata	vesiculosus	intestinalis	seeds
(µm)	(µm)	(µm)	(µm)	(µm)	(µm)	(µm)	(μm)	(µm)	(µm)
2.98	2.93	2.9	2.92	2.91	2.91	2.93	2.95	2.92	2.95
3.3	-			3.3	3.3				3.3
3.4	3.4	3.4	3.4	3.4	3.4	3.4	3.4	3.4	3.4
3.5	3.5			3.5	3.5				3.5
				5.7	5.7				5.7
		5.8			5.8				
6.2	6.1	6.1	6.1	6.1	6.1	6.2	6.2		6.1
		6.4	6.4		6.45			6.47	6.48
-	-			6.5	6.58		-		
6.89	6.9	6.9	6.9	6.8	6.9	6.9	6.9	6.9	6.8
-	-								
7.2	7.2	7.2	7.2	7.2	7.2			7.2	7.2
				7.4	7.4				
7.6	7.6		7.6						
-		7.7		7.7	7.7	7.8	7.8	7.8	
8	8	8.1	8					8.0	8
		1			8.3				
8.6		8.5	8.6						8.6
					8.6	8.6	8.6	8.6	
8.9				8.86					
9.5	9.36	9.5						9.2	9.1
9.6			9.6	9.6	9.6	9.6	9.6	9.6	
		10.2							
11.3	11.1	11.2	11.3	11.3	11.3	11.3	11.3		
								11.8	
12.08	12.05	12.1	12			12.2	12.2		
12.4				12.5	12.5				
-	12.89								
-	-			13.4	13.5				13.7
14.3									
15	15			-					
16.1		16.6				16.1	16.1		
	19.3								

Table 3.3: Distribution of major infrared absorption wavelengths of experimental models and emission features of UIBs and PPNe

UIBs	PPNe	Algae	B. cereus	S. Aureus	Chlorophyll a	Chlorophyll b	Grass	Pelvetia	Enteromopha	Poppy
								canaliculata	intestinalis	seed
								&		
								Fucus		
								vesiculosus	,	
3.3	3.3	3.3	-	-	3.3	3.3	-	-	-	3.3
-	3.4	3.4	3.4	3.4	3.4	3.4	3.4	3.4	3.4	3.4
6.2	6.2	6.2	6.1	6.1	6.1	6.1	6.1	6.2	6.1	6.1
-	6.9	6.9	6.9	6.9	6.8	6.9	6.9	6.9	6.9	6.8
-	7.2	7.2	7.2	7.2	7.2	7.2	7.2	-	7.2	7.2
7.7	7.7	7.6	7.7	7.6	7.7	7.7	7.6	_	-	-
-	8.0	8.0	8.1	8.0	-	-	8.0	-	8.0	8.0
8.6	8.6	8.6	8.5	8.6	-	8.6	-	8.6	8.6	8.6
11.3	11.3	11.3	11.2	11.3	11.3	11.3	11.1	11.3	-	-
-	12.2	12.4	12.1	12.0	-	-	12.0	12.2	-	-
-	13.3	-	-	-	13.4	13.5	-	-	-	13.7

### 3.5. Discussion

Organic molecules and carbonaceous matter are present naturally in the interstellar medium and protoplanetary nebulae. They have been detected in carbonaceous meteorites found on Earth (Lorca, 2004). These findings support the theory of panspermia which proposes that organic molecules and precursors of building blocks for life and degradation products of biology are ubiquitous in the universe (Wickramasinghe, 2010; Wickramasinghe et al., 2010). One of the main aims of research in the field of PPNe or other astronomical sources including UIBs is to identify the individual molecules that are thought to be the carriers of infrared emission bands. Several astronomical sources have been reported to contain an interesting complex feature centred at ~3.4 µm (Willner et al., 1979). The source GC-IRS 7 in particular, has been an ideal choice for studying the properties of interstellar dust as it is located at a large distance (~10 kpc or ~3x10<sup>22</sup> cm) from the solar system towards the galactic centre (Allen and Wickramasinghe, 1981). The infrared spectrum of IRS 7 reveals a broad absorption feature over a waveband stretching from 2.9 to 3.6 µm. The absorption peaks in this region have been suggested to be caused by complex organic molecules consistent with biomaterial (Allen and Wickramasinghe, 1981). Furthermore, the diffuse ISM has been found to possess a set of emissions in the infrared waveband known as the unidentified bands or UIBs (Mattila et al., 1996; Onaka et al., 1996). The major features are centered at 3.3, 6.2, 7.7, 8.6, and 11.3 µm. The protoplanetary nebulae (PPNe) have also these same components (Hrivnak et al., 2000). Cataldo and Keheyan (2003) show that aromatic distillate of petroleum exhibits a good match with many of the unidentified infrared bands (UIBs). Although the infrared spectrum of PPNe appears similar to that of UIBs, detailed observation shows that the PPNe have additional features that are usually not detected in UIBs, and that these features are centered at 3.4, 6.9, 7.2, 12.2 and 13.3 µm (Hrivnak et al., 2000, Cataldo et al., 2002; Cataldo and Keheyan, 2003).

The present work aims to compare infrared spectra of algae (*Oedogonium sp.*), bacteria (*B. cereus* and *S. aureus*), poppy seed, chlorophyll 'a' and 'b', grass (*Panicum maximum*) and three species of seaweed (*Enteromopha intestinalis*, *Pelvetia canaliculata* and *Fucus vesiculosus*) with those of astronomical sources. Its objective

is to determine whether any of these biological materials of interest possess IR characteristics that appear distinctively similar to those of the unidentified infrared bands (UIBs) and emission spectra of protoplanetary nebulae. It is interesting to see if these materials could be proposed as the candidate models for the interpretation of the unidentified bands and the protoplanetary nebula emission spectra.

The results obtained from the present study show that algae treated at room temperature produced absorptions over a waveband stretching from 2.5 to 25 µm with a series of high absorption peaks centered at 2.9, 3.4, 6.2, 6.8, 7.2, 7.6, 8.0, 8.6, 8.9, 9.5, 11.3, 12.4 and 14.3 µm. A parallel experiment was also set up to check the stability of algae at high temperatures. The experimental results indicate that all those that were taken to high temperatures (100, 120, 140, 165 and 250 °C) displayed a similar pattern with strong absorption features centered at the specific wavelengths as shown in Fig.3.1a and Table 3.1. The data also confirm that subjection of algae to high temperatures up to 250 °C did not affect their stability (Table 3.1). It is however noted that the transparency of the KBr discs was reduced when the samples were heated to higher temperatures. In the present study, the spectra of all algae samples have been shown to contain a peak centred at 2.9 µm, which has been reported by Al-Mufti (1985) to be the absorption band of water in liquid form. According to Al-Mufti (1985), cellulose always contained a few percent of water, no matter how much precautionary measures were taken to make the samples dried, even when the cellulose was heated to temperatures around 400 °C.

It is remarkable that all 10 samples tested in the present study (algae, *B. cereus*, *S. aureus*, chlorophylls 'a' and 'b', poppy seed, grass and three species of seaweed) produced an infrared absorption peak at 3.4  $\mu$ m which is a prominent feature of PPNe (Table 3.3). This feature is attributed to the CH band and is thought to be the common organic functional group of the interstellar grains (Al Mufti, 1985). Wickramasinghe and Allen (1980) also detected a 3.4  $\mu$ m absorption feature in the galactic infrared source GC-IRS 7 using the 3.9m Anglo-Australian Telescope and an infrared photometer-spectrometer. They attributed this feature to the grains in the interstellar medium containing a polymer based on the H<sub>2</sub>CO molecule and have further suggested that this 3.4  $\mu$ m feature corresponds to the CH band. This 3.4  $\mu$ m band was

also detected in the spectra of protoplanetary nebulae (Hrivnak et al., 2000, Cataldo et al., 2002; Cataldo and Keheyan, 2003).

The present study reveals that the 3.3  $\mu$ m absorption peak (the common feature of UIBs and PPNe), is also found in the FTIR spectra of algae, chlorophyll 'a' and 'b' and poppy seed (Table 3.2). Furthermore, chlorophylls 'a' and 'b' and grass show a peak at 6.1  $\mu$ m, the position of which is close to that of the feature (6.2  $\mu$ m) of both PPNe and UIBs. On the other hand, all three species of seaweed show a peak centered at 6.2  $\mu$ m, another characteristic feature of PPNe and UIBs. This 6.2  $\mu$ m band has been ascribed to a stretching mode of C-C (Allamandola et al., 1989), and to the aromatic 'quadrant' stretching ring (Reynaud et al., 2001 and Cataldo et al., 2004). Moreover, algae, *B. cereus*, *S. aureus*, Chlorophyll 'b', seaweed and grass all display a peak at 6.9  $\mu$ m, which is also another characteristic component of PPNe emission band. On the contrary, poppy seed and chlorophyll 'a' show a peak shifted slightly away from the 6.9  $\mu$ m position (6.8  $\mu$ m). It is noteworthy that the 6.8  $\mu$ m is attributed to the aromatic 'semicircle' stretching ring as suggested by Reynaud et al. (2001) and Cataldo et al. (2004).

The present work also indicates that algae, *B. cereus*, *S. aureus* and chlorophylls 'a' and 'b', grass, poppy seed and green seaweed (*Enteromopha intestinalis*) exhibited a peak located in the Mid-IR region at 7.2 μm that was also found in the PPNe spectrum. *B.cereus*, chlorophyll (a and b) produced a peak at 7.7 μm which has been reported to be associated with a blending of vibration modes of C-C. The 7.7 μm has also been detected in both, the UIBs and PPNe emission spectra (Hrivnak et al., 2000, Cataldo et al., 2002; Cataldo and Keheyan, 2003). Algae, *S. aureus* and grass expressed a feature centered at 7.6 μm which is near to the 7.7 μm of UIBs and PPNe.

The characteristic feature of PPNe which is centered at 8 µm has been found in the FTIR spectra of algae, grass, S. aureus, poppy seed and green seaweed (Enteromopha intestinalis). All temperature treated algae, S. aureus, chlorophyll 'b' green seaweed (Enteromopha intestinalis) and poppy seed samples display a peak at 8.6 µm, which is a perfect match with that of UIBs and PPNe. According to Allamandola et al. (1989), the 8.6 µm feature is attributed to an in-plane bending mode of C-H. The 11.3 µm band which is an out-of-plane bending mode of C-H (Allamandola et al., 1989)

detected in the spectra of UIBs and PPNe (Hrivnak et al., 2000, Cataldo et al., 2002; Cataldo and Keheyan, 2003), was also found in the FTIR spectra of both brown seaweed, *S. aureus*, chlorophyll 'a' and 'b' and all samples of algae.

The spectra of laboratory biological models exhibited absorptions at most of the relevant astronomical wavelengths as seen in Table 3.3. Figure 3.1b shows the Mid-IR spectra of algae samples, which are seen to correspond approximately to portions of the spectra displayed by a variety of galactic sources as shown in Fig. 3.9 (Smith et al., 2007). Traces of water cannot be ruled out in these samples, showing a strong 2.9-3 μm band that is attributed to H<sub>2</sub>O, whilst the elevated complex of features around 10 µm is assignable to polysaccharides. The unidentified interstellar absorption bands in the IR spectra have been suggested to be attributed to aromatic molecules within biological cells (Hoyle and Wickramasinghe, 1989; Rauf and Wickramasinghe, 2010). The current study reveals that amongst all samples tested, algae produced the largest number of absorption peaks, most of which matched those of the emission spectra of PPNe and UIBs. The Mid-IR waveband of algae resembles the Spitzer telescope emission spectra of galactic sources showing PAH emissions (Fig 3.9 compiled by Smith et al., 2007). Based on the above observations, the present study proposes that algae could be used as a biological model for the spectral interpretation of UIBs and PPNe and a potential candidate for the study of interstellar dust.

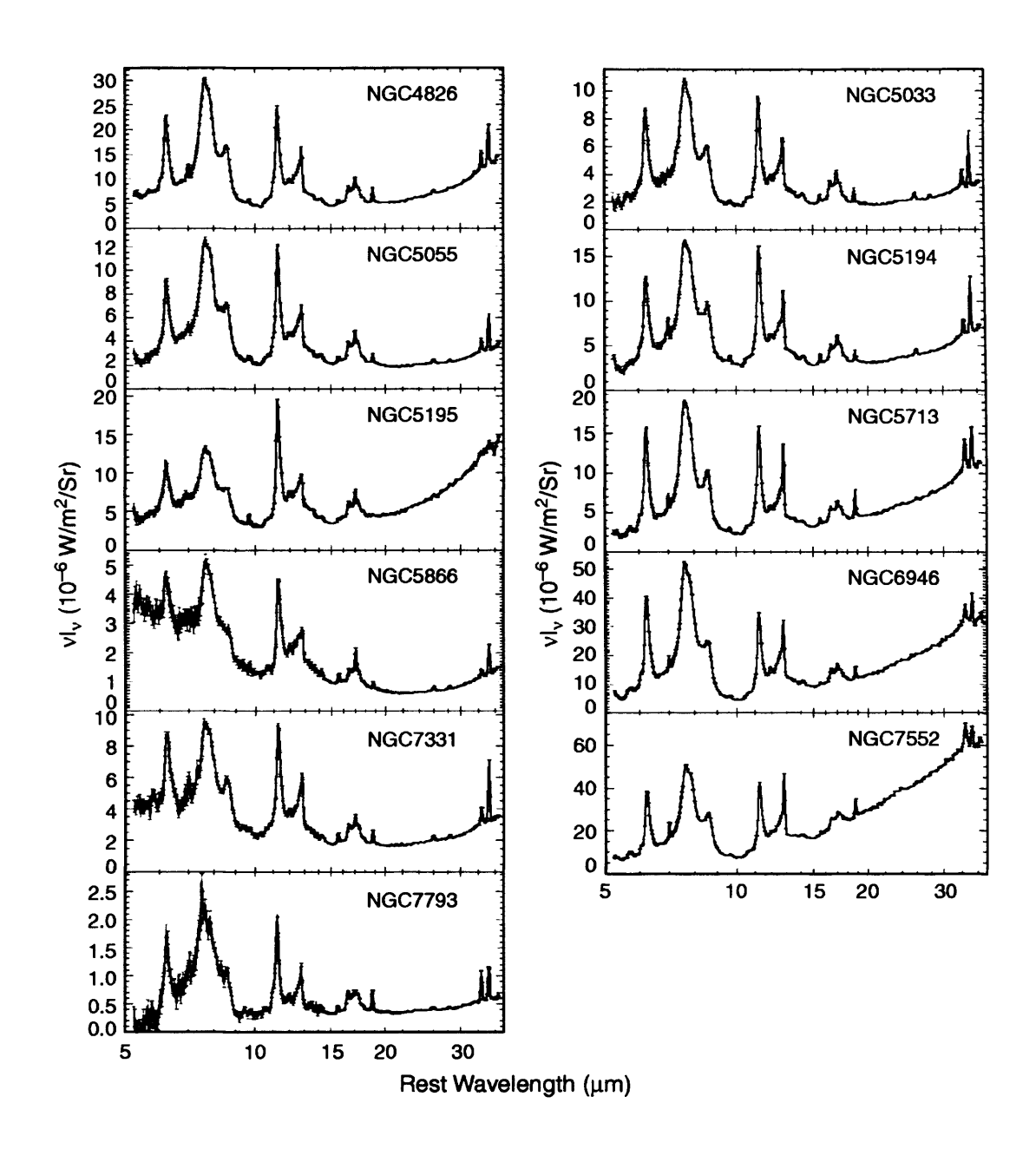


Fig. 3.9: Recent compilation of Spitzer telescope emission spectra of a variety of galactic sources showing PAH emissions (Smith et al., 2007).

# **CHAPTER 4**

Interpretation of Laboratory Models as
Possible Analogues of Carriers for the
Unidentified Infrared Bands and
Protoplanetary Nebulae

# 4.1. Summary

The present study analysed four compounds by Fourier Transform Infrared (FTIR) spectroscopy. Their infrared (IR) absorptions were compared with the emission spectra of unidentified infrared bands (UIBs) and protoplanetary nebulae (PPNe). The compounds under investigation included: graphite, bituminous coal (semi anthracite coal), anthracite coal and naphthalene. The results support unequivocally the early proposal that certain types of coal are suitable models for the interpretation of carriers for the emission spectra of UIBs and PPNe. The evidence obtained from the study confirms that bituminous coal is the best model, and this is based on the observation that its spectrum contains the highest number of prominent features that match those of UIBs and PPNe. Pure anthracite on the other hand is found to be the least suitable because its matching absorption peaks are weaker than those of bituminous coal. Furthermore, naphthalene is less suitable than both types of coal because the number of its peaks that match those of PPNe and UIBs is low even though it produces more absorption bands than its counterparts.

## 4.2. Introduction

Materials found in the diffuse interstellar medium and circumstellar environments are unquestionably of an organic nature (Hoyle and Wickramasinghe, 1989; Wickramasinghe et al., 1999; Irvine, 1996; Ehrenfreund and Charnley, 2000 and Cataldo et al., 2002), and very similar material is embedded in meteorites found on Earth (Llorca, 2004). Comets and interplanetary dust particles have also been reported to contain these same materials (Bradley, 2005). Following the discovery of organic materials in outer-space, attempts to identify their origin have never ceased. Irvine (1996) has reported that more than 100 molecular species in the interstellar medium of the Milky Way Galaxy have so far been characterised using spectroscopy. A number of chemical elements such as hydrogen, carbon, oxygen, nitrogen, sulfur, phosphorus and metals that play a role in the origin of life on Earth, have been identified as the products of nucleosynthesis in the cores of evolved stars and in stellar explosions (Burbidge et al, 1957; Matteucci, 1991). According to Lovas (2004 and 2005), 129

molecules mostly organic have been found in interstellar space, and 114 of these have been detected by radio astronomy, and the rest by infrared or ultraviolet astronomy.

Larger and much more complex organic molecules have also been detected in the stellar environments, and a number of reports have confirmed the presence of a rather more complex emission profile with wavelengths stretching from 2 to 14 μm, featuring both narrow and broad bands, which are now referred to as the 'unidentified infrared bands (UIBs) (Irvine, 1996; Hudgins and Allamandola., 1997; Ehrenfreund and Charnley, 2000; Reynaud et al., 2001). Although these characteristic bands have been identified, their carriers remain obscure (Hudgins and Allamandola, 1997). According to Sloan et al. (1999), these bands are the strongest interstellar features found in a variety of astronomical objects. As suggested by Leger and Puget (1984), Allamandola et al. (1987), Puget and Leger (1989) and Ehrenfreund and Charnley (2000), these bands are attributed to stretching and bending modes of C-H as well as the stretching vibrations of C=C in aromatic molecules.

Many materials have been suggested to be responsible for the emission of these interstellar infrared features. These include polycyclic aromatic hydrocarbons (Leger and Puget, 1984 and Allamandola et al., 1985), coal (Papoular et al., 1989, 1995), hydrogenated amorphous carbon or HAC (Ehrenfreund and Charnley, 2000), quenched carbonaceous composite or QCC (Sakata et al., 1987 and 1990) and aromatic molecules within biological cells (Hoyle and Wickramasinghe 1989; Rauf and Wickramasighe, 2010).

#### 4.2.1. Coal

It has been proposed that an alternative to polycyclic aromatic hydrocarbons is carbonaceous amorphous solid like coal (Guillois et al., 1999; and Cataldo et al., 2004). Coal is a black rock found in swampy forests where the dead plants were buried for several hundred million years during which time the plants were transformed into carbon and then became compressed under relentless heat and pressure. Different types of coal have been identified based on the degree of their transformation into carbon:

- Lignite is the lowest rank and the softest coal of all types with a brown or black coloration.
- Sub-bituminous coal contains more moisture and is harder than lignite but much softer than the bituminous coal.
- Semi-anthracite or bituminous coal contains a tar-like material, known as bitumen. This type of coal is an organic sedimentary rock formed by compression of peat material. Its appearance is dark brown or black consisting of layers of bright and dull materials.
- Anthracite is the hardest type of coal and appears glossy. It is generally found in areas such as flanks of mountains where movements of earth are considerable. It appears glossy and contains a high level of carbon. Anthracite is the product of transition stage between bituminous and graphite where the volatile constituents of the former are completely eliminated.
- Graphite is technically the purest and highest rank of all coal types.

Coal has been shown to be possible carriers for the unidentified infrared bands (UIBs) (Papoular et al., 1993; Guillois et al., 1994). One of the most interesting types of coal is semi-anthracite, which shows an infrared spectrum that mimics the spectrum of UIBs (Guillois et al., 1996, 1999; Cataldo et al., 2002).

# 4.2.2. Aim of the study

The present study analyses graphite, bituminous coal, anthracite and naphthalene samples using a Fourier Transform Infrared (FTIR) spectrophotometer. The resulting infrared spectra are compared with those of astronomical observations. The objective is to determine if these materials can produce infrared absorption wavelengths that mimic the emission spectra of UIBs and protoplanetary nebulae (PPNe). The results could be used to infer the existence of carriers for the unidentified infrared bands (UIBs) and protoplanetary nebulae (PPNe). This study may provide direction to advance research on the complexity of the chemistry of the interstellar medium, and

may lead to a better understanding of the processes which produce key molecules for the development of life.

#### 4.3. Materials and Methods

The following materials were used in the study:

- Graphite was supplied by Agar Scientifics Ltd., UK.
- Both anthracite and bituminous coal were obtained from Geo Supplies Ltd.,
   UK.
- Naphthalene in vacuum sealed bottle was purchased from Sigma Ltd., UK.

All samples were prepared according to the methods as described in detail in Chapter 2. Briefly, the samples were first subjected to vigorous grinding using an agate pestle until fine flour was obtained. The sample (0.2 mg) was embedded in KBr (20 mg). The mixture was then transferred into a small blending mill (SPECAmill TM, Kent, UK) for further grinding. After 10 mins, the mixture was subjected to drying under high vacuum (2x-7MB) for 3-4 hours. The dried sample was subsequently transferred into the Evacuable Pellet Dies (SPECAC Ltd, Kent, UK) to make the KBr disc as described in chapter 2. The resulting KBr disc was analysed using a FTIR spectrometer (JASCO Model FT/IR 660 Plus series).

# 4.4. Results

# 4.4.1. Infrared absorption of Graphite

The FTIR spectrophotometric analysis of graphite embedded in KBr disc produced absorption peaks centered at 2.9, 4.2 and 6.1  $\mu$ m. The spectrum tails off from 6.1  $\mu$ m to form an almost straight line as shown in Fig. 4.1.

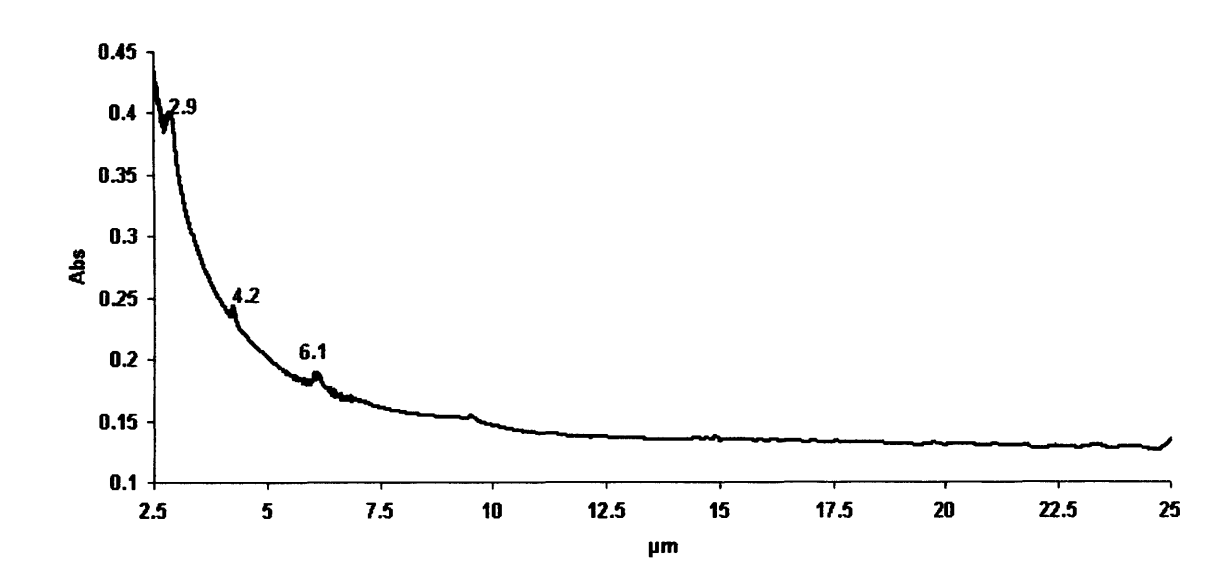


Fig.4.1: Infrared absorption spectrum of KBr-embedded graphite showing low peaks centered at 2.9, 4.2 and  $6.1\mu m$ .

# 4.4.2. Infrared absorption of Anthracite

The FTIR analysis of KBr-embedded anthracite produced an absorption spectrum stretching from 2.5 to 25  $\mu$ m. Absorption peaks were detected with the following wavelengths: 2.9, 3.4, 5.8, 6.2, 6.85, 7.2, 7.7, 8.8, 9.4, 11.3, 12.5, 13.4  $\mu$ m. The strongest absorption bands are centered at 2.9 and 3.4  $\mu$ m. The remaining features appear weak as shown in Fig. 4.2.

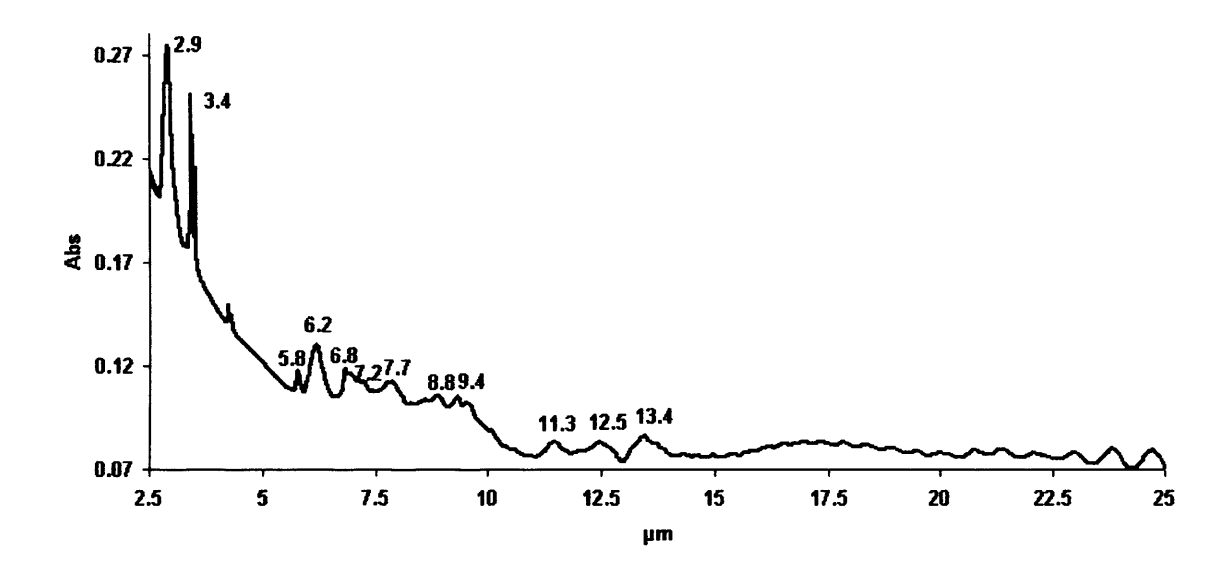


Fig.4.2: FTIR spectrum of KBr embedded anthracite showing a number of distinctive IR absorption peaks.

# 4.4.3. Infrared absorption of Bituminous Coal

The FTIR analysis of bituminous coal shows a broad absorption spectrum stretching from 2.5 to 25  $\mu$ m. Two interesting bands in the near infrared region are located at 3.3  $\mu$ m and 3.4  $\mu$ m flanked by two peaks centered at 3.37 and 3.5  $\mu$ m, respectively (Fig.4.3.a). As shown in Fig.4.3.b, the spectrum also contains three peaks located at 6.2, 6.9 and 7.2  $\mu$ m which match the emission bands of protoplanetary nebulae spectrum (Table 4.3). The broad waveband stretching from 7.2 to 9.6  $\mu$ m displays a series of weaker absorption peaks. Other bands are also detected at 11.5, 12.3, 13.3  $\mu$ m. Furthermore, the spectrum exhibits a peak at 14.4  $\mu$ m which is the characteristic emission band of PPNe. The peaks centered at 18.3, 20.7 and 22.8  $\mu$ m appear broader as shown in Fig.4.3.c.

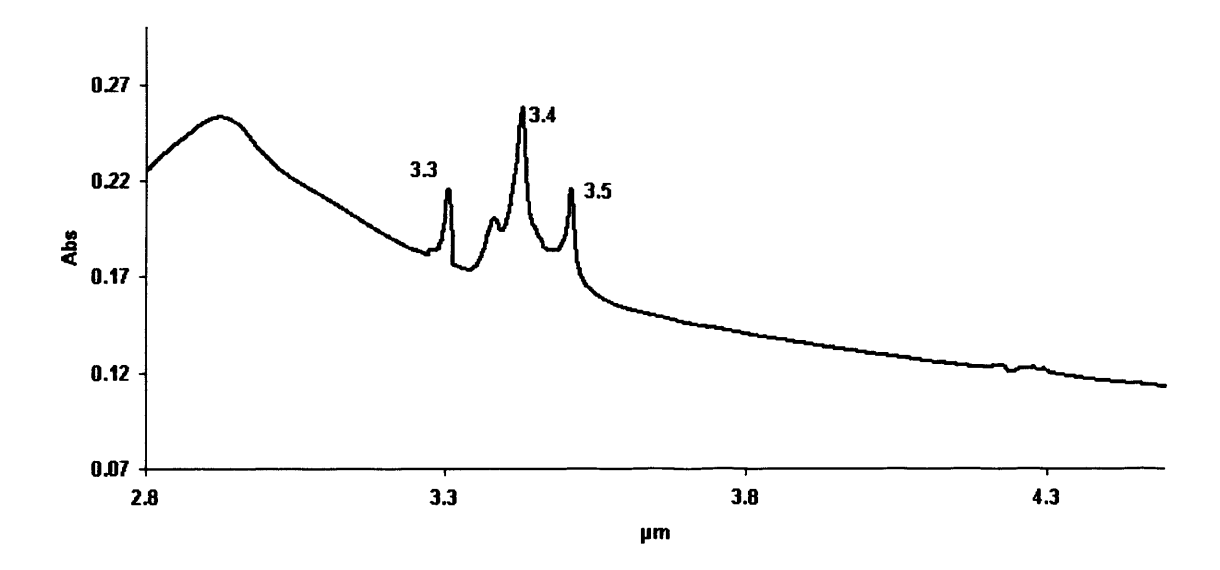


Fig.4.3.a: FTIR spectrum of KBr embedded bituminous coal showing a waveband stretching from 2.8 to 4.5  $\mu$ m. Two major absorption peaks are centered at 3.3 and 3.4  $\mu$ m.

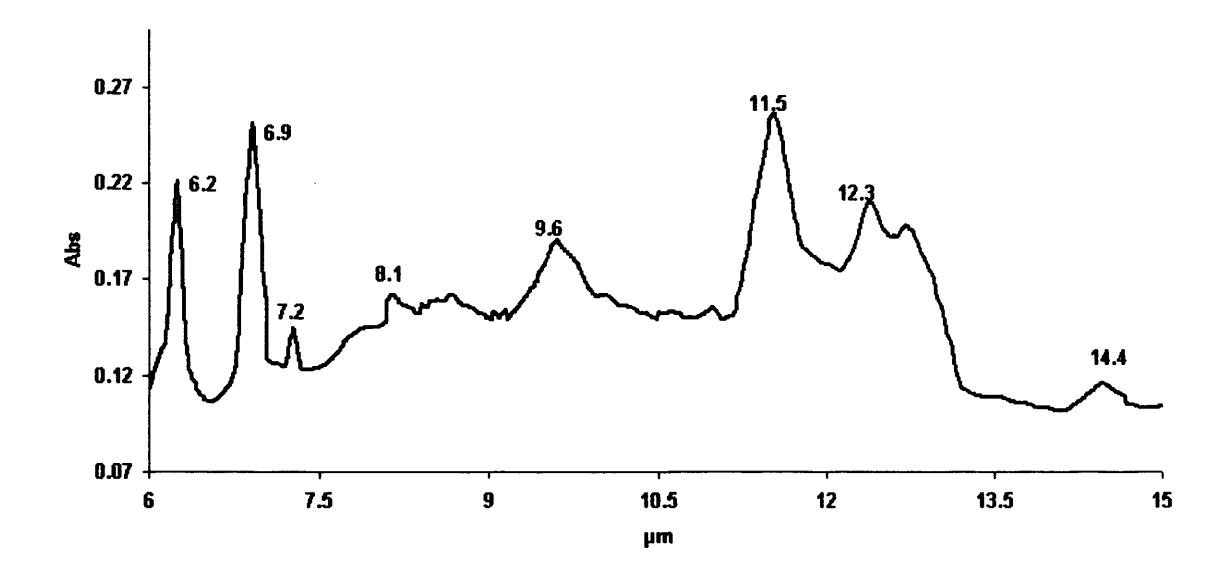


Fig.4.3.b: Expanded FTIR spectrum of bituminous coal showing a waveband in the mid infrared region stretching from 6 to 15  $\mu$ m. The most interesting peaks are centered at 6.2, 6.9, 7.2, 8.1, 8.6, 9.6, 11.5, 12.3, 13.3 and 14.4  $\mu$ m.

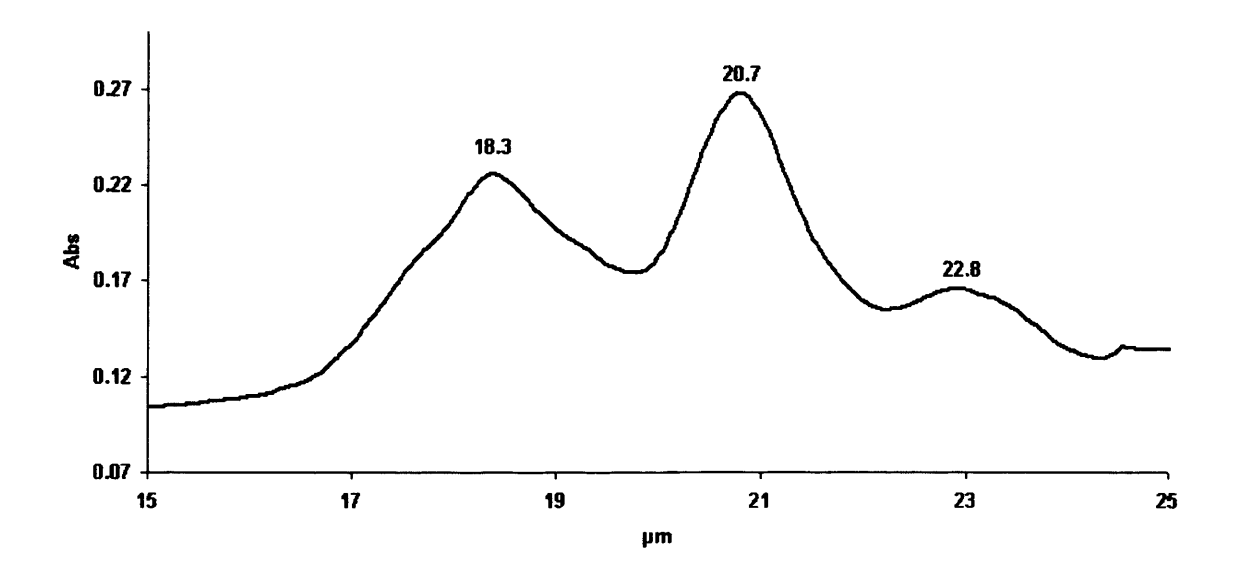


Fig.4.3.c: Bituminous coal FTIR waveband continued from Fig.4.3.b showing a mid infrared region stretching from 15 to 25  $\mu m$ .

# 4.4.4. Infrared absorption of Naphthalene

As shown in Figs. 4.4a, and 4.4b, the spectrum of naphthalene exhibits a series of absorption features located at 3.3, 6.2, 6.65, 7.2, 7.34, 7.87, 8.0, 8.27, 8.6, 8.9, 9.9, 10.4, 11.8, 12.8, 16.2, 20.7 and 21.2  $\mu$ m.

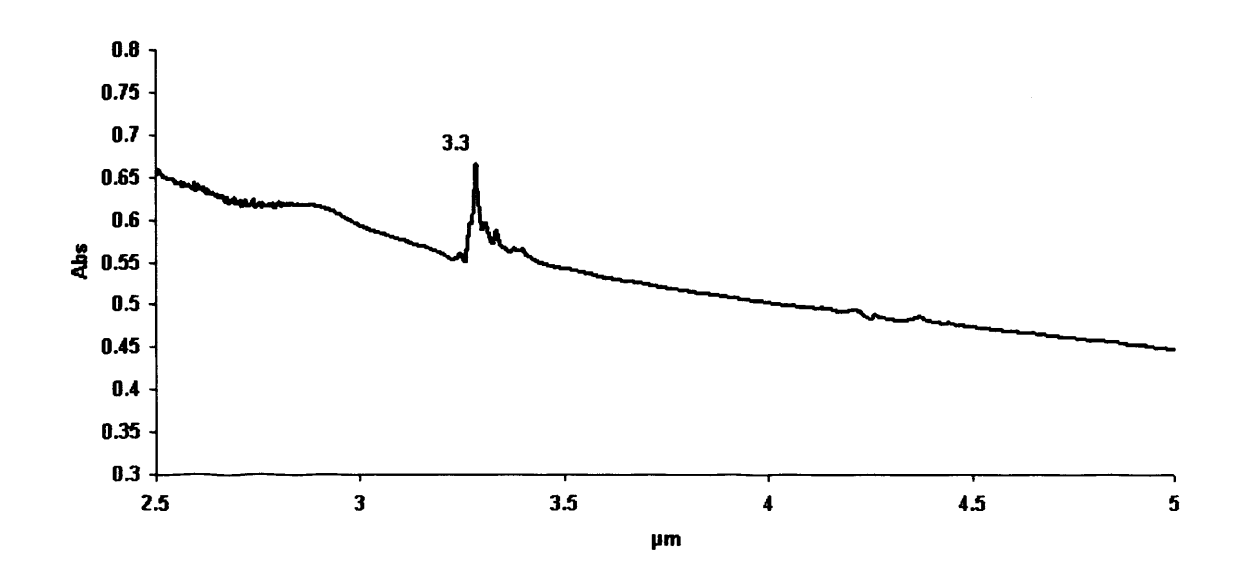


Fig.4.4.a: Naphthalene waveband showing a feature centered at 3.3 μm.

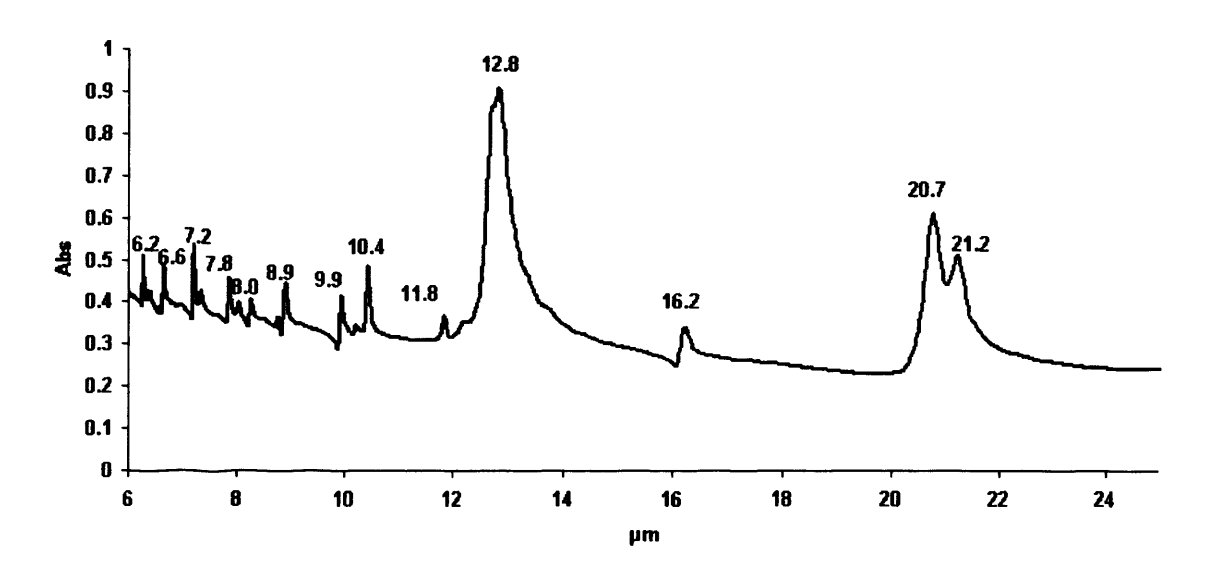


Fig.4.4.b: Continued waveband of naphthalene showing a series of peaks centered at 6.2, 6.65, 7.2, 7.34, 7.87, 8.0, 8.27, 8.6, 8.9, 9.9, 10.4, 11.8, 12.8, 16.2, 20.7 and 21.2  $\mu m$ .

Table 4.1: Spectroscopical detection of infrared absorption bands in laboratory models. The figures represent wavelength  $(\mu m)$  of the bands.

Bituminous coal	Anthracite coal	Graphite	Naphthalene
2.9	2.9	2.9	
3.3			3.3
3.4	3.4		
3.5	3.5		
		4.2	
5.8	5.8		
6.2	6.2	6.1	6.2
			6.65
6.9	6.85		
7.2	7.2		7.2
			7.34
	7.7		
			7.87
8.1			8.0
			8.27
8.6			8.6
	8.8		
			8.9
	9.4		
9.6	9.6		
			9.9
			10.4
11.5	11.3		
			11.8
12.3	12.5		
			12.8
13.3	13.4		
14.4			
			16.2
18.3			
			20.7
20.7			21.2
22.8			
24.5			

Table 4.2: Nature of unidentified infrared bands (UIBs) and emission bands of protoplanetary nebulae (PPNe)

Astronomical		Nature of	Modes		References
observat	io <u>n</u> s	components			
UIBs	PPNe		СН	CC	
3.3	3.3	aromatic	Stretching		Dulley and Williams, 1981;
-	3.4	aliphatic	Stretching		Joblin et al., 1995; Sloan et al.,
6.2	6.2	aromatic		stretching	1999; Hudgins and Allamanola,
-	6.9	aliphatic	Stretching		1997; Chiar et al., 2006;
-	7.2	aliphatic			Reynaud et al., 2001; Cataldo et
7.7	7.7	aromatic		stretching	al., 2004; Mulas et al., 2006;
-	8.0	aromatic			Kwok, 2009; Rauf and
8.6	8.6	aromatic	in plane bend		Wickramasinghe, 2010.
11.3	11.3	aromatic	out of plane		
			bend(wagging)		
-	12.2	aromatic	out of plane		
			bend(wagging)		
_	13.3	aromatic	out of plane		
			bend		

Table 4.3: Distribution of two astronomical observations (UIBs and PPNe) and major infrared absorption bands produced by laboratory models of terrestrial origin.

UIBs	PPNe	Bituminous coal	Anthracite coal	Naphthalene
3.3	3.3	3.3	-	3.3
-	3.4	3.4	3.4	-
6.2	6.2	6.2	6.2	6.2
-	6.9	6.9	6.8	-
-	7.2	7.2	7.2	7.2
7.7	7.7	-	7.7	-
-	8.0	8.1	-	8.0
8.6	8.6	8.6	-	8.6
11.3	11.3	11.5	11.3	-
-	12.2	12.3	12.5	-
-	13.3	13.3	13.4	-

### 4.5. Discussion

The macromolecular structure of coal has been well documented as being made of layers of condensed polycyclic aromatic rings containing both naphtenic and aliphatic chains (Van Krevelen, 1993). Formed by compression of peat material, bituminous coal is one of the lowest ranks of coal after lignite; it is composed of a mixture of molecules different in size and composition, and becomes soft at relatively low temperatures (Cataldo et al., 2004).

Coal in general and anthracite in particular have been suggested as components of interstellar carbon dust (Guillois et al., 1999), and as the carrier of UIBs (Cataldo et al., 2003). Earlier studies of coal by IR absorbance spectroscopy have shown that this material displays a broad spectral continuum. Papoular et al. (1993) reported that raw coal in general shows IR bands at 2.7-3.1, 3.3, 3.4, 5.25, 5.7, 6.0, 6.2, 6.9, 7.5-9, 9-10, 11.3, 12.3, 13.3, and 18-23 µm and that the wavelengths of the bands depend on the rank and heat treatment of the coal. Their study demonstrated further that the -OH blend (2.7-3.1) and that of mineral (9-10 and 18-23) µm disappear from the spectrum, and that the intensity of absorption peak at 6.9 µm is also reduced if the coal is demineralised and mildly heated. These observations seem to confirm that heat is the accelerating factor in the evolution of coal. According to Papoular et al. (1993), the spectra of coal showed loss of OH groups and a significant reduction in aliphatic C-H if the coal is heated at 600 °C and a further decrease in the aromatic C-H groups when the coal is allowed to progress towards graphitisation at a temperature reaching up to 700 °C. Thus, the graphitisation of coal involves high temperature and is accompanied by aromatisation of carbon atoms.

The present study used Fourier Transform Infrared Spectroscopy to examine four compounds: graphite, bituminous coal (semi anthracite coal), anthracite and naphthalene. Their IR absorption bands were compared with the emission spectra of unidentified infrared bands (UIBs) and protoplanetary nebulae (PPNe). The objective was to determine whether their infrared (IR) bands have the same wavelengths as those of astronomical observations. This comparative study could provide tests for the carriers for the interstellar bands. The results show that amongst all laboratory

compounds tested, graphite fitted least well, containing only three significant infrared absorption features centered at 2.9, 4.2 and 6.1 µm, which do not match those of any interstellar spectra. The present study used pure graphite as a control showing no IR absorption features comparable to interstellar emission bands. Thus, the results obtained from the IR spectroscopical analysis of graphite confirm the view of Mathis and Whiffen (1989) and Wickramasinghe et al. (1992) that graphite crystals are not likely to form under the interstellar or circumstellar conditions. However, it is reasonable to argue that although pure graphite grains are not expected to be present in the interstellar or circumstellar environments, the graphite-like coal may be present in the interstellar medium (ISM), resulting from the degradation of biological cells in the panspermia model.

The present study also shows that both bituminous and anthracite coal produced a broad spectral continuum. However, the spectrum of the former contains more absorption features than that of the latter (Table 4.1, Figs.4.3.a, 4.3.b & 4.3.c). Bituminous coal exhibits an IR spectrum with absorption features centered at 2.9, 3.3, 3.4, 3.5, 5.8, 6.2, 6.9, 7.2, 8.1, 8.6, 9.6, 11.5, 12.3, 14.4, 18.3, 20.7, 22.8 and 24.5  $\mu$ m. In comparison with the bituminous coal, anthracite produces a reduced number of infrared bands located at 2.9, 3.4, 3.5, 6.2, 6.8, 7.2, 7.7, 8.8, 9.4, 11.3, 12.5 and 13.4  $\mu$ m (Table 4.1, Fig.4.2). On the other hand, naphthalene which is the petroleum refinement product, has been found to exhibit a much higher number of features centered at 3.3, 6.2, 6.65, 7.2, 7.34, 7.87, 8.0, 8.27, 8.6, 8.9, 9.9, 10.4, 11.8, 12.8, 16.2, 20.7 and 21.2  $\mu$ m (Table 4.1, Figs.4.4.a & 4.4.b).

Earlier studies have proposed that the astronomical feature centered at 3.3μm is attributed to the C-H stretching mode of aromatic hydrocarbons as shown in Table 4.2. The 3.3μm C-H stretch band is a blend of at least two features that involve one being aromatic at 3.286 μm and the other, alkenic (CH<sub>2</sub>) at 3.314 μm, and this aromatic blend is dominant in interstellar space (Papoular et al., 1993). Interestingly, detailed observations made by Joblin et al. (1995) of the emission spectrum of planetary nebulae IRAS 21282+5050 reveal the presence of a 3.3 μm major band as well as additional bands centred at 3.4, 3.46, 3.57 μm. According to Barker et al. (1987) the major band at 3.4 μm was proposed to be the band of the C-H aromatic stretching mode.

Both bituminous coal and anthracite used in the present study produced the features located at 6.2 µm and 6.9 µm whereas the spectrum of naphthalene displayed the 6.2 μm but lacked the 6.9 μm. As proposed by Cataldo and Keheyan (2003), the strong bands at 6.2 and 6.9 µm are caused by the aromatic ring stretching. The 6.9 µm band is related to CH<sub>2</sub> and CH<sub>3</sub> groups (Papoular et al., 1993). As shown by the present study, the IR absorptions of bituminous coal match those of UIBs and PPNe, and these findings suggest that this type of coal is a perfect model to date for these astronomical bands (Table 4.3). According to Fuller (1992), these bands are assigned to C-O-C, C-O-H and C-C-O stretching and or bending modes. Furthermore, the bituminous coal tested in the present study produced the bands at 9.6 and 18.3, 20.7, 22.8 µm and their presence seems to suggest that this type of coal contains minerals since those far-infrared bands located at 9-10 and 18-23 µm have been attributed to minerals (Papoular et al., 1993). The infrared bands of bituminous coal located at 11.5-12.3 µm fall within the range of 11.3- 12.4 µm which have been ascribed to the C-H wagging of aromatic compounds. The band expressed by the bituminous coal at 12.4 µm is near 12.2 µm of the out-of-plane C-H bending feature of semi anthracite and lower ranking coals (Hudgins and Allamanola, 1997; Kwok, 2009). Moreover, the weaker band at 14.4 µm (Table 4.1) confirms the presence of hydrogenated compounds in the bituminous coal as these highly hydrogenated rings are reported to exhibit this band (Hudgins and Allamanola, 1997; Cataldo et al., 2004; Kwok, 2009).

The results as described above thus confirm that many IR features of the absorption spectra found in bituminous coal, anthracite coal and naphthalene correspond to the major unidentified infrared bands (UIBs) in the interstellar medium and protoplanetary (PPNe) (Table 4.3). These findings seem to agree with the earlier proposal that coal, which belongs to a group of natural materials of terrestrial origin, is the most suitable for the interpretation of emission spectra of different circumstellar and interstellar emission bands (Papoular et al., 1993; Guillois et al., 1999; Reynaud et al., 2001) and in particular, bituminous coal for the dark material on the surface of comets and meteorites (Moroz et al., 1998). As proposed by Papoular et al. (1993) since coal, petroleum and bitumen are found on Earth, these materials are also expected to be present in space, in particular on comets and meteorites.

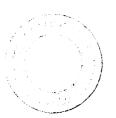
On the subject of naphthalene, Snow (1992) and Krelowski et al. (2001) attempted to search for naphthalene in the interstellar medium but their search proved inconclusive (Iglesias-Groth et al., 2008). The present study however reveals a number of strong peaks centered at 3.3, 12.8, 20.7 and 21.2  $\mu$ m and other much weaker bands from 6.0 to 25  $\mu$ m in an expanded spectrum of naphthalene as shown in Figs.4.4.a & 4.4.b. A set of similar features was also detected in naphthalene by Mulas et al. (2006).

The present study supports unequivocally the early proposal that certain types of coal are suitable models for the interpretation of carriers for the emission spectra of PPNe and UIBs. The evidence obtained from the present study confirms that bituminous coal (or semi-anthracite) is the best fit, and this is based on its absorption spectrum containing the highest number of strong features that match those of PPNe and UIBs. Pure anthracite on the other hand is found to be the least suitable because its matching absorption peaks are weaker than those of bituminous coal. Furthermore, naphthalene is less suitable than both types of coal due to the lower number of its matching peaks for PPNe and UIBs although it produces more absorption bands than its counterparts.

Combined with result of investigations of algae discussed in chapter 3 it is possible to assert that algae and the ultimate degradation product -coal- together provide a good model for the PPNe feature and the UIBs in general.

# **CHAPTER 5:**

A Proposed Ensemble of
Degraded and Non-Degraded
Biomaterials as a Carrier of the
217.5 nm (2175 Å) Interstellar
Extinction Feature



# 5.1. Summary

The interstellar absorption band centered at 217.5 nm (2175 Å), conventionally attributed to monodisperse graphite spheres of 20 nm radius, is more plausibly explained as arising from biologically derived aromatic molecules. On the basis of panspermia models interstellar dust includes a substantial fraction of biomaterials in various stages of degradation. The present study has modeled such an ensemble of degraded and non-degraded biomaterials with laboratory spectroscopy of algae, seaweed, grass pigments, naphthalene, bituminous coal and anthracite. The averaged ultraviolet absorption profile for these materials centred at 217.5 nm (2175 Å) with a FWHM of 25 nm (250 Å), is in full agreement with the interstellar extinction observations.

#### 5.2. Introduction

#### 5.2.1. Interstellar dust and its extinction curve

Interstellar dust has been suggested to play an important role in the evolution of galaxies and the formation of stars and planetary system (Wang et al., 2004). The space between the stars of the Galaxy and external galaxies is rich in dust grains of different sizes. According to Trumpler (1930), distant stars appeared dimmed, and the interstellar space in the galactic plane was occupied largely by fine cosmic dust particles of various sizes resulting in the selective absorption. The size and composition of interstellar dust are determined respectively by the extinction curve and its spectral features (Draine, 2003). The extinction curves have been studied in a number of galaxies (Wang et al., 2005), and the best quantitatively measured ones are related to the Milky Way galaxy (Fitzpatrick and Massa, 1986; Cardelli et al., 1989) and to both, the Large (Koornneef and Code, 1981; Misselt et al., 1999), and the Small Magellanic Cloud (Lequeux et al., 1982; Prevot et al., 1984).

An interstellar absorption band centred at 217.5 nm (2175 Å) with a half-width at full maximum of  $\sim 25$  nm (250 Å) was discovered in the spectra of most reddened stars, and the average interstellar extinction curve showing this feature is shown in Fig.5.1

(Stecher, 1965; Wickramasinghe, 1967). According to Hoyle and Wickramasinghe (2000) and Wickramasinghe et al. (2010), the observed extinction curve is in theory decomposed into three components: (i) component 1 corresponds to scattering by dielectric grains with sizes and properties resembling bacteria, (ii) component 2 is the extinction caused by an absorber that produces the mid-ultraviolet band, and (iii) component 3 represents a population of nanometric-sized dielectric particles.

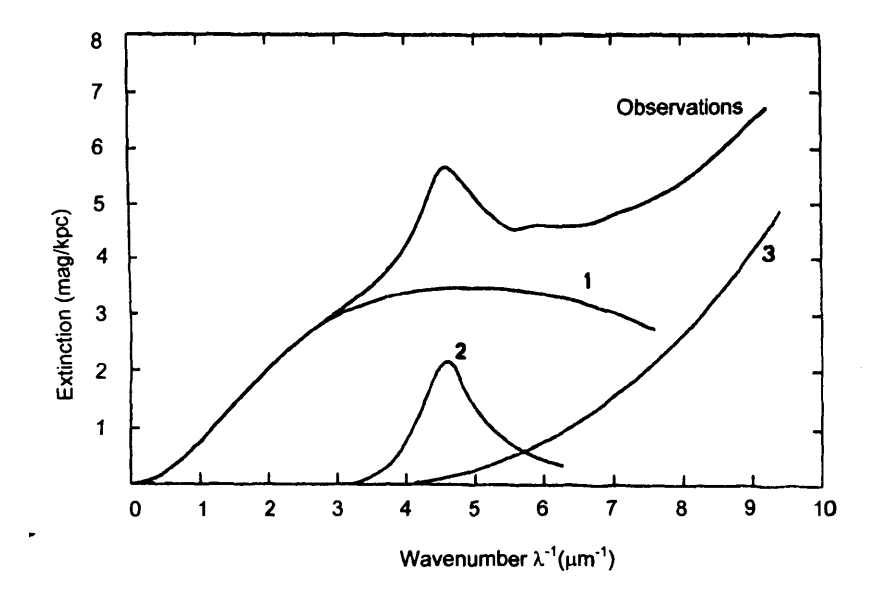


Fig.5.1: Interstellar extinction curves. (1) A composite of dielectric grains of radii 0.3μm; (2) molecular absorption due to aromatics; (3) dielectric particles of radii 0.01μm. (from Sapaar and Kuusik, 1978)

The averaged extinction curve for dust in the solar surroundings is well represented by the uppermost curve in Fig.5.1. However, stars in other regions of the galaxy and in external galaxies show a modest degree of variability which is consistent with varying proportions of the components 1, 2 and 3. Furthermore, Fig.5.2 illustrates how individual stars show varying relative amounts of the 217.5 nm (2175 Å) carrier. Boulanger et al. (1994) also discuss the correlation between the strength of the UV absorption peak and mid-infrared emission bands which could be interpreted as arising from a common molecular carrier (Hoyle and Wickramasinghe, 1989).

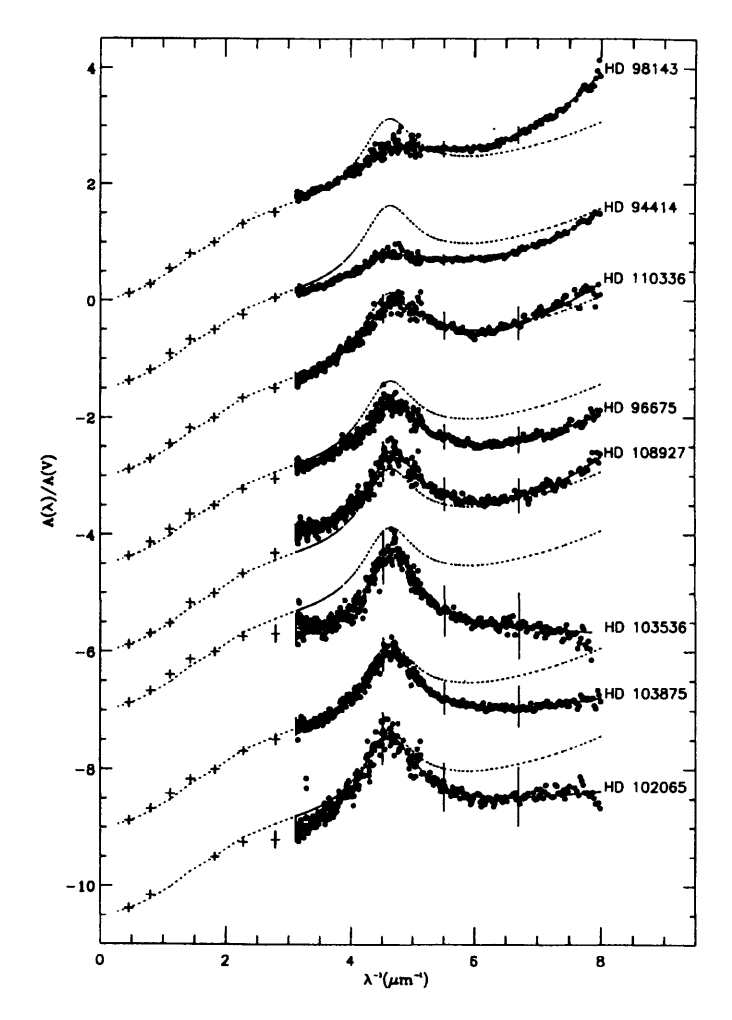


Fig.5.2: Normalised interstellar extinction curves for stars in our Galaxy showing varying strengths of the 2175 Å absorption feature. Crosses and dashed curve represent mean interstellar extinction (adapted from Boulanger et al., 1994).

#### 5.2.2. The extinction curve feature and its carrier

Our knowledge about interstellar grains comes from observations of features in their emission, polarization, and absorption spectra (Fitzpatrick and Massa, 1990; Sanford, 1996; Bradley, 2005). A prominent feature in the interstellar extinction curve was first detected by the Aerobee rocket observations (Stecher, 1965; Wang et al., 2004), and later observed by the International Ultraviolet Explorer (IUE) satellite (Stecher, 1969). This strongest feature is observed at 217.5 nm (2175 Å) in the range of UV-visible wavelengths (Fitzpatrick and Massa, 1990; Bradley, 2005). The dust extinction feature in the Milky Way is also believed to be the strongest of all with a broad bandwidth (≤25 nm) and a wavelength of 217.5 nm, corresponding to 4.6 μm<sup>-1</sup> or 5.7 eV.

While showing an almost unchanged central wavelength, this feature has a bandwidth that is variable from one line of sight to another, thus indicative of multiple carriers or a single carrier with different properties. As proposed by Steel and Duley (1987) and Sanford (1996), the carrier may be either oxygen-rich (e.g., oxides or silicates) or carbon-rich (e.g., graphite or organic compounds). However, the exact carrier responsible for this feature is still controversial. According to Kwok (2009), the strength of the feature depends on the amount of chemical elements present such as C, Mg, Si, Fe, etc, and the carrier of this feature must contain at least one of these elements (Wang et al., 2004). This view has been further supported by the suggestion that some form of graphitic carbon may be responsible for this feature (Draine, 2003), and most likely to be of polycyclic aromatic hydrocarbons (Joblin et al., 1992; Rouleau et al., 1997). Furthermore, photo- reflective measurements of anthracite produce a feature close to 217.5 nm, suggesting that this feature probably arises from a complex carbonaceous compound (Kwok, 2009).

#### 5.2.3. Dust models

A number of carbon models have been proposed to reproduce the 217.5 nm (2175 Å) interstellar extinction band. These consist of two different groups based on their ordered or disordered solid structure. The former is made up of randomly oriented pure graphite spheres (Draine and Lee, 1984). Sakata et al. (1983) synthesized a quenched carbonaceous composite material known as QCC that exhibited a UV absorption near 2000 Å (Papoular and Papoular, 2009), and proposed it as the disordered carbon model for the 217.5 nm (2175 Å).

Some recent models of interstellar dust include an abiotic PAH component that could produce a  $\lambda$  2175 Å absorption band under appropriate circumstances (Witt et al., 2006). However, for PAH's and other complex organic molecules to form abiotically may pose serious problems, in particular with the requirement that compact PAH's are in high ionisation states. An alternative model that fits the general context of panspermia is that organic dust and molecules in interstellar space may include a substantial component derived from biology itself. According to this point of view microbial cells replicate in liquid interiors of primordial comets and are distributed

widely across the galaxy (Wickramasinghe et al., 2010). As suggested by Rauf and Wickramasinghe (2010), interstellar material would include the detritus of biologymicrobial cells in various stages of degradation and break-up, and thus degradation of cells in H II regions and in other high radiation environments is inevitable. Whilst wholesale destruction if it occurs would vitiate a panspermia model, the requirement for panspermia to operate unhindered is that a fraction, less than one part in  $10^{20}$ , survives from one amplification site to the next; and this condition would seem impossible to violate (Wickramasinghe et al., 2010).

# 5.2.4. Aim of the study

The present study is primarily concerned with the precise position of a 2175 Å absorption feature. It sets out to perform spectroscopic analyses using a JASCO V-570 UV/VIS/NIR spectrophotometer on a number of biomaterials. The objective is to determine whether any of the models produces a feature that perfectly fits the interstellar extinction observation of 217.5 nm. The results could give an insight into their absorption properties and hence into the nature of their degradation from the astrobiological perspective.

#### 5.3. Materials and Methods

#### 5.3.1. Materials

In order to model the effects of sequential degradation, the present study took algal cells, seaweed and grass as a starting point, and measured their absorption properties as well as those of several other degraded biological products. The sources of the materials were as follows:

- 1. *Oedogonium sp.* (a fresh water species of green algae) collected from Roath Park, Cardiff, Wales, UK.
- 2. Enteromopha intestinalis (green seaweed) and Pelvetia canaliculata (brown seaweed), collected from Barry Island, Wales, Cardiff.

- 3. Grass from Santa Cruz Island of the Galapagos provisionally identified as *Panicum* maximum.
- 4. Naphthalene in vacuum sealed ampoule was supplied by Sigma Ltd, UK.
- 5. Bituminous coal (semi-anthracite) and anthracite were obtained from Geo Supplies Ltd., UK.

Samples (5) represent the last stages in a putative biodegradation sequence.

#### 5.3.2. Methods of sample mounting and preparation

The samples were dissolved in cyclohexane, a non-polar solvent. Algae, seaweed, grass, naphthalene, semi-anthracite and anthracite (approximately 70 mg in each case) were individually added to cyclohexane (500  $\mu$ l) and dissolved. The use of a non-polar solvent eliminates the effect of wavelength-shifts. All samples were agitated for a few minutes and allowed to stand still on the bench for 15 min to allow the sedimentation to complete. A clear solution (100  $\mu$ l) was carefully pipetted out from the top and placed in a test-tube containing the solvent (3.5 ml). The tube was briefly agitated and transferred into a spectrophotometer (JASCO V-570 UV/VIS/NIR spectrophotometer).

#### 5.4. Results

Figures 5.3 - 5.9 show ultraviolet spectra of algae, grass, seaweed species, semi-anthracite (bituminous coal), anthracite and naphthalene respectively. Fig. 5.10 shows the normalized (averaged) absorption spectrum of the whole sequence. Algae produced a band of 3 major peaks located at 216, 427 and 662 nm (Fig. 5.3) while grass gave a band containing a peak centered at 216 nm (Fig. 5.4). *Enteromopha intestinalis* (green seaweed) produced a waveband with 3 prominent peaks centred at 215.5, 413.0 and 667.0 nm whereas *Pelvetia canaliculata* (brown seaweed) displayed a spectral pattern with peaks of almost similar wavelengths 216.0, 413.5 and 667.5 nm (Figs. 5.5 & 5.6). Algae and the two seaweed species used in the present study produced additional peaks with a broader bandwidth. These peaks are located within the waveband stretching from 413.0 nm to 667.5 nm. The additional absorption bands

correspond to those of chlorophyll pigments which are generally within the waveband of 410-673 nm (RayChaudhuri and Bhattacharyya, 2008).

Both anthracite and semi-anthracite show a band with two peaks, the strongest at 213 nm and the less intense at 274 nm (Figs. 5.7 & 5.8). Naphtahlene on the other hand shows a prominent peak at 220.5 nm (Fig. 5.9). Figure 5.10 represents the normalized (averaged) absorption spectrum of the whole sequence. The normalised UV-Vis spectrum produces a peak centered precisely at 217.5 nm (2175 Å) which corresponds with the interstellar extinction observation (Figs. 5.1 & 5.2). The full width at half maximum (FWHM) of 25 nm (250 Å) also agrees with that of the interstellar absorption feature.

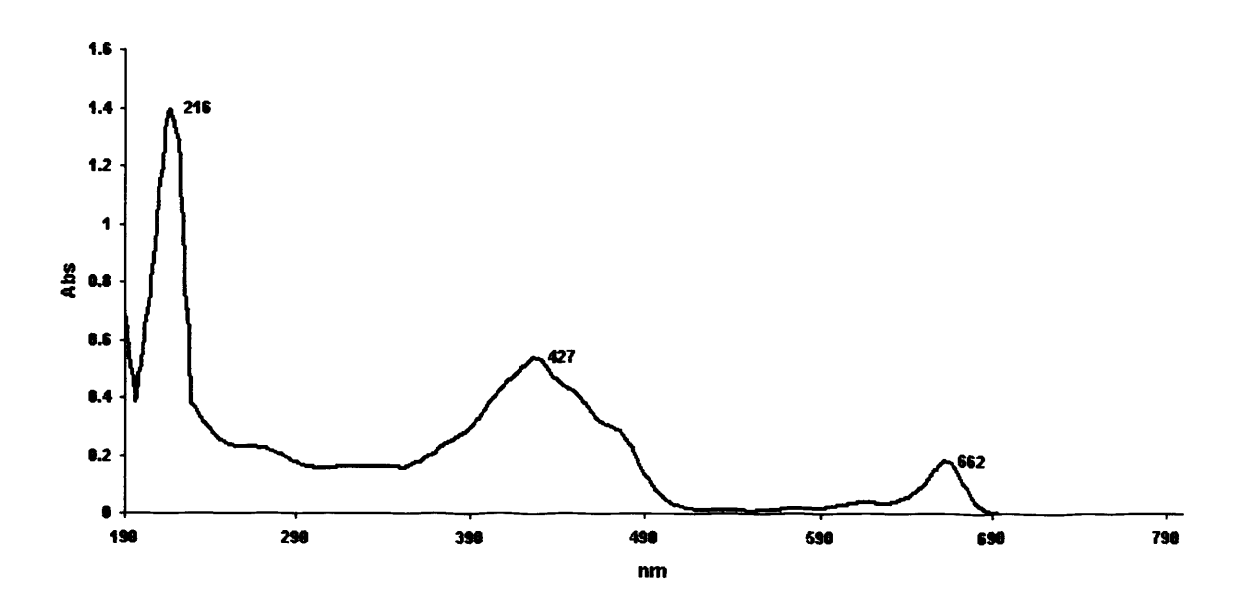


Fig.5.3: UV-Vis spectrum of algae dissolved in cyclohexane.

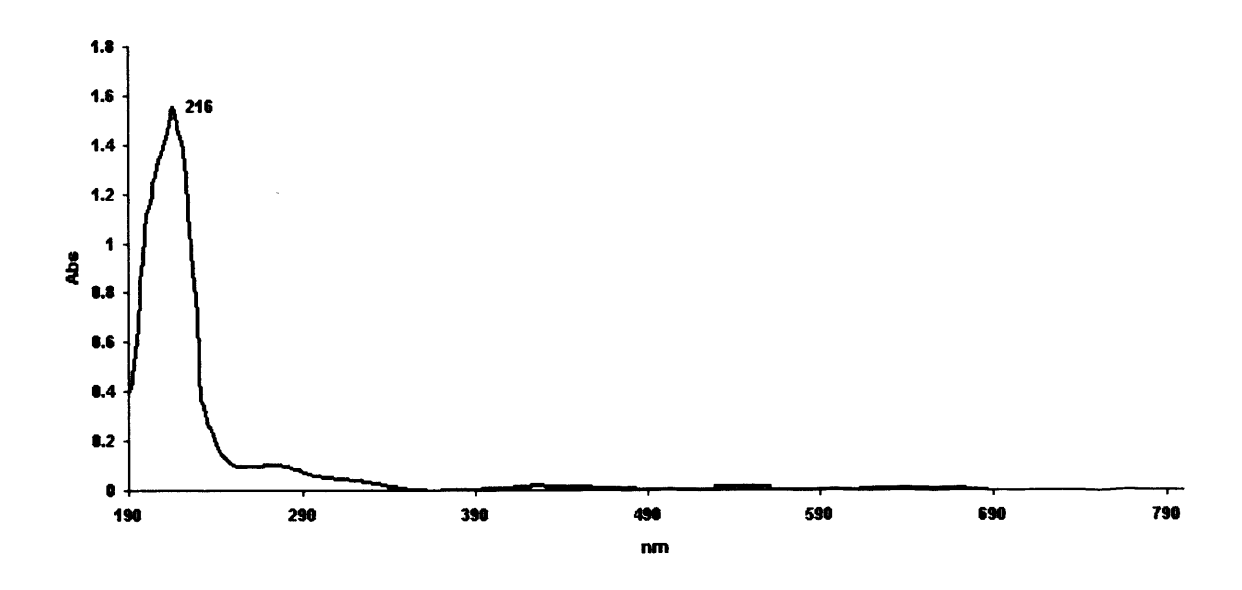


Fig.5.4: UV-Vis spectrum of grass (Panicum maximum) dissolved in cyclohexane.

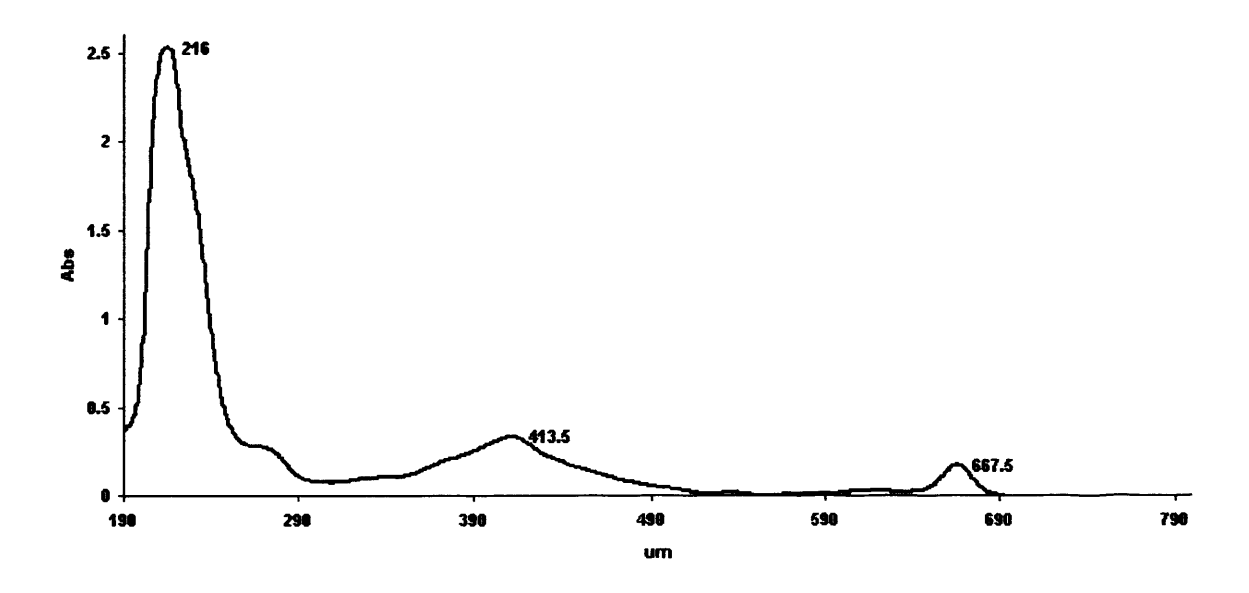


Fig.5.5: UV-Vis spectrum of *Pelvetia canaliculata* (brown seaweed) dissolved in cyclohexane.

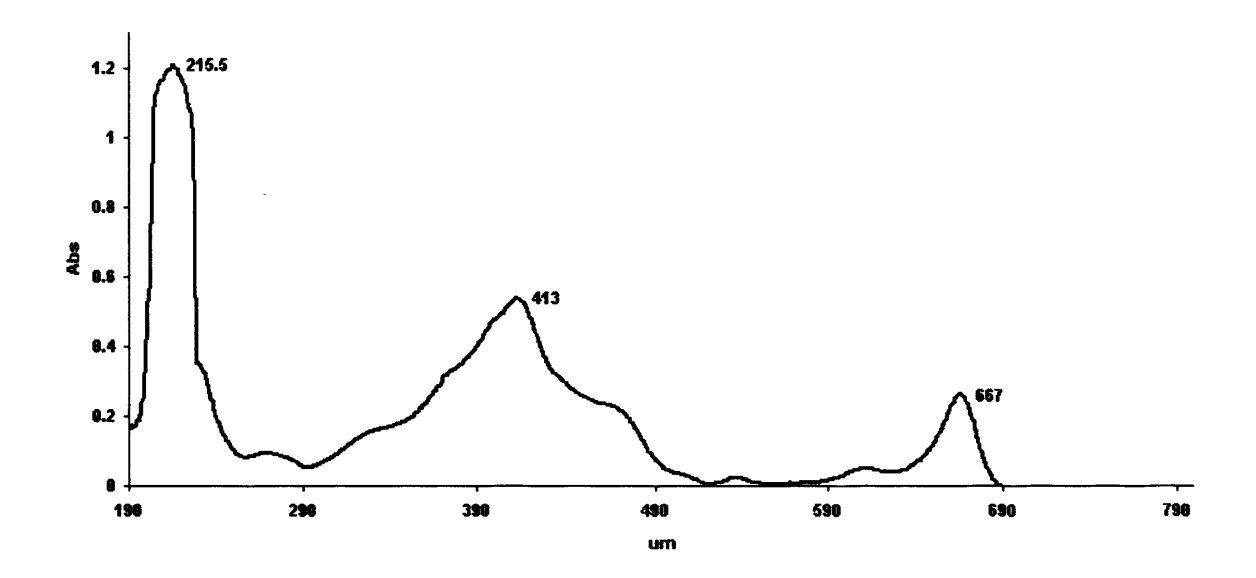


Fig.5.6: UV-Vis spectrum of *Enteromopha intestinalis* (green seaweed) dissolved in cyclohexane.

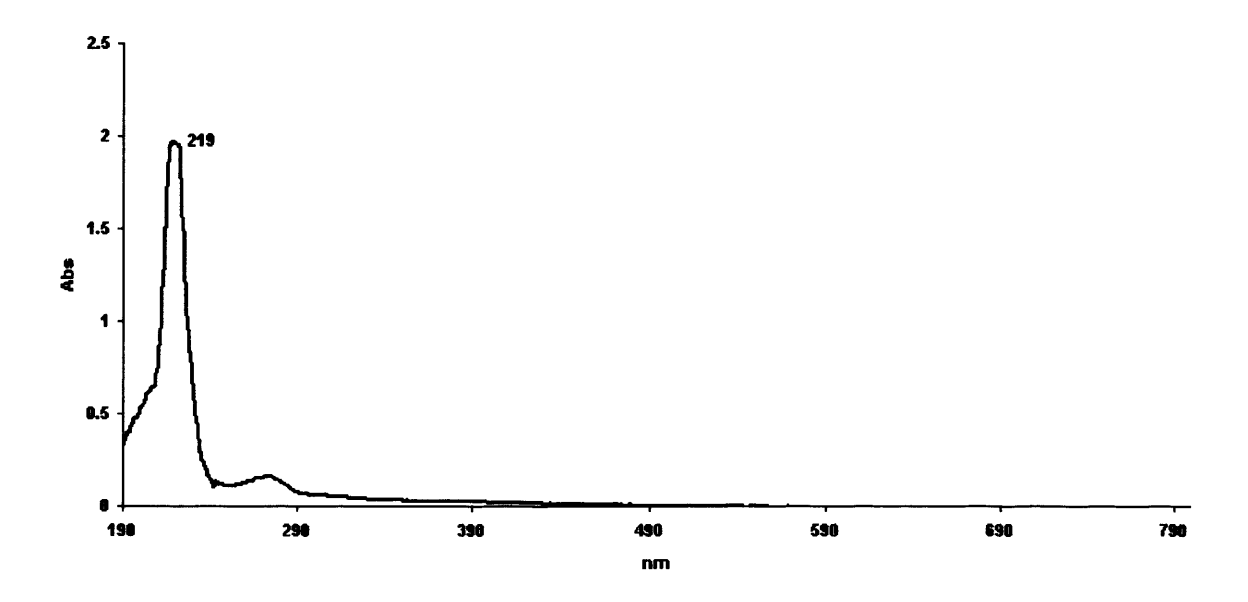


Fig.5.7: UV-Vis spectrum of semi-anthracite dissolved in cyclohexane.

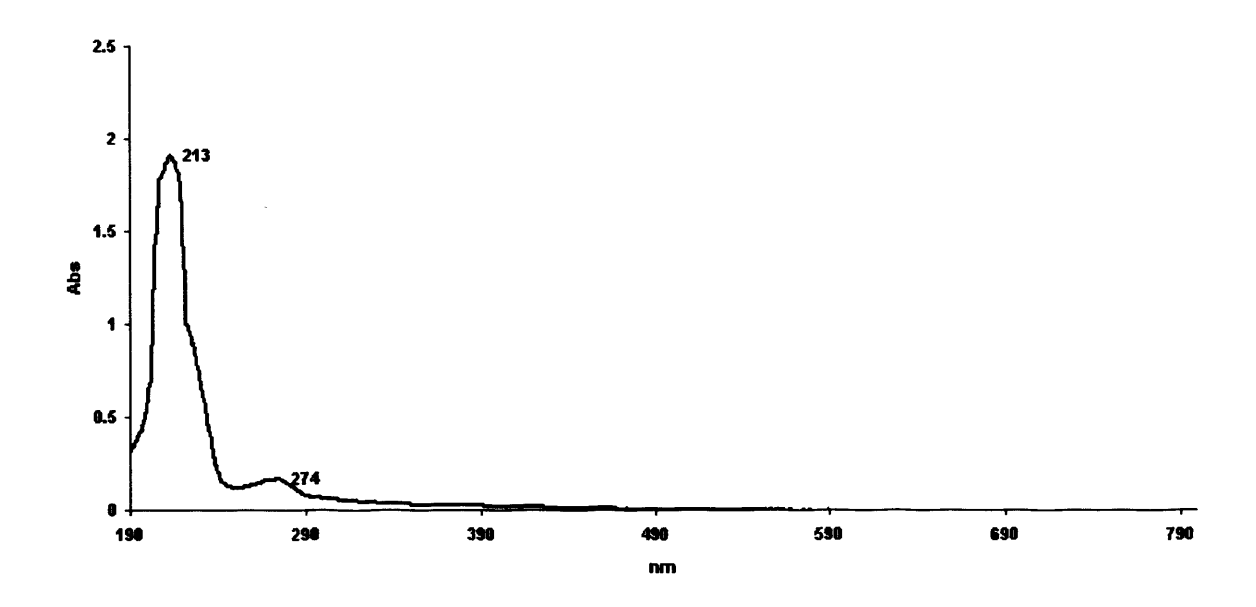


Fig.5.8: UV-Vis spectrum of anthracite dissolved in cyclohexane.

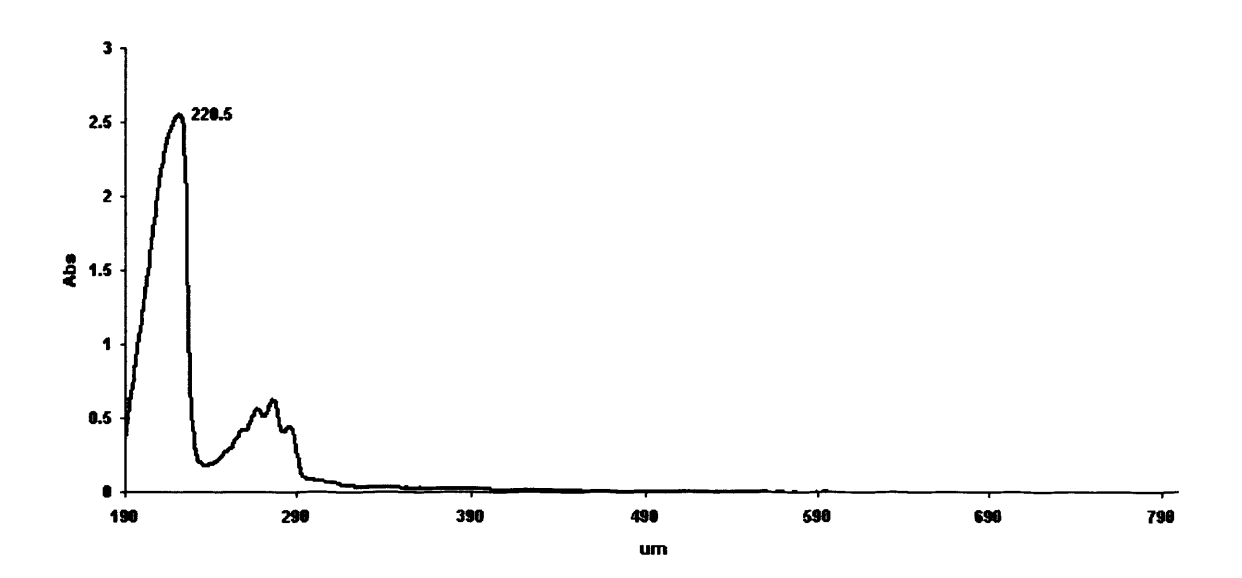


Fig.5.9: UV-Vis spectrum of naphthalene dissolved in cyclohexane.

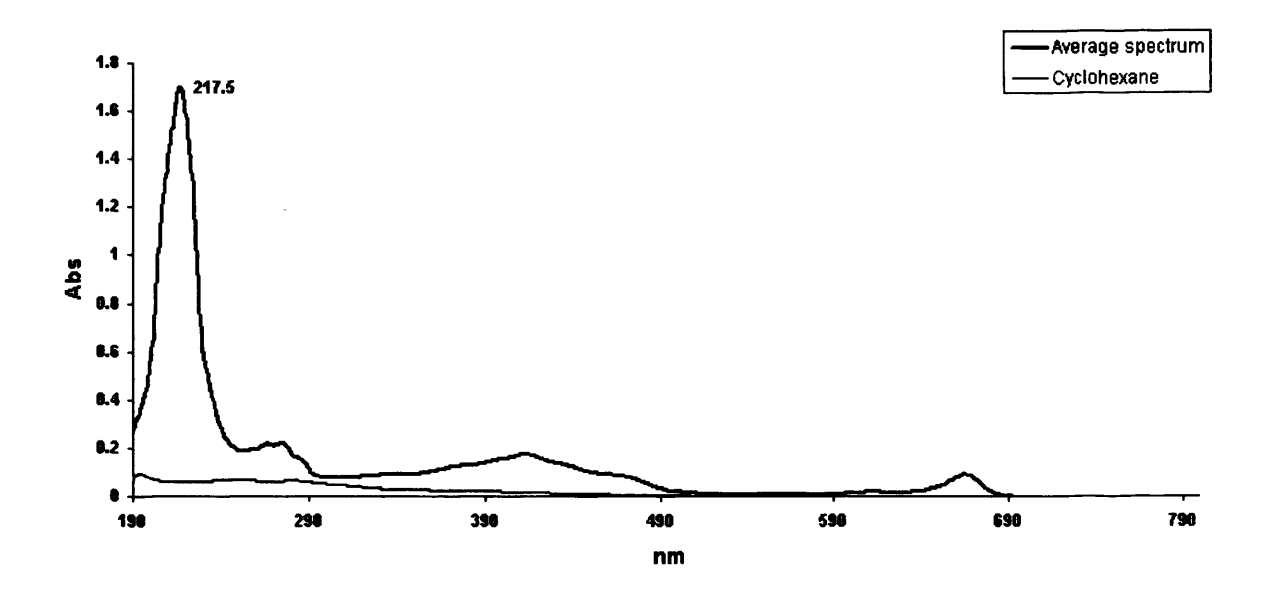


Fig.5.10: Averaged spectrum of a putative interstellar microbiota in various stages of degradation.

# 5.5. Discussion

Study of the UV spectra of stars have revealed a new molecular component associated with interstellar dust. Stecher (1965) first discovered an intense feature in the spectrum of interstellar dust, and the central peak was located at  $\lambda^{-1} = 4.6 \, \mu \text{m}^{-1}$ , or  $\lambda =$ 2175 Å. As pointed out by Draine, (2003), this feature was observed in many different dust clouds; and whilst the center of the peak was always exactly at 217.5 nm (2175 Å), the peak width of the feature varied from one region to another. Draine (1989) suggested that on the basis of the strength of this feature, the material responsible for this absorption must be abundant and that it must be made from H, C, N, O, Mg, Si, S, or Fe. On the other hand, Stecher and Donn (1965) suggested that the feature could be due to the presence of small graphite particles which would have a strong absorption peak due to  $\pi \to \pi^*$  electronic excitations. Furthermore, Draine (2003) proposed that as the carbon skeleton that composes polycyclic aromatic hydrocarbon (PAH) molecules resembles a portion of a graphite sheet, such molecules also are inclined to have strong electronic transitions, and therefore it is likely that the 217.5 nm (2175 Å) feature is due to some form of carbon material. As cited from Duley and Seahra (1998), Gilra (1972) studied the effect of particle size and shape and showed that interstellar graphite particles must be spherical and must have a radius of 20 nm in order to produce the 217.5 nm (2175 Å) feature. Although earlier studies showed that graphite particles could be constructed to fit the profile of the feature, Czyzak et al. (1982) argued that it would be unlikely that crystalline graphite particles could form with the size and shape to match the theoretical band profile.

The above observations generally seem to accept the proposal made earlier by Hoyle and Wickramasinghe (1962 and 1969) that the 217.5 nm (2175 Å) extinction bump is attributed to small spheres of graphite. According to Wickramasinghe et al. (1992), there are however serious problems associated with the graphite model; they explained that the requirement of graphite which has a planar lattice structure to be in the form of small spheres in interstellar space appears scarcely plausible. Alternative molecular explanations of the 2175 Å absorption were first proposed by Hoyle and Wickramasinghe in 1977, and these involve aromatic organic molecules.

The present study analysed the following materials using UV-Vis spectroscopy: biological (algae, grass, and seaweed species), polycyclic aromatic hydrocarbon (naphthalene), and 2 types of coal (semi-anthracite and anthracite). The results obtained from the study show that all the UV-Vis spectra displayed a prominent peak located within the region of 213.0- 220.5 nm, but none of which shows a peak that matches perfectly the interstellar extinction feature of 217.5 nm. However, attempts to average the whole sequence of spectra through normalization produced an impressive spectral band with a peak centered at 2175 Å that fits the interstellar extinction observations. Interestingly, the full width at half maximum (FWHM) of 250 Å also correlates with that of the interstellar feature.

Many models have been proposed for the carrier of this feature and these include graphite, dehydrogenated and hydrogenated amorphous carbon, coals, PAHs etc... However, Li and Greenberg (2003) claimed that, none of these single compounds provide a perfect model. A variation (±12%) has been observed with line of sight in the width and extinction band, and this observation may be indicative of a large chemical dispersion in the Galaxy (Fitzpatrick and Massa, 2007). The interstellar grain population has been proposed to include a substantial amount of ultra-small grains with PAH composition (Muthumariappan et al., 2008). Because PAH has strong absorption in the wide region (2000 to 2500 Å), the expected carrier of the

2175 Å feature could be a mixture of PAHs and the observed variation in the width of the feature may be attributed to differences in the PAH mix (Muthumariappan et al., 2008).

Chen et al. (2008) have reported that buckyonions are able to reproduce a peak close to the 2175 Å extinction feature, but argued that it is not clear if dust models consisting of the combined materials (buckyonions, amorphous silicates, PAHs, amorphous carbon, hydrogenated amorphous carbon and graphite) are capable of matching the 2175 Å extinction feature since the almost perfect feature produced by buckyonions might be affected by the addition of other dust components that must surely exist. They have however constructed an ensemble of silicate-graphite-PAH-buckyonions and this model has been shown to give an almost perfect match to the interstellar extinction curve at  $\lambda^{-1} \sim 3.5-7 \, \mu m^{-1}$  with a bump centered at  $4.5 \, \mu m^{-1}$ .

The results obtained from the present study using these materials appear to support the hypothesis of Hoyle and Wickramasinghe (1977) that the interstellar absorption feature 2175 Å is likely to be attributed to aromatic molecules within biological materials and such molecules may be interpreted as degradated biological products.

# **CHAPTER 6**

Microstructure and Elemental
Composition of the Tagish Lake
Meteorite and its Astrobiological
Implications

# 6.1. Summary

The present study examines the complex microstructure of the Tagish Lake meteorite. It also sets out to determine its elemental composition, and in particular the structural localization of carbon, oxygen and sulfur, which are the important elements of the insoluble organic species. Furthermore, the study analyses the samples by Fourier Transform Infrared (FTIR) spectroscopy to ascertain whether organic compounds are present in the meteorites.

The Tagish Lake meteorite, which fell in January 2000 in Canada has provided the most pristine cosmic materials for laboratory studies. It is made up of loosely formed aggregates, making it one of the most friable carbonaceous chondrites found on Earth. Its complex structure is composed of plaquettes of crystallised minerals, hexagonshaped metals, chondrules and granules, all of which are embedded in a matrix of fine grains and fibril-like materials. Those components with sizes larger than 350 nm in diameter are affected to variant degrees by solar hydrothermal reactions whereas a majority of smaller bodies (<350 nm in diameter) appear unscathed despite severe aqueous alterations on the parent body. A high population of granules (100-300 nm in diameter) consists of a wall (20-40 nm in thickness) and a larger core, the former is rich in organic elements such as carbon, oxygen and sulfur, and the core contains Ni-Fe-Mg rich silicates. The organic matter has both characters, aromatic and aliphatic, and such evidence suggests that the granules may be the carriers of large organic species with distinct astrobiological implications. The Tagish lake meteorite shows structural and chemical imprints, which are reminiscent of the characteristics of Pand D-type asteroids in the outer belt.

#### 6.2. Introduction

Meteorites are extraterrestrial materials that are now recognized as fragments of comets or asteroids that survived entry through the atmosphere of the Earth. When a meteorite enters the Earth's atmosphere, its speed rapidly decelerates, and its initial kinetic energy E=mv<sup>2</sup>/2 (where m is the mass and v is the speed of meteorite) is converted into heat, leading to the emission of light, and as a result, the meteorite

appears as a fireball. For a long time, there was reluctance to believe that meteorites could be extraterrestrial in origin. According to McSween (1989), a German physicist first claimed that these fragments originated in outer space.

According to the theory of panspermia, life is widespread across the universe, and the Earth has been seeded with space objects of variable sizes. A total of some 10<sup>11</sup> comets contain 10<sup>30</sup> g of material largely comprised of carbonaceous material (organics), mineral dust and water-ice. In the early history of the planetary system water in the form of liquid would be expected to persist for millions of years within cometary interiors (Hoyle and Wickramasinghe, 2000; Wickramasinghe et al, 2010).

One of the early life transporters between planets including Earth is proposed to be meteorites. This theory has been supported by the results obtained from the isotopic analysis of Murchison meteorite that fell in 1969 in Australia (Llorca, 2004). The analysis of the sample has shown that the meteorite contains organic compounds that are not related to terrestrial origin (Martins et al., 2008). This discovery provides evidence that the transfer of life across the inner Solar System is possible, and may constitute a powerful argument against the claims that evolution of life on Earth occurs in isolation from the rest of the universe (Coulson, 2004).

As described in detail in Chapter 1 'General Introduction' of the present thesis, meteorites and comets have been found to contain carbon, nitrogen, oxygen, hydrogen and minerals, which are essential for the production of large organic compounds. According to Oró (1961), water and the precursors of organic matter on Earth came from the comets that collided with our planet and this idea was later developed thoroughly by Delsemme (1984), Anders (1989) and Chyba and Sagan (1992). Complex organic molecules have been found in both the diffuse and dense clouds (Hollenbach and Thronson, 1987; Irvine, 1996), the atmosphere of Titan (Somogyi et al., 2005), and grains in interstellar space (Sandford et al., 1991). This organic matter may represent an important source of prebiotic molecules that are essential for the evolution of the origin of life on Earth.

Organic compounds as well as putative microbial fossils discovered in carbonaceous meteorites bear testimony to a possible connection between terrestrial life and comets.

These ideas are supported by the results obtained from the isotopic analysis of Murchison meteorite showing that the organic compounds do not have a terrestrial origin (Martins et al., 2008). Similarly, recent studies of Hoover et al. (2009) that support a long-standing argument for the presence of microbial fossils in the same meteorite provide further evidence in support of panspermia.

# **6.2.1. Types of meteorites**

Meteorites can be classified into three major families according to their mineralogy, and these include:

- 1. Iron meteorite: this type of meteorite is composed mainly of nickel-iron metal alloys. This type of meteorite is believed to be the important part of asteroids. Iron meteorites are the biggest type of meteorites because their surface layers are less affected by the impact during their passage through the Earth's atmosphere (Lewis, 1995; McBride, 2004).
- 2. Stony meteorite: most of meteorites that fell on Earth are stony meteorites which are composed mainly of silicates together with oxide minerals. The stony meteorites can be further divided into two main types: Chondrites and Achondrites. The former forms primitive cosmic rocks of early solar system, which have not been subjected to major alterations from the asteroidal parent, and most of them contain small glassy or crystalline spheroidal beads, called chondrules, having diameters ranging from 100nm to a few millimeters (Lewis, 1995). By contrast, the latter is made up of igneous rocks having chemical composition different from that of the sun and solar system resulting from the melting and crystallization processes.
- 3. Stony iron meteorites: these meteorites are rare and are composed of nearly equal amounts by weight of metals and silicate minerals.

# 6.2.2. Relationships between meteorites and asteroids

The meteorites are normally classified according to their mineralogy and their relationship with asteroids. According to Hiroi et al. (2001), the parent asteroid of each class of meteorite can be determined by reflectance spectroscopy. The largest asteroid is Ceres of type-C, and its surface has been found to contain water-bearing clays and organic material, reflecting the mineralogy of the matrix of CI and CM carbonaceous chondrites (Buseck and Hua, 1993; Llorca, 2004). Type-S asteroids are the sources of ordinary chondrites that are rich in olivine, pyroxene, and iron-nickel metals whereas enstatite chondrites containing (MgSiO<sub>3</sub>) metals belong to Types-E and -R asteroids.

# 6.2.3. Tagish lake meteorite

Fragments of the Tagish Lake meteorite fell on the Earth in January 18, 2000 in the region of Tagish Lake, Canada, after a large meteoric explosion in the upper atmosphere. This meteorite has been considered as a pristine sample because they have been kept in a frozen state which minimized the loss of organic molecules and potential contamination. Its fragments appear from dark grey to almost black with small light-colored inclusions (Brown et al., 2000). This meteorite was quickly collected after its fall was reported to reduce terrestrial contamination (Brown et al., 2000; Nakamura-messenger, 2006). According to Brown et al. (2000), the Tagish Lake meteorite is a carbonaceous chondrite of uncertain classification. However, Hiroi and his colleagues (2001) reported that this meteorite may be the first sample from D-type asteroids as its reflectance spectrum shows similarity with the spectra of the D-type asteroids. The Tagish lake meteorite also has characteristics similar to those of the two most primitive carbonaceous chondrites, the CI and CM2 (Brown et al., 2000; Nakamura et al., 2006). These meteorites also contain residual organic matter of interstellar origin, showing H and N isotopic anomalies (Busemann et al., 2006; Nakamura et al., 2006). It has been found in other studies to contain organic globules of sub-micrometer to nanometric sizes (Nakamura et al., 2002; Hoover, et al., 2003). Nanometric to sub micron sized organic granules as well as filaments and trichomes were interpreted as putative microfossils by Hoover et al. (2003). Similar objects were first reported in meteorite extracts from the 1960's (Claus and Nagy, 1961), and have since been reported in several other carbonaceous chondrites (Garvie and Buseck, 2006). Initial criticisms that all such structures were modern contaminants appears to have been ruled out by the work of Hans Pflug (see Hoyle and Wickramasinghe, 1982; Wickramasinghe, et al., 2010) and Hoover (2009), but their biogenic origin still remains controversial. As suggested by Nakamura et al. (2006), these organic globules may be linked to prebiotic organic matter that was delivered to the early Earth by comets and meteorites and thus there is ground for a further investigation into these objects to ascertain whether their composition and membrane-like structures play an important role in the building blocks for the origin of life.

# 6.2.4. Aim of the study

The present work examines the complex microstructures of the Tagish Lake meteorite using transmission and scanning electron microscopy. Also, the investigation sets out to determine the elemental composition of their contents by X-ray nanoprobe analysis. A particular interest is concerned with the structural localization of carbon, oxygen and sulfur, the important elements that make up the insoluble organic species. Furthermore, the samples are analysed by Fourier Transform Infrared (FTIR) spectroscopy to confirm the presence of bulk organic compounds in the meteorite.

#### 6.3. Materials and Methods

All materials together with the equipment used to prepare the samples for electron microscopy, X-ray nanoprobe analysis and infrared spectroscopy are described in detail in Chapter 2 of the present thesis. Briefly, fragments of the meteorite were embedded in LR White resin (London resin co. Ltd, UK) at 55 °C for 48 hours, and the resulting polymerized resin blocks were cut into thin sections (90-100 nm thick) on a Reichert E ultracut microtome (Reichert-Jung, Austria). The thin sections were mounted on pioloform-coated copper grids and examined using a Philips EM 208. The X-ray nanoprobe analysis of thin sections was carried out in a Philips CM12 fitted with an EDAX analytical system. The following operating conditions were

maintained constant throughout the X-ray analyses: electron beam size (20 nm), condenser aperture (30 μm), magnification (10,000x), analysis time (200 cps). For surface structure observations, a Philips XL20 SEM was used. For infrared spectroscopy the sample (0.15 mg) were prepared in KBr powder (20 mg). The mixture was transferred into a small blending mill (SPECAC mill<sup>TM</sup>) for grinding, and into the Evacuable Pellet Dies (SPECAC Ltd) under a pressure of 10 tons cm<sup>-2</sup> to make a KBr disc.

#### 6.4. Results

# 6.4.1. Electron Microscopy

The Tagish Lake meteorite is made up of loosely formed aggregates, making it one of the most friable carbonaceous chondrites found on Earth. High resolution transmission and scanning electron microscopy reveal its complex structure (Figs. 6.1, 6.2 & 6.3).

Scanning electron microscopical observations reveal that the aggregate is composed of plaquettes or chunks of crystalllised minerals, hexagonal bodies, chondrules of globular structure with variable sizes, all of which are embedded in a matrix of fine granules and fibril-like materials (Fig. 6.1). The mineral particles have irregular shapes, many displaying concentric rings (Plate C of Fig.6.1). Many plaquettes of minerals are partially embedded in the matrix of the parent body (Plate E of Fig.6.1). The hexagonal bodies (0.4-2.0 µm in diameter) appear electron black, have no internal structure, and are clustered in large groups (Plates D & F of Fig.6.1). Some of these bodies have lost their original hexagonal shape to become almost spherical (Plates D & F of Fig.6.1). Chondrules with diameters ranging from 3 to 6 µm are either clustered in groups (Plate A of Fig. 6.3), or individually attached to the matrix (Plates B & C of Fig. 6.3). However, a large population of them is covered with granules (100-300 nm in diameter) on their surface, making it appear rough and irregular (Plates A, B & C of Fig. 6.3). Many similar granules also form large clumps in the chondrule-free zones (arrows in Plate C of Fig. 6.3).

The imaging analysis by transmission electron microscopy of 90-100 nm thick sections cut from 1x2 mm fragment shows granules having an internal structure which consists of a rim (or wall) with an average thickness of 20-40 nm and a larger core (Plates D & E of Fig. 6.2 and D, E & F of Fig. 6.3). While numerous granules have a high electron dense core (Plates D & E of Fig.6.2), many others also show a hollow interior with their bodies partially embedded into the matrix (Plate E of Fig. 6.3). Lateral diffusion of probably volatile minerals can be seen in many large granules (Plate F of Fig. 6.2). The matrix of the parent body is made up of tiny grains with sizes ranging from 5 nm to 100 nm in diameter and a network of fibril-like materials (Plates B, D & E of Fig. 6.2), into which are embedded plaquettes of minerals, hexagonal bodies of metal, chondrules and granules of smaller sizes. The parent body shows intense aqueous alterations in places (Plates D & E of Fig. 6.2 and E & F of Fig. 6.3).

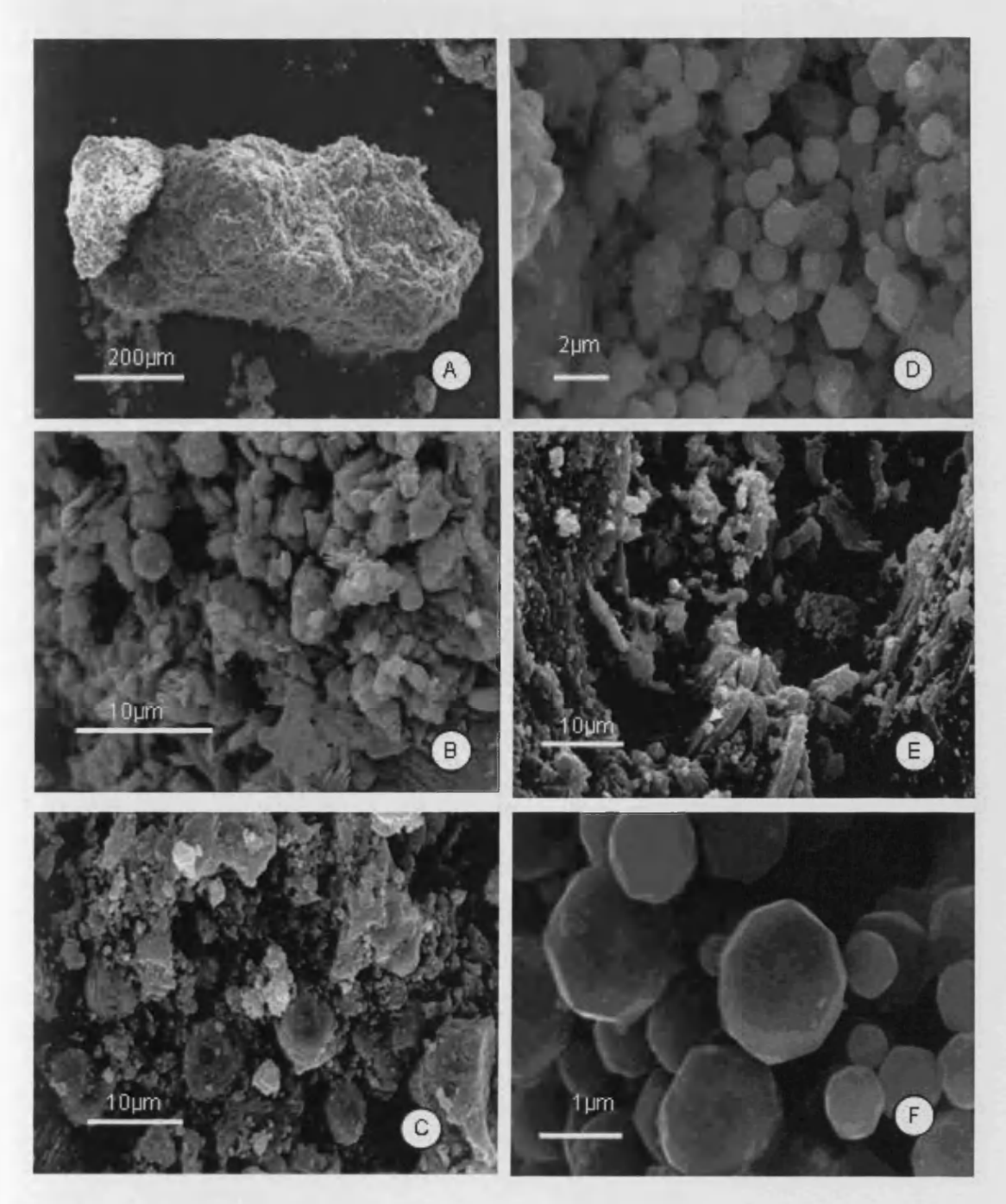


Fig.6.1: Scanning electron microscopy images of the Tagish Lake meteorite. (A) A fragment of the meteorite. (B) Plaquettes of crystallized minerals. (C) Chunks of minerals showing a concentric and layered structure. (D) A group of hexagonal bodies, some of which appear almost spherical. (E) Plaquettes of crystallized minerals partially integrated into the matrix. (F) High magnification of hexagonal bodies showing a smooth surface, suggestive of metal alloys.

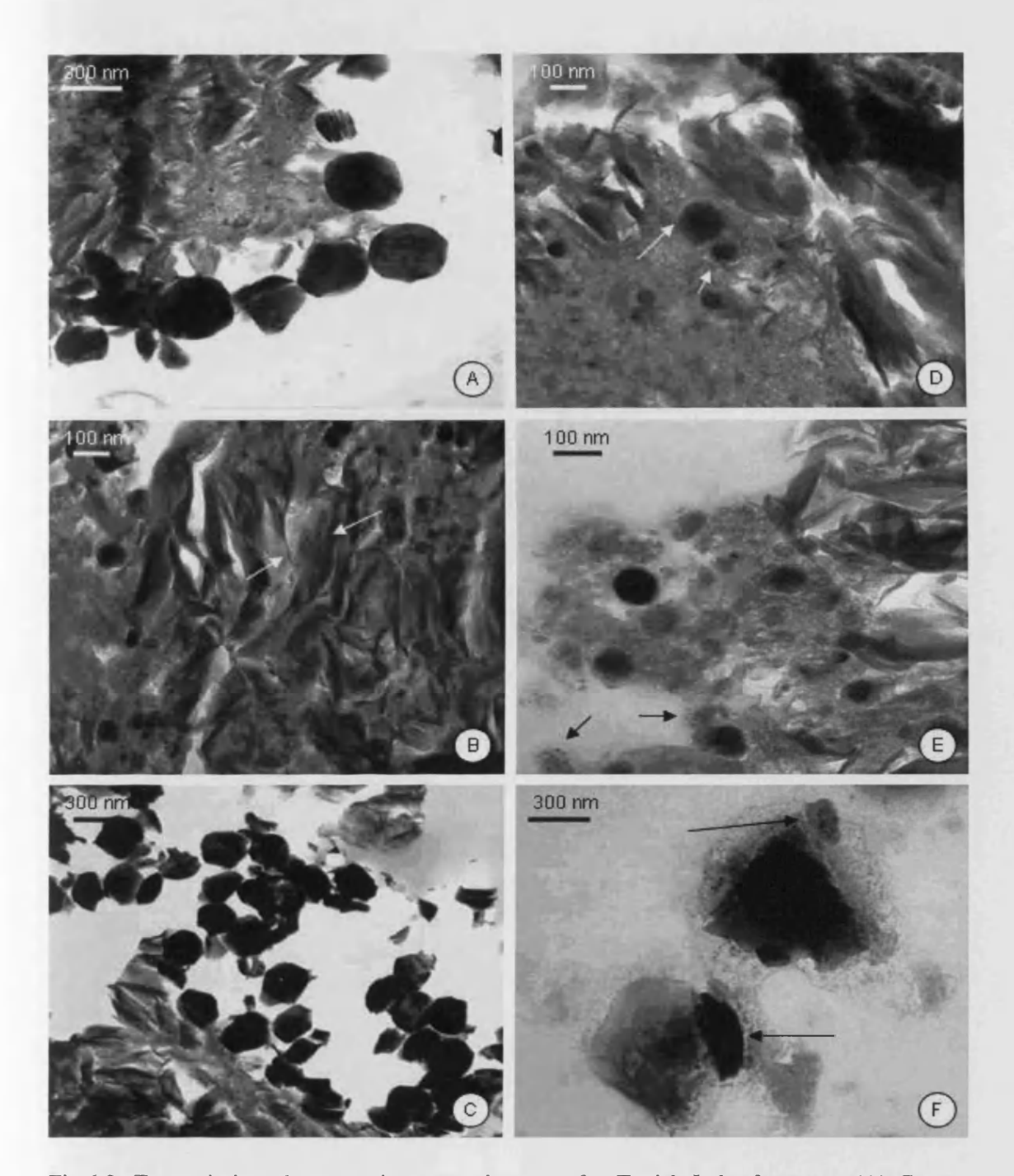


Fig.6.2: Transmission electron microscopy images of a Tagish Lake fragment. (A) Cross-section of a fragment showing black hexagonal bodies partially attached to the granular matrix of the parent body. (B) Plaquettes of minerals (arrows) embedded into the matrix of the parent body. (C) A group of metal alloys, some showing their hexagonal structure and many others becoming almost spherical. (D) A partial view of the matrix of the parent body showing granules of variable sizes and fibril-like materials, onto which plaquettes of minerals are attached; the arrows show granules with an electron dense core. (E) Plaquettes of crystallized minerals partially integrated into the altered matrix; the arrows show granules with an electron dense core. (F) Diffusion of minerals as a result of hydrothermal reaction; the arrows show diffused minerals.

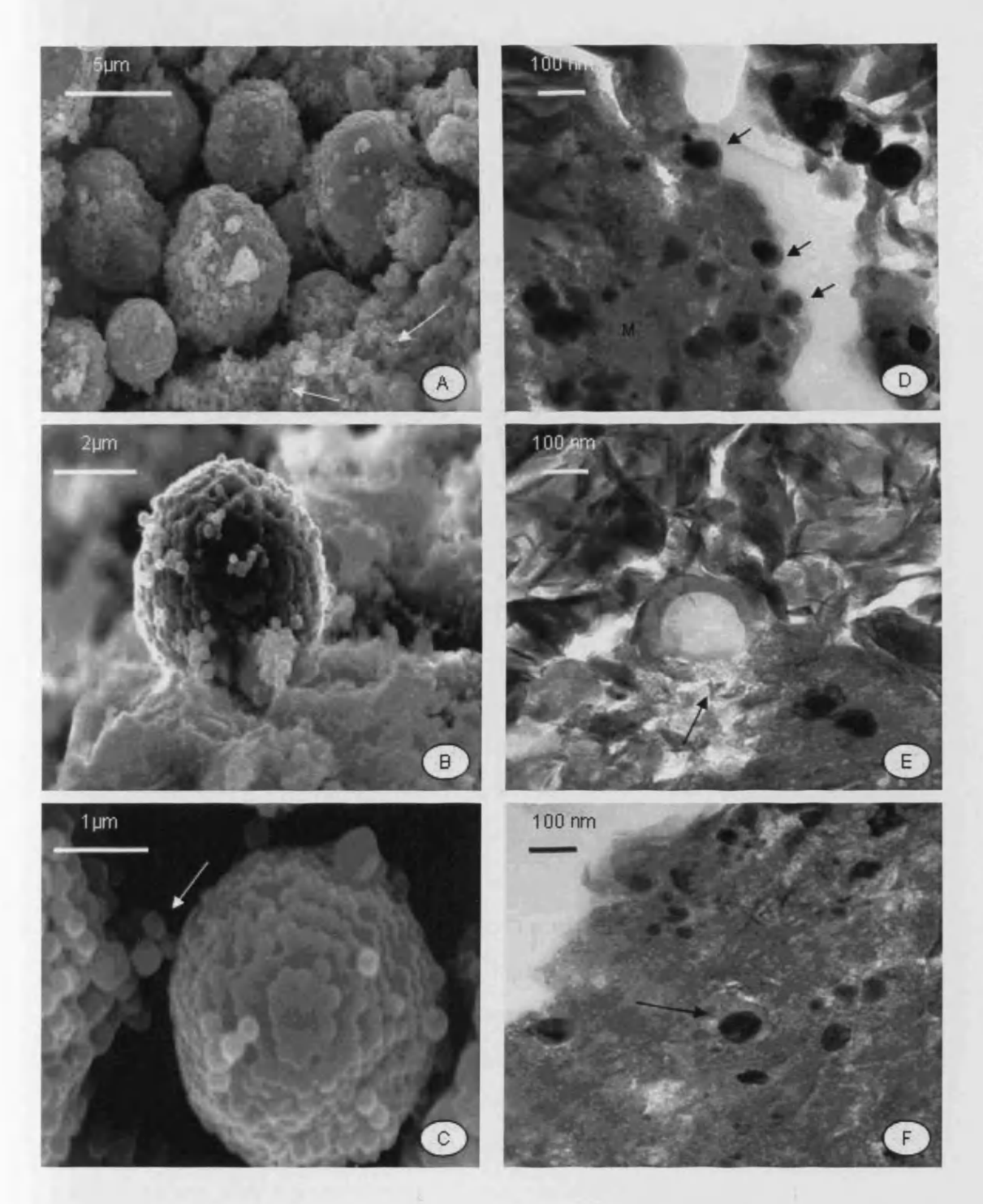


Fig.6.3: Scanning and transmission electron micrographs of the Tagish Lake components. (A) Chondrules covered with granules; the arrows show granules in the chondrule-free area. (B) A chondrule partially embedded in the parent body. (C) A high-magnification scanning electron micrograph showing a chondrule covered with granules; the arrow shows isolated granules. (D) Granules showing a wall (arrows) and an electron dense core. (E) A hollow chondrule partially embedded in the parent body; the arrow shows leakage of materials into the parent body. (F) The arrow shows a granule in the parent body.

#### 6.4.2. X-ray nanoprobe analysis

Plaquettes or chunks of crystallized minerals are mainly composed of carbon, oxygen, iron, magnesium and silicon (Fig.6.4 & Table 6.1). Other elements such as aluminum, sulfur, calcium, chromium and nickel are also detected, but their relative weight (0.2 - 1.6 wt %) is much less significant. The hexagonal bodies contain high concentrations of iron, zinc and nickel, but a low amount of carbon, manganese, sulfur, and chromium (Fig.6.4 & Table 6.1). Traces (<1 wt %) of magnesium, silicon, phosphorus, calcium, and aluminum are also detected in these bodies.

Chondrules with a smooth surface are generally rich in carbon, oxygen, iron, magnesium and silicon, but significantly low in sulfur, nickel, calcium, aluminum, phosphorus, manganese and zinc (Fig. 6.4 & Table 6.1). The chondrules with granules on their surface are comparable to those with a smooth surface in terms of their chemical composition (Fig. 6.4 & Table 6.1). These granules have variable sizes (100– 300 nm), mostly with an electron dense core, and contain a high level of carbon, silicon, magnesium, iron, nickel, sulfur, phosphorus, manganese and zinc. Many of them also form clusters in the chondrule-free regions, and basically have the same chemical composition as those on the chondrules (Fig.6.4 & Table 6.1). A large population of these granules is also integrated into the matrix of the parent body; those with a hollow core show a reduced amount of silicon, magnesium, nickel and iron, but are rich in carbon and sulfur elements, mostly confined to the wall (Fig. 6.4 & Table 6.1). The grains and fibril-like materials that make up the matrix of the Tagish Lake meteorite contain high concentrations of carbon, oxygen and sulfur. A significant amount of iron, silicon, magnesium and nickel is also detected in the matrix together with traces of calcium, aluminium, manganese, sodium, zinc and chromium (Fig.6.4 & Table 6.1).

Table 6.1: Relative concentrations (wt %) of minerals in the Tagish Lake meteorite.

Element	Hexagonal	Chondrule	Non-hollow	Hollow	Mineral	Matrix
			granule	granule	chunk	
CO	$10.9 \pm 0.85$	54.0 ±3.3	57.8 ±3.4	63.5±3.7	56.3 ±4.3	48.4±2.6
Na <sub>2</sub> O	0.3±0.06	0.0	0.2±0.05	0.1±0.06	0.2 ±0.01	0.1 ±0.04
MgO	0.4±0.06	8.9± 0.47	1.0±0.1	1.4±0.1	1.6±0.04	6.6±1.05
Al <sub>2</sub> O <sub>3</sub>	0.3±0.05	0.8±0.06	0.3±0.03	0.1± 0.06	0.4± 0.07	1.1±0.06
SiO <sub>2</sub>	0.4± 0.05	5.7±0.21	1.1±0.1	0.7±0.1	3.0±0.2	2.9±0.07
P <sub>2</sub> O <sub>5</sub>	0.4±0.06	1.7± 0.12	0.3±0.05	0.1±0.09	0.2±0.05	0.4±0.07
SO <sub>3</sub>	1.6± 0.1	0.4±0.06	3.2±0.2	2.9±0.07	0.8±0.3	0.9±0.1
CaO	0.3± 0.06	1.0±0.1	0.1±0.06	0.0	0.4±0.04	0.6±0.05
Cr <sub>2</sub> O <sub>3</sub>	0.4±0.05	1.1±0.1	0.1±0.05	0.0	0.0	0.5±0.04
MnO	1.0± 0.1	0.1±0.05	0.5±0.04	0.2±0.05	0.0	0.0
Fe <sub>2</sub> O <sub>3</sub>	35.3± 2.8	1.0±0.1	4.1±0.3	1.2±0.06	2.1±0.2	2.5±0.05
NiO	18.4±1.09	0.1±0.04	0.6±0.04	0.1±0.04	0.1±0.05	0.3±0.06
CuO **	31.1±2.2	25.1±1.8	29.2±1.6	30.5± 2.1	34.9±2.2	35.7±2.3
ZnO	5.2±0.42	0.1±0.05	0.5±0.04	0.2±0.04	0.0	0.0

Values ± SD (standard deviations), which were obtained from nanoprobe analysis of randomly selected materials, are shown as means of 25 measurements. \*\* CuO represents copper grid used to mount thin sections of the Tagish Lake sample

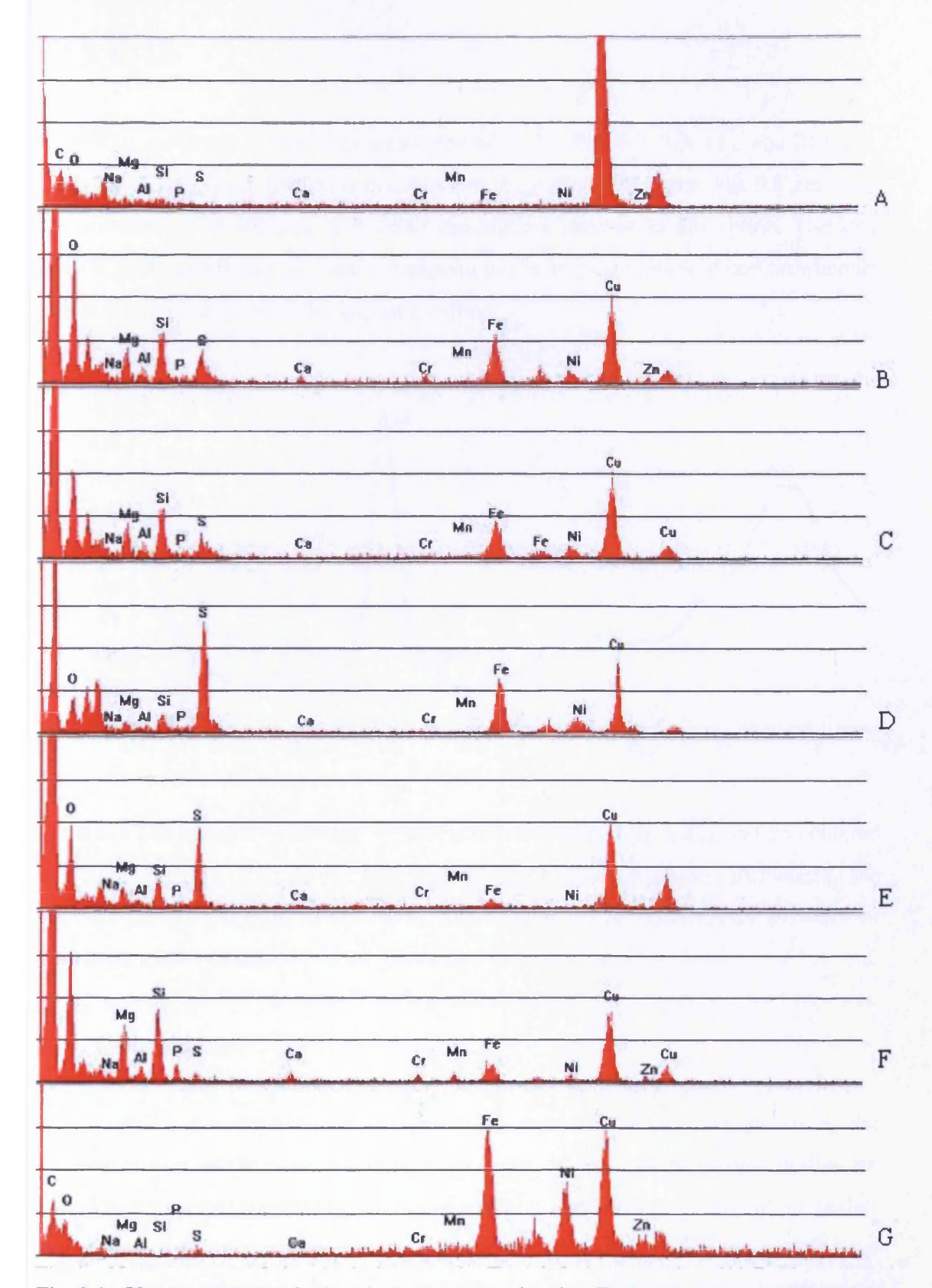


Fig.6.4: X-ray spectra of chemical elements in the Tagish Lake meteorite. (A) Background of film-coated copper grid. (B) Matrix of parent body. (C) Mineral chunk. (D) Non-hollow granule. (E) Hollow-granule. (F) Chondrule. (G) Hexagonal body.

#### 6.4.3. FTIR

The FTIR spectrum displays features centered at 2.9, 6.1, 6.9, 9.8, 11.3 and 21.6  $\mu$ m (Fig. 6.5). The 2.9  $\mu$ m feature is indicative of the presence of water. The 9.8  $\mu$ m band is characteristic of silicates and shows the highest intensity of absorption. The less intense peaks at 6.1 and 11.3  $\mu$ m correspond to the aromatic nature of carbon whereas that at 6.9  $\mu$ m is related to the aliphatic carbon.

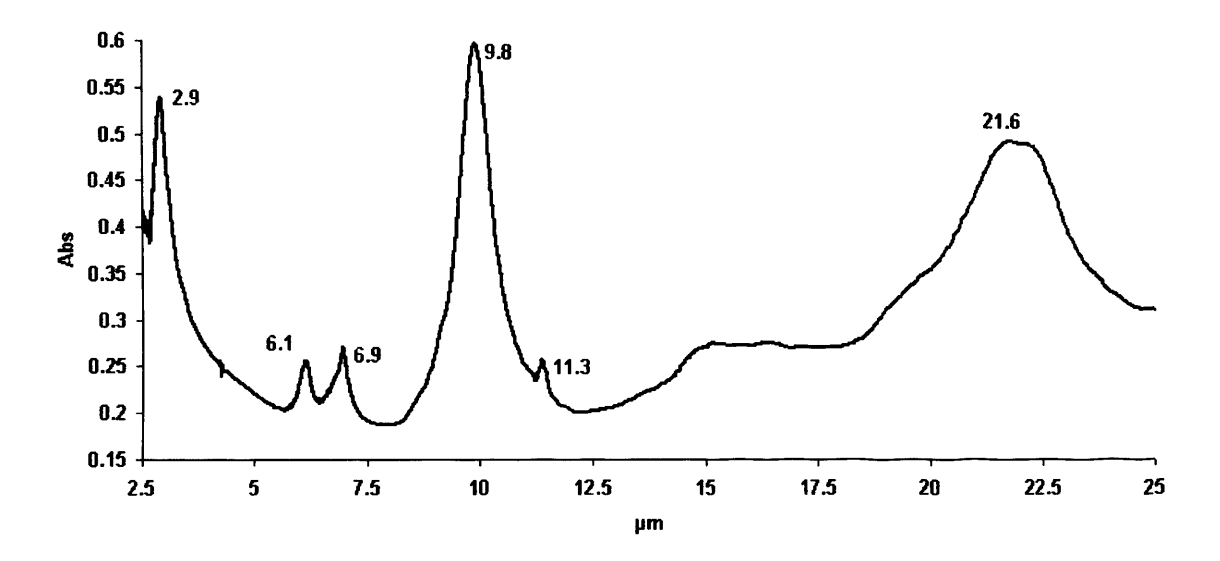


Fig.6.5: FTIR spectrum showing the characteristic bands of aromatic carbon centered at 6.1 and 11.3  $\mu$ m (Cataldo and Keyahan, 2003). A peak at 6.9  $\mu$ m is attributed to the aliphatic carbon (Papoular et al., 1993). The band at 2.9  $\mu$ m confirms the presence of water (Al-Mufti, 1985).

#### 6.5. Discussion

The Tagish Lake meteorite is composed of minerals loosely intergrown in the granular matrix of the carbonaceous parent body. Most of the hexagonal bodies are bound to each other, suggesting that this formation has taken place before the bodies are integrated into the matrix. Many of the hexagonal bodies within the groups have become almost spherical, this evidence indicates that they have been subjected to continuous interfrictional motion in space. Containing high concentrations of iron, zinc and nickel but having no distinguishable internal structure, these bodies are most likely to be metal alloys. The occasional detection in minute quantity of carbon,

magnesium, silicon, sulfur, calcium and aluminum, is an indication that the bodies may be contaminated with these elements after they have been incorporated into the mineral-rich matrix.

Chondrules in general appear to have a smooth surface, and are rich in carbonates, iron, silicon and magnesium, but also contain a less significant amount of sulfur, calcium and aluminum. This mineralogy suggests that the chondrules are not the same materials as the hexagonal bodies although both appear similar in sizes. The most spectacular transformation that the chondrules have experienced is the aggregation of granules on their surface (Plates A, B & C of Fig. 6.3). These granules may have formed as a result of condensation of interstellar grains under the effects of high temperature and rapid cooling in cold molecular clouds or in the outer regions of the protoplanetary disk (McSween, 1989).

Many of these granules are also found in clusters in the chondrule-free regions, suggesting that the molten ice grains may have formed before they are integrated into the parent body. Although most granules appear intact, many others show structural and chemical alterations in aqueous solution before they reach the Earth. The granules consist of two layers, an exterior wall and a core. The apparent changes in structure can be seen on the surface and the inside of the granules. A cross-section of the affected granules reveals partial degradation of their wall through which materials appear to leak profusely from the inside into the matrix, eventually leaving the granules with a hollow core. Breakdown of the wall and subsequent release of minerals are shown in Plate B in Fig. 6.3. These structural characteristics expressed by the affected granules are associated with the matrix of the parent body, and confirm that hydrothermal alteration has occurred, resulting in mass fractionation. Lateral diffusion of the interior materials through the wall followed by a massive loss of materials, is suggestive of hydrothermal reactions taking place in the parent body, leading to chemical fractionation. The transformation from the non-hollow to hollow granules gives an indication that the core which is rich in carbonates and waterbearing minerals, is very susceptible to hydrothermal conditions. The hydrous minerals in meteorite are similar to terrestrial clay, and are believed to be the products of low-temperature aqueous alterations of pre-existing anhydrous minerals in asteroids (Llorca, 2004). The hydrated mineralogy of the Tagish Lake and its richness

in carbonaceous matter are reminiscent of the expected characteristics of P- and D-type asteroids which are situated in the outer part of the belt (Hiroi et al., 2001; Grady et al., 2002). The Tagish Lake meteorite also shows characteristics strikingly similar to the Mars meteorite ALH84001 (McKay et al., 1996).

Mineral chunks including those with concentric structures are mainly composed of C-O-Fe-Mg-Si elements; their predominance in the Tagish Lake meteorite reflects that the chondrite is rich in minerals and metals, probably MgSiO<sub>3</sub>. The formation of concentric rings and layers of crystallised minerals suggests that these materials have been subjected to a cycle of high temperature and rapid cooling processes. Another unique composition of the Tagish Lake meteorite is that it contains high concentrations of iron-magnesium rich carbonates, but an unusual low amount of high temperature nebular elements such as calcium and aluminum, reflecting that these elements are probably altered to form Mg-Fe rich serpentine. These compositional characteristics are also consistent with those of extinct comets including P- and D-type asteroids (Bell et al., 1989).

The X-ray nanoprobe analysis of the granules shows that they are rich in carbon, silicon, magnesium, iron and sulfur, and that most of the carbon and sulfur are concentrated in the wall, indicating the existence in these granules of insoluble macromolecular organic material with the general formula  $C_{100}H_{60}N_7O_{12}S_2$  (Hayatsu and Anders, 1981). The presence of organic compounds in the Tagish Lake meteorite is further confirmed by the results obtained from the infrared spectroscopic analysis. The 6.1, 6.9 and 11.3  $\mu$ m features of the absorption waveband are all linked to organic species. Those at 6.1 and 11.3  $\mu$ m are characteristic of aromatic carbon whereas that at 6.9  $\mu$ m is linked to aliphatic character. These features match the emission bands of several astronomical objects, in particular the unidentified bands and the protoplanetary nebulae spectrum (Hudgins and Allamandola, 1997; Wickramasinghe et al, 2010; Rauf and Wickramasinghe, 2010).

The X-ray analytical data together with the infrared spectrum and electron microscopy are in agreement with the early observations that a high proportion of carbon in the Tagish Lake derives from organic species (Brown et al., 2000) and that the organic material occurs as submicrometer, hollow globules (Nakamura et al.,

2002; Nakamura et al., 2006). As reported by Pizzarello et al. (2001) and Busemann et al. (2006), over 99% of total organic carbon makes up the insoluble macromolecular group, and only 100 parts per million constitutes the soluble compounds. The unusual low concentration of soluble organic compounds is attributed to low temperature chemical oxidation as proposed by Cody and Alexander (2005). It is generally accepted that organic matter in meteorites is introduced into the asteroid belt from the interstellar space through radial turbulent mixing in the protoplanetary disk (Wooden et al., 2005). Most of the organic molecules remain unaffected on entering the region of the protosolar nebula (Bunch and Chang, 1980), and has survived the impact of intense aqueous alterations on its parent carbonaceous body due to the low ambient temperature in the asteroid belt (Busemann et al., 2006).

The microscopic and analytical data reveal that materials with sizes larger than 350nm are vulnerable to hydrothermal reactions whereas a majority of smaller granules appear unscathed despite severe aqueous alterations on the parent body. These granules (< 350 nm in diameter) are rich in carbon and sulfur, the important elements that compose the macromolecular organic material. Chemical biosignatures found in acid-dissolved samples by Pizarello et al. (2001), and the microstructure analysis of Hoover et al. (2003) support the speculation that the 5-100 nm grains have a biological origin, probably similar to nanobacteria claimed to be present in the Mars meteorite ALH84001 (McKay et al., 1996). The possibility of microfossils cannot be ruled out from our work, but further research is needed to resolve this important issue.

The present work reports the presence of structural and chemical imprints in the meteorite, which are reminiscent of the characteristics of the outer belt, and in particular of P- and D-type asteroids as previously suggested by Brown et al. (2000) and Grady et al. (2002). The granules reported in the present study have been described by Nakamura et al. (2006) as hollow organic globules. Since this material can survive entry into the Earth's atmosphere, it is reasonable to suggest that life on Earth could not have evolved independently, and that it must have been affected by the arrival of interplanetary or interstellar material. According to the theory of panspermia, this extraterrestrial material could have acted to seed the development of life on Earth and as its arrival on Earth is a continual process, it could also be responsible for the evolution of life.

# **CHAPTER 7**

The Carancas Meteorite: A Study by Electron Microscopy, Energy Dispersive X-Ray Microanalysis and Fourier Transform Infrared Spectroscopy

# 7.1. Summary

Fragments of the Carancas meteorite were examined by electron microscopy (TEM/SEM), energy dispersive analysis of X-rays (EDAX) and Fourier Transform Infrared (FTIR) spectroscopy. Scanning electron microscopical observations reveal that the fragment is composed of aggregates having a stony appearance and containing mostly mineral particles in various shapes and sizes. Many of these particles show fractures in places, thus confirming an ealier observation that the meteorite was subjected to a high velocity impact. The outer-rim of many aggregates displays a mud crack-like texture. At high magifications, this texture shows ovoid and elongated features which appear similar to microfossils found in other meteorites.

As revealed by both scanning and transmission electron microscopy, some aggregates contain particles with three clearly marked zones, distinguishable by their differences in electron density and texture: a light zone exhibiting a sheet-like structure, a dark zone displaying a pronounced radiating pattern and an intermediate zone depicting a smooth surface texture. The EDAX analysis of these particles shows that the light zone is composed of silicates rich in Fe, Ni and S (the elements of pyrrhotite and pentlandite). The dark zone contains high concentrations of Mg and Si (the major elements of high-temperature minerals such as forsterite, Mg2SiO<sub>4</sub> and enstatite, MgSiO<sub>3</sub>) intermixed with carbonates and traces of Al, Ca and Na. The intermediate zone also contains high-temperature minerals and Fe-Ni rich silicates.

The Carancas meteorite produces an infrared (IR) waveband stretching from 2.5  $\mu$ m to 25  $\mu$ m. This spectrum shows prominent features of amorphous and crystalline silicates in the range, 9-10.8  $\mu$ m. Hydrated silicates and hydroxyl groups are less abundant as shown by the presence of small humps between 2.5  $\mu$ m and 8.0  $\mu$ m. Some carbonate species (FeCO<sub>3</sub> in particular) are also present as shown by the presence of bands from 11.3 to 13.7  $\mu$ m (Knache and Kratschmer, 1980). Several infrared (IR) bands of olivine group are observed between 14.5  $\mu$ m and 20.0  $\mu$ m.

The data obtained from the FTIR and EDAX analyses indicate that the Carancas meteorite is composed of an assortment of materials that have presolar and solar

system origins. The abundance of high temperature minerals and iron rich metal confirms an earlier observation that the meteorite is an ordinary H4/5 chondrite. Some particles in the Carancas meteorite are found to have structural and chemical characteristics similar to those of 81P/Wild 2 comet.

#### 7.2. Introduction

The Carancas meteorite fell on 15 September 2007 approximately 10 km south of Desanguadoro, near Lake Titicaca, Peru. The impact excavated a crater having an overall diameter of 13.5 m, a 7.5 m central hole, 1 m high ejecta rim and a shallow (0.6 m deep) groundwater pond (del Prado et al., 2008). The estimated timing of the fall was recorded at approximately 11:45 A.M. (local time) (16:45 UT) (Macedo and Machare, 2007), but later claimed to be 11:40 AM (16:40:14.1 UT) (Tancredi et al., 2009). The meteorite was thought to travel from east to west, and the angle at which the meteorite entered the atmosphere was estimated to be between 45 and 60 degrees from the horizontal (Tancredi et al., 2007 and 2009). According to the initial report (Macedo and Machare, 2007), the locals claimed that a luminous object was seen about 1 km from the earth surface before a strong explosion lasting 15 minutes was heard. The fireball consisted of a head with strong bright light and a white smoky tail. The locals also reported that immediately after the explosion, a massive cloud of dust was seen followed by a 'sulphurous' smell from the site and groundwater evaporation. Neither explosion nor 'rained down' debris was reported to take place in the sky, suggesting that the meteorite remained intact on entering the atmosphere. According to the media reports (Diario Larepublica of 19/09/2007; Living in Peru of 19/09/2007 and BBC of 19/09/2007), many local witnesses became ill and several of them had to be hospitalised after they came into contact with the glowing rocks. The symptoms of the illness have been reported to include headache, dermal injuries, dizziness, nausea and vomiting. Arsenic vapour from the contaminated water in the crater was thought to be responsible for the outbreak of the sickness.

The mineralogical analysis of the fragments indicate that the meteorite is a chondrite composed of fine-grained materials with light grey coloration, rich in iron particles, pyroxene, olivine and kamacite (Macedo and Machare, 2007; Tancredi et al., 2009).

Other minerals such as forsterite, enstatite and troilite have also been detected in the fragments (del Prado et al., 2008). The Carancas has been proposed to be an ordinary H4/5 chondrite (del Prado et al., 2008; Tancredi et al., 2008 and 2009). The meteorite was found to survive the atmosphere entry without major fragmentation (Le Pichon et al., 2008). The trajectory of its fall has recently been reviewed by Tancredi et al. (2009); they have suggested that the crater was formed as a result of a hypervelocity impact. Earlier reports have presented several transmitted light optical images of the fragments (Macedo and Machare, 2007; Harris et al., 2008; Tancredi et al., 2009). However, so far there has been little information on the microstructural characteristics and elemental composition of the particles that formed the Carancas fragments.

# 7.2.1. Aim of the study

The present work examines the complex microstructure of the Carancas meteorite using transmission and scanning electron microscopy. The grains embedded in KBr powder are analysed by Fourier Transformer Infrared (FTIR) spectroscopy to determine their chemical composition. The results obtained from these studies could provide further evidence to confirm the earlier reports that the Carancas meteorite is a H4/5 ordinary chondrite.

#### 7.3. Materials and Methods

# 7.3.1. Scanning Electron Microscopy

The Carancas samples were mounted onto a metal stub using a piece of carbon double-sided sticky tape, and coated with gold in an Emscope sputter coater. The samples were examined using a Philips SEM XL 20 operated at 20kV accelerating voltage.

# 7.3.2. Transmission Electron Microscopy

Fragments of the Carancas meteorite were embedded in LR White resin (London resin Co. Ltd, UK) at 55 °C for 48 hours, and the resulting polymerized resin blocks were cut into thin sections (100 nm thick) using a diamond knife on a Reichert E ultracut microtome (Reichert-Jung, Austria). The thin sections were collected on pioloform-coated copper grids and examined using a Philips EM 208.

# 7.3.3. EDAX Analysis

A Philips CM12 fitted with an EDAX system (EM-400 Detecting Unit, EDAX, UK) was used to analyse the thin sections. The following operating conditions were maintained constantly throughout the analyses: electron beam size (20 nm), condenser aperture (30 µm), magnification (13,000x) and analysis live time (200 cps). During the analyses, the electron beam was focused onto the regions of interest, and a total of 25 similar measurements were randomly taken for each region. Both qualitative and quantitative analyses were performed using a 'Genesis' software.

# 7.3.4. FTIR Spectroscopy

The samples (0.15 mg) were prepared in KBr powder (20 mg). The mixture was transferred into a small blending mill (SPECAC mill<sup>TM</sup>) for grinding, and into the Evacuable Pellet Dies (SPECAC Ltd) under a pressure of 10 tons cm<sup>-2</sup> to make a KBr disc. The KBr embedded sample was analysed using a FTIR spectrometer (JASCO Model FT/IR-660 Plus series).

#### 7.4. Results

# 7.4.1. Scanning Electron Microscopy

The Carancas fragment contains particles, mostly minerals having variable sizes and shapes (Figs. 7.2A and 7.2B). The most common features include conchoidal, cuboidal and irregularly shaped bodies (Fig. 7.2B). The surface of some individual particles displays a mud crack-like texture. At high magnifications, this texture contains ovoid and rod-shaped objects which are similar to microfossils of terrestrial origin (Figs. 7.3A and 7.3B). A large number of particles have crusts on their surface (Fig. 7.2C) whereas many others show fractures (Fig. 7.3D) and cavities (Figs. 7.3C and 7.3D). Some particles exhibit three zones, distinguishable by their differences in both electron opacity and texture: a light zone showing a layered or sheet-like structure, a darker zone at the centre displaying a pronounced radiating pattern and an intermediate zone with a smooth texture (7.2 D).

# 7.4.2. Transmission Electron Microscopy

Most of the sections cut from the resin-embedded fragment were brittle and damaged by the electron beam bombardement. The ultrastructual observations of these sections reveal the presence of numerous holes, indicating that the samples were poorly embedded. As shown in figure 7.1, some well embedded particles show three zones distinguishable by their differences in electron density and structural characteristics: (i) a light zone displays a layered or thin sheet-like structure; (ii) a darker region displays aligned 'chatter pits'; and (iii) an intermediate zone has a surface structure that appears rather smooth.



Fig.7.1: A transmission electron micrograph of particles in the well embedded-resin section. Three large particles appear to have a similar structure. Each particle shows three clearly defined zones: a light zone (Z1) showing a layered or sheet-like structure (dark arrows); a darker zone (Z2) at the center displaying aligned 'chatter pits', probably resulting from the diamond knife cutting (white arrows); an intermediate zone (Z3) having a smooth surface structure.

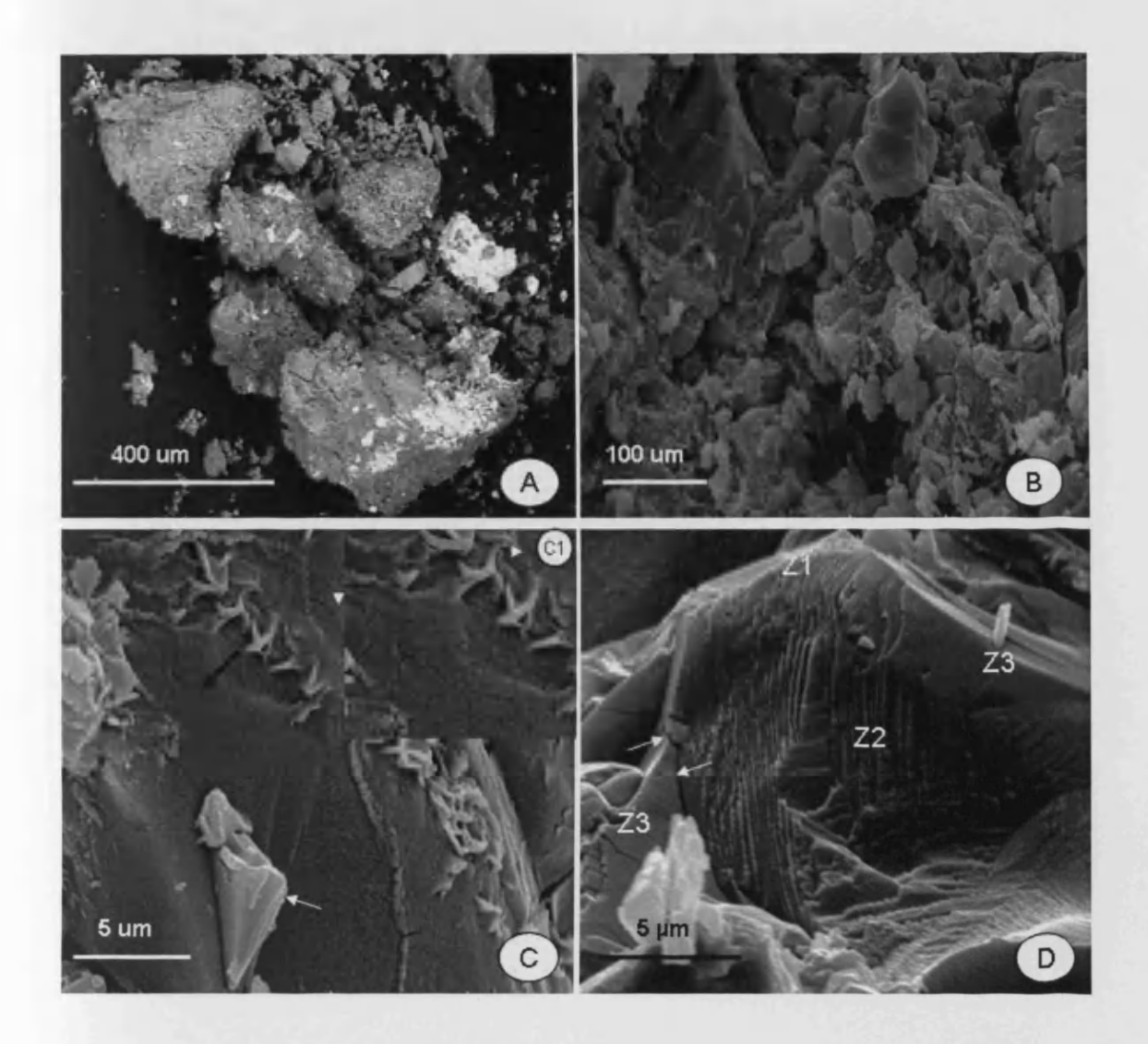


Fig.7.2: Scanning electron micrographs of the Carancas meteorite. (A) Carancas fragments. (B) A general view of the central region of the fragment showing mineral particles in various forms and sizes. (C) A partial view of the peripheral region of the fragment showing a mud-crack like texture; streaks of fusion crusts on the surface (arrow head); the inset (C1) shows an enlarged picture of the mud crack-like structure. (D) A particle showing three clearly delineated regions: a light zone (Z1) shows a layered or sheet-like structure; a darker zone (Z2) at the center displays a pronounced radiating texture; an intermediate zone (Z3) is distinguishable by its smooth surface structure where cracks can be seen as shown by the arrows.

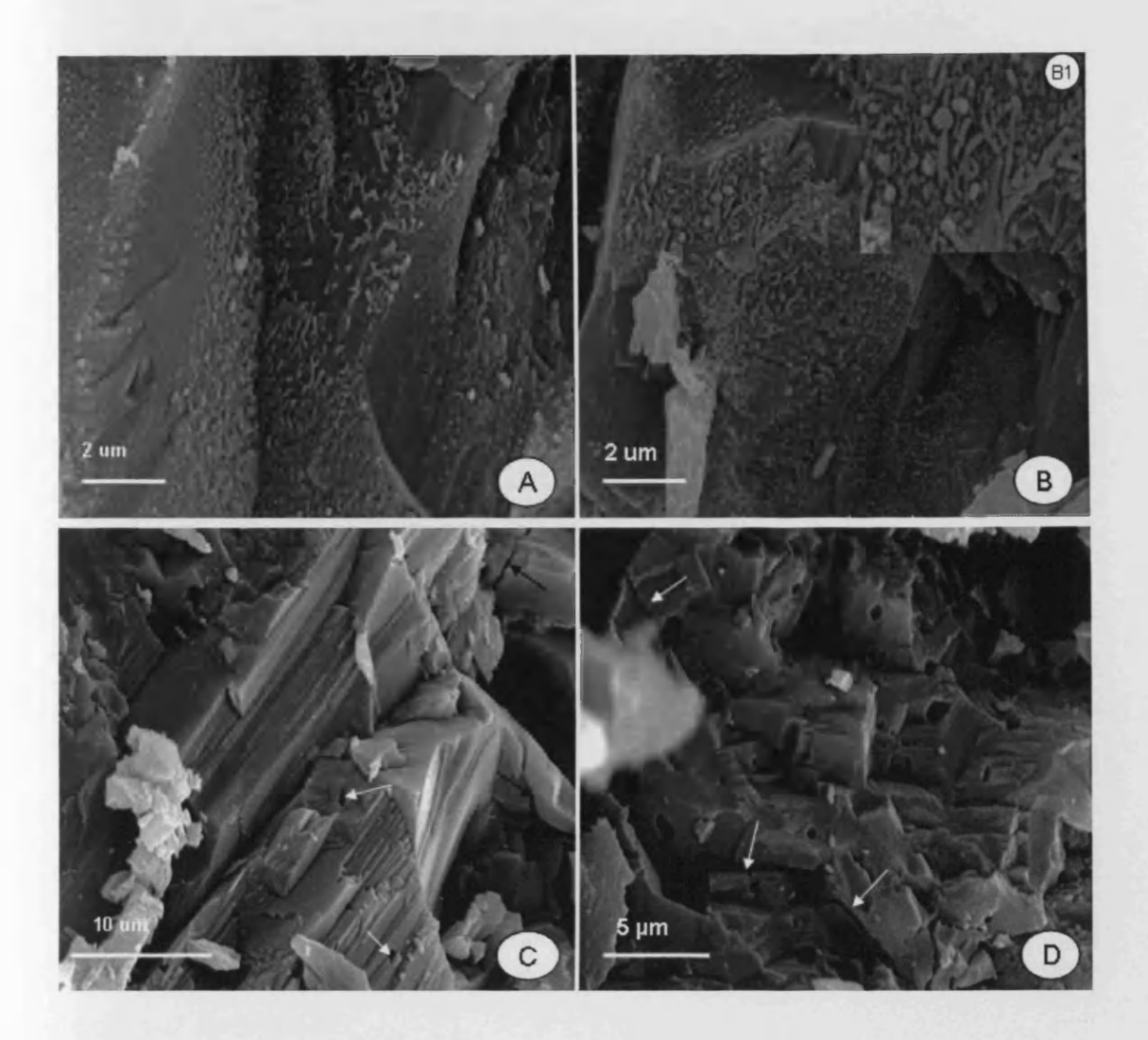


Fig.7.3: SEM micrographs of the Carancas fragments. (A) A high magnification electron micrograph of the peripheral region of a fragment: ovoid and elongated features are apparent. (B) An electron micrograph of the same region as (A); the inset (B1) illustrates the close-up of microfossil-like features. (C): An electron micrograph of the layered texture showing cracks (black arrows) and cavities (white arrows). (D) An electron micrograph of the central region of a fragment showing fractures (arrows) and numerous cavities.

### 7.4.3. X-Ray nanoprobe analysis

The results obtained from the X-ray nanoprobe analysis of the thin sections show that the resin-embedded particles are composed of three different regions, distinguishable by the differences not only in structural characteristics but also in chemical composition (Table 7.1). For convenience, they are labelled in the present study as Z1, Z2 and Z3. During the analyses, attempts were also made to determine whether arsenic element (As) was present in the sample. As Fig. 7.4 shows, the spectra do not reveal the presence of the characteristic X-ray emission peak of arsenic (As) element which should normally be located at 10.5 KeV energy. The chemical composition of Z1 is similar to that of Z3, but the former contains less magnesium and silicon than the latter. The amounts of major elements in Z1 such as sulfur, iron and nickel are much higher than those in Z2 and Z3. On the other hand, the chemical composition of Z2 is unique since it contains no nickel, but is rich in magnesium and silicon as compared to Z1 and Z3. Traces of sodium, aluminium and calcium are detected in Z2 but they are not present in Z1 and Z3.

Table 7.1: Relative concentrations (wt %) of major elements that make up the three regions of the particle.

Element	Z1	Z2	<b>Z</b> 3
CO	38.4±2.1	37.8±2.8	36.3±3.2
Na <sub>2</sub> O	0.0	1.2±0.05	0.0
MgO	2.1±0.08	12.2±0.6	10.8±0.9
$Al_2O_3$	0.1±0.05	0.9±0.08	0.0
SiO <sub>2</sub>	1.8±0.15	19.8±0.9	13.8±1.2
SO <sub>3</sub>	9.0±0.9	1.7±0.12	6.2±0.2
CaO	0.0	0.5±0.03	0.0
Fe <sub>2</sub> O <sub>3</sub>	35.2±3.8	25.9±2.3	22.9±2.5
NiO	13.4±1.68	0.0	10.0±1.4

Values ± SD (standard deviations) represent the average of twenty-five measurements. The data are computed by the 'Genesis' thin section software which calculates the weight percentages of the elements based on the known concentrations of the standard samples.

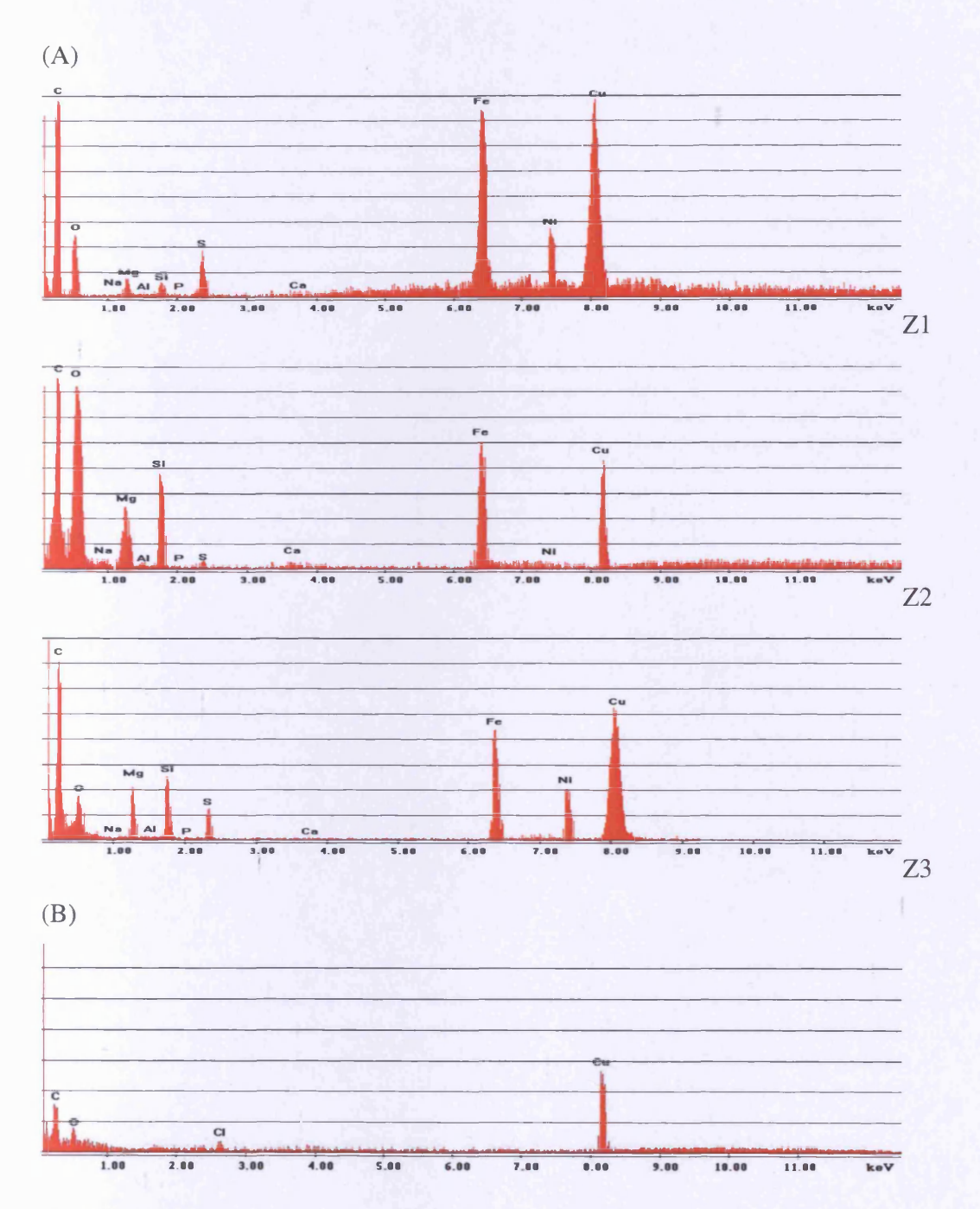


Fig. 7.4: X-ray spectra obtained from the analyses of a thin section. (A): X-ray spectra of a particle with three zones: a light zone Z1 showing a sheet-like structure, a darker zone Z2 exhibiting a pattern of 'chatter pits', and an intermediate zone Z3 with a smooth surface structure. The X-ray intensity of the elements detected is variable depending on the zones. C, Fe, S and Mg are detected in Z1, Z2 and Z3. Nickel is found only in Z1 and Z3. The presence of Na, Al and Ca is confined to Z2. The Cu peak represents the element from the copper grid used for mounting thin sections. (B): A background area in the same section containing no sample. The X-ray intensity of C and Cl is negligible.

#### 7.4.4. FTIR

The analysis by FTIR spectroscopy of the Carancas grains embedded in KBr shows a spectrum containing a series of absorption features located at 9.5, 9.8, 10.2, 10.5, 10.8, 11.3, 11.9, 13.7, 14.5, 15.6, 16.8, 18.4, 20.0 and 24.4  $\mu$ m (Fig.7.5). Several small peaks are located within the range of 2 - 3  $\mu$ m and 6 - 7  $\mu$ m.

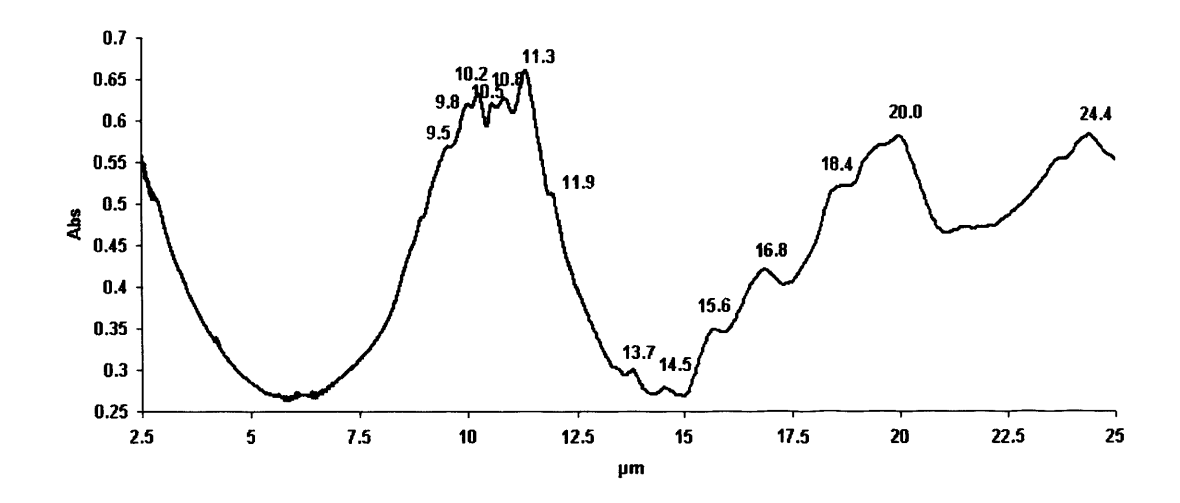


Fig.7.5: FTIR spectrum of the Carancas meteorite showing infrared bands centred at 9.5, 9.8, 10.2, 10.5, 10.8, 11.3, 11.9, 13.7, 14.5, 15.6, 16.8, 18.4, 20.0 and 24.4  $\mu$ m.

#### 7.5. Discussion

Scanning electron microscopy of the Carancas fragments indicates that they have a stony appearance and are composed of a large population of mineral particles in variable shapes and forms (Figs. 7.2A and 7.2B). Some particles show numerous cavities (Fig. 7.3D), which may suggest the occurrence of a steam phase. Many particles also show fractures (Figs. 7.3C and 7.3D), probably as a result of the impact brecciation. Furthermore, the surface of many particles is covered in places with crusts, most of which show fusion melt along the fissures (Fig. 7.2C). These findings support an ealier observation made by Miura et al. (2008) that the Carancas meteorite was subjected to two major step processes: melting in atmosphere and steaming after impacting the Earth. The melting process resulted in the formation of fusion crusts rich in Fe and Si and melt flakes of Fe- Ni composition. The steam phase occured as a result of the reaction between the hot meteorite metal and cold groundwater at the

excavation site. Fractured or broken fragments were discovered around the crater, suggesting that the Carancas fragmented on impact with the Earth. The impact velocity on the ground was estimated at between 3 km s<sup>-1</sup> and 6 km s<sup>-1</sup> (Tancredi et al., 2009).

Some particles show a mud crack-like texture intermixed with ovoid and elongated features, which appear similar to microfossils of terrestrial origin (Figs. 7.3A and 7.3B). These features have also been found in Martian meteorite ALH84001 (McKay et al., 1996) and in other carbonaceous chondrites (Hoover et al., 2003 and 2009). The origin of these objects is however uncertain and remains to be properly determined. One possible explanation is that the mud crack-like structure may originate from the terrestrial contamination. It is possible that some of the fragments were exposed to the terrestrial muddy water or wet-ground at the excavation site. This explanation is further supported by the observation that the Carancas fall was immediately followed by a massive cloud of dust and groundwater evaporation from the impact crater (Macedo and Machare, 2007; Miura et al., 2008; Schultz et al., 2008; del Prado et al., 2008).

Concerning the ovoid and elongated features, an explanation could be offered that these may be the broken products of carbonate crystallisation since they appear similar to the bundles of carbonate crystal precipitation induced by bacteria as suggested by Buczynski and Chafetz (1991) and McKay et al. (1996). Rauf et al. (2010) on the other hand have suggested that the assembly of features into monodisperse particles resembling nanobacteria and micrococi invites an alternative interpretation in terms of biological activity within aqueous niches of a parent body.

The FTIR analysis of grains in the Carancas meteorite reveals a waveband stretching from 2.5 to 25  $\mu$ m showing IR absorption peaks centred at 9.5, 9.9 and 10.2 $\mu$ m whose characteristics are of amorphous (9.5  $\mu$ m) and crystalline (9.9 and 10.2  $\mu$ m) silicates (Knacke and Kratschmer, 1980). The presence of many bands around 10  $\mu$ m may be indicative of the band shift from amorphous to crystalline silicates, and this shift may result from the annealing of amorphous silicates at high temperatures. This process is believed to take place in the hot inner-region of the solar nebular (Bockelee-Morgan et al., 2002). Amorphous silicates are found in abundance in interstellar medium

(Zolensky et al., 2006) and IDPs (Molster and Kemper, 2005) whereas crystalline silicates are predominant in primitive meteorites (Nuth et al., 2005; Busemann, 2006). On the other hand, the C1 and C2 chondrites are rich (50-60%) in hydrated silicates, which show a sharp absorption at 2.71 µm in Orgueil and Murchison meteorites (Knacke and Kratschmer, 1980). Furthermore, the carbonaceous chondrites have been shown to display strong absorptions at 6.1 µm and 6.8 µm (Kancker and Krastchmer, 1980). Recently, Rauf et al. (2010) have detected these absorption features in the Tagish Lake meteorite. The 6.1 µm feature is known to be related to water absorption in many clay minerals (Farmer, 1974a) whereas the 6.9 µm is caused by carbonate minerals (Knacker and Kraschmer, 1980). Unlike these carbonaceous chondrites, the Carancas meteorite shows considerably weaker absorptions in the infrared range of 2.5-4.0 µm and 5.0-7.0 µm (Fig. 7.5). The occurrence of such small humps indicates that hydrated silicates (probably phyllosilicate minerals), hydroxyl (OH) groups and carbonates are less common. There is no evidence of aliphatic functioning groups as confirmed by the absence of a 3.4 µm peak. However, aromatic hydrocarbons may be present in the Carancas meteorite as shown by the presence of a band centered at 11.3 µm which is known to be the absorption feature of aromatic hydrocarbons in many astronomical objects (Cataldo and Keyehan, 2003; Rauf et al., 2010; Rauf and Wickramasinghe, 2010) including comets and 81P/Wild 2 in particular (Sandford, 2008). The IR bands observed in the 14.5-20 µm region may be due to the presence of olivine group (Saikia and Parthasarathy, 2009).

Attempts to section the resin-impregnated fragments were met with little success. Most of the sections showed perforations and became brittle, suggesting that the fragments were poorly embedded. However, there are some small grains that were reasonably well preserved. As shown in Figs. 7.1 and 7.2 D and Table 7.1, these grains are composed of three phases distinguishable not only by the differences in their electron density and texture, but also their chemical composition. The light zone (Z1) showing a mica sheet-like structure, is composed of sulfide minerals rich in Fe and Ni. In contrast, the darker region (Z2) displays a spectacular pattern of 'chattering pits', rich in Mg and Si (the major elements of high temperature minerals such as forsterite Mg<sub>2</sub>SiO<sub>4</sub> and enstatite MgSiO<sub>3</sub>). The richness of chemical elements such as Mg, Si, and Fe in Z2 also suggests the existence of olivine and pyroxene. The third zone (Z3) showing a rather smooth surface structure, is composed of crystalline

silicates rich in Mg, Fe and Si (the major elements of olivine and pyroxene). The X-ray microanalysis also confirms that there is no evidence for the presence of arsenic element (Fig. 7.4 and Table 7.1), thus ruling out the claim that the illness experienced by the locals in Carancas was arsenic-related. Cr, P and K were not detected in the present study; these elements are normally found in small amounts in ordinary H chondrites like H4/5 (Reimold et al., 2004; del Prado et al., 2008).

The results obtained from the elemental analysis, electron microscopy and FTIR spectroscopy suggest that the chemical composition of some particles in the Carancas meteorite is similar to that of particles of 81P/Wild 2 comet where both amorphous and crystalline silicates are present in abundance (Keller et al., 2006; Zolensky et al., 2006). The 8 µm terminal particle (known as Sitara) of this comet is composed of bright regions of sulfides rich in iron and nickel, a central grey region of enstatite marked by aligned 'chatter pitts' and a smooth grey region rich in crystalline Mg-silicates (Brownlee et al., 2006).

Using FTIR spectroscopy, EDAX analysis and electron microscopy to analyse the Carancas fragments, the current investigation presents the following findings: (1) the meteorite is composed of a large population of minerals that are abundant in space; (2) it is rich in chemical elements that compose olivine, pyroxene and high temperature minerals such as fosterite and enstatite; (3) the richness of these minerals and iron metal support the early proposal that the meteorite is an ordinary H4/5 chondrite (del Prado et al., 2008; Tancredi et al., 2008 and 2009); (4) some particles show structural characteristics and chemical composition of minerals similar to comet 81P/Wild 2; and (5) the ovoid and elongated features look like microfossils found in other meteorites, many of which resemble bacterial microfossils of terrestrial origin. Based on the above findings, it may be concluded that the Carancas meteorite is composed of presolar and solar system materials.

# **CHAPTER 8**

# Astrobiological Aspects of Kerala Red Rain

# 8.1. Summary

The current controversial aspects of the Kerala red rain have prompted me to reexamine the sample using a number of laboratory techniques. Under a transmitted light microscope, the Red rain cells appear red-brown in coloration and show variations in size (5-10  $\mu$ m) and shape (spherical, ellipsoidal and oval). Electron microscopy confirms that the red particles are biological materials with a structure resembling that of spores of a microorganism yet to be properly identified. The red rain cells contain an abnormally large nucleus that occupies almost the entire volume of their cytoplasm. Their exceptionally thick wall (850 nm thick including capsule) suggests that they may be one of the toughest microorganisms that can survive in extremely harsh environmental conditions. The cells contain all the biogenic elements that are ubiquitous in the interstellar medium and their mineralogy is similar to that of carbonaceous meteorites. Spectroscopical analyses of the red rain cells by UV-Visible, IR and fluorescence show spectral characteristics mostly resembling those of astronomical observations. On the other hand, the IR absorption spectrum is remarkably similar to that of seaweed species.

The evidence presented in this study seems to suggest that the red rain cells could be closely related to the original species of a microorganism that was involved in the evolution or introduction of early life on Earth. The issue of whether the red rain cells contain DNA remains in dispute. Further studies are required to help resolve this contentious issue.

#### 8.2. Introduction

#### 8.2.1. Brief historical accounts of red rain

McCafferty (2008) has reported historical events in relation to red rain. According to his account, different types of rain have fallen from the sky in many different parts of the world. Throughout the centuries, from Classical Rome to medieval Ireland, Norman Britain and 19<sup>th</sup> century California to 21<sup>st</sup> century India, about eighty falls of red rain have been reported together with a further twenty relating to lakes and rivers

that turned blood-red, and sixty eight instances of other falls which included milky, honey, wine, black rain and even blood-red coloration. Sixty of one hundred reported instances were found to be associated with meteorite or comet activity and of these sixty, twenty three were related to the red rain events, thirteen to red blood rivers and the remaining twenty four to other types of rain coloration. These historical events of different colors of rainfall suggest that materials of different nature in variable shapes and sizes could have been brought down from space. Thunderstorms and even meteor bursts are believed to play a crucial role in bringing down these materials in the form of rain.

#### 8.2.2. Controversial aspects of Kerala red rain

The most recent mysterious phenomenon that has attracted much attention amongst astrobiologists, who are interested in extraterrestrial microorganisms, is that of the red rain which fell in Kerala, India, on 25 July 2001. The rain has been reported to contain red particles, the amount of which was estimated at about 50000 kg (Louis and Kumar, 2006). These particles appeared like biological cells (Louis and Kumar, 2006), looked like red blood cells with an average size of 10 µm in diameter, and showed some characteristics of algae. The mysterious aspect of the rain is that it fell for two months accompanied by colored hailstones, and that in most cases the color was red but in some cases it was also yellow. The cells appeared in low magnifications as smooth glass beads and at high magnifications showed large variations in size (Louis and Kumar, 2003). Their shapes ranged from spherical to ellipsoidal. As reported by the locals in Kerala, the fall of the rain started a few hours after a meteor airburst took place. The analyses of red particles performed by Louis and Kumar (2006) using an energy dispersive analytical X-ray system revealed a spectrum of major peaks of carbon and oxygen with other minor elements such as silicon (Si), iron (Fe), chlorine (Cl), aluminum (Al) and sodium (Na). Furthermore, Louis and Kumar (2006) have demonstrated that when subjected to certain harsh physical and chemical conditions such as high concentration of H<sub>2</sub>SO<sub>4</sub>, high temperature (300 °C) and low pressure (0.01 millibar), the cells remained intact and survived. The UV-Vis spectroscopic analysis of red rain revealed a spectrum with a very clear absorption peak near a wavelength of 200 nm. The dilemma facing astrobiologists is whether this absorption peak correlates with the extinction peak at 217.5 nm that has been widely observed in the interstellar medium. The above findings obtained from the laboratory analysis of red rain samples together with the coincidence of meteor events may be taken as evidence that the red rain particles probably have an extraterrestrial origin. This claim if it is scientifically supported, would agree with the theory proposed by Hoyle and Wickramasinghe (2000) that comets can act as transporters of microorganisms to Earth.

The claim made by Louis and Kumar (2003 and 2006) that the red rain in Kerala is of extraterrestrial origin, is considered by some to be flawed because there has been a lack of supportive evidence to confirm the presence of well-defined meteoric events that took place over India at that precise time. To many critics, such an idea that a comet may contain red cells, is hard to imagine, let alone to accept. The report of a meteorite or comet explosion is still in dispute, and the origin of this huge quantity of red particles is far from clear. So when faced with the suggestion that the fall of red rain in Kerala is extraterrestrial in origin, there is an attempt to treat any connection between red rain and a meteor as a coincidence.

Fitzsimmons (2006) has raised doubt about the Kerala Red Rain by making the following statement: "The report sounds completely improbable; it would be a fantastic result if it were true and would tell us once and for all if there was extraterrestrial life, but the report is assuming that these micro-organisms came from a comet when no comet has been observed". Sampath et al. (2001) also confirmed that they found no meteor debris in the colored rainwater. According to Veerabuthiran and Satyanarayana (2003) and Satyanarayana et al. (2004), the reported coloration of red rain was probably caused by the dusty storm from the desert in the west region of Asia. It has also been suggested that these red particles are either fungal spores (Sampath et al., 2001) or red dust that was swirled up from the Arabian dessert (Veerabuthiran and Satyanarayana, 2003; Satyanarayana et al., 2004) or even a splash of blood cells caused by a meteor hitting a flock of bats while flying in the sky (Reed, 2006). Finally it should be noted that the claim made by Louis and Kumar (2006) that the red rain cells have no DNA, is highly controversial since it is well known that all living organisms on earth contain this genetic material.

#### 8.2.3. Aim of the study

Research on the Kerala red rain may give a new perspective to the origin and evolution of life on Earth, and to the question of the possible existence of life beyond our planet. The present study has used a number of laboratory techniques to reexamine the red particles in the Kerala rain sample. Its main aim is to find some answers to the following critical questions: (1) Are there any real structural differences between the red rain particles and normal mammalian red blood cells? (2) Do these rain particles produce spectroscopic characteristics similar to those of astronomical observations? (3) Do these red particles contain phosphorus, a known chemical element that involves in the genetic encoding? (4) Is their chemical composition comparable to that of a comet or meteorite? In order to answer these questions, the present study has made the following attempts: (i) to compare the fine structure of red rain particles with that of mammalian red blood cells using both transmission and scanning electron microscopy; (ii) to carry out spectroscopic analyses of the red rain particles and to determine whether there is any match between the resulting spectra and the astronomical observations; (iii) to analyse the elemental composition of red rain cells using an Energy Dispersive Analyser of X-rays (EDAX); and (iv) to ascertain if there is any similarity in terms of chemical composition between the red rain particles and the Tagish Lake meteorite.

#### 8.3. Materials and Methods

The following methods are used in the present study: FTIR, UV-Vis and Fluorescence Spectroscopy, Light and Electron Microscopy and Energy Dispersive Analysis of X-Rays (EDAX). Details of instruments and their operation are described in Chapter 2 of the present thesis. Specific sample preparative steps are described as follows:

# 8.3.1. Electron Microscopy

Briefly, the red rain sample for transmission electron microscopy was centrifuged at 13000 rpm for 10 mins and the resulting pellet fixed for 1 hour in 2.5% glutaraldehyde in phosphate buffer (pH7.4). The fixed sample was dehydrated in a

graded series of ethanol concentrations and embedded in araldite resin. The polymerized resin block was cut into 90 nm thick sections on a Reichert ultracut microtome (Leica Ltd., UK) with a diamond knife. The thin sections were collected on a pioloform coated grid and stained in 2% uranyl acetate and Reynolds lead citrate. Ultrastructural examination was carried out using a Philips transmission electron microscope (Philips 208 TEM, FEI Ltd., Eindhowen, The Netherlands).

For scanning electron microscopy, the sample was prepared as above up to the final steps of ethanol dehydration, transferred onto a 0.2 µm millipore filter in a capsule and dried under a high pressure (90 bars) in a critical point drying unit for 4 hours using liquid CO<sub>2</sub>. The dried sample was then mounted on a metal stub, coated with a thin layer of gold and examined in a scanning electron microscope (Philips XL20 SEM, FEI Ltd., Eindhowen, The Netherlands).

# 8.3.2. FTIR Spectroscopy

For the FTIR spectroscopical analyses, the red particles in rain water were centrifuged at 13000 rpm for 10 mins, the supernatant carefully removed and the pellet dried under a high pressure (-7 MB) for 48 hours in a 360 Edwards vacuum unit (Agar Scientific Ltd., Stansted, UK). The dried sample (0.5 mg) was mixed with KBr powder (20 mg), crushed with a pestle in a mortar until a fine powder was obtained and transferred into Evacuable pellet Dies (SPECAC Ltd, Kent, UK) to make a disc.

# 8.3.3. UV-Visible Spectrophotometry

Two different types of samples (DMSO extract and neat red rain) were analysed using UV-Visible Spectrophotometry. The DMSO extract was obtained using the following procedure: (1) the rain water containing red particles (1 ml) was centrifuged at 13000 rpm for 10 mins and the supernatant removed; (2) the resulting pellet was mixed with DMSO for 10 mins and the whole mixture centrifuged at 13000 rpm for 10 mins; and (3) the clear red supernatant was transferred to the UV-Visible spectrophotometer for analysis. The neat rain water containing red particles (1 ml) was transferred directly to the UV-Visible spectrophotometer for analyses.

# 8.3.4. Fluorescence Spectroscopy

The DMSO extract of red rain sample prepared as above was analysed using fluorescence spectroscopy at different excitation bands ranging from 412 to 600 nm.

# 8.3.5. Energy Dispersive Analysis of X-rays (EDAX)

Red rain sample (100  $\mu$ l) was pipetted out onto a 0.2 Millipore filter in a capsule, allowed to air dry overnight at room temperature and analysed using an EDAX system fitted into an environmental SEM (Philips ESEM-XL30).

#### 8.4. Results

# 8.4.1. Structural Analysis

#### 8.4.1.1. Light Microscopy

Under a transmitted light microscope, the cells appear generally red brown in coloration; their shapes vary from spherical to ellipsoidal or oval and their sizes are between 5  $\mu$ m and 10  $\mu$ m. The cells are outlined by a thick wall that appears darkly stained (Fig.8.1).

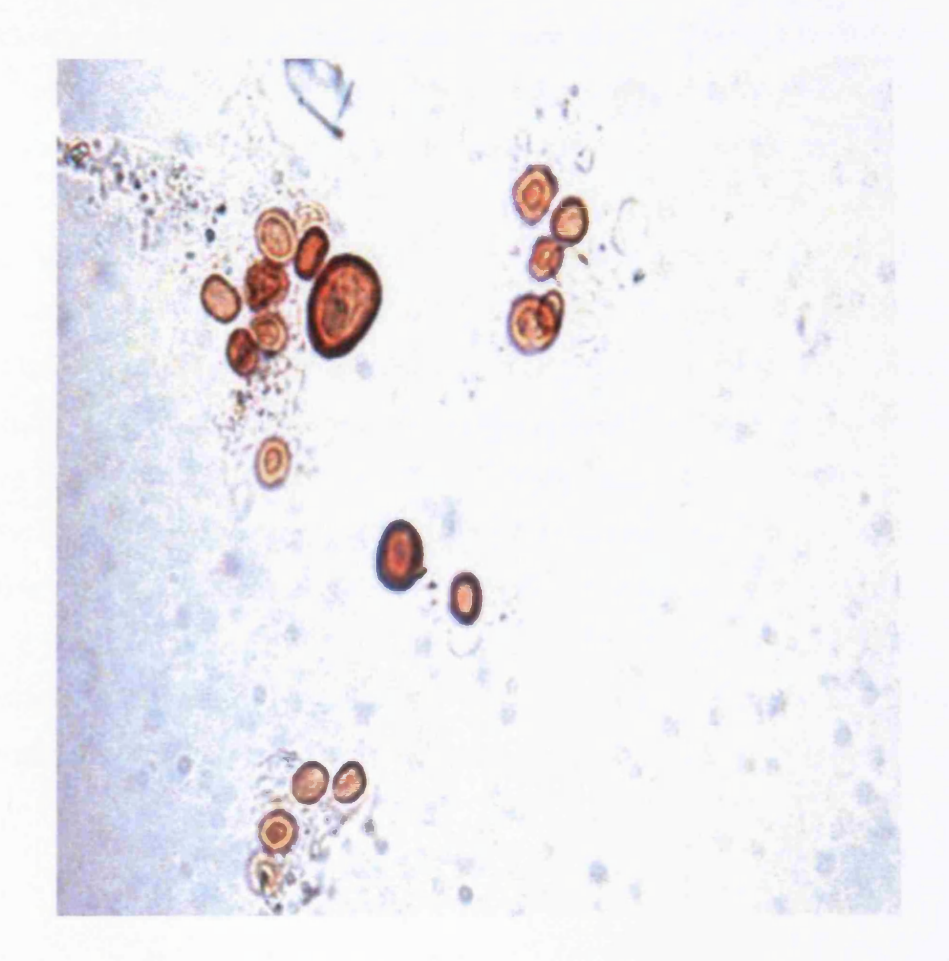


Fig.8.1: Light microscopy (LM) photograph of red rain cells showing variations in shape (spherical, ellipsoidal and oval) and size (5-8  $\mu$ m). The cells have a thick wall outlined by darkly stained membranes. In general, the cells appear red-brown in coloration. Magnification: 100x.

#### 8.4.1.2. Electron Microscopy

Figs. 8.2 and 8.3 show cross-sections of red rain cells cut from a pellet. The representative electron micrographs illustrate the internal structure of different parts of the cells. The cells show variations in shape, size and cellular contents; these variations depend on the area where the cells were sectioned. In general, all cells show an exceptionally thick wall outlined by two darkly stained membranes, internal and external. The wall has an average thickness of 600 nm. Many cells also have additionally a 200-300 nm thick protective exterior coat, known as capsule or exosporium (Fig. 8.2). Some cells reveal their core or cytoplasm containing densely stained materials of variable shapes and sizes, some of which appear almost spherical

with clearly defined membranes and an average size of 1000 nm in diameter. These nanometer-sized objects have been identified as 'daughter' cells by Louis and Kumar (2003 and 2006), and they are squeezed out at some stage through the openings in the wall of the 'mother' cells (Fig. 8.3). Other organelles are not found in the cytoplasm of red rain cells such as mitochondria, endoplasmic reticulum and golgi apparatus. It is noteworthy however that whilst some 'mother' cells show an empty core, many others have an abnormally large nucleus occupying almost the entire volume of their cytoplasm (Fig. 8.2). The nuclear membrane is clearly defined by its electron dense opacity as shown by the arrows in Fig. 8.2. Dark inclusions, apparently aggregates of chromatins, are seen scattered in the inside of the nucleus. The present study also used scanning electron microscopy (SEM) to illustrate the surface structure of the red rain cells. Fig.8.4 shows many cells with a concave surface structure. This inward depression at the centre of the cells is comparable to the cup-like structure of mammalian erythrocytes (Fig. 8.5) and as a result, the red rain cells were thought by some to be the normal red blood cells.

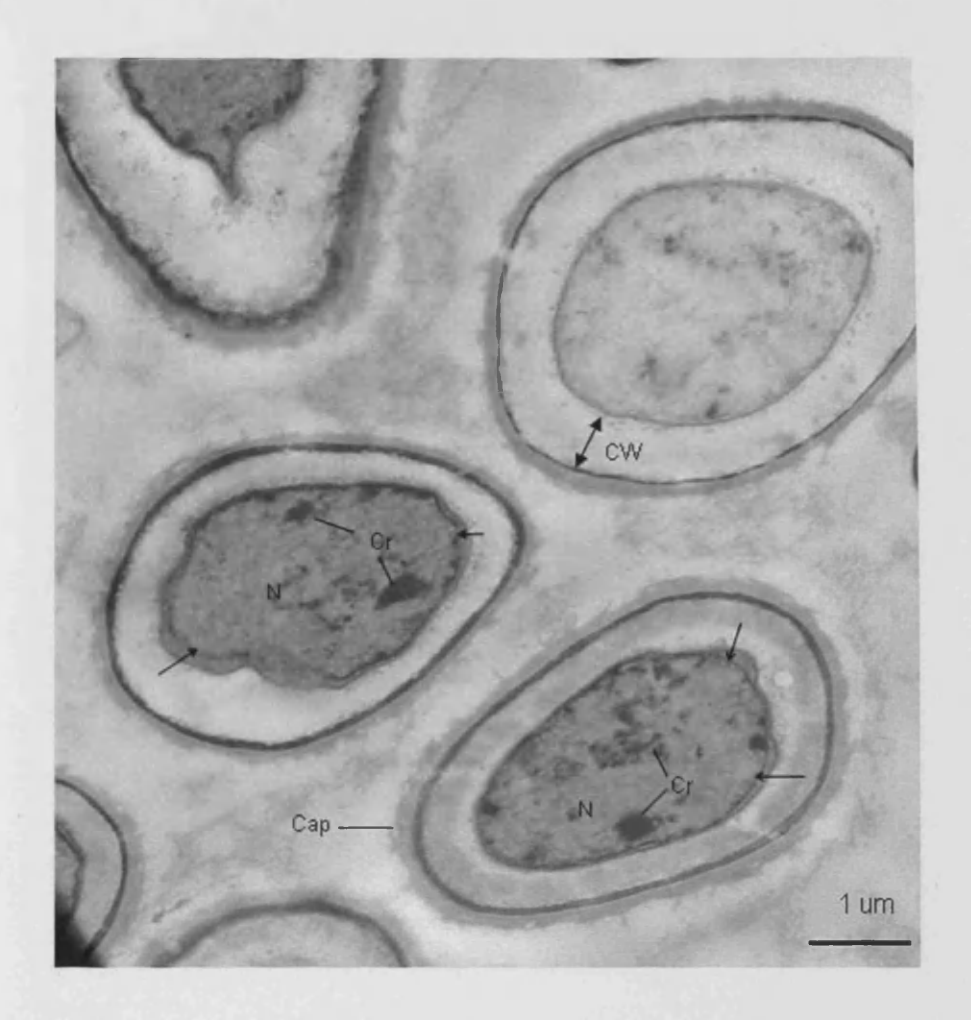


Fig.8.2: Transmission electron microscopy of cross- sections of red rain cells. The cells show a large nucleus which is delineated by an electron dense membrane as shown by the black arrows. Aggregates of chromatins are scattered within the nuclear enclosure. The nucleus occupies almost the entire area of cytoplasm. In general the cell wall has an average thickness of 600 nm. The wall is coated with a 250 nm thick layer of fibrillar materials, known as capsule or exosporium. Nucleus (N); Chromatin (Cr); Cell wall (CW); Capsule (Cap).

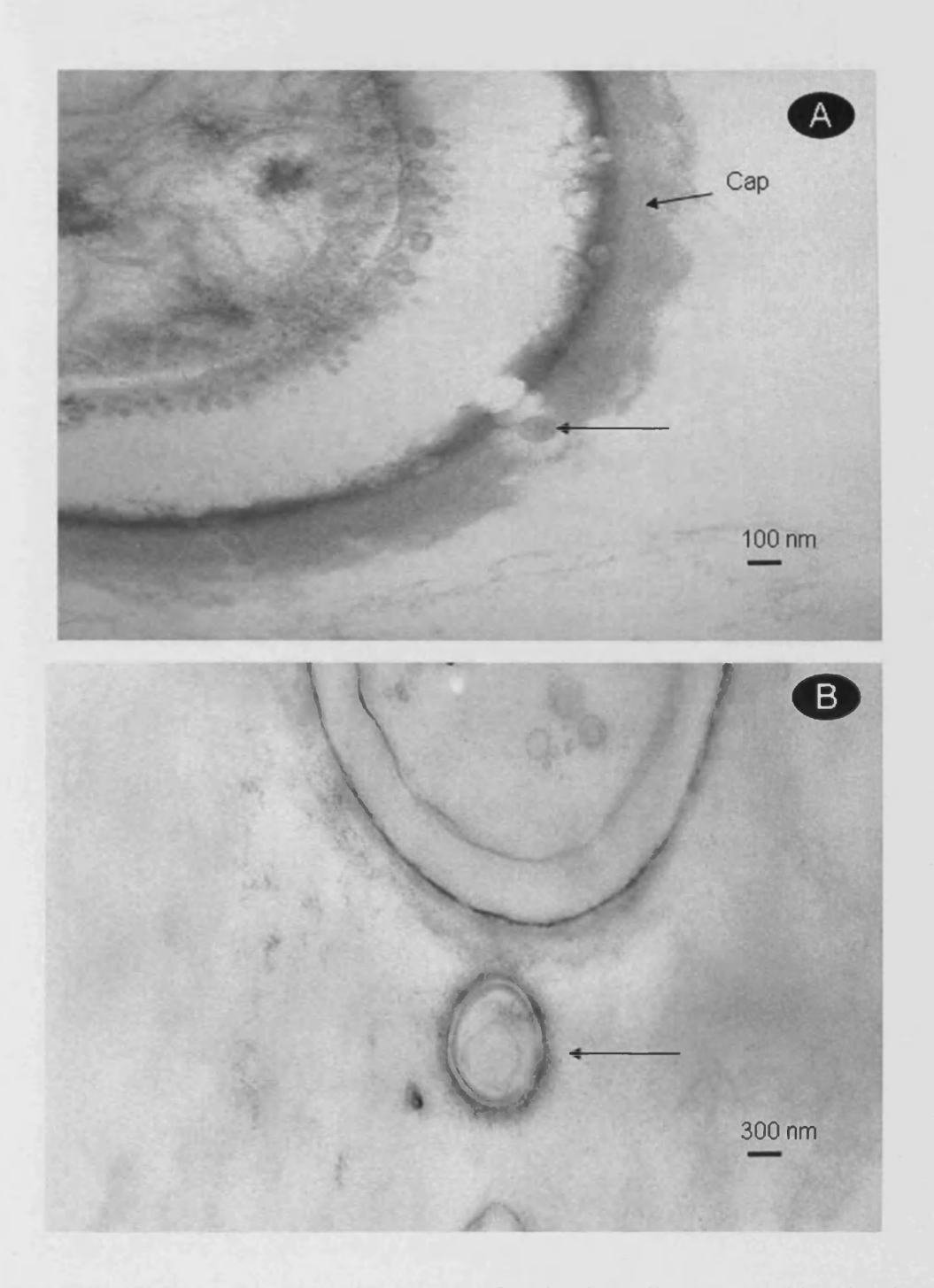


Fig.8.3: Transmission electron micrograph of red rain cells. (A): A 'daughter' cell (arrow) is just released from the 'mother'. (B): A daughter cell (arrow) has enlarged, showing some structural characteristics of the 'mother' cells. Capsule (Cap).

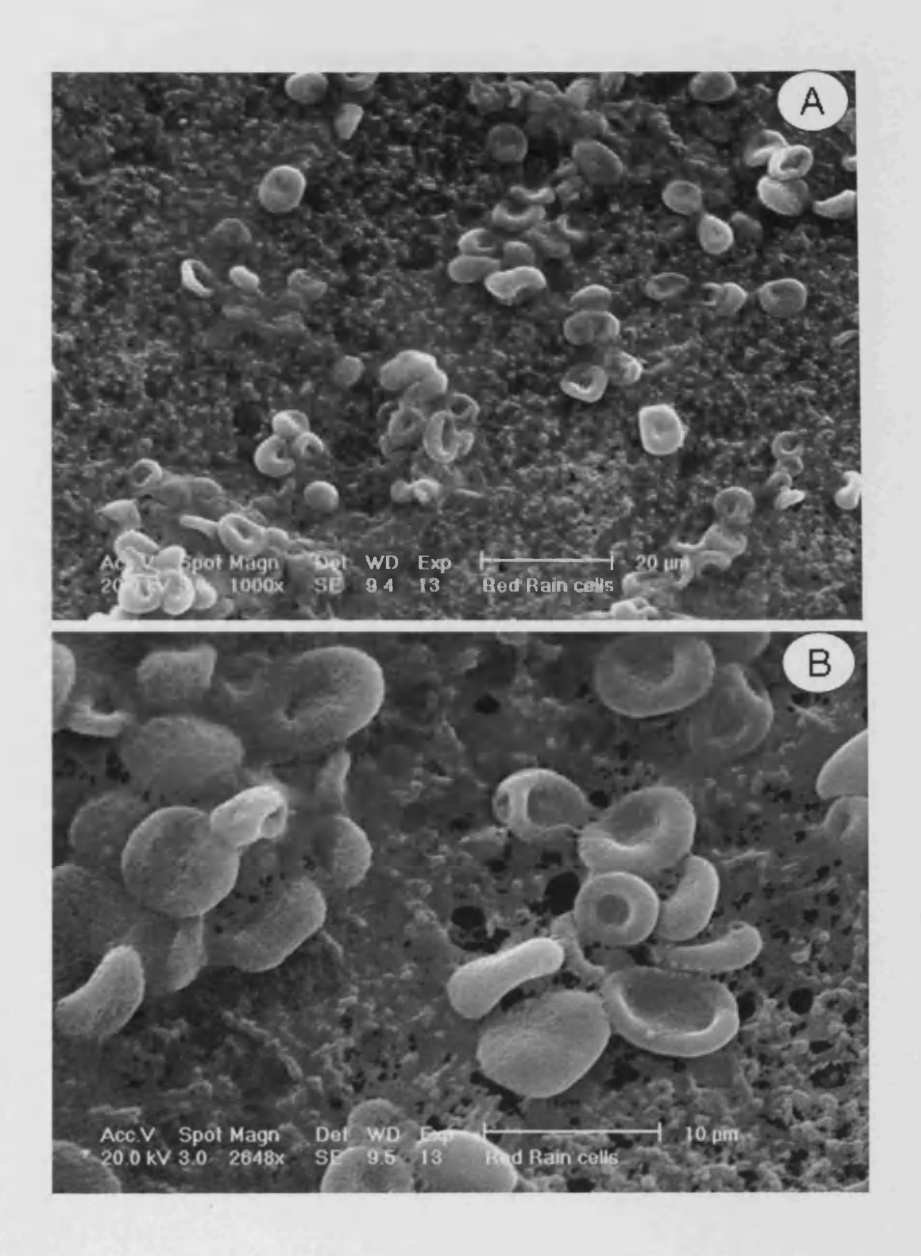


Fig.8.4: Scanning electron microscopy of red rain cells. (A): A low magnification micrograph showing a concave structure. (B): A high magnification image showing the cup-like structure; the cell surface appears granular.

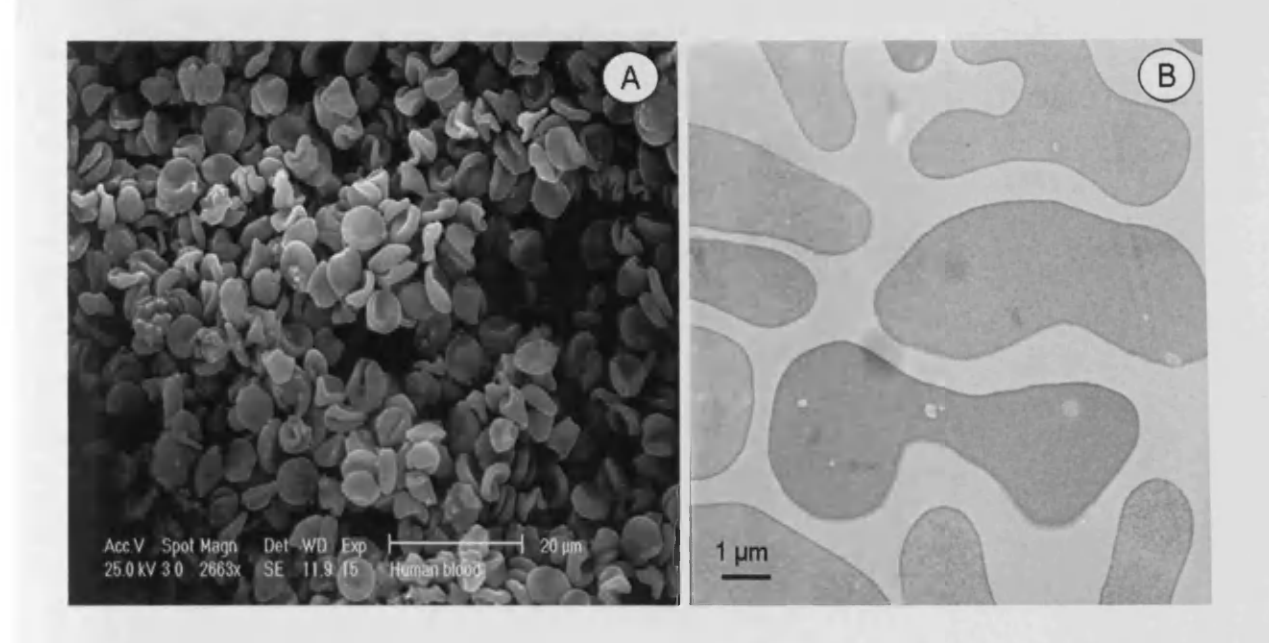


Fig. 8.5: Electron micrographs of mammalian red blood cells. (A) A scanning electron micrograph of erythrocytes illustrating a concave (cup-like) structure. (B) A transmission electron micrograph of erythrocytes showing a thin wall; the cytoplasm appears granular but has no organelles.

# 8.4.2. UV-Vis Spectrophotometry

The results obtained from the present study using a UV-Visible spectrophotometer are shown in Figs. 8.6 and 8.7. The spectrum of neat (untreated) red rain samples contains an absorption peak at 207 nm (Fig.8.6). The red rain cells dissolved in DMSO produce a UV-Vis spectrum with two major absorption peaks centered at 338 nm and 435 nm in the visible region (Fig.8.7).

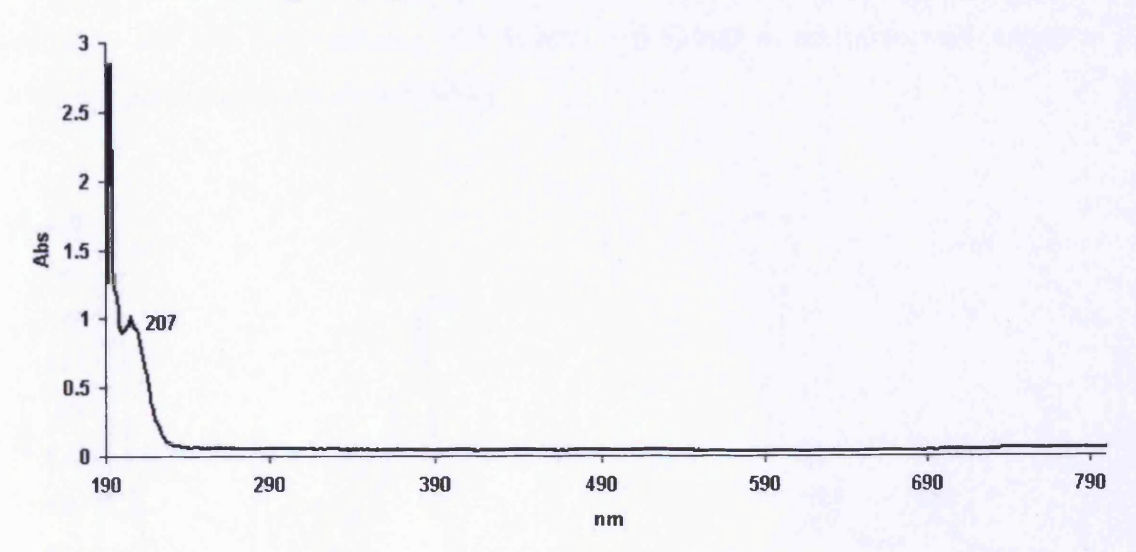


Fig.8.6: UV- Vis spectrum of neat sample of red rain showing a prominent bump centered at 207 nm.

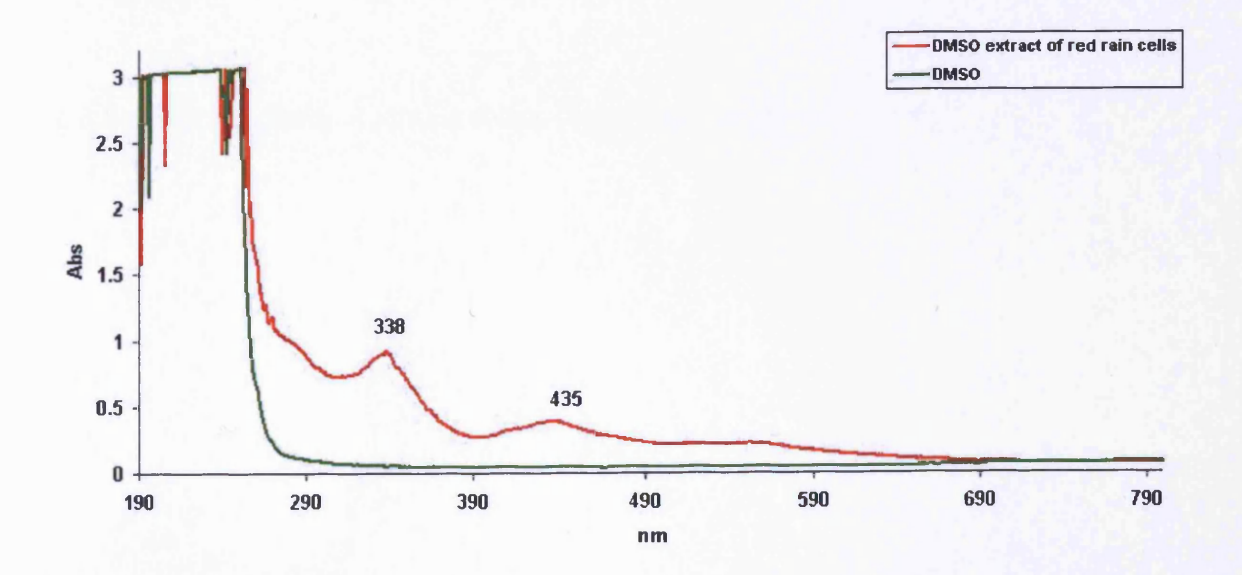


Fig.8.7: UV- Vis spectrum of DMSO extracted red rain sample showing two peaks centered at 338 and 435 nm.

# 8.4.3. FTIR Spectroscopy

The analysis of red rain samples by FTIR spectroscopy shows an IR spectrum containing a series of absorption peaks centered at 2.9, 3.4, 6.0, 6.2, 6.8, 7.2, 7.7, 9.6, 10.3, 11.0, 12.4, 13.3, 18.5 and 21.0  $\mu$ m (Fig.8.8), most of which match those of UIBs and PPNe (Chapter 4 of the present thesis). Fig. 8.9 displays four overlaid spectra (the first three tops representing species of seaweed and the fourth at the very bottom relating to the red rain sample). All spectra are found to resemble each other in waveband pattern and absorption peaks.

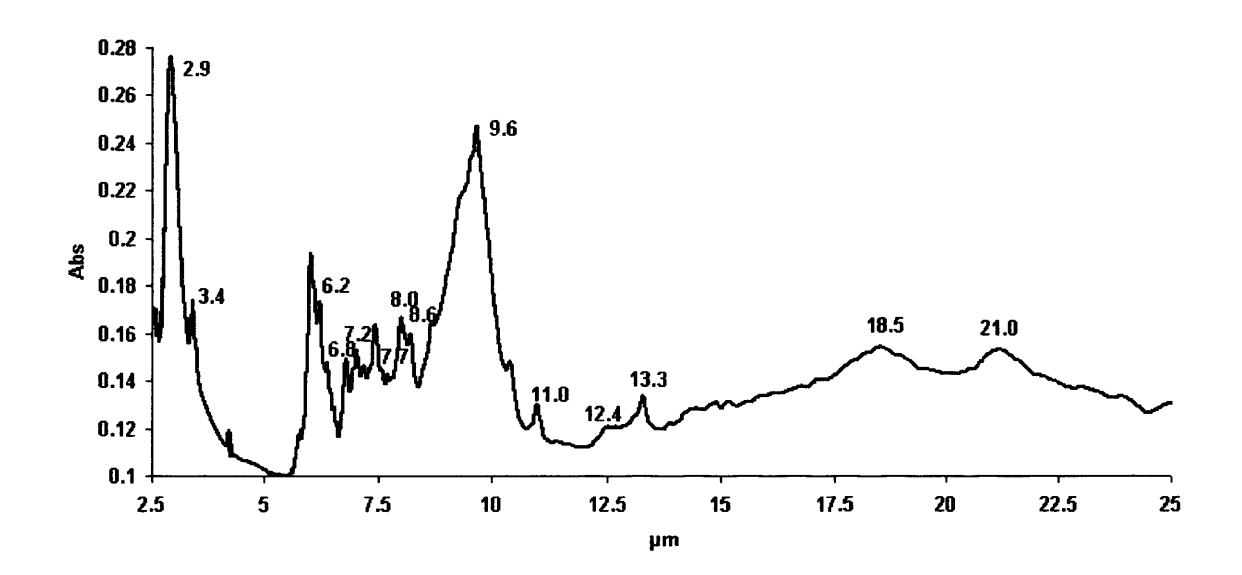


Fig.8.8: FTIR spectrum of KBr-embedded red rain sample.

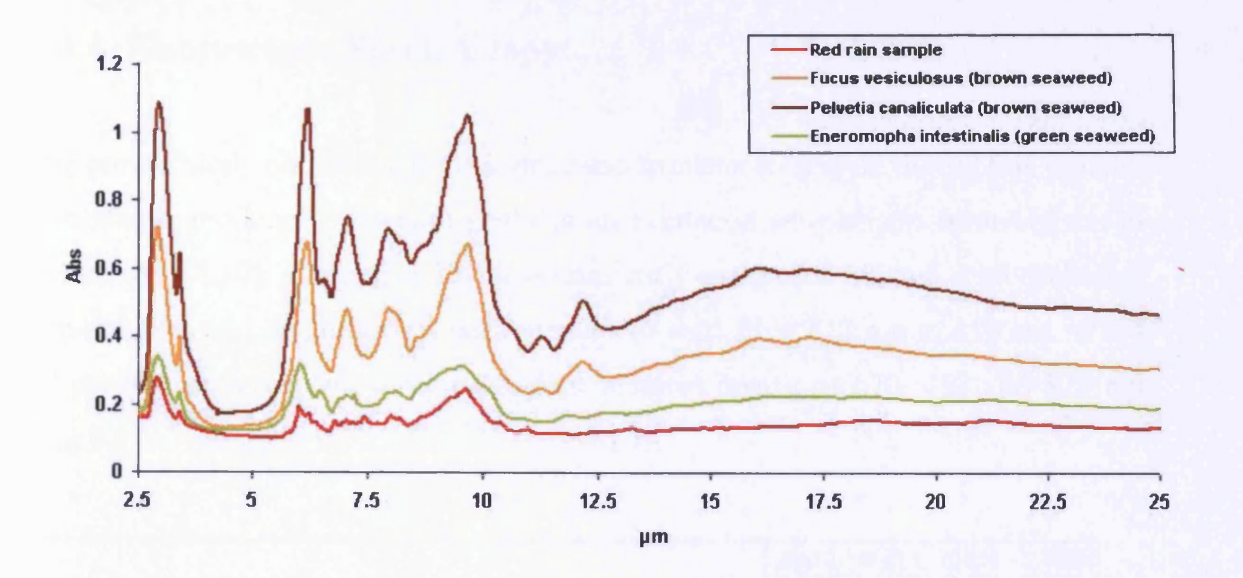


Fig.8.9: Overlaid FTIR spectra of three different species of seaweed and red rain. All wavebands appear similar to each other and exhibit almost identical features, centered at 2.9, 3.4, 6.0, 6.2, 6.8, 7.2, 7.7, 9.6, 10.3, 11, 12.2, 13.2, 18.5 and 21.1µm.

Table 8.1: Distribution of infrared absorption peaks of red rain cells and astronomical emission bands

UIBs (µm)	PPNe (µm)	Red rain (µm)
3.3	3.3	
	3.4	3.4
6.2	6.2	6.2
	6.9	6.8
	7.2	7.2
7.7	7.7	7.7
1.78 FT	8.0	8.0
8.6	8.6	8.6
11.3	11.3	11.0
-	12.2	12.4
(CR)(G-)	13.3	13.3

## 8.4.4. Fluorescence Spectroscopy

The present study has used a fluorescence spectrometer to analyse the red rain sample. The sample produces two major peaks at all excitation wavelengths from 412 nm to 600 nm (Fig.8.10). A prominent peak is constantly centered at 670 nm at all excitation wavelengths, and an additional peak appears to shift from 813 nm to 850 nm. When all spectra are averaged, three prominent features appear at 670, 763 and 823 nm (Fig.8.11).

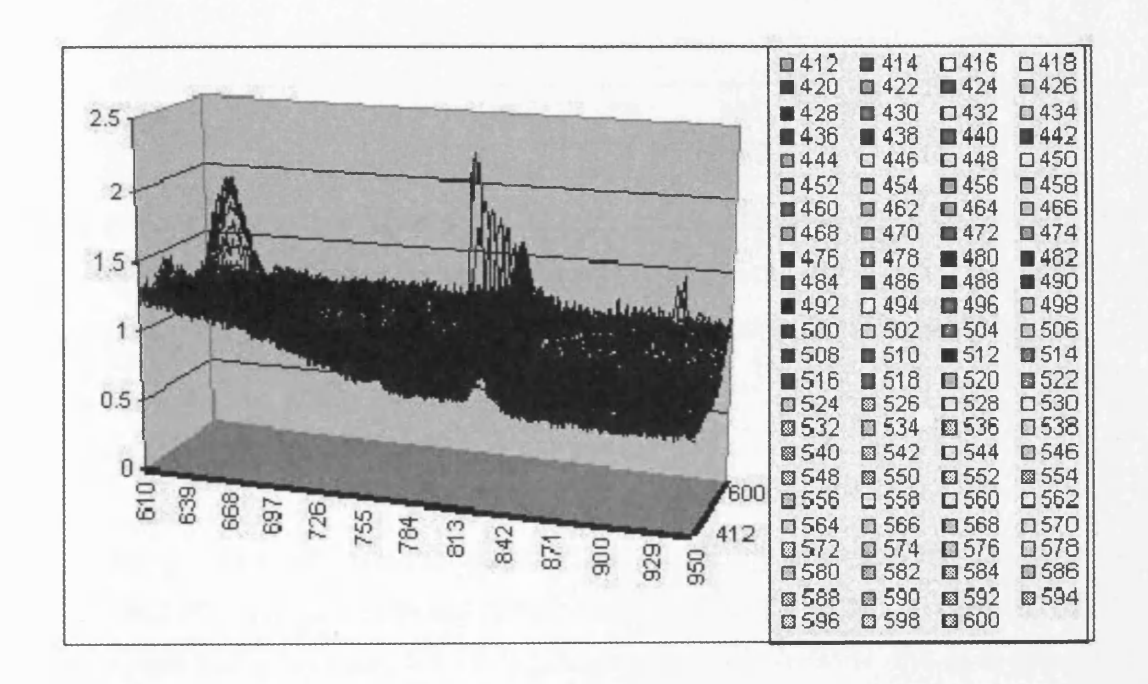


Fig.8.10: Emission spectra of red rain particles at different excitation wavelengths (412-600 nm).

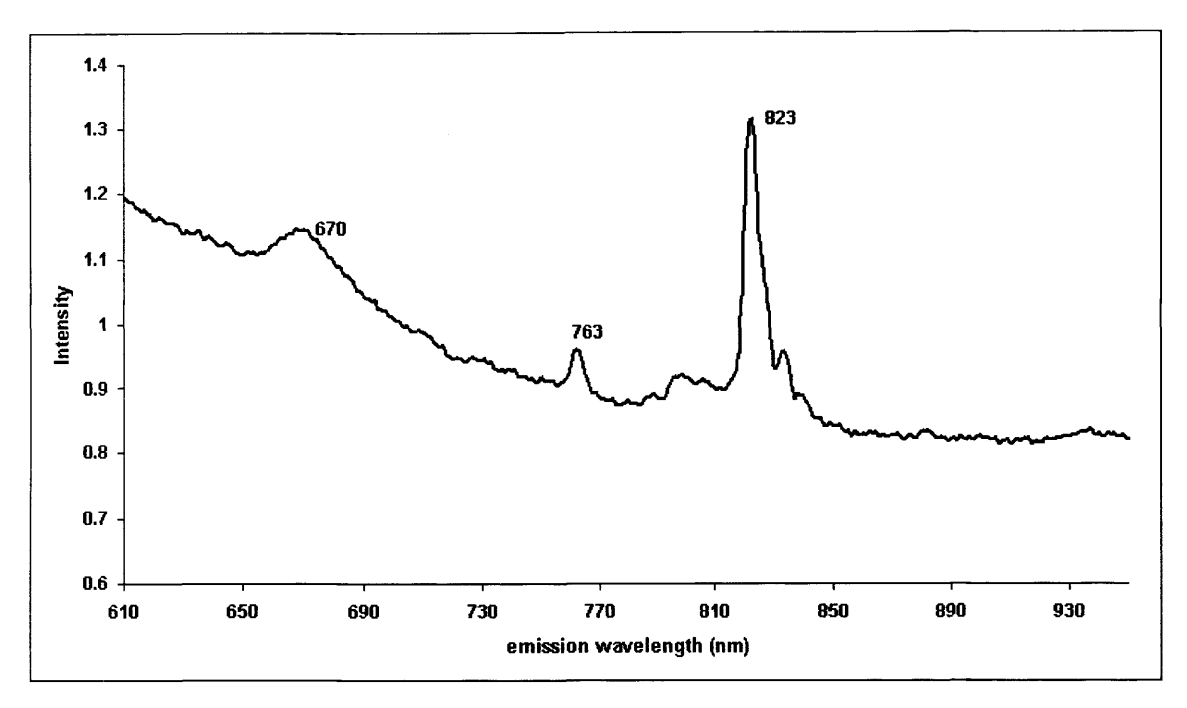


Fig.8.11: The average of emission spectra at excitation wavelengths 412-600 nm shows three majors peaks, 670, 763 and 823 nm, located within the extended red emission or (ERE) band of 540-940 nm (Ehrenfreund and Charnley, 2000).

#### 8.4.5. EDAX

The results obtained from the energy dispersive X-ray microanalysis are shown in Table 8.2. The red rain cells are rich in carbon (52.1±3.3 wt %), oxygen (33.04±2.6 wt %) and nitrogen (8.8±0.4 wt %). Silicon (3.21±0.3 wt %) is the most prominent amongst the less (<1 %) abundant elements such as Al, Fe, Na, Co, P, S, Cl, K, Ca and Cu. Most of the chemical elements detected in the red rain cells are also found in the Tagish Lake meteorite such as carbon, oxygen, silicon, sulfur, iron, phosphorus and aluminum (Table 8.2). By contrast, Louis and Kumar (2003 and 2006) did not detect some of the crucial elements such as phosphorus, sulfur and calcium that are commonly found in biological materials.

Table 8.2: Relative weight (%) of chemical elements detected in the red rain particles obtained from the energy dispersive X-ray microanalysis in comparison with those of Louis and Kumar (2006) and the Tagish Lake meteorite (See Chapter 6 of the present thesis). The figures are mean  $\pm$  SD (standard deviation) of 25 measurements taken at random.

Elements	Weight %±	Louis and	Weight %±STD
	STD(Red Rain	Kumar	(Tagish Lake
	particles)	( 2006)	meteorite)
Carbon	50.0±3.3	49.53	47.9±3.1
Nitrogen	8.8±0.4	_	0
Oxygen	35.01±2.6	45.42	36.0±3.0
Cobalt	0.24±0.05	-	0
Aluminium	0.8 ±0.2	0.41	0.7±0.06
Silicon	3.21±0.3	2.85	3.9±0.3
Phosphorous	0.2±0.04	-	0.5±0.05
Copper	0.04±0.01	-	0
Sulphur	0.2±0.02	-	2.2±0.2
Calcium	0.1±0.02	-	0.5±0.04
Iron	0.7±0.05	0.97	7.5±0.3
Sodium	0.5±0.02	0.69	0.1±0.01
Chlorine	0.1±0.02	0.12	0
Potassium	0.1±0.07	-	0

#### 8.5. Discussion

According to panspermia theory, the Earth was seeded in the past with microorganisms from outer space, and this activity is still taking place. This theory is recently supported by the work of Louis and Kumar (2003 and 2006) who have claimed that comets may harbor red rain particles in the form of biological cells. Their claim is based on the results obtained from the laboratory analyses on the rain samples. Studies on the Kerala red rain cells have provided insights into extreme environmental conditions in which life can inhabit in the Universe. The Red Rain cells could be a new algal species, or they may represent entirely new forms of life that would link the origin of life on Earth to life forms that might be present elsewhere. There are some speculations about Venus that it may be harbouring life in the clouds (Wickramasinghe and Wickramasinghe, 2008). Since Louis and Kumar (2003 and 2006) have proposed a comet as the transporter of red rain cells, this idea has attracted criticism.

The current controversial topic relating to the Kerala red rain cells has prompted me to re-examine the samples using a number of laboratory techniques and instruments. Under a transmitted light microscope, the natural cells appear generally red brown in coloration and their shape varies from spherical to ellipsoidal or oval with a densely stained thick wall (Fig. 8.1). Observed in a transmission electron microscope, this wall has an average diameter of 600 nm and is outlined by two thick membranes, internal and external; its external membrane is further coated with a 200-300 nm thick layer of fibrillar material, generally known as capsule or exosporium. The overall thickness of their protective layers (cell wall, outlining membranes and capsule) is about 850 nm, thus making the red rain cells microoganisms that have the thickest cell wall. It may be argued that the presence of such a thick wall should make the red rain cells perhaps the toughest microorganism on Earth. Louis and Kumar (2003 and 2006) have demonstrated that these cells can sustain growth at extremely harsh conditions but this result has still to be verified independently.

Their cytoplasm contains organelles of variable sizes, some of which appear almost spherical with an average size of 1000 nm in diameter. These nanometer sized

globules have been identified as 'daughter' cells by Louis and Kumar (2003); they are released at some stage through the openings in the wall of their 'mother' cell' (Fig.8.3). Many of these so called 'mother' cells show an almost empty core which may be attributed to the loss of the 'daughter' cells. The cells have a huge nucleus which takes up almost the entire volume of their cytoplasm (Fig.8.2). The nuclear boundary is delineated by clearly defined membranes as shown by the arrows in Fig.8.2. Electron dense inclusions, probably aggregates of chromatins, are scattered within the nuclear enclosure.

The present study used scanning electron microscopy (SEM) to illustrate the surface structure of the red rain cells. Many cells show a concave structure (Fig. 8.4); this inward depression may be attributed to the release of the daughters and other materials by the mother cells. It may also be argued that the structural deformation could result from the cytoplasmic shrinkage caused by the EM processes using chemical fixation and dehydration. Although both the red rain and the normal red blood cells show a similar surface structure as shown in Figs. 8.4 and 8.5A, their internal morphology is completely different (Figs. 8.2 & 8.5B). Whilst the red rain particles show a thick wall and cytoplasmic organelles, the normal mammalian red blood cells in contrast have a much thinner wall and contain no cytoplasmic organelles (Fig. 8.5B). Based on these ultrastructural differences, the present study confirms that the red rain cells are not the normal mammalian red blood cells and therefore rules out the concern raised by Reed (2006) that the red particles could be red blood cells from the bats that were hit by some strange objects while flying in the sky. Furthermore, the discovery of biological elements such as membraneous walls and cellular organelles confirms that the red rain particles are neither dust nor sand.

The results obtained from the present study using UV-Visible spectrophotometry show that the spectrum of neat (untreated) red rain samples contains an absorption peak at 207 nm (Fig. 8.6). When the red rain cells were treated in DMSO and the resulting DMSO extract solution was analysed, the acquired spectrum displayed two major absorption peaks at 338 nm and 435 nm in the visible region (Fig. 8.7); the 435 nm peak is known to be associated with the chlorophyll pigment (Raychaudhuri and Bhattacharyya, 2008). The detection of a feature at 207 nm in the present study is in agreement with the observation of Louis and Kumar (2003) who have reported the

presence of an absorption peak near 200 nm. Louis and Kumar (2003) have attempted to link this near 200 nm peak to the UV extinction bump at 217.5 nm of the interstellar dust by assuming that the red particles are a component in the interstellar dust clouds. According to Louis and Kumar (2003), the shift of wavelength in the extinction peak may be attributed to the effect of interstellar conditions such as low temperature and high pressure to which the particles are subjected.

The present study using FTIR spectroscopy reveals that the red rain cells produce an infrared spectrum containing a series of peaks centered at 3.4, 6.2, 6.8, 7.2 7.7, 8, 8.6, 9.6, 11.0, 12.4 and 13.3 nm, most of which match those of UIBs and PPNe (Fig. 8.8 and Table 8.1). When compared with a number of biological materials, the red rain cells produce a waveband resembling those of seaweed species (Fig. 8.9). This discovery is rather unexpected for the following reasons: (1) the red rain particles were suspended in rain water fallen on Kerala, the state of India from the sky whereas the seaweed samples were collected from seawater in Barry, Wales, UK; and (2) their nature is not related to each other.

The results obtained from the fluorescence spectroscopic analysis of red rain show two interesting features, the first constantly peaked at 670 nm and the second shifted from 813 nm to 850 nm (Fig. 8.10). These bands are within the range of the extended red emission (ERE), 500-800 nm that has been observed in many astronomical sources (Gordon et., 1998; Wickramasinghe et al., 2002). Such sources include planetary nebulae (Furton and Witt, 1990), dark nebulae (Mattila, 1979), and entire galaxies (Darbon et al., 1998). According to Ehrenfreund and Charnley (2000), the ERE is broader (540-940 nm) and results from the photoluminence of particular dust grains. The carriers of ERE are the same carbonaceous compounds as those proposed for the interstellar extinction UV bump at 217.5 nm such as hydrogenated aromatic carbon, HAC (Duley, 1985), quenched carbonaceous composite, QCC (Sakata et al., 1992), coal (Papoular et al., 1996) and polycyclic aromatic hydrocarbons, PAHs (d'Hendecourt et al., 1986).

The present study using EDAX shows that the red rain cells are rich in carbon, oxygen and nitrogen (Table 8.2). Silicon is found to be the most prominent amongst the less (<1 %) abundant elements such as Al, Fe, Na, Co, P, S, Cl, K, Ca and Cu.

According to Louis and Kumar (2006), carbon and oxygen were found to be the major elements but nitrogen, phosphorus and sulfur were not detected. In contrast, the present study has detected nitrogen, phosphorus and sulfur in the red rain cells. Furthermore, most of the chemical elements detected in the red rain cells are also found in the Tagish Lake meteorite such as carbon, oxygen, silicon, sulfur, iron, phosphorus and aluminum (Table 8.2). Six elements (C, H, O, N, S and P) crucial for terrestrial lifeforms that have been found in the red rain cells, are also reported to be present in comets (Huebner and Boice, 1997) and interstellar clouds (Ehrenfreud et. al., 2002). Sulfur is one of the constituents of the insoluble organic matter found in meteorite (Hayatsu, and Anders, 1981; Rauf et al., 2010). Phosphorus on the other hand is one of the main chemical constituents of DNA molecule that is essential for living systems. Three phosphorus bearing molecules, PN (Turner and Bally, 1987), CP (Gue'lin et al., 1990) and HCP (Agu'ndez et al., 2007) have so far been detected in the interstellar medium (ISM) or circumstellar sources. Louis and Kumar (2003) did not detect phosphorus in the red rain cells; their experiments on cell culture also confirmed that phosphorus was not required to sustain growth.

Furthermore, Louis and Kumar (2006) did not find DNA in the red rain cells using dische diphenylamine reagent and ethidium bromide fluorescent dye; they have explained that the red rain cells may have evolved without DNA as a survival strategy to protect themselves from the stellar radiation damage. Unlike Louis and Kumar (2003 and 2006), Miyake (2009) has recently found DNA in the red rain cells using a DAPI (4', 6- diamidino-2-phenylindole) staining method. The present study using electron microscopy also confirms the presence of a large organelle having the characteristics of a nucleus (Fig. 8.2). The fundamental question still remains unanswered as to whether the red rain cells like any terrestrial living organisms carry thermally unstable DNA as their genetic molecule or thermostable proteins as their first informational macromolecules. It may be suggested that to sustain growth, the red rain cells may rely on more stable proteins than DNA (Louis and Kumar, 2003). All known living systems on earth are known to be unable to survive at 100 °C, let alone 300 °C. Under these temperatures, their metabolic activities completely shut down. However, there are reports that some microorganisms isolated from the ocean hydrothermal vent systems and deep-sea oil wells can grow even at 121 °C, such as Pyrolobus fumarii (Blochl et al., 1997), and Strain 121 (Kashefi and Lovley, 2003).

These microorganisms are known as hyperthermophiles, and can thrive in such a high temperature because of their ability to evolve either by altering their metabolism or genetic make-up (Grogan, 1998).

Electron microscopy confirms that the red particles are biological materials with a structure resembling that of spores of a microorganism yet to be properly identified. Their amazingly thick cell wall may suggest that the red rain cells can survive in extremely harsh environmental conditions. The present investigation using EDAX has shown that the red rain cells contain all biogenic elements that are ubiquitous in the interstellar medium. Their mineralogy is also similar to that of carbonaceous meteorites. The cells display UV-Visible, IR and fluorescence wavebands containing features whose wavelengths mostly match those of astronomical observations. The IR spectrum of the red rain cells remarkably resembles those of seaweed species. The cells are equipped with an abnormally large nucleus that takes up almost the entire volume of their cytoplasm.

The evidence presented in this current study seems to offer a plausible explanation that the red rain cells could be closely related to the original species of a microorganism that was involved in the evolution of early life on Earth. It would be interesting to study the survival behaviour of this organism in space conditions, and this study could provide an insight into its origin. The issue of whether the red rain cells contain DNA still remains controversial. Further studies are required to help resolve this contentious topic. One of the contemporary methods that may be suggested is to characterize the DNA molecular structure by polymerase chain reaction (PCR).

# **CHAPTER 9**

Study of Putative Microfossils in Space

Dust from the Stratosphere by Scanning

Electron Microscopy and UV-Vis

Spectroscopy

# 9.1. Summary

Interplanetary dust particles (IDPs) have recently been recovered from the stratosphere using a cryosampler flown below a balloon flying at altitudes of 20-41 km. The present study uses high resolution scanning electron microscopy (SEM) and UV-Visible spectrophotometry to examine samples collected by this method at 38-41 km. The SEM observations confirm the presence of 7-32 µm sized clusters of coccoidal (0.4-1.3 µm in diameter) and rod shaped (0.6-2.5 µm in length) objects as components of the IDPs complex. Many single globules (1.6-9.0 µm in diameter) are also observed, some of which exhibit a rough surface with filamentous features of variable lengths. The spectrophotometry of the particles in aggregate reveals a prominent peak centered at 216 nm, remarkably similar to that of diatoms and close to the UV astronomical feature of 217.5 nm which has been identified as the spectral characteristic of aromatic hydrocarbons. The evidence presented here suggests that the stratospheric particles are IDPs comprising an assortment of materials among which are included microfossil-like features in variable sizes and forms such as coccoids, rods and filaments.

#### 9.2. Introduction

# 9.2.1. The Earths' Atmosphere

The atmosphere of the Earth is thick near its surface and gradually thins out as altitude increases until it completely merges with space. The total thickness of the atmosphere takes up approximately 1 % of the Earth's radius. The Earth's atmosphere is made up of the following layers distinguishable by their specific temperatures as shown in Table 9.1.

**Troposphere** is the lowest and denser layer of the atmosphere, with altitudes extending from 8 km at the poles to 16 km over the equator, and contains about 75 % of the total mass of atmospheric gases. Nearly all atmospheric water vapour and aerosols are found in this layer. The average temperature decreases from 15 °C at sea

level to about -56.5 °C at the top. A narrow transition zone, known as tropopause, is at the upper edge of the troposphere.

**Stratosphere** is the second layer of the atmosphere immediately above the troposphere but below the mesosphere. It contains about 10 % of the atmospheric mass and extends upward about 50 km from the surface of Earth. The highest temperature in the stratosphere is only around 0 °C, this is because of the localized concentration of ozone gases that absorb ultraviolet sunlight, thus creating heat energy which warms the stratosphere (Barry and Chorley, 2003). A transition zone that separates the stratosphere from the mesosphere is known as stratopause.

**Mesosphere** is immediately above the stratosphere, extending to about 90 km. This is the region where the atmosphere reaches its coldest temperatures (-133 °C). The top of the mesosphere is another transition zone known as the mesopause.

**Thermosphere** is the last atmospheric layer where the temperature can rise to 1,200 °C. The lower part of the thermosphere, from 80 to 550 km above the Earth's surface, is ionosphere. The zone extending from the ionosphere to about 10,000 km forms the exosphere which gradually merges with space.

Forming a protective shield and maintaining a continuous circulation of hot and cold air around the Earth, these atmospheric layers provide favourable conditions for life to exist on our planet. The Earth's atmosphere contains gases and aerosols of various forms. The major gases are made up of nitrogen (79 %) and oxygen (20 %) (Barry and Chorley, 2003).

Table 9.1: Some Characteristics of Atmospheric Layers

Layers of the	Height from the	Temperature (°C)	Pressure
atmosphere	surface of Earth		(mbar)
	(km)		
Troposphere	8-16	25 to -56.5	500
Stratosphere	50	-56.5 to 0	1
Mesosphere	90	0 to -133	0.01
Thermosphere	> 90	-133 to 1200	< 0.001

#### 9.2.2. Aerosols

The aerosols that were found in the stratosphere, originate from Earth and space; these include particles suspended in sea salt, mineral dust (particularly silicates), organic matter and smoke (Barry and Chorley, 2003). According to Renard et al. (2001 and 2005), the aerosols in various forms are present in significant quantities in the middle atmosphere.

## 9.2.3. Interplanetary Dust Particles (IDPs)

The IDPs are either cometary dust particles, or fragments resulting from collision between asteroids. They are considered as 'primitive meteorites' since they contain preserved materials that pre-exist the formation of the solar system (Messenger, 2000). These have become known as IDPs (interplanetary dust particles) and have distinctive compositions (similar to carbonaceous and stony meteorites) and morphologies. Numerous IDPs have bulk mineralogy resembling that of C1 and CM carbonaceous chondrites whereas many other are C-rich materials similar to comets (Rietmeijer et al., 1998). Tens of tons of these particles are believed to enter daily the Earth's atmosphere, but during the entry most of which (about 70%) vaporised into smoke of sub-micrometer sized particles (Biermann et al., 1996). However, large particles with sizes up to 500 µm, remain intact and are mostly detected into the stratosphere (Brownlee, 1985; Maurette et al., 1991).

## 9.2.4. Microorganisms in space

The theory of cometary panspermia proposes that grains in space consist of a mixture of complex organics, and that their inclusion in many hundred billions of comets leads to transition from prebiotic matter into primitive bacterial cells (Wickramasinghe, 1974; Hoyle and Wickramasinghe, 1976; Wickramasinghe, et al., 1977; Hoyle and Wickramasinghe, 1977). It has been suggested that pre-existing viable bacterial cells derived from the interstellar space may have been present in comets in the primitive solar system. This proposal is based on the following evidence: (1) the extinction properties of interstellar dust match precisely the expected behaviour of freeze-dried bacteria. (Hoyle and Wickramasinghe, 1979); (2) the infrared absorption by dust in the 2.9–3.9 µm waveband for the galactic centre source GC-IRS7 has a distinctly bacterial signature (Hoyle, et al., 1982; Rauf and Wickramasinghe, 2010); and (3) the 217.5 nm (2175 Å) ultraviolet extinction is better explained by an ensemble of biological aromatics than by spherical graphite grains (Hoyle and Wickramasinghe, 1991; Rauf and Wickramasinghe, 2010). Other astronomical evidence such as the diffuse IR bands, the complex organic composition of cometary dust and the extended red emission in the red rectangle, also serve to corroborate this proposal. However, the suggestion that the universe is replete with cosmic life, is slow to gain wide acceptance.

In the early years of the space age, attempts were made to probe the upper atmosphere for the presence of microorganisms. The NASA-supported balloon program (Bruch, 1967) and Soviet rocket experiments (Lysenko, 1979) made attempts to show direct evidence for the presence of extraterrestrial microorganisms in the upper atmosphere, but the results were judged to be inconclusive due to the primitive nature of the sterilization procedures. Using rocket probes, Imshenetsky et al. (1978) claimed to have detected and isolated a wide range of common bacteria and fungi from the stratosphere at heights of 48-77 km. This claim has attracted an interest amongst astrobiologists since it has long been known that most microorganisms are restricted to the lower atmosphere at a height less than 17 km (Wainwright et al., 2006). In recent years, improved methodologies have been developed for the identification of microorganisms and stringent protocols applied to almost eliminate contamination

from sampling and laboratory processes (Smibert and Kreig, 1994; Lopez-Amoros et al., 1995; Lal et al., 1996; Narlikar et al., 1998).

Claims to find viable microorganisms in the upper stratosphere met with much scepticism. A common criticism concerns terrestrial contamination from sample handling and laboratory processes. In recognition of this criticism, stringent procedures have been used in the present investigation to prevent possible contamination during sample preparation. Experience at Cardiff with scanning electron microscopy (SEM) gives high confidence in distinguishing contaminant particles from IDP-like cluster particles, while elemental composition identified via the EDAX facility adds credibility and confirmation (Miyake, 2009). The current uses investigation high resolution environmental **UV-Visible** SEM and spectrophotometry to examine in detail some microdust samples collected at 38-41 km altitude.

#### 9.2.5. Aim of the study

The present work re-examined the stratospheric air samples collected by the Indian group (Indian Space Research Organisation/Tata Institude Balloon Facility) using scanning electron microscopy and UV-Visible Spectrophotometry. The findings obtained from this independent investigation may help to confirm whether the samples show structural characteristics similar to those previously reported. Furthermore, the UV-Vis spectrophtometric data should provide an insight into the nature of these samples and possibly their origin.

## 9.3. Materials and Methods

# 9.3.1. Collection of stratospheric air samples

The stratospheric air samples were collected at altitudes between 30 km and 41 km using a cryosampler attached to a balloon according to the procedure as described in detail by Narlikar et al. (2003). The cryosampler was made of stainless steel and fitted with 16 probes. The whole assembly was electron-beam welded and electron plated.

The cryosampler in pre-testing was found to be capable of withstanding temperatures between -246  $^{\circ}$ C and 140  $^{\circ}$ C. Before use, the interior components (probes and manifolds) were cleaned with acetone and thoroughly washed in de-mineralized water, steam-baked and heated with an infrared lamp to 140  $^{\circ}$ C. During the balloon ascent, the probe inlet was closed via a metallic valve. The inlet was opened and closed via radio-signal from ground. The air samples were passed through cellulose acetate filters (0.2  $\mu$ m and 0.45  $\mu$ m pore sizes) as described by Harris et al. (2001). Due to limited availability of the samples, the present study examined only the 0.45  $\mu$ m pore membranes.

### 9.3.2. Scanning Electron Microscopy

Millipore filters (0.45 µm pore size) carrying the samples were cut into pieces (12 mm x12 mm) with a sharp razor blade, attached with sticky carbon tape onto metal stubs and gold coated. This sample preparation was conducted in a clean double-filtered air chamber. The samples were examined using a high resolution environmental scanning electron microscope (Philips XL 30-ESEM) operated at 25-30 kV. Filter membranes containing no stratospheric samples were used as controls, being mounted and examined by SEM in exactly the same way.

# 9.3.3. UV- Visible Spectrophotometry

The filter containing the stratosphere particles was placed in cyclohexane in a glass container and the particles removed by sonication for 15 mins. The particles were suspended in cyclohexane (1 ml) for 30 mins, and the mixture centrifuged at 13000 rpm for 10mins. The clear supernatant was transferred to the UV-Visible spectrophotometer (JASCO V-570 UV/VIS/NIR spectrophotometer) for analysis.

#### 9.4. Results

# 9.4.1. Scanning Electron Microscopy of stratospheric air samples

Scanning electron microscopic observations reveal that the membranes contain materials of variable shapes and sizes, most of which appear in clusters. The clusters are sized between 3 and 32  $\mu$ m across (Figs. 9.1-9.6), and are formed by coccoidal particles that are intermixed in places with rod or tubular objects (Figs. 9.1, 9.2 and 9.3). The sizes of coccoids are measured between 0.4  $\mu$ m and 1.3  $\mu$ m whereas those of rod or tubules vary from 0.6  $\mu$ m to 2.5  $\mu$ m in length (Fig.9.1A). Many globules with sizes ranging from 1.6  $\mu$ m to 9  $\mu$ m can also be observed in places (Figs. 9.3B, 9.4 and 9.5), some of which show a surface covered with small granules of 40-300 nm in diameter (Fig. 9.3) and filamentous features (Fig. 9.6). None of the above features were found on the filter membranes used as controls.

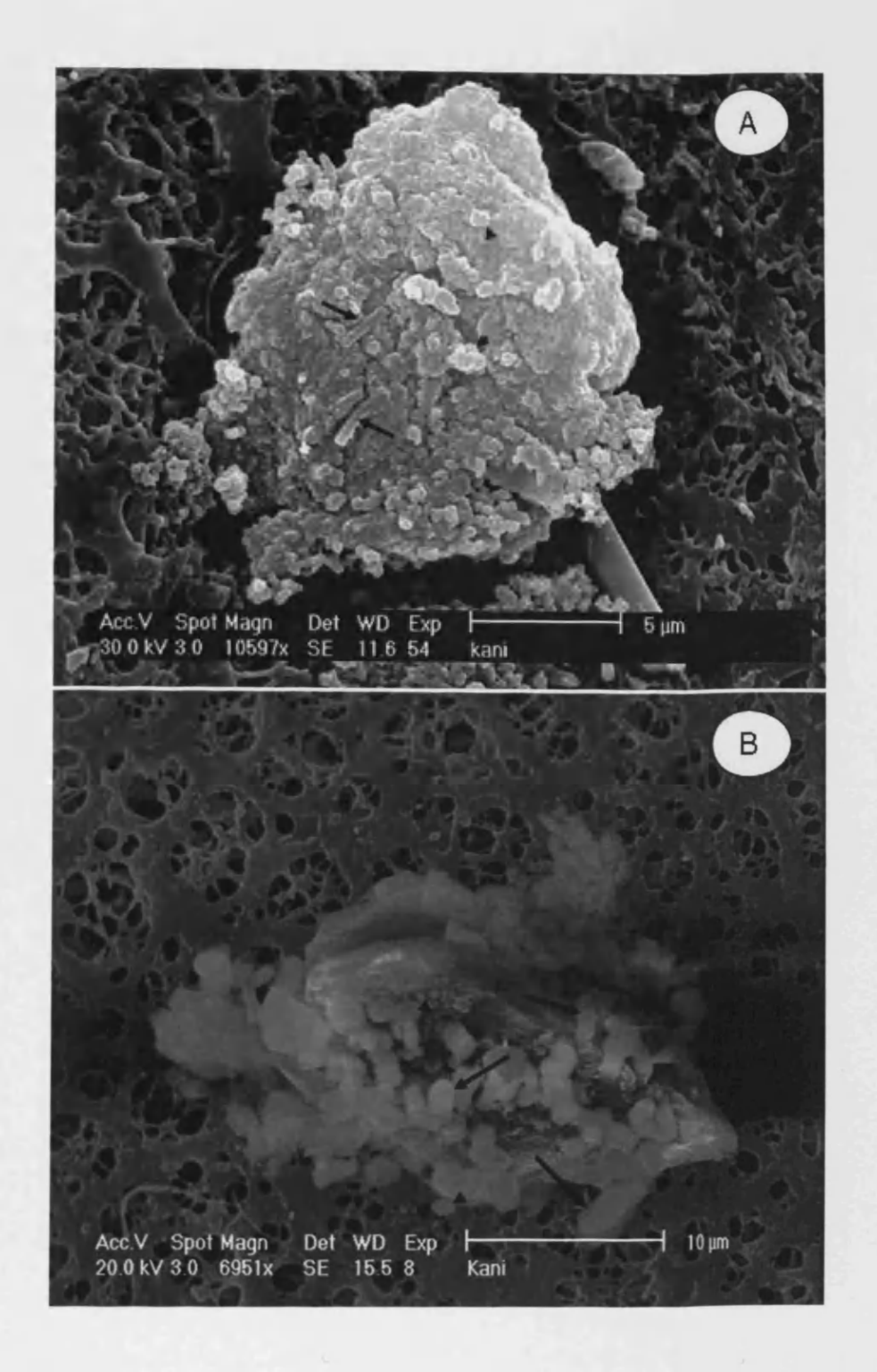


Fig. 9.1: Scanning electron micrographs of stratospheric air samples on 0.45  $\mu m$  cellulose acetate filter. (A) A 20  $\mu m$  sized clump formed by spherical particles (0.4-1.3  $\mu m$  in diameter) as shown by arrow heads and rod shaped particles (0.6-2.5  $\mu m$  in length) as shown by arrows. (B) A 32  $\mu m$  clump formed by rod shaped (2.0-5.0  $\mu m$  in length) as shown by arrows and spherical features (0.4-2.0  $\mu m$ ) as shown by arrow heads.

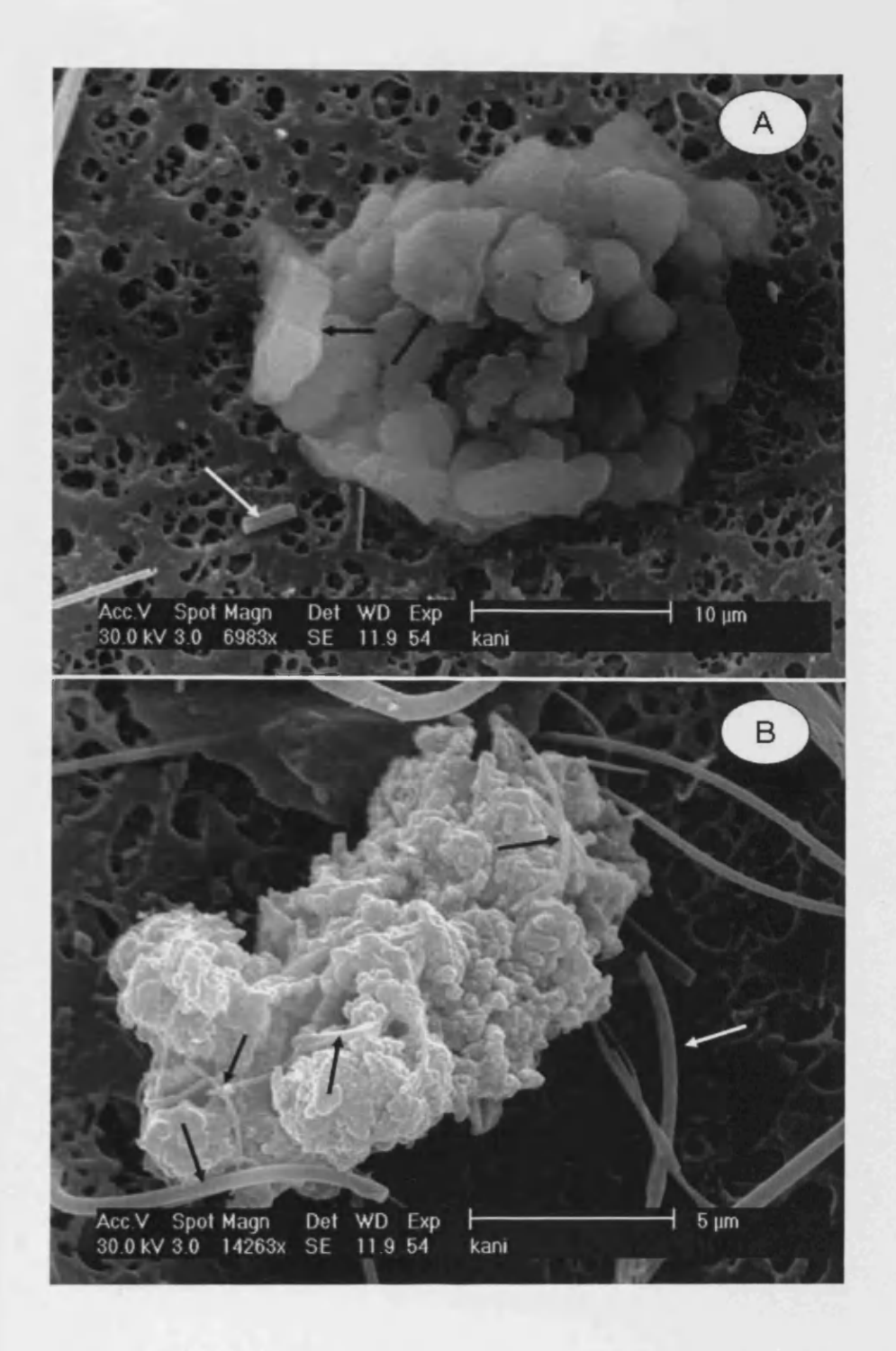


Fig.9.2: Scanning electron micrographs of stratospheric air samples. (A) A 28 μm cluster of materials showing variable shapes from spherical (1.5-4.0 μm in diameter) as shown by arrow heads to irregular shaped objects (4.0-9.0 μm) as shown by arrows; few isolated filamentous or tubular objects can be occasionally seen (white arrow). (B) A 16 μm clump formed by aggregates (2.5-4.5 μm across); these aggregates are composed of smaller granules; tubular features of variable thickness (90-500 nm) as shown by arrows, some of which are intermixed with the granules (40-300 nm) as shown by arrows.

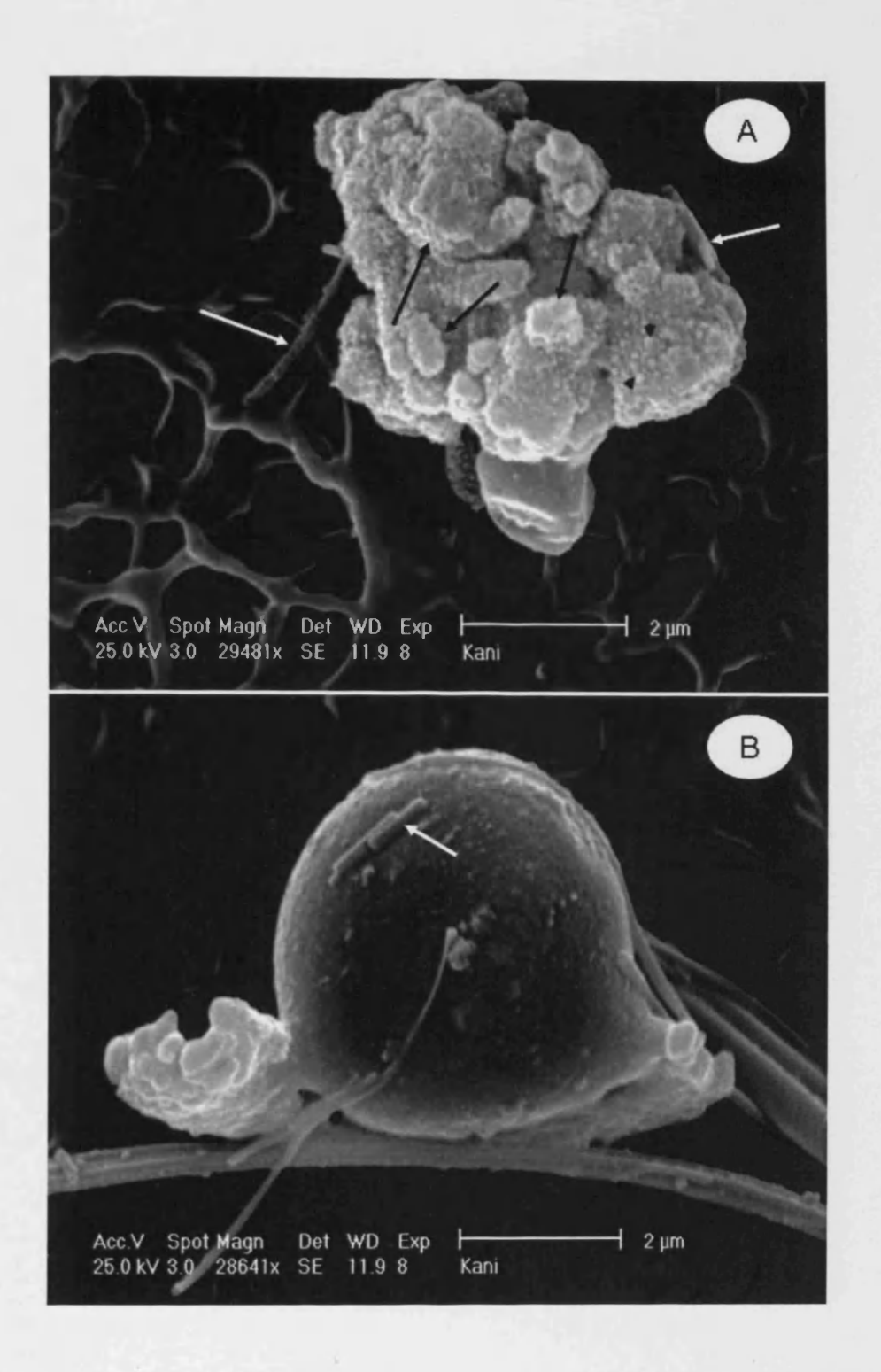


Fig.9.3: Scanning electron micrographs of stratospheric air samples. (A) A 7.0 μm sized clump formed by small aggregates (0.6-3.0 μm) as shown by arrows; these aggregates are covered with granules (40-200 nm) as shown by arrow heads; white arrows show filamentous or tubular objects. (B) A 7.0 μm globule with a rough surface structure covered with tiny granules and rod shaped features as shown by arrow.

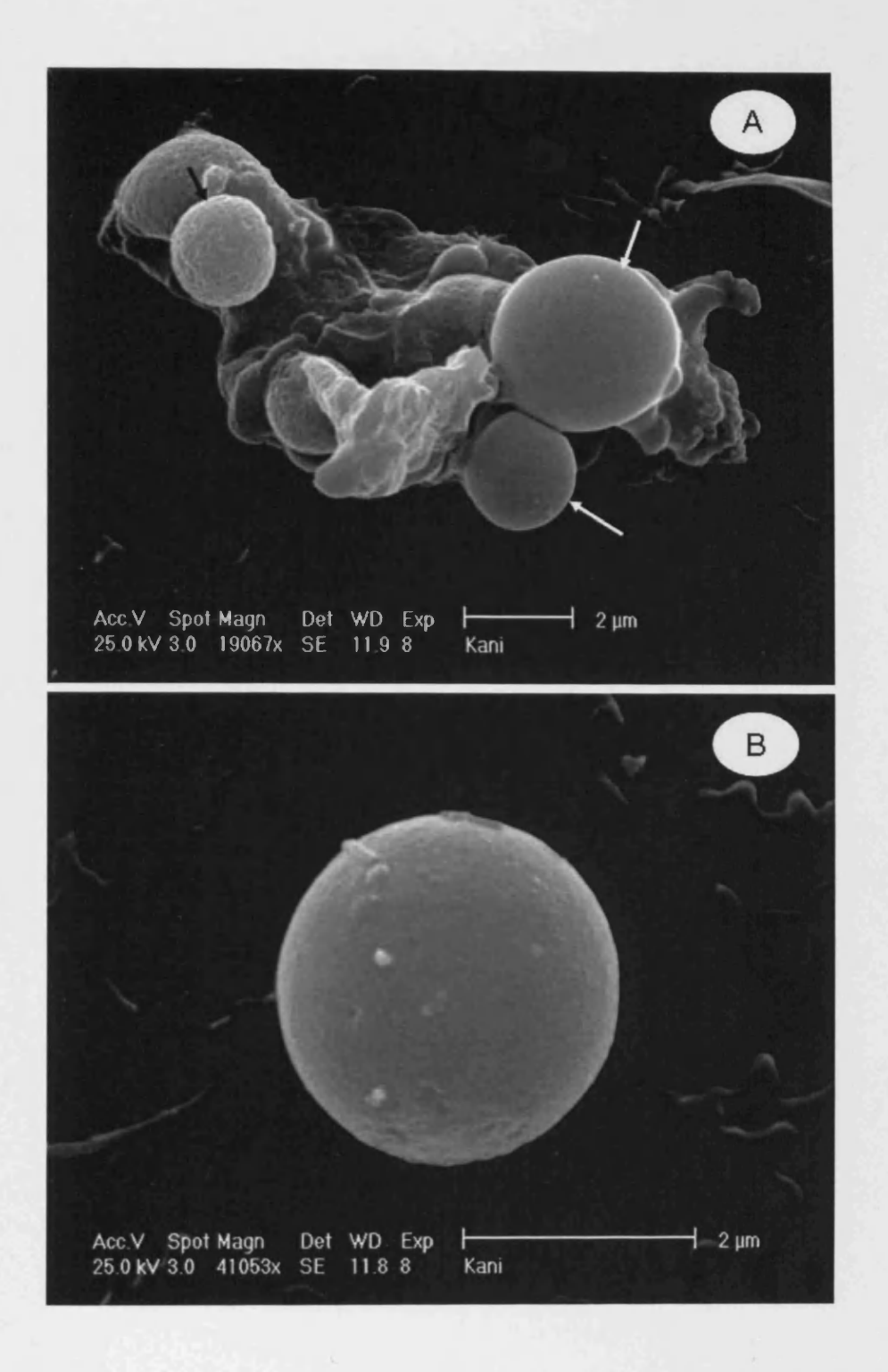


Fig.9.4: SEM micrograph of stratospheric air particles. (A) A 12  $\mu$ m clump showing globules with a smooth surface structure of variable sizes arranging from 2.0  $\mu$ m to 3.3  $\mu$ m (as shown by white arrows); some globules showing a rough surface are sized between 1.6  $\mu$ m and 1.8  $\mu$ m (as shown by a black arrow). (B) A 3  $\mu$ m globule showing a rough surface structure.

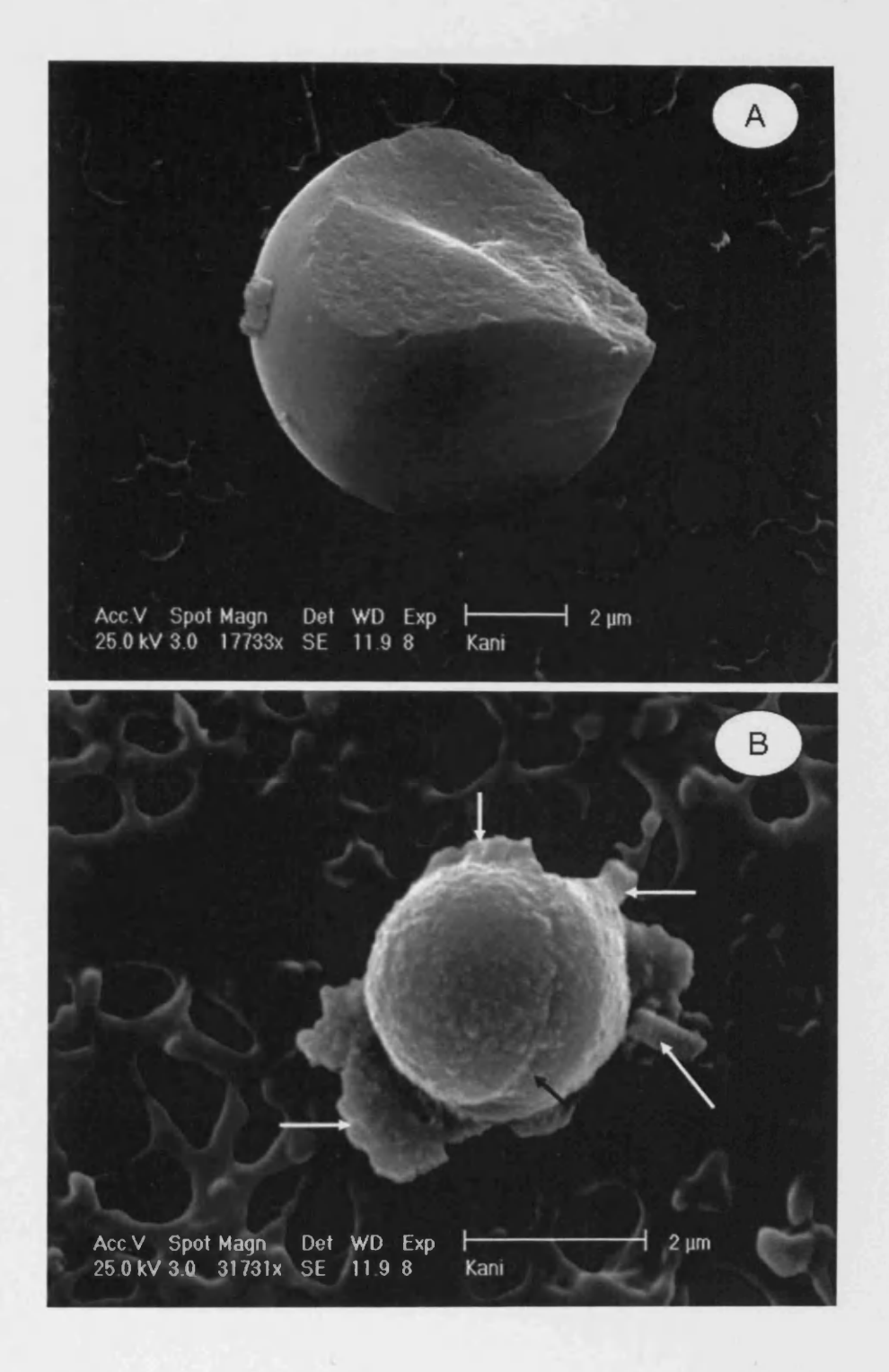


Fig.9.5: SEM micrograph of stratospheric air particles. (A) A partially broken 9  $\mu$ m globule showing its internal structure. (B) A 3  $\mu$ m globule showing its coccoidal shape and rough surface structure; its appearance looks like a cell division with a septa in the middle separating two cells as shown by a black arrow; extracellular materials can be seen attached to the globule as shown by white arrows.

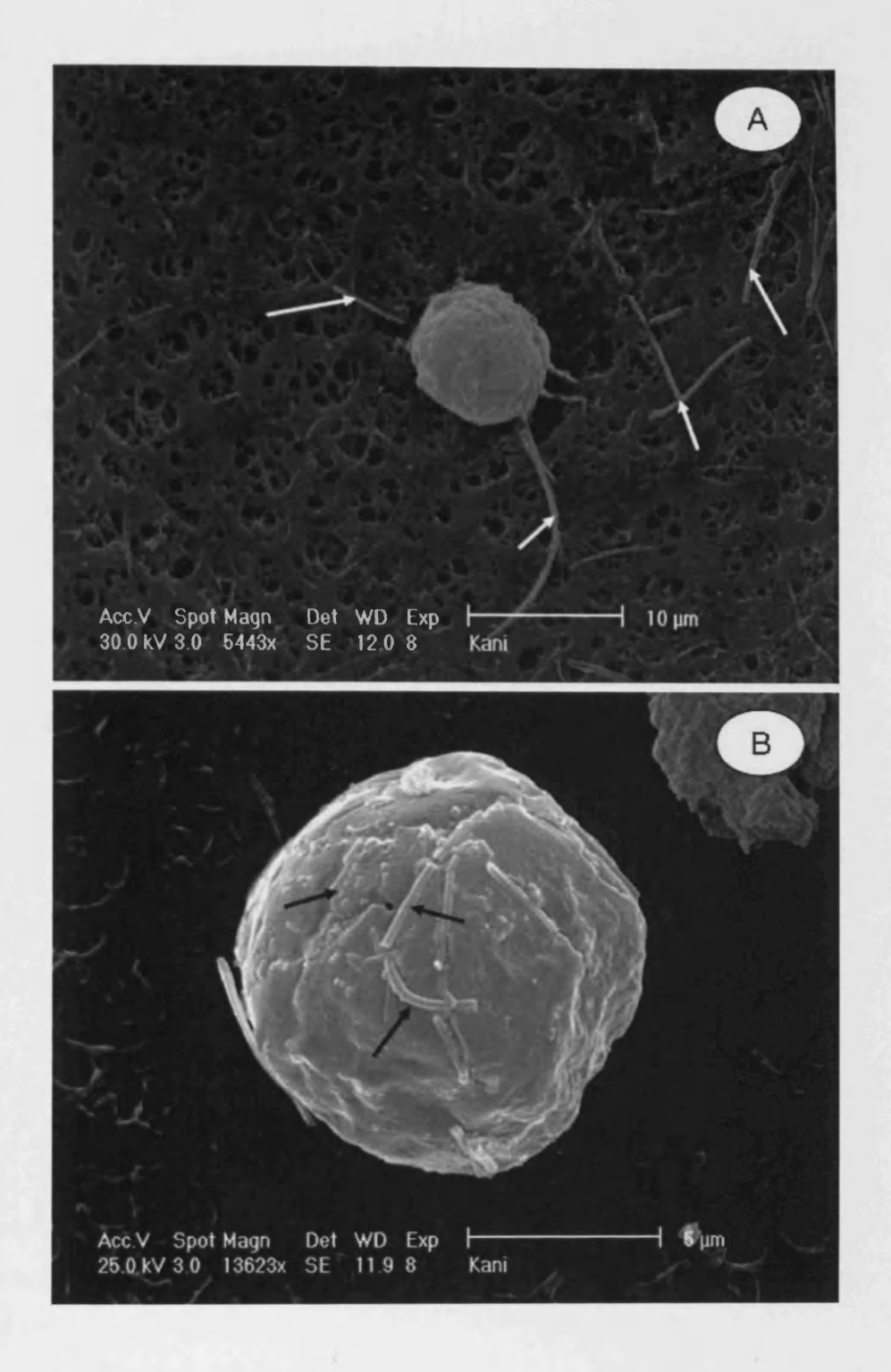


Fig.9.6: SEM micrograph of stratospheric air particles. (A) A 9 μm sized globule showing extra cellular filaments (arrows). (B) A 11 μm globule showing its rough surface covered with filamentous objects of variable lengths (as shown by arrows).

# 9.4.2. UV-Vis Spectroscopy of stratospheric air samples

The UV-Visible spectrophotometric analysis of cyclohexane-dissolved samples produce a prominent peak shifted to 216 nm, close to the 217.5 nm UV astronomical feature (Fig. 9.7).

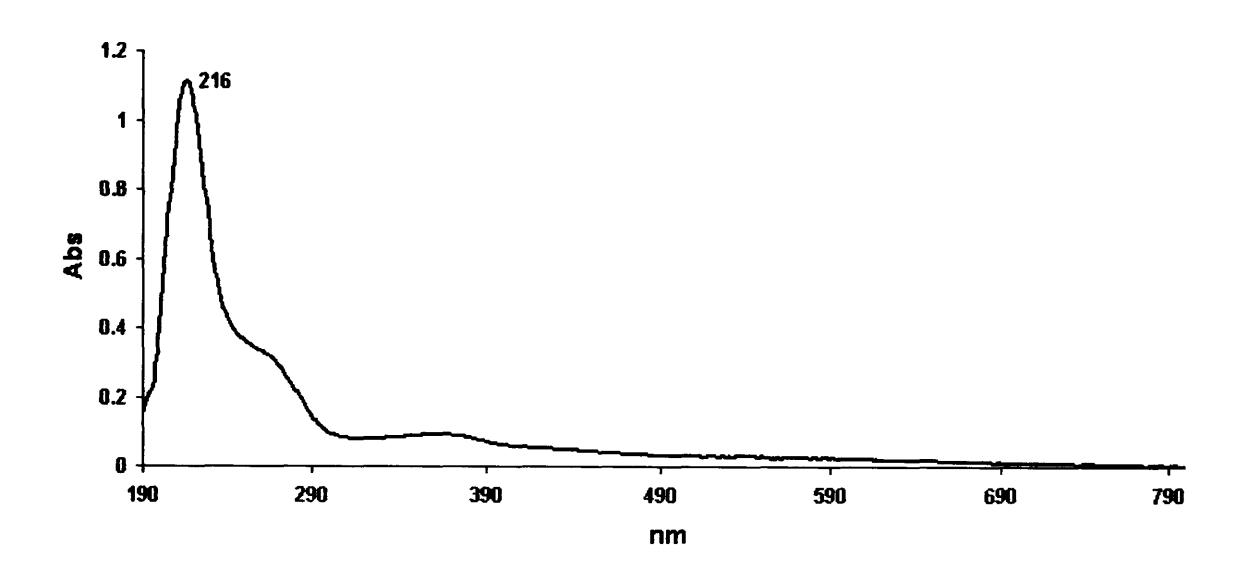


Fig.9.7: UV-Visible spectrum of stratospheric air samples dissolved in cyclohexane. A prominent feature is observed at  $216 \mu m$ .

#### 9.5. Discussion

The present study using UV-Visible spectrophotometry shows that sample dissolved in cyclohexane displayed a band centered at 216 nm which is close to the 217.5 nm astronomical UV feature (Fig. 9.7). This astronomical feature has been found along every galactic line of sight (Mathis, 1993; Draine and Malhotra, 1993; Sandford, 1996; Bradley et al., 1992 and 1999).

The presence of microorganisms in stratosphere has been confirmed by a number of studies using a cryosampler attached to a balloon flying at altitutes of 20-41 km (Harris et al., 2001; Narlikar et al., 2003; Wainwright et al., 2003; Griffin, 2004). In early years, Imshenetsky et al. (1978) detected microorganisms even at much higher

altitudes (48-77 km). In some cases, several microorganisms found in the stratosphere were successfully isolated and cultured in normal terrestrial growing conditions (Imshenetsky et al., 1978; Wainwright et al., 2003 and 2004b).

The present study using a high resolution environmental scanning electron microscope reveals the presence of 3-32 µm sized-clusters of coccoids intermixed with elongated features (Figs. 9.1 and 9.2). Other materials that were also found include globules, some of which appear to have a granular surface structure (Figs. 9.3B, 9.4A and 9.5B). Some of these globules display structural characteristics of bacteria such as coccoids showing an apparent cell-division with extracellular materials (Fig. 9.5B) and flagella (Fig. 9.6A). The ovoid features as shown in Fig. 9.1A appear similar in size and shape to nanobacteria found in travertine and limestone (Folk, 1993) and in Pleistocene ground water (McBride, 1994). The above features may possibly be regarded as products of terrestrial contamination from sample handling and laboratory processing. However, none of these were observed on the membranes used as controls, thus suggesting an endogenous origin. The discovery of macrosized clusters of coccoids by the present study goes to confirm the observations made by Harris et al. (2001) and Wainwright et al. (2003 and 2004a). Furthermore, the long filamentous features as shown in Figs. 9.2B, 9.3A and 9.6 appear similar in structural characteristics to microfossils that have been found embedded in some carbonaceous meteorites such as Orgueil and Murchison (Hoover, 2009). Miyake (2009) and Miyake et al. (2009) ascribed these clusters to aggregates of interplanetary dust particles (IDPs) rich in carbon and found the rods are siliceous, suggesting that they are fragments of diatoms. Both diatoms and bacteria display an absorbance feature near 220 nm (2200Å) similar to the observed UV spectral properties of interstellar grains, thus supporting the concept of a cosmic microbiological system in which these microorganisms might exist on comets (Hoover et al., 1999).

Although the present data obtained from morphological and UV spectral analyses of stratospheric particles suggest that materials of biological origin are likely to be present in the samples, it may be argued that not all of the observed particles are of the same nature. The ovoid and elongated features could be the products of partial dissolution of the carbonate which is abundant in IDPs, and have been reported to be

similar to bacterially induced carbonate precipitation (Buczynsik and Chefetz, 1991; McKay et al., 1996). A study made by Wainwright et al. (2004a) using SIMS has demonstrated that several clusters of bacteria-like particles found in the same stratospheric air samples are not biological, and thus pointed out that the SEM- based observation in itself cannot be used as evidence for the presence of bacteria in the stratosphere.

The early claim (Imshenetsky et al., 1978) to have detected and isolated a wide range of common bacteria and fungi via rocket probes to heights of 48-77 km is beset with contamination objections. The recent studies using cryosamplers attached to balloons flying at altitudes of 20-41 km have largely overcome that problem (Harris et al., 2001; Narlikar et al., 2003; Wainwright et al., 2004b). The microorganisms recovered from the stratosphere include bacteria-like particles (Harris et al., 2001; Narlikar et al., 2003; Wainwright et al., 2004b), two bacteria (B. simplex and S. pasteuri) and one fungus (Engyodontium album) (Wainwright et al., 2003), P. Stutzeri (Narlikar et al., 2003) and species of Penicillium and two bacteria (B. luciferensis and B. sphaericus) (Griffin, 2004). While most microorganisms appear unlikely to survive under the harsh stratospheric conditions with low temperature and strong ultraviolet radiation, some microorganisms utilise protective strategies such as clumping, forming thick cell walls, carbonising outer layers and embedding in carbonaceous dust (Narlikar et al., 2003; Wainwright et al., 2006). Furthermore, microorganisms can survive quite extreme conditions of temperature, pressure and even radiation (Hoyle and Wickramasinghe, 2000). Secker et al. (1994) have shown that a few microns thick carbonaceous coating of bacterial cells provides a protective shield against radiation. Microorganisms such as spore forming bacilli (B. simplex) (Whisler, 1940) and clump forming bacteria (B. subtilis and Staphylococcus aureus) (Horneck, 1998; Darling, 2001) are relatively resistant to radiation. The pigmented microbes in the mesosphere discovered by Imshenetsky (1946) led him to propose that UV resistance is given by protective pigments (melanins and carotinoids) and suggest natural selection for these pigments.

The conclusion that microorganisms found in the stratosphere are extraterrestrial is contested by some on the basis of possible terrestrial contamination resulting from sample handling or laboratory processes. If laboratory contamination can be excluded,

an extraterrestrial origin is supported by the argument that terrestrial microbes can not be lofted easily above 17 km except in rare exceptional situations. This is because the tropopause forms a barrier that restricts their upward movement to higher altitudes. However, there have been attempts in recent years to explain the possible mechanisms whereby microorganisms could reach the stratosphere from Earth. For example, Wainwright et al. (2006) have cited the following mechanisms that are thought to be able to transport microorganisms into the stratosphere from Earth: (1) volcanic eruption by which microorganism could be ejected into the stratosphere through the tropopause, (2) blue lightening strikes causing conical blue jets transporting microorganisms upward to an altitude of 70 km, (3) thunderstorms and Forrest fires sending upward plumes of smoke including microbial particles into the stratosphere and (4) gravito-photophoresis (GP), a mechanism whereby materials including microorganism could be transported upward to the stratosphere or at altitude of 10-85 km. Some of these mechanisms have also been suggested in early reports such as the blue lightening strikes (Pasko et al., 2002) and gravito-photophoresis GP (Rohatschek, 1996). Imshenetsky et al. (1978) claimed that microorganisms were registered in a great number in the mesosphere during dust storms as compared to the absence of strong winds, but that is consistent with contaminants collected in flight through the troposphere. Terminal speeds for settling through the atmosphere are higher for larger sizes (and mean density). Moreover lofting mechanisms are likely to discriminate in favour of smaller sizes, yet the recovered IDP-like particles show no statistical weighting to micrometer sizes.

Some may argue that not all microorganisms found in the stratosphere originated from the earth, especially those clumps of bacteria-like particles reported by Harris et al. (2001). These bacteria-like particles cells were found to express some non-terrestrial characteristics; for example, they appeared viable but lacked one of the important characteristics of terrestrial microorganisms, that is an ability to proliferate in normal culturing conditions. It may be argued that the non-culturable cells may have been carbonized or deactivated and subsequently degraded by exposure to cosmic rays and UV radiation, thus resulting in the production of free organic molecules. Evidence for such disintegrations has been presented for years (Bigg, 1983) and organic structures found in the particles collected by U2 aircraft were shown to remain intact (Clemett et al., 1993). However, it has been reported that some microorganisms found in the

stratosphere were successfully isolated and cultured in normal terrestrial growing conditions (Imshenetsky et al., 1978; Wainwright et al., 2003 and 2004b).

The absence of a plausible explanation for lofting our 7-32 µm clusters through the stratosphere to 40 km altitude adds weight to our identifying these materials as interplanetary dust particles (IDPs) and particularly carbonaceous IDPs (Miyake, 2009). Although the detection in the samples of microfossil-like materials such as coccoids, rods and filaments suggests a biological origin, and the UV spectral data is consistent with this biological identification, more substantive evidence is needed to confirm this identification.

# **CHAPTER 10**

# **Concluding Remarks**

The primary aim of the present thesis was to explore the current status and validity of various models of interstellar and cometary dust. Panspermia theories require a substantial mass fraction of sub-micron particles in the galaxy to be derived from biology. Astronomical spectroscopy from the far-infrared to the ultraviolet provides stringent constraints on permissible models. The 'standard' models of interstellar dust involve mixtures of silicates, graphite and organics, the organics being the carriers of spectral features, such as the UIBs and the 2175 Å interstellar absorption feature. It is shown that abiotically generated mixtures of organic grains appear to be contrived to fit the data and are therefore unsatisfactory.

Biologically generated cells – algae, bacteria, grasses – together with their degradation products match astronomical data over the IR and UV wavebands without further ad hoc assumption. Investigations of the Tagish lake and Carancas meteorites and stratospheric dust, all of which have a generic link to comets, show evidence of biology and putative microfossils to varying degrees.

Evidence in the thesis is consistent with life being a cosmic phenomenon. The biosphere of our planet could extend to the edge of our galaxy at least and possibly beyond.

#### **Future Directions**

The work on the Carancas meteorite has left several unanswered questions. Are the ovoid and elongated features artefacts resulting from terrestrial contamination or space weathering? If they are of terrestrial orgin, when and where did the contamination occur? Large scale studies may be required to determine the origin of these objects, and to find out whether they are of biological nature. If they are biomarkers, are they bacterial cells and if so, do they remain viable? Baterial cell viability can be determined using a fluorescent membrane sensitive dye, cationic carbocyanine or Live/Dead BacLight Bacterial Viability Kit. Both methods require the use of a fluorescence microscope. The latter can also be used with a fluorescence microplate reader, flow cytometer or fluorometer. High resolution imaging will require deployment of a confocal microscope. The subsequent procedures (isolation,

culturing and identification of viable cells) can also be followed with the use of microbiological techniques. Moreover, the bacterial material (if successfully cultured) can then be compared with microbial flora around the impact crater where the original meteoritic fragment was collected.

Since the work of Louis and Kumar (2003 and 2006) on the Kerala red rain was published, the suggestion that the red cells are of cometary origin has been hottly disputed. Furthermore, my current work (Chapter 8) and that of Miyake (2009) have revealed the presence of DNA materials in the Kerala red rain cells, and these findings contradict the claim made by Louis and Kumar (2003) that these cells are devoid of DNA. This highly controversial issue remains to be resolved. One of the contemporary biochemical methods that may be proposed is to use polymerase chain reaction or PCR to determine whether the red rain cells contain DNA materials. It would also be useful to study the cultureability of the red rain cells under very extreme environmental conditions and their adaptability to the living environment of extrememophiles.

# References

Adamson, A. J., Whittet, D. C. B., Chrysostomou, A., Hough, J. H., Aitken, D. K., Wright, G. S. and Roche, P. F. (1999) Spectropolarimetric Constraints on the Nature of the 3.4 Micron Absorber in the Interstellar Medium. *The Astrophysical Journal*, 512: 224–229.

Agu'ndez, M., Cernicharo, J. and Gue'lin, M. (2007) Discovery of Phosphaethyne (HCP) in Space: Phosphorus Chemistry in Circumstellar Envelopes. *The Astrophysical Journal*, 662: 91 94.

Alexander, C.M.O.'D., Russell, S.S., Arden, J.W., Ash, R.D., Grady, M.M. and Pillinger, C.T. (1998) The origin of chondritic macromolecular organic matter: A carbon and nitrogen isotope study. *Meteor. Planet. Sci.*, 33: 603–622.

Allamandola, L. J., Tielens, A. G. G. M. and Barker, J. R. (1985) Polycyclic aromatic hydrocarbons and the unidentified infrared emission bands – Auto exhaust along the Milky Way. *Astrophysical Journal*, 290: 25-28.

Allamandola, L. J., Tielens, A. G. G. M. and Barker, J. R. (1989) Interstellar polycyclic aromatic hydrocarbons - The infrared emission bands, the excitation/emission mechanism, and the astrophysical implications. *Astrophysical Journal Supplement Series*, 71: 733-775.

Allamandola, L.J., Sandford, S.A. and Valero, G.J. (1988) Photochemical and thermal evolution of interstellar/precometary ice analogs. *Icarus*, 76:225-252.

Allamandola, L.J., Sandford, S.A., and Wopenka, B. (1987) Interstellar Polycyclic Aromatic Hydrocarbons and Carbon in Interplanetary Dust Particles and Meteorites. *Science* 237: 56.

Allen, D.A. and Wickramasinghe, D.T. (1981) Nature, 294: 239.

Al-Mufti, A.R.S. (1985) Laboratory studies relating to a bacterial model of interstellar grains, PhD thesis, University College Cardiff.

Anders, E. (1989) Pre-biotic organic matter from comets and asteroids. *Nature*, 342: 255-257.

Arrhenius, S. (1908) World in the Making, Harper and Row, New York.

Bains, W. (2004) Many chemistries could be used to build living systems, Astrobiology 4 (2): 137–167.

Barker, J. R., Allamandola, L. J. and Tielens, A. G. G. M. (1987) Anharmonicity and the interstellar polycyclic aromatic hydrocarbon infrared emission spectrum. *Astrophys. J.* 315: 61-65.

Baross, J.A. and Deming, J.W. (1983) Growth of 'black smoker' bacteria at temperatures of at least 250 °C. Nature 303: 423 – 426.

Barry, R.G. and Chorley, R.J. (2003) Atmosphere, weather and climate. Eight edition by Routledge, London & New York.

Bauschlicher, C.W., Langhoff, S.R., Sandford, S.A. and Hudgins, D.M. (1997) Infrared Spectra of Perdeuterated Naphthalene, Phenanthrene, Chrysene, and Pyrene. *J. Phys. Chem. A*, 101(13): 2414–2422.

BBC News: http://news.bbc.co.uk/2/hi/7001897.stm

Beegle, L.W., Wdowiak, T.J., Robinson, M.S., Cronin, J.R., McGehee, M.D., Clemett, S.J. and Gillette, S. (1997) Experimental Indication of a Naphthalene Base Molecular Aggregate for the Carrier of the 2175 Å Interstellar Extinction Feature. ApJ, 487: 976-982.

Bell, J.F., Davis, D.R., Hartmann, W.K. and Gaffey, M.J. (1989) Asteroid: The big picture. In Asteroids II, Univ. Arizona Press, Tucson, Arizona, USA, 921–945.

Biermann, U.M., Presper, T., Koop, T., Mobinger, J., Crutzen, P.J. and Peter, T. (1996) The unsuitability of meteoritic and other nuclei for polar stratospheric cloud freezing. *Geophys.Res.Lett.*, 23: 1693-1696.

Bigg, E.K. (1983) Particles in the upper atmosphere. Fundamental Studies and the Future of Science (ed. Wickramasinghe, C.) Cardiff. University Press, Cardiff, 38–51.

Blochl, E., Rachel, R., Burggraf, S., Haphenbradl, D., Jannasch, H.W. and Stetter, K.O. (1997) *Pyrolobus fumarii*, gen. and sp. nov., represents a novel group of archaea, extending the upper temperature limit for life to 113 degrees C. *Extremophiles* 1: 14-21.

Bockelée-Morvan, D., Gautier, D., Hersant, F., Huré, J.-M. and Robert, F. (2002) Turbulent radial mixing in the solar nebula as the source of crystalline silicates in comets. *Astron. Astrophys.*, 384: 1107–1118.

Boulanger, F., Prévot, M. L. and Gry, C. (1994) The contribution of small particles to the extinction curve. Astronomy and Astrophysics 284(3): 956-970.

Bradley, J.P. (1994) Chemically Anomalous, Preaccretionally Irradiated Grains in Interplanetary Dust from Comets. *Science*, 265: 925-929.

Bradley, J.P. (2003) in: Treatise on Geochemistry. Davis, A. M., Holland, H. D., Turekian, K. K., Eds., Elsevier, London, 1: 689-711.

Bradley, J.P., Dai, Z.R., Erni, R., Browning, N., Graham, G., Weber, P., Smith, J., Hutcheon, I., Ishii, H., Bajt, S., Floss, C., Stadermann, F., Sandford, S. (2005) An Astronomical 2175 Å Feature in Interplanetary Dust Particles. *Science*, 307(5707): 244-247.

Bradley, J.P., Humecki, H.J. and Germani, M.S. (1992) combined infrared and analytical electron microscope studies of interplanetary dust particles. *Ap. J.* 394: 643-651.

Bradley, J.P., Keller, L.P., Snow, T.P., Hanner, M.S., Flynn, G.J., Gezo, J.C., Clemett, S.J., Brownlee, D.E. and Bowey, J.E. (1999) An Infrared Spectral Match Between GEMS and Interstellar Grains. *Science*, 285(5434): 1716-1718.

Brock, T.D. (1978) Thermophilic Microorganisms and Life at High Temperatures. Springer, New York.

Brocks, J.J., Buick, R., Summons, R.E. and Logan, G.A. (2003) A reconstruction of Archean biological diversity based on molecular fossils from the 2.78–2.45 billion year old Mount Bruce Supergroup, Hamersley Basin, Western Australia. *Geochim. Cosmochim. Acta* 67 (22): 4321-4335.

Brown, P.G., Hildebrand, A.R., Zolensky, M.E., Grady, M., Clayton, R.N., Mayeda, T.K., Tagliaferri, E., Spalding, R., MacRae, N.D., Hoffman, E.L., Mittlefehldt, D.W., Wacker, J.F., Bird, J.A., Campbell, M.D., Carpenter, R., Gingerich, H., Glatiotis, M., Greiner, E., Mazur, M.J., McCausland, P.J.A., Plotkin, H.and Rubak-Mazur, T. (2000) The fall, recovery, orbit, and composition of the Tagish Lake meteorite: A new type of carbonaceous chondrite. *Science* 290: 320-325.

Brownlee, D.E. (1985) Cosmic dust-collection and research. Annual review of earth and planetary science, 13: 147-173.

Brownlee, et al. (2006) Comet 81P/Wild 2 under a microscope. *Science*, 314: 1711-1716.

Bruch, C. W. (1967) Microbes in the upper atmosphere and beyond. *In Airborne Microbes, Society for General Microbiology Symposium*, Cambridge: Cambridge University Press, 17: 345–373.

Buczynski, C. and Chafetz, H.S. (1991) Habit of bacterially induced precipitates of calcium carbonate and the influence of medium viscosity on mineralogy. *J. Sediment. Petrol.* 61: 226–233.

Bunch, T. E. and Chang, S. (1980) Carbonaceous chondrites—II. Carbonaceous chondrite phyllosilicates and light element geochemistry as indicators of parent body processes and surface conditions. *Geochim.Cosmochim.Acta.*, 44: 1543 1577.

Burbidge, E. M., Burbidge, G. R., Fowler, W. A. and Hoyle, F. (1957) Synthesis of the Elements in Stars. *Rev Mod Phy.*, 29 (4): 547.

Buseck, P.R. and Hua, X. (1993) Matrices of carbonaceous chondrite meteorites. *Annu Rev Earth Planet Sci* 21: 255-30.

Busemann, H., Young, A.F., Alexander, C.M.O'D., Hoppe, P., Mukhopadhyay, S. and Nittler, L.R. (2006) Interstellar chemistry recorded in organic matter from primitive meteorites. *Science* 312: 727-730.

Butchart, I., McFadzean, A.D., Whittet, D.C.B., Geballe T.R. and Greenberg, J.M. (1986) Three micron spectroscopy of the galactic centre source IRS 7. *Astron. Astrophys.*, 154: 5–7.

Cardelli, J. A., Clayton, G. C. and Mathis, J. S. (1989) The relationship between infrared, optical, and ultraviolet extinction. *ApJ*, 345: 245-256.

Cataldo, F. and Keheyan, Y. (2003) Heavy petroleum fractions as possible analogues of carriers of the unidentified infrared bands. *International Journal of Astrobiology* 2 (1): 41–50

Cataldo, F., Keheyan, Y. and Heymann D. (2004) complex organic matter in space:about the chemical composition of carriers of the unidentified infrared bands (UIBs) and protoplanetary emission spectra recorded from certain astrophysical objects. *Origins of Life and Evolution of the Biosphere* 34: 13–24.

Cataldo, F., Keheyan, Y. and Heymann, D. (2002) A new model for the interpretation of the unidentified infrared bands (UIBS) of the diffuse interstellar

medium and of the protoplanetary nebulae. *International Journal of Astrobiology* 1(2): 79-86.

Ceplecha, Z. (1977) Meteoroid populations and orbits. In: Delsemme AH (ed) Comets, asteroids, meteorites. University of Toledo Press, Ohio, 143-152.

Chen, J., Li, M., Li, A. and Wang, Y. (2008) On buckyonions as a carrier of the 2175 °A interstellar extinction feature. *Organic Matter in Space Proceedings IAU Symposium*, 251: 71-72.

Chiar, J. E., Adamson, A. J., Whittet, D. C. B., Chrysostomou, A., Hough, J. H., Kerr, T. H., Mason, R. E., Poche, P. F. and Wright, G. (2006) Spectropolarimetry of the 3.4 µm feature in the diffuse ISM toward the Galactic center quintuplet cluster. *The Astrophysical Journal*, 651:268-271.

Chyba, C.F. and Sagan, C. (1992) Endogenous production, exogenous delivery and impact-shock synthesis of organic molecules: an inventory for the origin of life. *Nature*, 355: 125-132.

Chyba, C.F., Thomas, P.J., Brookshaw, L. and Sagan, C. (1990) Cometary delivery of organic molecules to the early Earth. *Science*, 249:366-373.

Claus, G. and Nagy, B. (1961) A microbiological examination of some carbonaceous chondrites. *Nature*, 192: 594-596.

Clemett, S., Maechling, C., Zare, R., Swan, P. and Walker, R. (1993) Identification of Complex Aromatic Molecules in Individual Interplanetary Dust Particles. *Science*, 262(5134):721-725.

Cockell, C.S. (2008) The Interplanetary Exchange of Photosynthesis. *Orig Life Evol Biosph*, 38: 87-104.

Cody, G.D. and Alexander, C.M.O'D. (2005) NMR studies of chemical structural variation of insoluble organic matter from different carbonaceous chondrite groups. *Geochim. Cosmochim. Acta.*, 69: 1085-1097.

Coulson, S.G. (2002) Resistance of motion to a small, hypervelocity sphere, sputtering through a gas. *Mon. Not. R. Astron. Soc.*, 332: 741-744.

Coulson, S.G. (2004) On panspermia and the survivability of micrometre-sized meteoroids within the Earth's atmosphere. *Int. J. Astrobiology* 3 (2): 151–156.

Coulson, S.G. and Wickramasinghe, N.C. (2003) Frinctional heating of micron sized meteoroids in the Earth's upper atmosphere. *Mon. Not. R. Astron. Soc.*, 343: 1123-1130.

Cox, A.N. (2000) Allen's astrophysical quantities. *Springer/Verlag*, ISBN 978-0387987460.

Crawford, M. K., Tielens, A. G. G. M. and Allamandola, L. J. (1985) Polycyclic Aromatic Hydrocarbon Cations and the Diffuse Interstellar Bands. *Astrophys. J.*, 293: 45-48.

Crick, F.H.C. and Orgel, L.E. (1973) Directed Panspermia. Icarus 19: 341-346.

Cronin, J.R., Pizzarello, S. and Cruikshank, D.P. (1988) Organic matter in carbonaceous chondrites, planetary satellites, asteroids and comets. Meteorites and the early solar system. *The University of Arizona Press, Tucson, AZ*, 819-857.

Crovisier, J., Brooke, T.Y., Leech, K., Bockelée-Morvan, D., Lellouch, E., Hanner, M.S., Altieri, B., Keller, H.U., Lim, T., Encrenaz, T., Griffin, M., de Graauw, T., van Dishoeck, E. and Knacke, R.F. (2000) The thermal infrared spectra of Comets Hale-Bopp and 103P/Hartley 2 observed with the Infrared Space Observatory. *Thermal Emission Spectroscopy and Analysis of Dust, Disks, and Regoliths*, M.L. Sitko, A.L. Sprague and D.K. Lynch edts, ASP Conf. Series 196: 109-117.

Crovisier, J., Leech, K., Bockelée-Morvan, D., Brooke, T.Y., Hanner, M.S., Altieri, B., Uwe- Keller, H. and Lellouch, E. (1997) The Spectrum of Comet Hale Bopp (C/1995 O1) Observed with the Infrared Space Observatory at 2.9 Astronomical Units from the Sun. *Science*, 275(5308): 1904-1907.

Cruikshank, D.P., Roush, T.L., Bartholomew, M.J., Geballe, T.R., Pendleton, Y.J., White, S.M., Bell, III J.F., Davies, J.K., Owen, T.C., de Bergh, C., Tholen, D.J., Bernstein, M.P., Brown, R.H., Tryka, K.A. and Dalle-Ore, C.M. (1998) The composition of centaur 5145 Pholus. *Icarus* 135:389-407.

Czyzak, S. J., Hirth, J. P. and Tabak, R. G. (1982) The formation and properties of grains in the interstellar medium. *Vistas Astron.*, 25: 337-382.

d'Hendecourt, L. and Ehrenfreund, P. (1997) Spectroscopic properties of polycyclic aromatic hydrocarbons (PAHs) and astrophysical implications. *Advances in Space Research*, 19(7): 1023-1032.

Darbon, S., Perrin, J.M. and Sivan, J.P. (1998) Extended red emission (ERE) detected in the 30 Doradus nebula. *Astronomy and Astrophysics*, 333: 264-268.

Darling, D. (2001) Life Everywhere. Basic Books, New York.

Davies, B. H. (1976) Chemistry and biochemistry of plant pigments (T. W. Goodwin, ed.), 2, Academic press, New York.

de Heer, W. A. and Ugarte, D. (1993) Carbon Onions Produced by Heat Treatment of Carbon Soot and Their Relation to the 217.5 nm Interstellar Absorption Feature. *Chem. Phys. Lett.*, 207: 480.

Dehel, T. (2006) Uplift and Outflow of Bacterial Spores via Electric Field. 36<sup>th</sup> COSPAR Scientific Assembly. Held 16, in Beijing, China.

del Prado, H.N., Macharé, J., Macedo, L., Chirif, H., Pari, W., Ramirez-Cardona, M., Aran-da, A., Greenwood, R.C., Franchi, I.A., Canepa, C., Bernhardt H. –J.

and Plascencia, L.(2008) The meteorite fall in Carancas, lake Titicaca region, southern Peru: first results. Lunar and Planetary Science XXXIX abstract.

Delsemme, A. (1984) The cometary connection with prebiotic chemistry. *Orig Life*, 14:51-60.

Desert, F.-X., Boulanger, F. and Puget, J.L. (1990) Interstellar dust models for extinction and emission. *Astronomy and Astrophysics*, 237(1): 215-236.

d'Hendecourt, L., Léger, A., Olofsson, G., Schmidt, W. (1986) The Red Rectangle - A possible case of visible luminescence from polycyclic aromatic hydrocarbons. *Astron. Astrophys.* 170: 91–96.

Diario La Republica Online '600 afectados en Puno por caída de meteorite' (09/19/2007), <a href="http://www.larepublica.com.pe/component/">http://www.larepublica.com.pe/component/</a>.

Dose, K., Bieger-Dose, A., Dillmann, R., Gill, M., Kerz, O., Klein, A., Meinert, H., Nawroth, T., Risi, S. and Stridde, C. (1995), ERA-experiment 'space biochemistry'. *Adv. Space Res.* 16(8): 119-129.

Draine B.T., Li A. (2007) Infrared emission from interstellar dust .IV. The = silicate-graphite-PAH model in the post-spitzer era. The astrophysical journal, 657:810-837.

Draine, B. T. (1994) Dust in Diffuse Interstellar Clouds. The First Symposium on the Infrared Cirrus and Diffuse Interstellar Clouds. ASP Conference Series, 58: 227-241.

Draine, B. T. and Lee, H.M. (1984) Optical properties of interstellar graphite and silicate grains. *ApJ* 285: 89-108.

Draine, B.T. (1989) On the Interpretation of the  $\lambda$  2175Å Feature. *Interstellar Dust* (Proceedings of IAU Symposium 135), ed. L.J. Allamandola & A.G.G.M. Tielens (Dordrecht: Kluwer), 313-327.

Draine, B.T. (2003) Interstellar Dust Grains, Ann. Rev. Astron. Astrophys. 41: 241-289.

Draine, B.T. and Anderson, N. (1985) Temperature fluctuations and infrared emission from interstellar grains. *ApJ*, 292: 494-499.

Draine, B.T. and Malhotra, S. (1993) On Graphite and the 2175A Extinction Profile. Astrophys. J., 414: 632.

Duley, W.W. and Seahra (1998) Graphite, polycyclic aromatic hydrocarbons, and the 2175Å extinction feature. *The astrophysical journal*, 507: 874-888.

Duley, W.W. and Seahra, S.S. (1999) 2175 Å and 3.4 Micron Absorption Bands and Carbon Depletion in the Diffuse Interstellar Medium. *The Astrophysical Journal*, 522:129-132.

Duley, W.W. and Williams, D.A. (1979) Are there organic grains in the interstellar medium?. Nature, 277, 40-41.

Duley, W. W. (1985) Evidence for hydrogenated amorphous carbon in the Red Rectangle. *Royal Astronomical Society, Monthly Notices*, 215, 259-263.

Dwek, E. (1997) Can Composite Fluffy Dust Particles Solve the Interstellar Carbon Crisis?. *Astrophysical Journal*, 484: 779-784.

Ehrenfreund, P. and Charnley, S. (2000) Organic Molecules in the Interstellar Medium, Comets, and Meteorites: A Voyage from Dark Clouds to the Early Earth. *Annu. Rev. Astron. Astrophys.*, 38: 427-483.

Ehrenfreund, P., Foing, B. H. (1996) Resolved profiles of diffuse interstellar bands: Evidence for rotational contours of gas-phase molecules. *Astronomy and strophysics*, 307: 25–28.

Ehrenfreund, P., Irvine, W., Becker, L., Blank, J., Brucato, J.R., Colangeli, L., Derenne, S., Despois, D., Dutrey, A., Fraaije, H., Lazcano, A., Owen, T., Robert, F. and an International Space Science Institute ISSI-Team (2002) Astrophysical and astrochemical insights into the origin of life. *Rep. Prog. Phys.* 65: 1427-1487.

Ehrenfreund, P., Robert, F., D'Hendencourt, L. and Behar, F. (1991) Comparison of interstellar and meteoritic organic matter at 3.4 microns. *Astronomy and Astrophysics*, 252(2): 712-717.

Encrenaz, T., D'Hendecourt, L. and Puget, J. L. (1988) The interpretation of the 3.2-3.5 micron emission feature in the spectrum of Comet P/Halley – Abundances in the comet and in interstellar matter. *Astronomy and Astrophysics*, 207(1): 162 173.

Farmer, V.C. (1974a) The Infrared Spectra of Minerals. *Monograph* 4. Mineralogical Society, London, 539.

Fitzpatrick, E. L. and Massa, D. (1986) An analysis on the shapes of ultraviolet extinction curves. I - The 2175 Å bump. *ApJ*, 307: 286-294.

Fitzpatrick, E. L. and Massa, D. (1990) An analysis of the shapes of ultraviolet extinction curves. III - an atlas of ultraviolet extinction curves. Astrophysical Journal Supplement Series, 72: 163-189.

Fitzpatrick, E. L. and Massa, D. (2007) An Analysis of the Shapes of Interstellar Extinction Curves. V. The IR-through-UV Curve Morphology. *ApJ.*, 663: 320 341.

Fitzsimmons, A. (2006) Quoted in 'Red rain may have extraterrestrial origin'. Sunday Herald, by Jenifer Johnston.

Floss, C. and Stadermann, F. (2004) Lunar Planet. Sci. XXXV, abstr. 1281.

Foing, B.H. and Ehrenfreund, P. (1997) New evidences for interstellar  $C_{60}^{+}$  Astronomy and Astrophysics, 317: 59–62.

Folk, R. L. (1993) SEM imaging of bacteria and nannobacteria in carbonate sediments and rocks. *Journal of Sedimentary Research*, 63(5): 990-999.

Franks, F. (1985) Biophysics and Biochemistry at Low Temperatures. Cambridge Univ. Press, Cambridge.

Fuller, E. L. Jr. (1992) in *Carbon* 92, Proceedings of the 5th Int. Carbon Conf., Essen. pp. 192–198. Edited by R. B. Hoover, G. V. Levin, Paepe, R. R. & A. Y. Rozanov.

Furton, D.G. and Witt, A.N. (1992) Extended red emission from dust in planetary nebulae. *Astrophy.J.*, 386, 587-603.

Gaffey, M.J. (1997) The early solar system. Origins of Life and Evolution of the Biosphere, 27: 185-203.

Gallo, G. and Colombo, U. (1974) Chimica Industriale, 4, Uses Edizioni Scientifiche, Italia.

Garvie, L.A.J. and Buseck, P.R. (2006) Carbonaceous Nanospheres in Chondrites. Lunar Planet. Sci. 37, Abstract 1455.

Gillett, F. C., Forrest, W. J. and Merrill, K. M. (1973) 8-13 Micron Observations of Titan. *Astrophysical Journal*, 184: 93.

Gilra, D. P. (1972) Collective Excitations and Dust Particles in Space. *Scientific Results from OAO-2*, (Greenbelt, MD: NASA SP-310), 295.

Gordon, K.D., Witt, A.N. and Friedmann, B.C. (1998) Detection of Extended Red Emission in the Diffuse Interstellar Medium. *Astrophys.J.*, 498: 522.

Grady, M.M., Verchovsky, A.B., Franchi, I.A., Wright, I.P. and Pillinger, C.T. (2002) The light element geochemistry of the Tagish Lake CI2 chondrite: comparisons with CI and CM chondrites. *Meteoritics & Planet. Sci.*, 37: 713–735.

Grant, W. B., Browell, E.V., Fishman, J., Brackett, V.G., Veiga, R.E., Nganga, D., Minga, A., Cros, B., Butler, C.F., Fenn, M.A., Long, C.S. and Stowe, L.L. (1994) Aerosol-associated changes in tropical stratospheric ozone following the eruption of Mount Pinatubo. *J. Geophys. Res.*, 99 (D4), 8197–8211.

Greenberg, J.M. and Hong, S.S. (1974) Galactic Radio Astronomy, Proc. IAU Symp. No. 60, ed. F.J. Kerr and S.C. Simonson III, (Dordrecht: Reidel), 155.

Griffin, D.W. (2004) Terrestrial microorganisms at an altitude of 20,000 m in Earth's atmosphere. *Aerobiologia*, 20: 135–140.

Grogan, D. W. (1998) Hyperthermophiles and the problem of DNA instability. *Mol Microbiol*. 28: 1043-1049.

Gross, J. (1991) Pigment in vegetables. Van Nostrand Rienhold, New York, 8-13.

Gue lin, M., Cernicharo, J., Paubert, G. and Turner, B. E. (1990) Free CP in IRC + 10216. *A&A*, 230(1): 9-11.

Guillois, O., Ledoux, G., Nenner, I., Papoular, R. and Reynaud, C. (1999) Present Situation of the Coal Model for Interstellar Carbon Dust. Solid Interstellar Matter: The ISO Revolution, Les Houches. EDP Sciences and Springer-Verlag, 103.

Guillois, O., Nenner, I., Papoular, R. and Reynaud, C. (1994) The dust heating mechanism in the coal model. *Astrophysical Journal*, 179: 483 – 491.

Guillois, O., Nenner, I., Papoular, R. and Reynaud, C. (1996) Coal Models for the Infrared Emission Spectra of Proto--Planetary Nebulae. *Astrophysical Journal* 464: 810.

Gustvson, B.A.S. (1994) Physics of zodiacal dust. Ann. Rev. Earth Planet Sci., 22: 553-595.

Hanner, M.S. and Bradley, J.P. (2005) in Comets II, M. Festou et al., Eds. (Univ. of Arizona Press, Tucson, AZ), 555–564.

Harker, D.E., Woodward, C.E. and Wooden, D.H. (2005) The Dust Grains from 9P/Tempel 1 Before and After the Encounter with Deep Impact. *Science*, 310 (5746): 278-280.

Harker, D.E., Woodward, D.H., Wooden, C.E. and Lisse, C.M. (2004) Grain Properties of CometC/1995O1 (Hale-Bopp). *Astrophys J.*, 615: 1081-1081.

Harper, C. L. (1996) Astrophysical site of the origin of the Solar System inferred from extinct radionuclide abundances. *Astrophys. J.*, 466: 1026-1038.

Harris, M.J., Wickramasinghe, N.C., Lloyd, D., Narlikar, J.V., Rajaratnam, P., Turner, M.P., Al-Mufti, S., Wallis, M.K. and Hoyle, F. (2001) The detection of living cells in stratospheric samples. *Proc. SPIE*, 4495: 192–198.

Harris, R. S., Schultz, P. H., Tancredi, G. and Ishitsuka, J. (2008) Petrology of ejecta from the Carancas (Peru) crater: Insights into the dynamics of an "unusual" impact event. *Asteroids, Comets, Meteors*, LPI Contribution, No. 1405, p. 8302.

Hayatsu, R. and Anders, E. (1981) Organic compounds in meteorites and their origins. *Topics Current Chemistry*, 99:1-37.

Helou, G., Lu, N. Y., Werner, M. W., Malhotra, S. and Silbermann, N. A. (2000) The Mid-Infrared Spectra of Normal Galaxies. *ApJ*, 532: 21-24.

Henkel, C., Mauersberger, R. and Baan, W. A. (1991) 9 Galaxies and the universe. *Astron. Astrophys. Rev.*, 3(47): 270-296.

Henning, Th. and Salama, F. (1998) Carbon in the Universe. *Science*, 282: 2204-2208.

Herbig, G. H. (1995) The Diffuse Interstellar Bands. Annual Review of Astronomy and Astrophysics, 33: 19-74.

Hildebrandt, S.R., Rebolo, R., Rubino-martin, J.A., Watson, R.A., Gutierrez, C.M., Hoyland, R.J. and Battistelli, E.S. (2007) Cosmosomas observations of the cosmic microwave background and Galactic foregrounds at 11 GHz: evidence for anomalous microwave emission at high Galactic latitude. *Monthly Notices of the Royal Astronomical Society*, 382(2): 594-608.

Hiroi, T., Zolensky, M.E. and Pieters, C.M. (2001) The Tagish Lake Meteorite: A Possible Sample from a D-Type Asteroid. *Science*, 293: 2234.

Hobbs, L. M., York, D. G., Snow, T. P., Oka, T., Thorburn, J. A., Bishof, M., Friedman, S. D., McCall, B. J., Rachford, B. L., Sonnentrucker, P. and Welty, D. E. (2008) A Catalog of Diffuse Interstellar Bands in the Spectrum of HD 204827. *Astrophysical Journal*, 680: 1256.

Hollenbach, D. J. and Thronson Jr, H. A. (1987) Interstellar processes. *Proceedings of the Symposium, NASA, American Astronomical Society*, Dordrecht, D. Reidel Publishing Co., Astrophysics and Space Science Library, 134: 819.

Hong, S.S. and Greenberg J.M. (1980) A unified model of interstellar grains – A connection between alignment efficiency, grain model size, and cosmic abundance. *Astronomy and Astrophysics*, 88: 194-202.

Hoover, R.B. (2009). Proc. SPIE, 7441, doi: 10.1117/12.832643.

Hoover, R.B., Jerman, G., Rozanov, A.Y. and Davies, P.C.W. (2003) Biomarkers and Microfossils in the Murchison, Rainbow, and Tagish Lake meteorites. *Proc. SPIE*, 4859: 15–31.

Horneck, G. (1998) Exobiological Experiments in Earth Orbit. A& Space Res., 22 (3):317-326.

Housecroft, C.E. and Constable, E.C. (2002) Chemitry 2<sup>nd</sup> Edition. Pearson education limited. ISBN 0130869244.

Hoyle, F. and Wickramasinghe, N.C. (1962) On Graphite Particles in Interstellar Grains. *Monthly Notices of the Royal Astronomical Society* 124(5): 417-433.

Hoyle, F. and Wickramasinghe, N.C. (1969) Interstellar grains. *Nature* 223(5205): 459-462.

Hoyle, F. and Wickramasinghe, N. C. (1976) Nature, 264, 45.

Hoyle, F. and Wickramasinghe, N. C. (1977) Nature, 270, 323.

Hoyle, F. and Wickramasinghe, N.C. (1977) The case for life as a cosmic phenomenon. *Nature*, 268: 610.

Hoyle, F. and Wickramasinghe, N.C. (1979) On the nature of interstellar grains. *Astrophysics and space science*, 66: 77-90.

Hoyle, F. and Wickramasinghe, N.C. (1980a) The Identification of the 3 MICRON Spectral Feature in Galactic Infrared Sources. *Astrophysics and Space Science*, 68(2): 499-503.

Hoyle, F. and Wickramasinghe, N.C. (1982) Proofs that Life is Cosmic. Mem Inst Fund Studies, Sri Lanka (<a href="http://www.astrobiology.cf.ac.uk/proofs...pdf">http://www.astrobiology.cf.ac.uk/proofs...pdf</a>)

Hoyle, F. and Wickramasinghe, N.C. (1985) Living comets. Univ. college, Cardiff press.

Hoyle, F. and Wickramasinghe, N.C. (1989) ESA SP., 290, 67.

Hoyle, F. and Wickramasinghe, N.C. (1990) The theory of cosmic grains. Kluwer Academic Publishers, Dordrect, The Netherlands.

Hoyle, F. and N.C. Wickramasinghe (1991) The Theory of Cosmic Grains. Kluwer Academic Press, Dordrecht, 307.

Hoyle, F. and Wickramasinghe, N. C. (1999) Comets - A Vehicle for Panspermia. *Astrophys. Space Sci.* 268: 333-341.

Hoyle, F. and Wickramasinghe, N.C. (2000) Astronomical Origins of Life. Kluwer Academic Publishers, Dordrect, The Netherlands.

Hoyle, F., Olavesen, A.H. and Wickramasinghe, N.C. (1978) The case for life as a cosmic phenomenon. *Nature*, 271: 229.

Hoyle, F., Wickramasinghe, N. C. and Al-Mufti, S. (1985) The case for interstellar micro-organisms. *Astrophys. Space Sci.* 110: 401-404.

Hoyle, F., Wickramasinghe, N.C. and Al-Mufti, S. (1982) 1. Organo-siliceous biomolecules and the infrared spectrum of the trapezium nebula; 2. Interstellar absorptions at 3.2μm and 3.3μm. *Astrophys. Space Sci.*, 86(2): 341-344.

Hrivnak, B. J., Volk, K. and Kwok, S. (2000) 2-45 Micron Infrared Spectroscopy of Carbon-rich Proto-Planetary Nebulae. *ApJ*, 535: 275-292.

Hudgins, D. M. and Allamandola, L. J. (1997) Complex organic molecules in space: the carries of the interstellar infrared emission features, A&. Space Res., 19(7): 999-1008.

Huebner, W. F. and Boice, D. C. (1997) Polymers and other macromolecules in comets. *Comets and the Origin and Evolution of Life*, 111-129.

Huebner, W.F. (1990) Physics and chemistry of comets. W. F. Huebner (ed.) Springer-Verlag New York, LLC, ISBN-13: 9780387512280, 376pp.

Iglesias-Groth, S., Manchado, A., Garcı´a-Herna´ndez, D.A., Gonza´lez Herna´ndez, J.I. and Lambert, D.L. (2008) Evidence for the naphthalene cation in a region of the interstellar medium with anomalous microwave emission. *The Astrophysical Journal*, 685: 55–58.

Imshenetsky, A.A. (1946) Mikrobiologiya, 15: 422.

Imshenetsky, A.A., Lysenko, S.V. and Kazakov, G.A. (1978) Upper boundary of the biosphere. *Appl Environ Microbiol.*, 35(1): 1-5.

Irvine, W. M. (1996) Extraterrestrial organic matter: a review. *Orig.Life Evol. Biosph.* 28 (4-6):365-383.

Ishii, H.A, Bradley, J.P., Dai, Z.R., Chi, M., Kearsley, A.T., Burchell, M.J., Browning, N.D. and Molster, F. (2008) Comparison of Comet 81P/Wild 2 Dust with interplanetary dust from comets. *Science*, 319(5862): 447-450.

Jabir, N.L., Hoyle, F. and Wickramasinghe, N.C. (1983) On the optical properties of bacterial grains, I. *Astrophysics and space science*, 91: 327-344.

Javaux, E.J. (2006) Extreme life on Earth—past, present and possibly beyond, Research in Microbiology 157, 37-48.

Joblin, C., Léger, A. and Martin, P. (1992) Contribution of polycyclic aromatic hydrocarbon molecules to the interstellar extinction curve. *Ap. J.* 393: 79–82.

Joblin, C., Tielens, A.G.G.M., Allamandola, L.J., Lkger, A. d'Hendecour, L. and Geballe, T.R. and Boisse, P. (1995) PAHs as the carriers of the 3.3 and 3.4 μm emission bands. *Planet. Space Sci.*, 43(10/11): 1189-1 194.

Joswiak, D.J., Matrajt, G., Brownlee, D.E., Westphal, A.J. and Snead, C.J. (2007) A Roedderite-bearing Terminal Particle from Stardust Track 56: Comparison with Rare Peralkaline Chondrules in Ordinary Chondrites. *Lun. Planet. Sci.*, 38: 2142.

Kashefi, K. and Lovley, D. R. (2003) Extending the Upper Temperature Limit for Life. *Science*, 301: 934.

Kasting, J.F. (1997) Environmental constraints on the origin of life. *Pontifical Academy of Sciences, Rome*, Commentarii 4(3): 133-147, Reprinted in: Encyclopedia Italiana.

Keller, L. P., Bajt, S., Baratta, G. A., Borg, J., Bradley, J. P., Brownlee, D. E., Busemann, H., Brucato, J. R., Burchell, M., Colangeli, L., d'Hendecourt, L., Djouadi, Z., Ferrini, G., Flynn, G., Franchi, I. A., Fries, M., Grady, M. M., Graham, G. A., Grossemy, F., Kearsley, A., Matrajt, G., Nakamura-Messenger, K., Mennella, V., Nittler, L., Palumbo, M. E., Stadermann, F. J., Tsou, P., Rotundi, A., Sandford, S. A., Snead, C., Steele, A., Wooden, D., Zolensky, M. (2006) Returned by Stardust Infrared Spectroscopy of Comet 81P/Wild 2 Samples. *Science*, 314: 1728-1731.

Knacke, R. F. and Kraetschmer, W. (1980) Infrared spectra of hydrated silicates, carbonaceous chondrites, and amorphous carbonates compared with interstellar dust absorptions. *A&A*, 92(3): 281-288.

Kogut, A., Banday, A. J., Bennett, C. L., Gorski, K. M., Hinshaw, G., Reach, W. T. (1996) High-Latitude Galactic Emission in the COBE Differential Microwave Radiometer 2 Year Sky Maps . *Astrophysical Journal*, 460: 1.

Koornneef, J. and Code, A. D. (1981) Ultraviolet interstellar extinction in the large Magellanic Cloud using observations with the International Ultraviolet Explorer. *ApJ*, 247: 860-868.

Krełowski, J., Galazutdinov, G.A., Musaev, F.A. and Nirski, J. (2001) Identification of the naphthalene cation in space? *MNRAS*, 328: 810.

Kwok, S. (2009) Organic matter in space: from star dust to the Solar System. Astrophys Space Sci., 319: 5–21.

Lal, S., Archarya, Y.B., Patra, P.K., Rajaratnam, P., Subbarya, B.H. and Venkataramani, S. (1996) Balloon-borne cryogenic air sampler experiment for the study of atmospheric trace gases. *Ind. J. Radio Space Phys.*, 25: 1-7.

Le Page, V., Keheyan, Y., Snow, T.P. and Bierbaum, V.M. (1999) Reactions of Cations Derived from Naphthalene with Molecules and Atoms of Interstellar Interest. J. Am. Chem. Soc., 121: 9435-9446.

Le'ger, A. and d'Hendecourt, L. (1985) Are polycyclic aromatic hydrocarbons the carriers of the diffuse interstellar bands in the visible? *Astronomy and Astrophysics*, 146(1): 81-85.

Léger, A. and Puget, J.L. (1984) Identification of the 'unidentified' IR emission features of interstellar dust?. *Astronomy and Astrophysics*, 137(1): 5-8.

Lemke, D., Mattila, K., Lehtinen, K., Laureijs, R.J., Liljestrom, T., Leger, A. and Herbstmeier, U. (1998) Detection of UIR bands in an isolated local interstellar cirrus cloud. *Astronomy and Astrophysics*, 331 (2): 742-748.

Le Pichon, A., Antier, K., Cansi, Y., Hernandez, B., Minaya, E., Burgoa, B., Drob, D., Evers, L.G., and Vaubaillon, J. (2008) Evidence of a meteoritic origin of the September 15, 2007, Carancas crater. *Meteoritics & Planetary Science*, 43:1797–1809.

Lequeux, J. and Jourdain de Muizon, M. (1990) The 3.4 and 12 micrometer absorption bands in the proto-planetary nebula CRL 618. Astronomy and Astrophysics, 240(2): 19-22.

Lequeux, J., Maurice, E., Prevot-Burnichon, M.-L., Prevot, L., Rocca-Volmerange, B. (1982) SK 143 - an SMC star with a galactic-type ultraviolet interstellar extinction. *Astronomy and Astrophysics*, 113(2): 15-17.

Lewis, J.S. (1995) Physics and chemistry of the solar system. Published by Academic press, Inc., A division of Harcourt Brace & Company. ISBN 0124467407.

Li, A. and Draine, B. T. (2001b) Infrared Emission from Interstellar Dust. II. The Diffuse Interstellar Medium. *The Astrophysical Journal*, 554:778–802.

Li, A. and Greenberg, J. M. (2002) Mid-Infrared Spectropolarimetric Constraints on the Core-Mantle Interstellar Dust Model. *The Astrophysical Journal*, 577: 789 794.

Li, A. and Greenberg, J. M. (2003) In dust we trust: an overview of observations and theories of interstellar dust. *Solid State Astrochemistry*, 37-84.

Li, A. and Greenberg, J.M. (1997) A unified model of interstellar dust. *Astronomy and Astrophysics*, 323: 566-584.

Living In Peru (Peru's online newspaper) <a href="http://www.livinginperu.com/news">http://www.livinginperu.com/news</a> 4732-environmentnature-medical-teams-aid-in -rising-number-of-illnesses-after meteorite crash, (19/09/2007).

Llorca J (2005) Organic matter in comets and cometary dust. *Int Microbiol*, 8(1):5-12.

Llorca, J. (2004) Organic matter in meteorite, Int Microbiol, 7(4):239-248.

Lopez-Amoros, R., Mason, D.J. and Lloyd, D. (1995) Use of two oxonols and a fluorescent tetrazolium dye to monitor starvation of *Escherichia coli* in sea water. *J. Microbiol. Meth.*, 22: 165-176.

Louis, G. and Kumar, A.S. (2006) The red rain phenomenon of Kerala and its possible extraterrestrial origin. *Astrophysics and Space Science*, 302: 175-187.

Louis, G. and Kumar, A. S. (2003) Cometary panspermia explains the red rain of Kerala. *eprint arXiv:astro-ph/0310120*.

Lovas, F. J. (2004) NIST Recommended Rest Frequencies for Observed Interstellar Molecular Microwave Transitions—2002 Revision. *J. Phys. Chem. Ref. Data*, 33: 177-355.

Lovas, F. J., McMahon, R. J., Grabow, J., Schnell, M., Mack, J., Scott, L.T. and Kuczkowski, R.L. (2005) Interstellar Chemistry: A Strategy for Detecting Polycyclic Aromatic Hydrocarbons in Space. *Journal of the American Chemical Society* 127 (12): 4345-4349.

Lysenko, S. V. (1979) Microorganisms of the upper layers of the atmosphere and the protective role of their cell pigments. *Life Sci Space Res.*, 17:105-110.

Macedo L. F. and Macharé J. O. (2007) The Carancas meteorite fall, 15 September 2007. Official INGEMMET initial report.

Mancinelli, R.L., Klovstad, M. (2000) Martian soil and UV radiation: microbial viability assessment on spacecraft surfaces. *Planet Space Sci*, 48:1093–1097.

Martin, P. G. (1995) On the value of GEMS (glass with embedded metal and sulphides). *The Astrophysical Journal*, 445(2): 63.

Martins, Z., Botta, O., Fogel, M., Sephton, M.A., Glavin, D.P., Watson, J.S., Dworkin, J., Schwartz, A.W. and Ehrenfreund, P. (2008) Extraterrestrial nucleobases in the Murchison meteorite. *Earth and Planetary Science Letters*, 270 (1-2): 130-136.

Mathis, J. S. (1993) Observations and theories of interstellar dust. Rep. Prog. Phys., 56: 605-652.

Mathis, J.S. (1996) Dust Models with Tight Abundance Constraints. *Astrophysical Journal*, 472: 643.

Mathis, J.S. and Whiffen, G. (1989) Composite interstellar grains. *Astrophysical Journal*, 341: 808-822.

Mathis, J.S., Rumpl, W., and Nordsieck, K.H. (1977) The size distribution of interstellar grains. *ApJ*, 217: 425.

Matteucci, F. (1991) The Role of SNs in the Chemical Evolution of Galaxies. European Southern Observatory, 703.

Mattila, K. (1979) Astronomy and Astrophysics, 78,253.

Mattila, K., Lemke, D., Haikala, L.K., Laureijs, R.J., Leger, A., Lehtinen, K., Leinert, Ch., Mezger, P.G. (1996) Spectrophotometry of UIR bands in the diffuse emission of the galactic disk. *Astronomy and Astrophysics*, 315 (2): 353-356.

Maurette, M., Olinger, C., Michel-Levy, C., Kurat, G., Pourchet, M., Braudstatter, M. and Bourot-Denise, M. (1991) A collection of diverse micrometeorites recovered from 100 tonnes of Antarctic blue ice. *Nature*, 351: 44-47.

Mautner, M. N. (1997) Directed panspermia: Strategies and motivation for seeding star-forming clouds. J. British Interplanetary Soc., 50: 93.

Mazur, P. (1980) Limits to life at low temperatures and at reduced water contents and water activities. *Origins of Life*, 10: 137-159.

McBride, E. F., Picard, M. D. and Folk, R. L. (1994) Oriented concretions, Ionian Coast, Italy; evidence of groundwater flow direction. *Journal of Sedimentary Research*, 64(3a): 535-540.

McBride, N. (2004) A tour of the solar system. In "An introduction to the solar system". Cambridge university press. McBride N., Gilmore I (Eds.) ISBN 0521837359.

McBride, N. and Gilmore, I. (2004) In "An introduction to the solar system", The Open University. Cambridge university press. McBride N., Gilmore I (Eds.) ISBN 0521837359.

McCafferty, P. (2008) Bloody rain again! Red rain and meteors in history and myth. *International Journal of Astrobiology*, 1-7.

McDonald, G.D., Whited, L.J., DeRuiter, C., Khare, B.N., Patnaik, A. and Sagan, C. (1996) Production and chemical analysis of cometary ice tholins. *Icarus* 122:107-117.

McDonnell, J.A.M., Alexander, W.M., Burton, W.M., Bussoletti, E., Clark, D.H., Grard, R.J.L., Grün, E., Hanner, M.S., Hughes, D.W., Igenbergs, E., Kuczera, H., Lindblad, B.A., Mandeville, J.C., Minafra, A., Schwehm, G.H., Sekanina, Z., Wallis, M., Zarnecki, J.C., Chakaveh, S.C., Evans, G.C., Evans, S.T., Firth, J.C., Littler, A.N., Massone, L., Olearczyk, R.E., Pankiewicz, G.C., Stevenson, T.J. and Turnerm, R.J. (1986) Dust density and mass distribution near comet Halley from Giotto observations. *Nature*, 321:338-341.

McKay C.P. (1991) Urey Prize lecture: Planetary evolution and the origin of life. *Icarus*, 91: 92–100.

McKay, D. S., Gibson, E. K., Thomas-Keptra, K. L., Vali, H., Romanek, C. S., Clemett, S. J., Chillier, X. D. F., Maechling, C. R. and Zare, R.N. (1996) Search for Past Life on Mars: Possible Relic Biogenic Activity in Martian Meteorite ALH84001. *Science*, 273(5277): 924-930.

McSween, H., Jr (1989) Meteorites and their parent planets. Cambridge University Press, Cambridge, UK.

Melosh, H. J. (1988) The rocky road to panspermia. Nature, 332: 687-688.

Mennella, V., Colangeli, L., Palumbo, P., Rotundi, A., Schutte, W. and Bussoletti, E. (1996) Activation of an Ultraviolet Resonance in Hydrogenated Amorphous Carbon Grains by Exposure to Ultraviolet Radiation. *Ap. J.*, 464:191 194.

Messenger, S. (2000) Identification of molecular-cloud material in interplanetary dust particles. *Nature*, 404(6781): 968-971.

Messenger, S., Keller, L.P., Stadermann, F.J., Walker, R.M. and Zinner, E. (2003) Samples of stars beyond the solar system: silicate grains in interplanetary dust. *Science*, 300(5616): 105-108.

Michell, A.J. and Scurfield, G. (1970) An assessment of infrared spectra as indicators of fungal cell wall composition. *Aust.J. Biol. Sci.*, 23, 345.

Misselt, K., Clayton, G. C., and Gordon, K. D. (1999) A Reanalysis of the Ultraviolet Extinction from Interstellar Dust in the Large Magellanic Cloud. *ApJ*, 515: 128-139.

Miura, Y. (2008) Multiple explosions during cratering at Carancas meteorite hit in Peru. Earth Sci., Graduate School of Sci. & Eng., Yamaguchi University, Yoshida 1677-1, Yamaguchi, 753- 8512, Japan. Lunar and Planetary Science XXXIX abstract.

Miyake, M., Wallis, M.K., and Wickramasinghe, N.C. (2009) Discovery in space Micro-dust: Siliceous fragments supporting the diatom hypothesis. EPSC abstract, 4.

Miyake, N. (2009) Laboratory studies of stratospheric dust – relevance to the theory of cometary panspermia. PhD thesis. Cardiff university, Cardiff. UK.

Mojzsis, S.J., Arrhenius, G., McKeegan, K.D., Harrison, T.M., Nutman, A.P., Friend, C.R.L. (1996) Evidence for life on Earth before 3800 million years ago. *Nature*, 384: 55–59.

Molster, F. and Kemper, C. (2005) Crystalline Silicates. *Space Science Reviews*, 119(1-4): 3-28.

Moore, E.A. (2004) The giant planets, In "An introduction to the solar system". The Open University. Cambridge university press. McBride N., Gilmore I (Eds.) ISBN 0521837359.

Moroz, L.V., Arnold, G., Korochantsev, A.V. and Wasch, R. (1998) Natural Solid Bitumens as Possible Analogs for Cometary and Asteroid Organics: 1. Reflectance Spectroscopy of Pure Bitumens. *Icarus*, 134(2): 253-268.

Mulas, G., Malloci, G., Joblin, C. and Toublanc, D. (2006) A general model for the identification of specific PAHs in the far-IR. *Astronomy & Astrophysics*, 460: 93-104.

Muthumariappan, C., Maheswar, G., Eswaraiah, C. and Pandey, A. K. (2008) A study of 2175 °A absorption feature with TAUVEX: An Indo-Israeli UV mission. *Organic Matter in Space Proceedings IAU Symposium*, 251: 73-74.

Nakamura, K., Messenger, S., Keller, L.P., Clemett, S.J. and Zolensky, M.E. (2006) Organic globules in the Tagish Lake meteorite: remnants of the protosolar disk. *Science*, 314(5804): 1439-1442.

Nakamura, K., Zolensky, M.E., Tomita, S., Nakashima, S. and Tomeoka, K. (2002) Hollow organic globules in the Tagish Lake meteorite as possible products of primitive organic reactions. *Int. J. Astrobiology* 1(3): 179-189.

Nandy, K., Thompson, G.I., Jamar, C., Monfils, A. and Wilson, R. (1975) Studies of ultraviolet interstellar extinction with sky-survey telescope of TD-1 satellite. 1. Results for 3 galactic regions. *Ast. Astrophys.* 44(1): 195-203.

Narlikar, J.V. et al. (1998) Proceedings of SPIE Conference on Instruments, Methods and Mission for Astrobiology, 3441: 301-305.

Narlikar, J.V., Lloyd, D., Wickramasinghe, N.C., Harris, M.J., Turner, M.P., Al Mufti, S., Wallis, M.K., Wainwright, M., Rajaratnam, P., Shivaji, S., Reddy, G.S.N., Ramadurai, S. and Hoyle, F. (2003) Balloon experiment to detect micro organisms in the outer space. *Astrophys Space Science* 285 (2): 555–62.

Nicholson, W.L., Munakata, N., Horneck, G., Melosh, H.J. and Setlow, P. (2000) Resistance of *Bacillus* endospores to extreme terrestrial and extraterrestrial environments. *Microbiol Mol Biol Rev.*, 64: 548-572.

Nicholson, W.L., Schuerger, A.C. and Setlow, P. (2005) The solar UV environment and bacterial spore UV resistance: considerations for Earth-to-Mars transport by natural processes and human spacecraft. *Mutat Res*, 571:249-264.

Nuth, J.A. Jr III, Brearley, A.J. and Scott, E.R.D. (2005) Microcrystals and amorphous materials in comets and primitive meteorites: keys to understanding processes in the early solar system. In *Chondrites and the Protoplanetary Disk*. ASP Conference Series, 341: 675-700.

Omont, A. (1991) in J. M. Greenberg and V. Pirronello (eds.), Chemistry in Space, *Kluwer Academic Publishers*, 171–197.

Onaka, T. (2000) Interstellar dust: What do space observations tell us?. Advances in Space Research, 25(11): 2167-2176.

Onaka, T., Yamamura, I., Tanabe, T., Roellig, T.L. and Yuen, L. (1996) Detection of the mid-infrared unidentified bands in the diffuse galactic emission by IRTS. *Publications of the Astronomical Society of Japan*, 48 (5): 59-63.

Oró, J. (1961) Comets and the formation of biochemical compounds on the primitive Earth. *Nature*, 190: 389-390.

Oró, J., Mills, T. and Lazcano, A. (1992) Comets and the formation of biochemical compounds on the primitive Earth-A review. *Orig Life Evol Biosph*, 21:267-277.

Pace, N.R. (2001) The universal nature of biochemistry. *Proc. Natl. Acad. Sci. USA*, 98: 805–808.

Papoular, R., Conard, J., Guiliano, M., Kister, J. and Mille, G. (1989) A coal model for the carriers of the unidentified IR bands. *Astronomy and Astrophysics*, 217(1-2): 204-208.

Papoular, R., Conard, J., Guillois, O., Nenner, I., Reynaud, C., Rouzaud, J.N. (1996) A comparison of solid-state carbonaceous models of cosmic dust. *Astron. Astrophys.* 315: 222-236.

Papoular, R., Ellis, K., Guillois O., Reynaud C. and Nenner, I. (1993) New Developments of the Coal Model of Interstellar Dust. *J. Chem. Soc. Farady Trans*. 89(13): 2289-2295.

Papoular, R., Guillois, O., Nenner, I., Perrin, J.M., Reynaud, C. and Sivan, J.P. (1995) On the nature of interstellar carbonaceous dust. *Planet. Space Sci.*, 43,(10 11): 1287-1291.

Papoular, R.J. and Papoular, R. (2009) A polycrystalline graphite model for the 2175Å interstellar extinction band. *Mon. Not. R. Astron. Soc.*, 394(4): 2175-2181.

Pasko, V.P., Stanley, M.A., Mathews, J.D., Inan, U.S. and Wood, T.G. (2002) Electrical discharge from thundercloud tops to the lower ionosphere. *Nature*, 416: 152-154.

Pavlov, A.A., Hurtgen, M.T., Kasting, J.F. and Arthur, M.A. (2003) Methane-rich Proterozoic atmosphere?. *Geology*, 31(1): 87-90.

Pizzarello, S. (2006) The Chemistry of Life's Origin: A Carbonaceous Meteorite Perspective. *Acc. Chem. Res.*, 39(4): 231–237.

Pizzarello, S., Huang, Y., Becker, L., Poreda, R.J., Nieman, R.A., Cooper, G., and Williams, M. (2001) The organic content of the Tagish Lake meteorite. *Science*, 293: 2236–2239.

Prevot, M. L., Lequeux, J., Prevot, L., Maurice, E. and Rocca-Volmerange, B. (1984) The typical interstellar extinction in the Small Magellanic Cloud. *A&A*, 132: 389-392.

Puget, J. L. and Le'ger, A. (1989) A new component of the interstellar matter-small grains and large aromatic molecules. *Annual review of astronomy and astrophysics.*, 27: 161-198.

Rauf, K. and Wickramasingh C. (2010) Evidence for biodegradation products in the interstellar medium. *Int. J. Astrobiology*, 9 (1): 29-34.

Rauf, K., Hann, A. and Wickramasingh C. (2010) Microstructure and elemental composition of the Tagish Lake meteorite and its astrobiological implications. Int. *J. Astrobiology* 9(1): 35-43.

Raulin-Cerceau, F., Maurel, M. amd Schneider, J. (1998) From panspermia to bioastronomy, the evolution of the hypothesis of universal life. *Origins of Life and Evolution of the Biosphere*, 28 (4-6), 597-612.

RayChaudhuri, B. and Bhattacharyya, S. (2008) Molecular level all-optical logic with chlorophyll absorption spectrum and polarization sensitivity. *Appl. Phys. B.*, 91: 545-550.

Reach, W. (2004) paper presented at the 36th Annual Division of Planetary Sciences Meeting, Louisville, KY.

Reach, W. T., Boulanger, F., Contursi, A. and Lequeux, J. (2000) Detection of mid-infrared aromatic hydrocarbon emission features from the Small Magellanic Cloud. *A&A*, 361: 895-900.

Reed, J. (2006) Myserious red cells might be aliens! Sited at <a href="http://www.viewzone.com/redrain.html">http://www.viewzone.com/redrain.html</a>. Popular Science.

Reimold, W. U., Buchanan, P.C., Ambrose, D, Koeberl, C., Franchi, I., Lalkhan, C., Schultz, L., Franke, L. and Heusser (2004) Thuathe, a new H4/5 chondrite from Lesotho: Histoy of the fall, petrography, and geochemistry.

Renard, J.-B., Hadamcik, E., Brogniez, C., Berthet, G., Worms, J.-C., Chartier, M., Pirre, M., Ovarlez, J. and Ovarlez, H. (2001) UV-visible bulk optical properties of randomly distributed soot. *Appl. Opt.*, 40: 6575–6580.

Renard, J.-B, Ovarlez, J., Berthet, G., Fussen, D., Vanhellemont, F., Brogniez, C., Hadamcik, E., Chartier, M. and Ovarlez, H. (2005) Optical and physical properties of stratospheric aerosols from balloon measurements in the visible and near infrared domains. III. Presence of aerosols in the middle stratosphere. *Appl. Opt.*, 44: 4086-4095.

Reynaud, C., Guillois, O., Herlin-Boime, N., Rouzaud, J. N., Galvez, A., Clinard, C., Balanzat, E. and Ramillon, J. M. (2001) Optical Properties of Synthetic Carbon Nanoparticles as Model of Cosmic Dust. *Spectrochim. Acta A.*, 57: 797 814.

Rietmeijer, F.J.M. (1998) Interplanetary dust particles. In: Papike, J.J. (Ed.), Planetary Materials, Review in Mineralogy 36, Mineralogical Soc. of America, Washington, 2-01–2-95.

Ristorcelli, I., Giard, M., Mény, C., Serra, G., Lamarre, J.M., Le Naour, C., Léotin, J. and Pajot., F. (1994) The diffuse galactic emission at 6.2 µm. *Astron. Astrophys.* 286(2): 23–26.

Robert, F. and Epstein, S. (1982) The concentration and isotopic composition of hydrogen, carbon and nitrogen in carbonaceous meteorites. *Geochimica et Cosmochimica Acra*, 46: 81-95.

Roche, P. F., Lucas, P. W. and Geballe, T. R. (1996) Mon. Not. Royal Ast. Soc., 281: 25.

Rohatschek, H. (1996) Levitation of stratospheric and mesophilic aerosols by gravitophosphophoresis. *J Aerosol Sci.*, 27: 467-475.

Rothschild, L.J. and Mancinelli, R.L. (2001) Life in extreme environments, *Nature*, 409: 1092-1101.

Rouleau, F., Henning, Th. and Stognienko, R. (1997) Constraints on the properties of the 2175Å interstellar feature carrier. *Astronomy & Astrophysics*, 322: 633-645.

Ruiz, A., Bret'on, J. and Gomez Llorente, J. M. (2005) *Phys. Rev. Lett.*, 94, 105501.

Saikia and Parthasarathy (2009) Spectroscopic investigation of Mahadevpur H4/5 ordinary chondrites. *Goldschmidt Conference*, Abstracts.

Sakata, A., Wada, S., Narisawa, T., Asano, Y., Iijima, Y., Onaka, T. and Tokunaga, A. T. (1992) Quenched carbonaceous composite – Fluorescence spectrum compared to the extended red emission observed in reflection nebulae. *Astrophysical Journal, Part* 2, 393: 83-86.

Sakata, A., Wada, S., Onaka, T. and Tokunaga, A. T. (1987) Infrared spectrum of quenched carbonaceous composite (QCC). II - A new identification of the 7.7 and 8.6 micron unidentified infrared emission bands. *Astrophysical Journal*, Part 2, 320: 63-67.

Sakata, A., Wada, S., Onaka, T. and Tokunaga, A. T. (1990) Quenched carbonaceous composite. III - Comparison to the 3.29 micron interstellar emission feature. *Astrophysical Journal*, Part 1, 353: 543-548.

Sakata, A., Wada, S., Okutsu, Y., Shintani, H. and Nakada, Y. (1983) Does a 2,200 Å hump observed in an artificial carbonaceous composite account for UV interstellar extinction?. *Nature*, 301: 493-494.

Salama, F., Bakes, E. L. O., Allamandola, L. J. and Tielens, A. G. G. M. (1996) Assessment of the Polycyclic Aromatic Hydrocarbon--Diffuse Interstellar Band Proposal. *Astrophysical Journal*, 458: 621-636.

Sampath, S., Abraham, T.K., Sasi Kumar, V. and Mohanan, C.N. (2001). Coloured rain: a report on the phenomenon. CESS-PR-114-2001, Center for Earth Science Studies and Tropical Botanic Garden and Research Institute.

Sandford, S. A., Allamandola, L.J., Tielens, A.G., Sellgren, K., Tapia, M. and Pendleton, Y. (1991) The interstellar C-H stretching band near 3.4 microns: constraints on the composition of organic material in the diffuse interstellar medium. The Astrophysical journal, 371: 607-620.

Sandford, S. A., Bernstein, M. P. and Dworkin, J. P. (2001) Assessment of the interstellar processes leading to deuterium enrichment in meteoritic organics. *Met. Planet. Sci.*, 36: 1117–1133.

Sandford, S.A. (1987) The collection and analysis of extraterrestrial dust particles. *Fund Cosmic Phys*, 12: 1-73.

Sandford, S.A. (1996) The inventory of interstellar materials available for the formation of the solar system. *Meteoritcs Planet Sci*, 31:449-476.

Sandford, S.A. (2008) Organics in the samples returned from comet 81P/Wild 2 by the Stardust Spacecraft. *Organic Matter in Space*, *Proceedings IAU Symposium*, 251, 299-307.

Satyanarayana, M., Veerabuthiran, S., Ramakrishna Rao D, Presennakumar B (2004) Colored rain on the west coastal region of India: Was it Due to a Dust Storm?. *Aerosol Science and Technology*, 38(1): 24-26.

Satyanarayana, M., Veerabuthiran, S., Rao, D. R. and Presennakumar, B. (2004) Colored Rain on the West Coastal Region of India: Was it Due to a Dust Storm? *Aerosol Science and Technology*, 38, 24-26.

Savage, B.D. (1975) Ultraviolet photometry from the Orbiting Astronomical Observatory. XX - The ultraviolet extinction bump. *Astrophysical Journal*, 199(1): 92-109.

Schmidt, G.D., Cohen, M. and Margon, B. (1980) Discovery of optical molecular emission from the bipolar nebula surrounding HD 44179. *ApJ*, 239: 133.

Schopf, J.W. (1992) in Major Events in the History of Life, J.William Schopf (ed.), Jones and Bartlett, p. 29.

Schopf, J.W. (1993) Microfossils of the Early Archean Apex chert: New evidence of the antiquity of life. *Science*, 260: 640-646.

Schramm, L.S., Brownlee, D.E. and Wheelock, M.M. (1989) Major element composition of stratospheric micrometeorites. *Meteoritics*, 24:99-112.

Schultz P.H., Harris R.S., Tancredi, G., Ishitsuka, J. (2008) Implications of the Carancas meteorite impact. *Lunar and Planetary Science*, #2409 abstract.

Secker, J., Wesson, P.S. and Lepock, J.R. (1994) Astrophys. Sp. Sci. 329, 1.

Sephton, M.A. (2005) Organic matter in carbonaceous meteorites: past, present and future research. *Phil. Trans. R. Soc. A.*, 363: 2729-2742.

Shafizadeh, F.J. (1971) Thermal Behavior of Carbodhydrates. *Journal of Polymer Sci.*, 36: 21-51.

Siebenmorgen R. and Krugel E. (1992) A&A, 259, 614-626.

Silverstein, R.M., Clayton Bassler G and Morrill T.C. (1974) Spectroscopic identification of organic compound, J. Wiley and Sons (Publishers), New York.

Sloan, G. C., Hayward, T. L., Allamandola, L. J., Bregman, J. D., DeVito, B. and Hudgins, D. M. (1999) Direct spectroscopic evidence for ionized polycyclic aromatic hydrocarbons in the interstellar medium. *ApJ*, 513: 65-68.

Smibert, R.M. and Kreis, N.R. (1994) in: P. Gerherdt, R.G.E. Murray, W.R. Wood and N.R. Kreig (eds.), *Methods for General and Molecular Bacteriology*, Am. Soc. Microbiol., 603.

Smith, J.D.T., Draine, B.T., Dale, D.A., Moustakas, J., Kennicutt, R.C., Helou, G., Armus, L., Roussel, H., Sheth, K., Bendo, G.J., Buckalew, B.A., Calzetti, D.A., Engelbracht, C.W., Gordon, K.D., Hollenbach, D.J., Li, A., Malhotra, S., Murphy, E.J. and Walter, F. (2007) The Mid-Infrared Spectrum of Star-Forming Galaxies: Global Properties of PAH Emission. *Astrophys. J.*, 656: 770-791.

Snow, T. P. (1992) On ionized napthalene (C10H8(+)) as a carrier of diffuse interstellar bands. The Astrophysical Journal, 401: 775.

Snyder, L. E., Buhl, D., Zuckerman, B., and Palmer, P. (1969) Microwave detection of interstellar formaldehyde. *Phys. Rev. Lett.*, 22: 679-681.

Somogyi, A, Oh, C, Smith, M.A., Lunine, J.I. (2005) Organic Environments on Saturn's Moon, Titan: Simulating Chemical Reactions and Analyzing Products by FT-ICR and Ion-Trap Mass Spectrometry. *American Society for Mass Spectrometry Published by Elsevier B.V.*, 16(6): 850-859.

Sorrell, W. H. (1990) The 2175Å feature from irradiated graphitic particles. *MNRAS*, 243: 570.

Stecher, T. P. (1969) Interstellar Extinction in the Ultraviolet. II. Astrophysical Journal, 157: 125.

Stecher, T.P. (1965) Interstellar Extinction in the Ultraviolet. *Astrophys. J.*, 142: 1683.

Stecher, T.P. (1965) Wavelength Dependence of Interstellar Polarization by Graphite Grains. *Astrophys. J.*, 142: 1683.

Stecher, T. P. and Donn, B. (1965) On Graphite and Interstellar Extinction. *ApJ.*, 142: 1681.

Steel, T. M. and Duley, W.W. (1987) A 217.5 nanometer absorption feature in the spectrum of small silicate particles. *Astrophys. J.*, 315: 337-339.

Stetter, K.O. (1982) Ultrathin mycelia-forming organisms from submarine volcanic areas having an optimum growth temperature of 105-degrees-C. *Nature*, 300: 258–260.

Swan, P., Walker, R.M., Wopenka, B., Freeman, J.J. (1987) 3.4 µm Absorption in interplanetary dust particles: Evidence for indigenous hydrocarbons and a further link to comet Halley. *Meteoritics*, 22: 510-511.

Szomoru, A. and Guhathakurta, P. (1998a) Optical Spectroscopy of Galactic Cirrus Clouds: Extended Red Emission in the Diffuse Interstellar Medium. *ApJ*, 494: 93-97.

Tanaka, M., Matsumoto, T., Murakami, H., Kawada, M., Noda, M., Matsuura, S. (1996) IRTS observation of the unidentified 3.3-micron band in the diffuse galactic emission. *Publ. Astron. Soc. Japan* 48: 53-57.

Tancredi, G. et al. (2007), LPSC 39, XXXIX abstract.

Tancredi, G., Ishitsuka, J., Rosales, D., Vidal, E., Dalmau, A., Pavel, D., Benavente, S., Miranda, P., Pereira, G., Vallejos, V., Varela, M.E., Brandstätter, F., Schultz, P., Harris, R.S. and Sánchez, L. (2008) What do we know about the

Carancas-Desaguadero' fireball, meteorite and impact crater?. Lunar and Planetary Science, #1216 abstract.

Tancredi, G., Ishitsuka, J., Schultz, P. H., Harris, R. S., Brown, P., Revelle, D. O., Antier, K., Le Pichon, A., Rosales, D., Vidal, E., Varela, M. E., Sánchez, L., Benavente, S., Bojorquez, J., Cabezas, D. and Dalmau, A. (2009) A meteorite crater on Earth formed on September 15, 2007: The Carancas hypervelocity impact. *Meteoritics & Planetary Science*, 44(12), 1967-1984.

Tansey, M. R. and Brock, T. D. (1978) Microbial life at high temperatures: ecological aspects. *Microbial Life in Extreme Environments* (ed. Kushner, D. J.), Academic press, London 159–216.

Thomas, K. L., Blanford, G.E., Keller, L.P. Klock, W. and McKay, D.S. (1993) Carbon abundance and silicate mineralogy of anhydrous interplanetary dust particles. *Geochim. Cosmochim. Acta*, 57: 1551–1566.

Thomson (Lord Kelvin), W. (1871) Inaugural Address to the British Association Edinburgh: "We must regard it as probably to the highest degree that there are countless seed-bearing meteoritic stones moving through space". *Nature*, 4: 262.

Tielens, A.G. (1993) PAHs and Astrochemistry. Dust and Chemistry in Astronomy. 103–136.

Tokunaga, A.T. (1997) A summary of the UIR bands. ASP Conf. Ser., 124: 149 160.

Trent, J. D. (2000) Extremophiles in astrobiology: per Ardua ad Astra. *Gravit. Space Biol. Bull.*, 13: 5-11.

Trimble, V. (1991) The Origin and Abundance of the Chemical Elements Revisited. Astron. Astrophys. Rev., 3: 1.

Trimble, V. (1997) Origin of the biologically important elements. *Origins of Life and Evolution of the Biosphere*, 27(1-3): 3-21.

Trumpler, R.J. (1930) Absorption of Light in the Galactic System. *Publications of the Astronomical Society of the Pacific*, 42(248): 214.

Tscharnuter, W. M. and Boss, A. P. (1993) in Protostars and Planets III, Levy E. H., Lunine J. I. (eds.), University of Arizona Press, 921.

Tulej, M., Kirkwood, D.A., Pachkov, M. and Maier, J.P. (1998) Gas-Phase Electronic Transitions of Carbon Chain Anions Coinciding with Diffuse Interstellar Bands. *The Astrophysical Journal*, 506(1): 69-73.

Turner, B. E. and Bally, J. (1987) Detection of interstellar PN - The first identified phosphorus compound in the interstellar medium. *ApJ*, 321, 75-79.

Vaidya, D.B., Gupta, R., Dobbie, J.S. and Chylek, P. (2001) Interstellar extinction by composite grains. *A&A*, 375: 584-590.

Van der Zwet, G.P. and Allamandola, L. J. (1985) Polycyclic Aromatic Hydrocarbons and the Diffuse Interstellar Bands. *Astron. Astrophys.*, 146(1): 76 80.

Van Krevelen, D. W. (1993) Coal. Typology, Physics, Chemistry and Constitution. *Elsevier Sciences*, Amsterdam, 89–110.

Vanysek, V. and Wickramasinghe, N.C. (1975) Astrophysics space science, 33: 19.

Veerabuthiran, S. and Satyanarayana, M. (2003) Lidar observations on atmospheric dust transported from south-west Asia to Indian west coast region: A case study of colour rain event occurred during July 2001. *Indian Journal of Radio & Space Physics*, 32: 158-165.

Wada, S. and Tokunaga, A. T. (2006) Natural Fulerenes and Related Structures of Elemental Carbon. *Dordrecht: Springer*, 31.

Wainwright, M., Alharbi, S. and Wickramasinghe, N.C. (2006) How do microorganisms reach the stratosphere?. *Int. J. Astrobiology*, 5 (1): 13-15.

Wainwright, M., Weber, P.K., Smith, J.B., Hutcheon, I.D., Klyce, B., Wickramasinghe, N.C., Narlikar, J.V. and Rajaratnam, P. (2004a) Studies on bacteria-like particles sampled from the stratosphere. *Aerobiologia*, 20: 237-240.

Wainwright, M., Wickramasinghe, N.C., Narlikar, J.V. and Rajaratnam, P. (2003) Microorganisms cultured from stratospheric air samples obtained at 41 km. *FEMS Microbiol. Lett.*, 218: 161–165.

Wainwright, M., Wickramasinghe, N.C., Narlikar, J.V., Rajaratnam, P. and Perkins, J. (2004b) Confirmation of the presence of viable but non-cultureable bacteria in the stratosphere. *Int. J. Astrobiology* 3 (1): 13–15.

Waite, J.H. Jr., Niemann, H., Yelle, R.V., Kasprzak, W.T., Cravens, T.E., Luhmann, J.G., McNutt, R.L., Ip, W., Gell, D., De La Haye, V., Müller-Wordag, I., Magee, B., Borggren, N., Ledvina, S., Fletcher, G., Walter, E., Miller, R., Scherer, S., Thorpe, R., Xu, J., Block, B. and Arnett, K. (2005) Ion Neutral Mass Spectrometer Results from the First Flyby of Titan, 308(5724): 982-986.

Waite, J.H. Jr., Young, D. T., Cravens, T. E., Coates, A., Crary, F. J., Magee, B. and Westlake, J. (2007) The Process of Tholin Formation in Titan's Upper Atmosphere. *Science*, 316(5826): 870 - 875.

Wang, J., Ge, J., Hall, P.B., Prochaska, J.X. and Li, A. (2005) Detection of the 2175Å dust feature from The Sloan Digital Sky Survey first and second data releases. *Probing Galaxies through Quasar Absorption Lines, Proceedings IAU Colloquium*, 199.

Wang, J., Hall, P. B., Ge, J., Li, A. and Schneider, D. P. (2004) Detections of the 2175 Å Dust Feature at 1.4<~z<~1.5 from the Sloan Digital Sky Survey. *ApJ*, 609: 589-596.

Watson, R.A., Rebolo, R., Rubino-martin, J.A., Hildebrandt, S.R., Gutierrez, C.M., Fernandez-Cerezo, S., Hoyland, R.J. and Battistelli, E.S. (2005) Detection of Anomalous Microwave Emission in the Perseus Molecular Cloud with the cosmosomas Experiment. *The Astrophysical Journal*, 624(2): 89-92.

Wdowiak, T.J., Flickinger, G.C. and Cronin, J.R. (1998) Insoluble organic material of the Orgueil carbonaceous chondrite and the unidentified infrared bands. *Astrophys J.*, 328(2): 75-79.

Weingartner, J. C. and Draine, B. T. (2001a) Dust Grain-Size Distributions and Extinction in the Milky Way, Large Magellanic Cloud, and Small Magellanic Cloud. *ApJ*, 548: 296-309.

Whisler, B.A. (1940) The efficacy of ultra-violet light sources in killing bacteria suspended in air. *Iowa State Coll. J. Sci.*, 14: 215-231.

Whittet, D. C. B. (1992) Dust in the Galactic Environment, Institute Physics Publishing.

Whittet, D.C.B. (1996) Is extraterrestrial organic matter relevant to the origin of life on earth?. Origin of life and evolution of the biosphere, 27: 249-262.

Wickramasinghe, D.T. and Allen, D.A (1980) Discovery of organic grains in comet Wilson. *Nature*, 287: 518-519.

Wickramasinghe, N.C. and Wickramasinghe, J.T. (2008) On the possibility of microbiota transfer from Venus to Earth. *Ap.Sp.Sci.*, 317, 133-137.

Wickramasinghe, J.T., Wickramasinghe, N.C. and Napier, W.M. (2010) Comets and the Origin of Life. World Scientific Publishing Co., Singapore.

Wickramasinghe, N. C., Brooks, J. and Shaw, G. (1977) Nature, 269, 674.

Wickramasinghe, N. C., Wickramasinghe, A. N. and Hoyle, F. (1992) The case against graphite particles in interstellar space. *Astrophys. Space Sci.*, 196: 167 169.

Wickramasinghe, N.C. (1967) Interstellar Grains. Chapman & Hall, London.

Wickramasinghe, N.C (1974) The case for life as a cosmic phenomenon. *Nature*, 252: 462.

Wickramasinghe, N.C. (2004) The universe: a cryogenic habitat for microbial life. *Cryobiology*, 48:113-125.

Wickramasinghe, N.C (2010) The astrobiological case for our cosmic ancestry. *International Journal of Astrobiology*, 1-11.

Wickramasinghe, N.C. and Guillaume, C. (1965) On the Origin of the Zodiacal Light. *Nature*, 207: 366.

Wickramasinghe, N.C., Wickramasinghe, A.N. and Hoyle, F. (1999) The case against graphite particles in interstellar space. *Astrophysics and Space Science*, 268: 289-292.

Wickramasinghe, N. C., Lloyd, D. and Wickramasinghe, J. T. (2002) Evidence of photoluminescence of biomaterial in space. *Proc. SPIE*, 4495: 255-260.

Willner, S. P., Puetter, R. C., Russell, R. W. and Soifer, B. T. (1979) Unidentified infrared spectral features. *Astrophysics and Space Science*, 65: 95-101.

Witt, A. N., Gordon, K. D., Vijh, U. P., Sell, P.H., Smith, T.L. and Xie R. (2006) The Excitation of Extended Red Emission: New Constraints on Its Carrier from Hubble Space Telescope Observations of NGC 7023. *Astrophys. J.*, 636: 303-315.

Witt, A.N. (1999) Overview of Grain Models. Astrophysics, 2: 1-14.

Wood, J. A. and Chang, S. (1985) The Cosmic History of the Biogenic Elements. National Aeronautics and Space Administration NASA SP-476. Washington, DC, 5-9.

Wooden, D.H., Harker, D.E. and Brearley, A.J. (2005). Thermal processing and radial mixing of dust: Evidence from Comets, Chondrules and Matrices of Primitive Meteorites. *Chondrites and the Protoplanetary Disk.* ASP Conference Series, 341: 774-808.

Wright, I. (2004) The origin of the solar system. In "An introduction to the solar system", The Open University. Cambridge university press. McBride N., Gilmore I (Eds.) ISBN 0521837359.

Yabushita, S., Wada, K., Takai, T., Inagaki, T., Young, D. and Arakawa, E.T. (1986) A spectroscopic study of the microorganism model of interstellar grains. *Astrophys. Space Sci.*, 124: 377-388.

Yayanos, A.A. (1995) Microbiology to 10,500 meters in the deep sea. *Annual Review of Microbiology*, 49: 777-805.

Yelle, R. V. N., Borggren, V., de la Haye, W. T., Kasprzak, H. B., Niemann, I., Muller-Woodarg and Waite, J. H., Jr (2006) The Process of Tholin Formation in Titan's Upper Atmosphere. *Icarus*, 72: 468.

Yung, Y.L., Allen, M. and Pinto, J.P. (1984) Photochemistry of the Atmosphere of Titan Comparison between Model and Observations. *Astrophys. J. Suppl. Ser.* 55: 465–506.

Zagury, F. (2002) The incompatibilities between the standard theory of interstellar extinction and observations. *New Astronomy*, 7: 185–189.

Zolensky, M.E., Zega, T.J., Yano, H., Wirick, S., Westphal, A.J., Weisberg, M.K., Weber, I., Warren, J.L., Velbel, M.A., Tsuchiyama, A., Tsou, P., Toppani, A., Tomioka, N., Tomeoka, K., Teslich, N., Taheri, M., Susini, J., Stroud, J., Stephan, T., Stadermann, F.J., Snead, C.J., Simon, S.B., Simionovici, A., See, T.H., Robert, F., Rietmeijer, F.J.M., Rao, W., Perronnet, M.C., Papanastassiou, D.A., Okudaira, K., Ohsumi, K., Ohnishi, I., Nakamura-Messenger, K., Nakamura, T., Mostefaoui, S., Mikouchi, T., Meibom, A., Matrajt, G., Marcus, M.A., Leroux, H., Lemelle, L., Le, L., Lanzirotti, A., Langenhorst, F., Krot, A.N., Keller, L.P., Kearsley, A.T., Joswiak, D., Jacob, D., Ishii, H., Harvey, R., Hagiya, K., Grossman, L., Grossman, J.N., Graham, G.A., Gounelle, M., Gillet, P., Genge, M.J., Flynn, G., Ferroir, T., Fallon, S., Ebel, D.S., Dai, Z.R., Cordier, P., Clark, P., Chi, M., Butterworth, A.L., Brownlee, A.D., Bridges, J.C., Brennan, S., Brearley, A., Bradley, J.P., Bleuet, P., Bland, P.A., Bastien, R. (2006) Mineralogy and Petrology of Comet 81P/Wild 2 nucleus samples. *Science*, 314(5806): 1735 – 1739.

Zubko, V., Dwek, E. and Arendt, R. G. (2004) Interstellar Dust Models Consistent with Extinction, Emission, and Abundance Constraints. *The Astrophysical Journal Supplement Series*, 152: 211–249.

## **Appendix**

#### **Abbreviations**

CP IDPs Chondritic Porous Interplanetary Dust Particles

DIBs Diffuse Interstellar Bands

DMSO Dimethyl Sulfoxide

E Kinetic energy

EDAX Energy Dispersive Analyser of X-rays

ELA l'Ensemble de Lancement Ariane

EM Electron Microscope

ERE Extended Red Emission

ESA European Space Agency

ESEM Environmental Scanning Electron Microscope

FIR Far-infrared

FTIR Fourier Transform Infrared Spectrometer

FWHM Full Width at Half Maximum

GC-IRS Galactic Centre- Infrared Astronomical Satellite

GEMS Glass with Embedded Metal and Sulfides

GP Gravito-Photophoresis

HAC Hydrogenated Amorphous Carbon

I Intensity

IAU International Astronomical Union

IDPs Interplanatery dust particles

I<sub>o</sub> Incident intensity

IR Infrared

IRAS Infrared Astronomical Satellite

IRIS Infrared Interferometer Spectrometer

ISAS Institute of Space and Astronomical Science

ISM Interstellar Medium

ISO Infrared Space Observatory

IUE International Ultraviolet Explorer

JAXA Japan Aerospace Exploration Agency

KBr Potassium bromide

LED Deuterium arc lamp light emitting

LM Light microscopy

m Mass

NASA National Aeronautics and Space Administration

NEAs Near Earth Asteorids

NIVR Nederlands Instituut voor Vliegtuigontwikkeling en Ruimtevaart

PAHs Polycyclic Aromatic Hydrocarbons

PCR Polymerase Chain Reaction

PHAs Potentially Hazardous Asteroids

PPNe Proto-Planetary Nebulae

QCC Quenched Carbonaceous Composite

RNA Ribonucleic Acid

RT Room Temperature

SD Standard Deviation

SEM Scanning Electron Microscope

SERC Science and Engineering Research Council

SIMS Second Ion Mass Spectrometer

SIRTF Space Infrared Telescope Facility

T Transmittance

TEM Transmission Electron Microscope

UIBs Unidentified Infrared Bands

UV Ultraviolet

UV-Vis Ultraviolet-Visible

v Speed

#### List of my peer-reviewed publications:

- 1- Rauf, K. and Wickramasingh C. (2010) Evidence for biodegradation products in the interstellar medium. *Int. J. Astrobiology*, 9 (1): 29-34.
- **2-** Rauf, K. Hann, A. and Wickramasingh C. (2010) Microstructure and elemental composition of the Tagish Lake meteorite and its astrobiological implications. *Int. J. Astrobiology*, 9(1): 35-43.
- **3-** Rauf, K., Hann, A., Wallis, M. and Wickramasingh C. (2010) Study of putative microfossils in space dust from the stratosphere. *Int. J. Astrobiology*. 9(3): 183-189.
- **4-** Rauf, K. Hann, A., Wickramasingh C. and DiGregorio, B. (2010) Interpretation of micro structures in Carancas meteorite. (In press)
- 5- Norimune Miyake, Kani Rauf, Anthony Hann and Chandra Wickramasinghe (2010) Astrobiological aspects of Kerala red rain. (In preparation)

# Evidence for biodegradation products in the interstellar medium

#### Kani Rauf and Chandra Wickramasinghe

Cardiff Centre for Astrobiology, Cardiff University, 2 North Road, Cardiff CF10 3DY, UK e-mail: Wickramasinghe@cf.ac.uk

Abstract: The interstellar absorption band centred on 2175 Å that is conventionally attributed to monodisperse graphite spheres of radii 0.02  $\mu m$  is more plausibly explained as arising from biologically derived aromatic molecules. On the basis of panspermia models, interstellar dust includes a substantial fraction of biomaterial in various stages of degradation. We have modeled such an ensemble of degraded biomaterial with laboratory spectroscopy of algae, grass pigments, bituminous coal and anthracite. The average ulrtraviolet absorption profile for these materials is centred at 2175 Å with a full width at half maximum of 250 Å, in precise agreement with the interstellar extinction observations. Mid-infrared spectra also display general concordance with the unidentified interstellar absorption features found in a wide variety of astronomoical sources.

Received 27 September 2009, accepted 18 October 2009, first published online 20 November 2009

Key words: degradation products of biomateria, interstellar dust, panspermia, polycyclic aromatic hydrocarbon, interstellar molecules.

#### Introduction

Some four decades ago. ultraviolet (UV) stellar spectroscopy was born with the deployment of telescopes and instruments flown above the atmosphere. When stellar spectra were first examined at wavelengths shortward of 3000 Å, an interstellar absorption band centred at 2175 Å with a half-width at full maximum of  $\sim 250 \text{ Å}$  was discovered in the spectra of most reddened stars (Stecher 1965: Wickramasinghe 1967). The average interstellar extinction curve showing this feature is shown in Fig. 1, where the observed interstellar extinction curve is decomposed theoretically into three components. Component 1 represents scattering by dielectric grains with sizes and properties resembling bacteria. Component 2 is the extinction due to an absorber producing the mid-UV band, and component 3 represents a population of nanometricsized dielectric particles (Hoyle & Wickramasinghe 1999; Wickramasinghe et al. 2009).

Whilst the mean extinction curve for dust in the solar vicinity is well represented by the uppermost curve in Fig. 1, stars in other regions of the Galaxy and in external galaxies show a modest degree of variability. Such variability is consistent with differing proportions of the components 1, 2 and 3. Fig. 2, from Boulanger *et al.* (1994), shows how individual stars show varying relative amounts of the 2175 Å carrier. Boulanger *et al.* (1994) also discuss the correlation between the strength of the UV absorption peak and the mid-infrared (IR) emission bands that could be interpreted as arising from a common molecular carrier (Hoyle & Wickramasinghe 1989).

The attribution of the 2175 Å extinction bump by Hoyle and Wickramasinghe to small graphite spheres is now widely accepted, with such a component included in most models of interstellar grains (Hoyle & Wickramasinghe 1962, 1969; Mathis 1990; Draine 2003). There are, however, serious problems associated with the graphite model (Wickramasinghe et al. 1992). The requirement of graphite, which has a planar lattice structure, to be in the form of small spheres in interstellar space appears scarcely plausible, as indeed does the requirement that the size dispersion around a central size 0.02 µm be vanishingly small. Alternative molecular explanations of the 2175 Å absorption, first proposed by Hoyle and Wickramasinghe in 1977, involve aromatic organic molecules (Hoyle & Wickramasinghe 1977). In this paper we show that such molecules are most reasonably interpreted as being degradation products of biology.

### Microbial dust and polycyclic aromatic hydrocarbons

Some recent models of interstellar dust have included an abiotic polycyclic aromatic hydrocarbon (PAH) component that, under appropriate circumstances, could produce a  $\lambda = 2175$  Å absorption band (Witt *et al.* 2006). However, for PAHs and other complex organic molecules to form abiotically poses serious problems, in particular with the requirement that compact PAHs are in high ionization states. An alternative model that fits the general context of panspermia is that organic dust and molecules in interstellar space include a substantial component derived from biology itself.

#### K. Rauf and C. Wickramasinghe

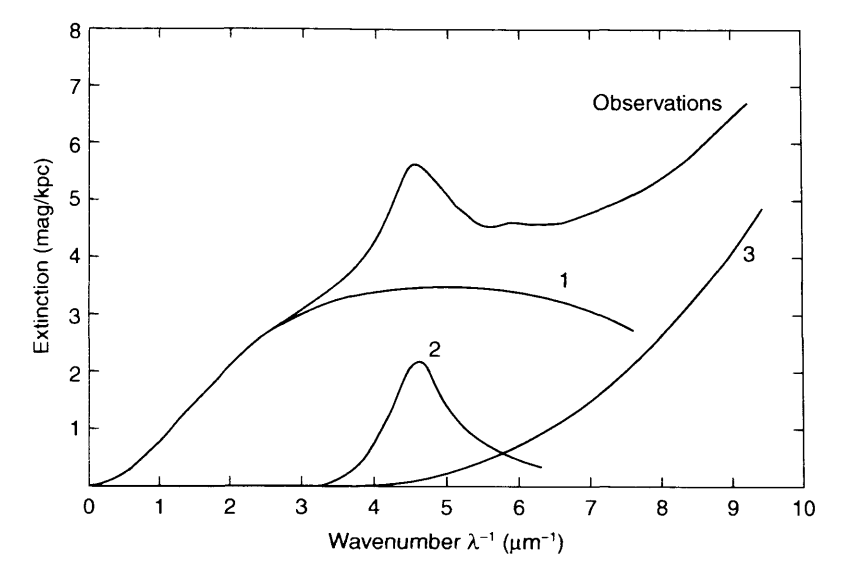


Fig. 1. Interstellar extinction observations from a compilation from Sapar & Kuusik (1978) interpreted as a composite of (1) dielectric grains of radii  $0.3 \, \mu m$ , (2) molecular absorption due to aromatics and (3) dielectric particles of radii  $0.01 \, \mu m$ .

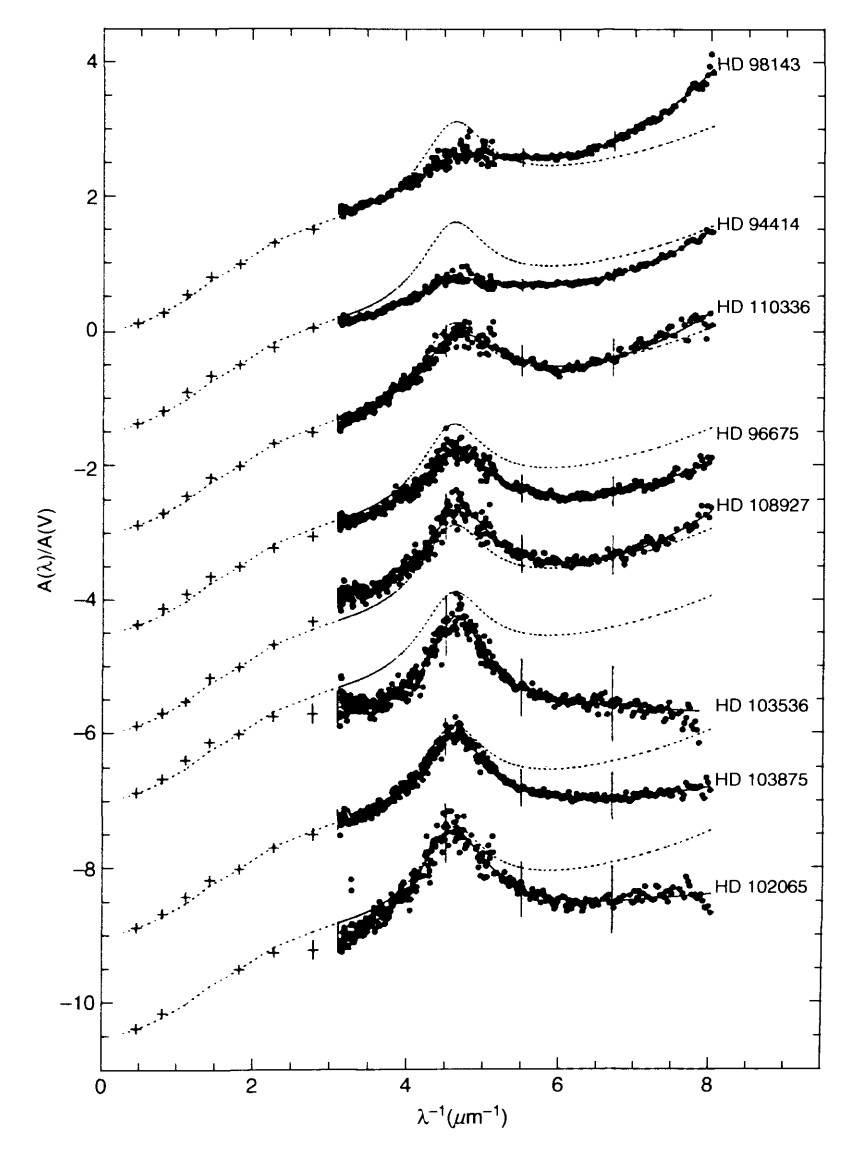


Fig. 2. Normalized interstellar extinction curves for stars in our Galaxy showing varying strengths of the 2175 Å absorption feature adapted from Boulanger *et al.* (1994). Crosses and the dashed curve represent mean interstellar extinction.

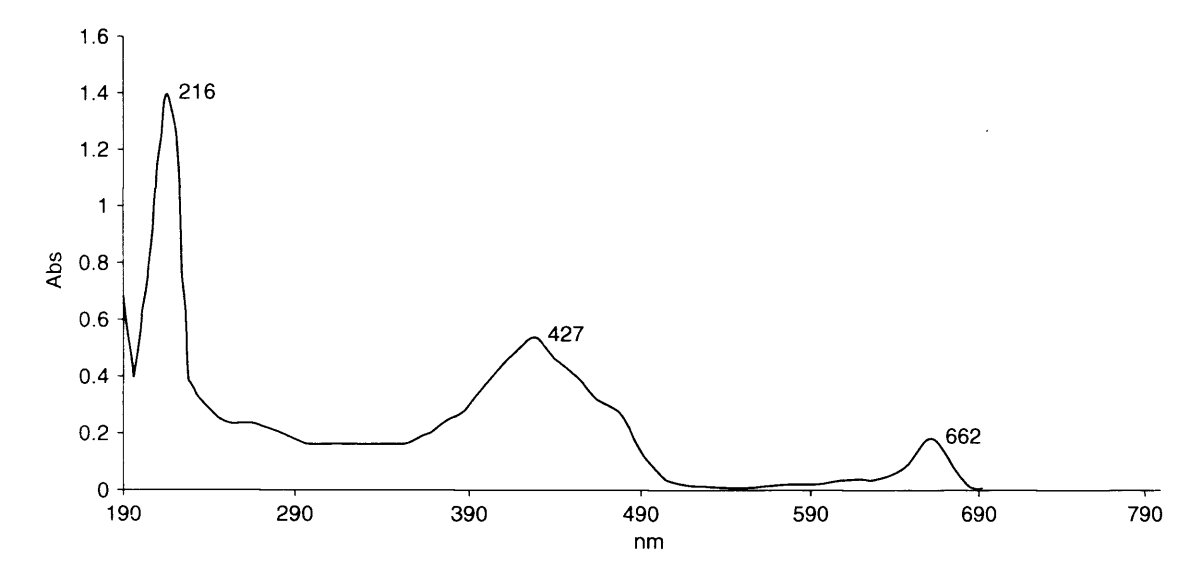


Fig. 3. UV-visible spectrum of algae dissolved in cyclohexane.

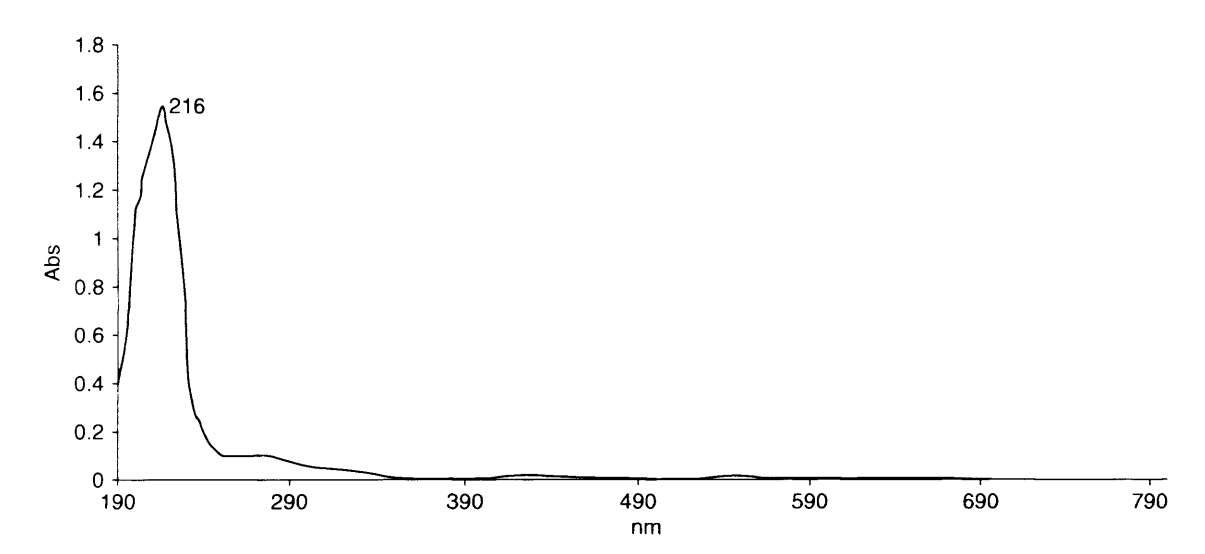


Fig. 4. UV-visible spectrum of grasses dissolved in cyclohexane.

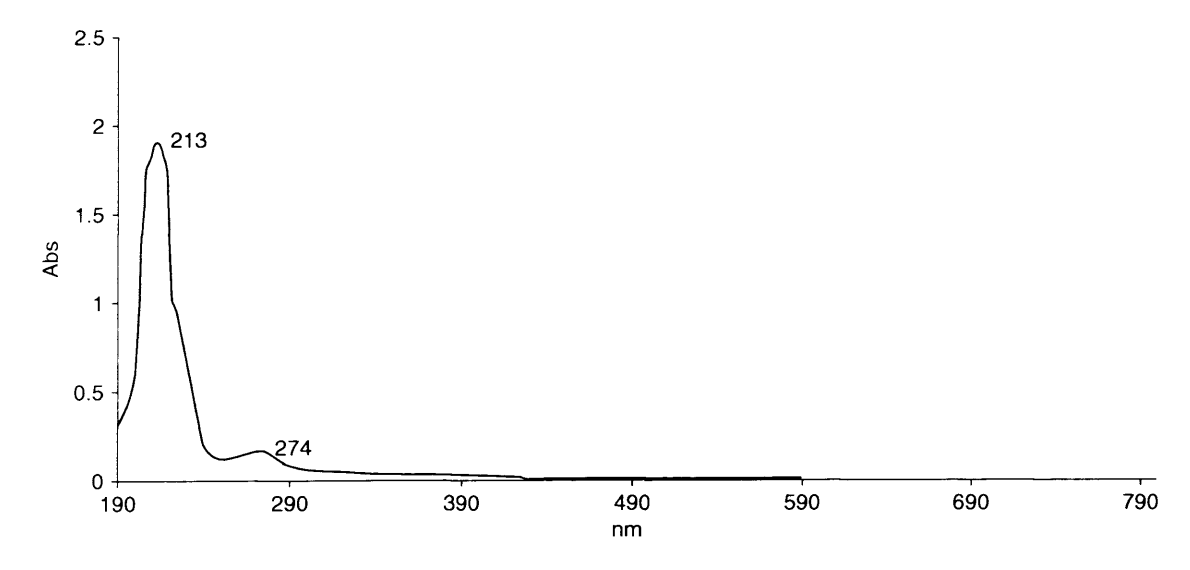


Fig. 5. UV-visible spectrum of anthracite dissolved in cyclohexane.

#### K. Rauf and C. Wickramasinghe

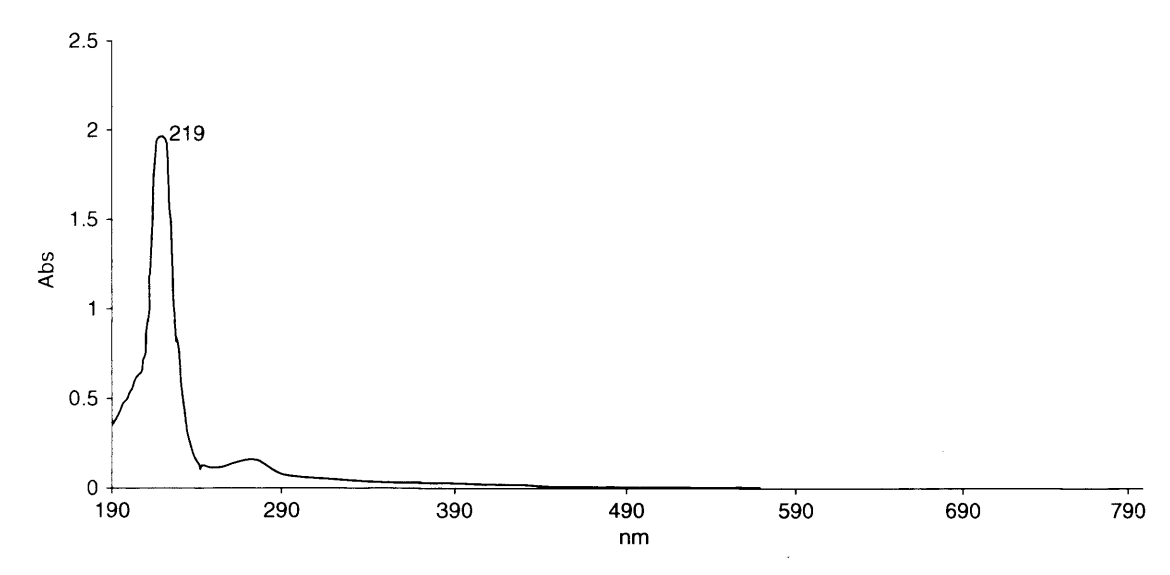


Fig. 6. UV-visible spectrum of semi-anthracite dissolved in cyclohexane.

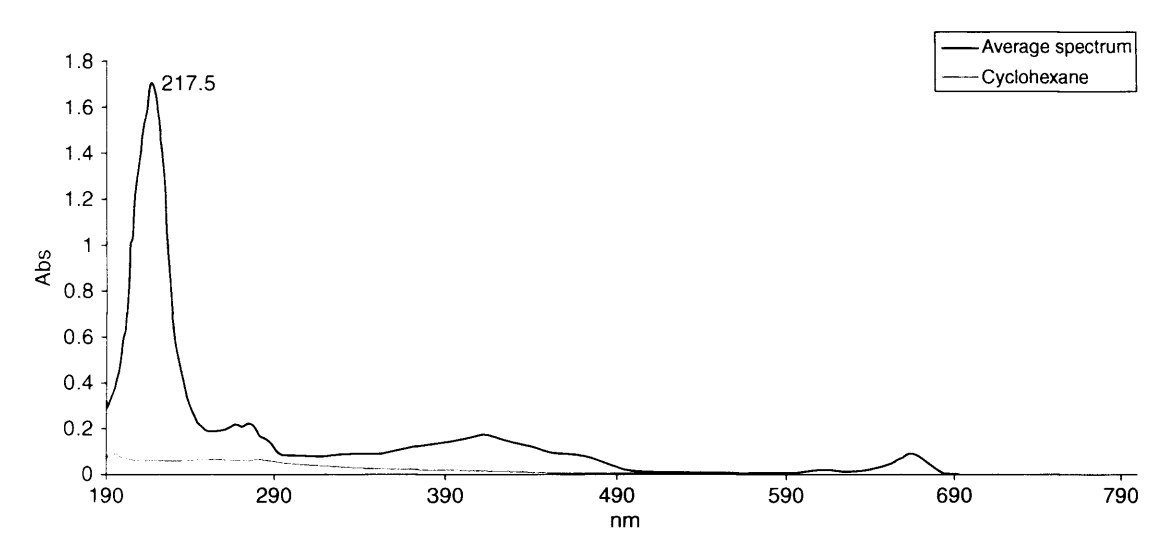


Fig. 7. Average spectrum of a putative interstellar microbiota in various stages of degradation.

According to this point of view, microbial cells replicate in liquid interiors of primordial comets and are distributed widely across the galaxy (Wickramasinghe et al. 2009). Interstellar material would then include the detritus of biology—microbial cells in various stages of degradation and break-up. The degradation of cells in HII regions and in other high radiation environments is of course inevitable. Whilst wholesale destruction, if it occurs, would vitiate a panspermia model, the requirement for panspermia to operate unhindered is that a fraction, less than one part in 10<sup>20</sup>, survives from one amplification site to the next; this condition would seem impossible to violate.

#### Experiments and materials used

Our model thus leads to a component of interstellar dust grains that start off as intact viable cells and end up as coal-like grains. In order to model the effects of sequential degradation we took algal cells and grasses as a starting point, and measured the absorption properties of the following:

- (1) algae and grasses;
- (2) semi-anthracite;
- (3) anthracite.

Samples (2) and (3) represent the last stages in a putative biodegradation sequence.

The sources of the material were as follows:

- Oedogonium sp (a fresh water species of green algae) collected from Roath Park, Cardiff;
- grass from the Santa Cruz island of the Galapagos provisionally identified as *Panicum maximum*;
- both bituminous coal (semi-anthracite) and anthracite were obtained from Geo Supplies Ltd., UK.

We were primarily concerned with the precise placement of a 2175 Å absorption feature in all of these systems, which were dispersed and dissolved in a non-polar solvent. We also

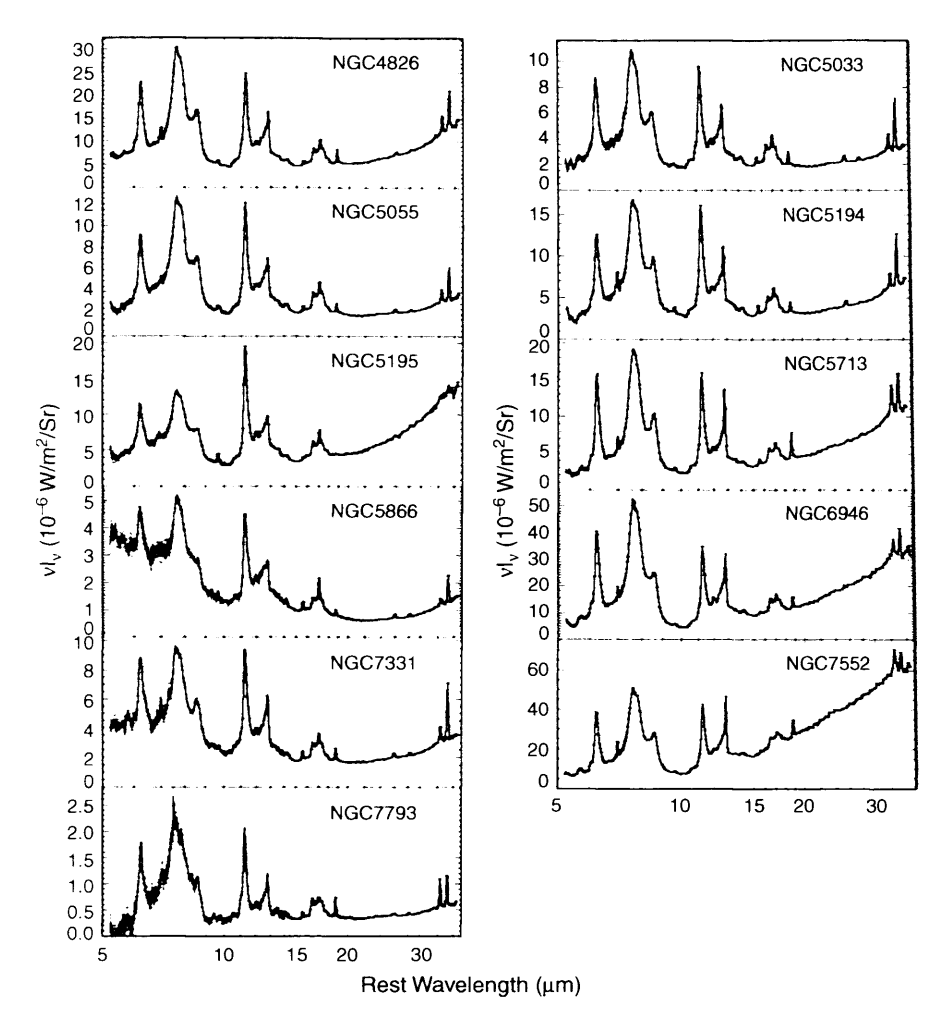


Fig. 8. Recent compilation of Spitzer telescope emission spectra of a variety of galactic sources showing PAH emissions (Smith et al. 2007).

examined mid-IR spectra of the same systems dispersed in KBr discs, with a view to comparing them with the Unidentified IR Bands (UIBs) in interstellar material.

#### Methods of sample mounting and preparation

For UV and visual spectroscopy, the samples were dissolved in cyclohexane – a non-polar solvent. Algae, grasses, semi-anthracite and anthracite (approximately 70 mg in each case) were individually added to cyclohexane (500  $\mu$ l) and dissolved. The use of a non-polar solvent eliminates the effect of wavelength shifts. All samples were agitated for a few minutes and allowed to stand still on the bench for 15 minutes to allow the sedimentation to complete. A clear solution (100  $\mu$ l) was carefully pipetted out from the top and placed in a test tube containing the solvents (3.5 ml). The tube was briefly agitated and transferred into a spectrophotometer (JASCO V-570 UV/visible imaging system (VIS)/near infrared (NIR) spectrophotometer).

For IR spectroscopy, the samples were first subjected to vigorous grinding using an agate pestle until a fine powder was obtained. The sample (0.2 mg) was embedded in KBr (20 mg), and the resulting mixture was transferred into a small blending mill (SPECAmill<sup>TM</sup>, Kent, UK) for further grinding. After 10 minutes, the sample was subjected to

Table 1. Distribution of two astronomical observations (UIBs and proto-planetary nebulae (PPNe)) and major IR absorption bands in laboratory models of terrestrial origin.

UIBs	PPNe	Algae	Grasses	Bituminous coal	Anthracite coal
3.3	3.3	3.3	_	3.3	3.3
_	3.4	3.4	3.4	3.4	3.4
6.2	6.2	6.0	6.1	6.2	6.2
_	6.9	6.9	6.9	6.9	6.9
_	7.2	7.2	7.2	7.2	7.2
7.7	7.7	_	7.6	_	7.7
_	8.0	8.0	8.0	_	_
8.6	8.6	8.6	_	_	_
11.3	11.3	11.3	11.1	11.5	11.3
_	12.2	12.1	12.05	12.3	12.5
_	13.3	_	_	_	13.4

drying under high vacuum for 3–4 hours, after which it was subsequently transferred into the Evacuable Pellet Dies (SPECAC Ltd, Kent, UK) to make the KBr disc. The resulting KBr disc was analysed using a Fourier transform IR (FTIR) spectrometer (JASCO Model FT/IR 660 Plus series).

#### K. Rauf and C. Wickramasinghe

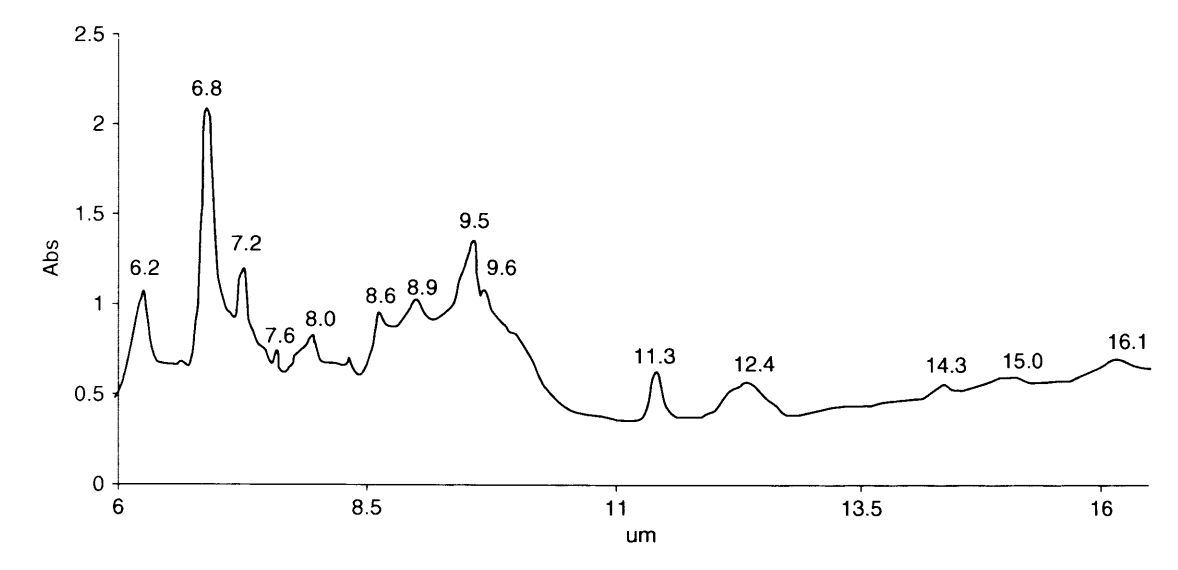


Fig. 9. Spectrum of algae dispersed in KBr disc.

#### Results and conclusion

#### Ultraviolet

Figures 3–6 show UV spectra of algae, grasses, semi-anthracite and anthracite, representing the UV-visual spectra of a putative interstellar microbiota in various stages of degradation. Figure 7 shows the average absorption spectrum of the whole sequence, a normalization being carried out to give an optical depth of 1.7 at the peak. We are particularly impressed with the precise correspondence between the 2175 Å peak in Fig. 7 and the interstellar extinction observations (Figs 1 and 2). The full width at half maximum (FWHM) of 250 Å agrees almost precisely with that of the interstellar absorption feature. Earlier attempts to construct an average UV spectrum from 115 aromatic biomolecules led to a synthetic 2175 Å band that is in general agreement with the curve in Fig. 7 (Wickramasinghe *et al.* 1989).

#### Infrared

Mid-IR spectra for a large number of galactic and extragalactic sources have recently been obtained using the Spitzer Space Telescope (Smith *et al.* 2007). A typical selection of such spectra are shown in Fig. 8.

The detailed spectra are variable from source to source, but strong recurring peaks occur at the wavelengths listed in Table 1. The IR spectra of the materials we studied also show peaks at wavelengths in general correspondence with the astronomical peaks. It has been suggested by many authors that these peaks arise from PAH structures, but objections cited initially by Schlemmer *et al.* (1994) would still appear to be largely valid. Moreover the formation of PAHs abiotically also poses problems. Our laboratory spectra exhibited absorptions at most of the relevant astronomical wavelengths as is seen in Table 1.

Figure 9 shows the IR spectrum of our sample of algae, which is seen to correspond approximately with portions of the spectra displayed in Fig. 8. It should be noted, however,

that whilst Fig. 7 shows emission spectra arising from molecular fragments (detritus of biomaterial?) under various excitation conditions, Fig. 9 shows the absorption spectrum of molecules within biological particles crushed and fused into KBr disks. Traces of water cannot be ruled out in the sample, with a strong 2.9–3  $\mu$ m band (not shown in Fig. 9) that is almost certainly attributed to H<sub>2</sub>O, whilst the elevated complex of features around 10  $\mu$ m is almost certainly assignable to polysaccharides.

In conclusion we note that the interstellar absorption feature at 2175  $\rm \mathring{A}$  in stellar spectra is plausibly attributed to aromatic molecules within biological cells. The unidentified interstellar absorption bands in the IR spectra may also have an origin in the same biomolecular structures (Hoyle & Wickramasinghe 1989).

#### References

Boulanger, R., Prevot, M.L. & Gry, C. (1994). Astron. Astrophys. 284, 956. Draine, B.T. (2003). Ann. Rev. Astron. Astrophys. 41, 241.

Hoyle, F. & Wickramasinghe, N.C. (1962). Mon. Not. Roy. Astron. Soc. 124, 417.

Hoyle, F. & Wickramasinghe, N.C. (1969). Nature 223, 459.

Hoyle, F. & Wickramasinghe, N.C. (1977). Nature 270, 323.

Hoyle, F. & Wickramasinghe, N.C. (1989). ESA SP 290, 67.

Hoyle, F. & Wickramasinghe, N.C. (1999). Astronomical Origins of Life. Kluwer Academic Publishers, Dordrecht.

Mathis, J.S. (1990). Ann. Rev. Astron. Astrophys. 28, 37.

Sapar, A. & Kuusik, I. (1978). Publ. Tartu. Astrophys. Obs. 46, 71.

Schlemmar, S. et al. (1994). Science 265, 1685.

Smith, J.D.T. et al. (2007). Astrophys. J. 656, 770.

Stecher, T.P. (1965). Astrophys. J. 142, 1683.

Wickramasinghe, J.T., Wickramasinghe, N.C. & Napier, W.M. (2009). Comets and the Origin of Life. World Scientific Publ. Co., Singapore.

Wickramasinghe, N.C. (1967). Interstellar Grains. Chapman & Hall, London.

Wickramasinghe, N.C., Hoyle, F. & Al-Jabory, T. (1989). Astrophys. Space Sci. 158, 135.

Wickramasinghe, N.C., Wickramasinghe, A.N. & Hoyle, F. (1992). Astrophys. Space Sci. 196, 167.

Witt, A.N. et al. (2006). Astrophys. J. 636, 303.

# Microstructure and elemental composition of the Tagish Lake meteorite and its astrobiological implications

#### Kani Rauf<sup>1</sup>, Anthony Hann<sup>2</sup> and Chandra Wickramasinghe<sup>1</sup>

<sup>1</sup>Cardiff Centre for Astrobiology, Cardiff University, Cardiff CF10 3DY, UK e-mail: Wickramasinghe@cf.ac.uk; newick@googlemail.com
<sup>2</sup>School of Biosciences, Cardiff University, Cardiff CF10 3US, UK

Abstract: Tagish Lake meteorite, which fell in January 2000 in Canada, has provided a sample of pristine cosmic materials for laboratory studies. It is made up of loosely formed aggregates, making it one of the most friable carbonaceous chondrites. Its complex structure is composed of plaquettes of crystalized minerals, hexagon-shaped metals, chondrules and granules, all of which are embedded in a matrix of fine grains and fibril-like materials. Those components with sizes larger than 250 nm in diameter are affected to varying degrees by hydrothermal reactions, whereas the majority of smaller bodies (<350 nm in diameter) appear unscathed despite severe aqueous alterations on the parent body. A high population of granules (100–300 nm in diameter) consist of a wall (20–40 nm in thickness) and a larger core: the former is rich in organic elements, such as carbon, oxygen and sulfur, and the core contains Ni-Fe-Mg rich silicates. The organic matter has aromatic and aliphatic characteristics, and such evidence suggests that the granules may be the carriers of large organic species with distinct astrobiological implications.

Received 12 October 2009, accepted 15 October 2009, first published online 20 November 2009

Key words: comets, meteorites, origin of life, panspermia.

#### Introduction

The Solar System is rich in biogenic elements. A total of some  $10^{11}$  comets contain  $10^{30}$  g of material, which is largely comprised of carbonaceous material (organics) mineral dust and water-ice. In the early history of the planetary system, water in the form of liquid would be expected to persist for millions of years within cometary interiors (Hoyle & Wickramasinghe 2000: Wickramasinghe *et al.* 2009). During this time microbial cells surviving from earlier episodes of planet-comet formation would be vastly amplified, and would be later re-frozen within cometary bodies. Subsequent sublimation at the surface and dynamical evolution leads to both the expulsion of viable microorganisms near perihelion and the sedimentation and concentration of biological structures within the cometary regolith.

Because carbonaceous chondrites are thought to have parent bodies that are comets, the existence of microbial structures in a fossilized form within such meteorites would not be entirely surprising. According to the theory of panspermia. Earth was seeded with microbial life during the epoch of late heavy bombardment that ended 3.8 billion years ago, the earliest geochemical evidence of life being found at precisely this time. However, an initial injection of life 3.8 billion years ago would not have been the end of the story.

Comets continue to interact with Earth with some 100 tonnes of comet debris being introduced to Earth on a daily basis even at the present time. Ongoing injections of cometary matter would thus be expected to show evidence of life.

Organic compounds as well as putative microbial fossils discovered in carbonaceous meteorites bear testimony to a possible connection between terrestrial life and comets. These ideas are supported by the results obtained from the isotopic analysis of the Murchison meteorite, showing that the organic compounds do not have a terrestrial origin (Martins et al. 2008). Similarly, recent studies by Hoover et al. (2009) that back up a long-standing contention for the presence of microbial fossils in the same meteorite provide further evidence in support of panspermia.

The Tagish Lake meteorite is classified as a type CI2 carbonaceous chondrite (Zolensky 2002). It has been found in other studies to contain organic globules of sub-micrometre to nanometric sizes (Nakamura et al. 2002; Hoover et al. 2003). Nanometric to sub-micrometre sized organic granules as well as filaments and trichomes were interpreted as putative microfossils by Hoover et al. (2003). Similar objects was first reported in meteorite extracts from the 1960s (Claus & Nagy 1961) and have since been reported in several other carbonaceous chondrites (Garvie & Buseck 2006). Initial criticisms that all such structures were modern contaminants

appears to have been ruled out by the work of Hans Pflug (see Hoyle & Wickramasinghe 1982; Wickramasinghe et al. 2009) and Hoover (2009), but their biogenic origin still remains controversial.

Our present work examines the complex microstructure of the Tagish Lake meteorite using both transmission and scanning electron microscopy. In addition, we set out to determine the elemental composition of its contents by X-ray nanoprobe analysis. Our particular interest is concerned with the structural localization of carbon, oxygen and sulfur, the important elements that make up the insoluble organic species localized within granules in the meteorite. Furthermore, we analyse the samples by Fourier Transformer Infrared (FTIR) spectroscopy to confirm the presence of bulk organic compounds in the meteorite.

#### Materials and methods

#### Transmission electron microscopy

The Tagish Lake sample ( $1 \times 2 \text{ mm}^2$  fragment) was embedded in LR White resin (London Resin Co. Ltd) in a gelatine capsule for 24 hours at 55 °C. The resulting polymerized resin block was cut into 90–100 nm thick sections on a Reichert ultracut microtome (Reichert-Jung, Austria) with a Diatom diamond knife. The thin sections were mounted on a pioloform-coated copper grid and examined using a Philips EM 208 transmission electron microscope operated at 80 kV accelerating voltage.

#### Scanning electron microscopy

The  $1 \times 2 \text{ mm}^2$  fragment was attached onto a metal stub with double-sided sticky tape, and coated with a thin layer of gold to protect it from beam irradiation. Ultrastructural examination was conducted in a scanning electron microscope (Philips XL 20 SEM), operated at 10 kV accelerating voltage.

#### X-ray nanoprobe analysis

The ultrathin sections as prepared above were analysed using a transmission electron microscope (Philips CM10), fitted with an X-ray microanalysis detector (EM-400 Detecting Unit, EDAX, UK). The following operating conditions were maintained constantly throughout the analyses: electron beam size (20 nm), condenser aperture (30  $\mu$ m), magnification (30  $\mu$ m) and analysis time (200 cps). The following components of the Tagish Lake meteorite were taken for analysis: mineral chunks, hexagonal bodies, chondrules, granules and the matrix of the parent body. During the analyses, the electron beam was focused onto the materials of interest, and a total of 25 similar objects were randomly taken for measurements. Both qualitative and quantitative analyses of the spectra were performed using the EDAX Genesis software for thin sections.

#### FTIR spectroscopy

The Tagish Lake sample (0.15 mg) was ground into very fine grains using an agate pestle and mixed thoroughly with

potassium bromide (KBr) powder (20 mg). The mixture was transferred into a small blending mill (SPECAmill<sup>TM</sup>, Kent, UK) for further grinding. The sample was subsequently transferred into the Evacuable Pellet Dies (SPECAC Ltd., Kent, UK) under a pressure of 10 tons to make a KBr disc. The resulting KBr disc was analysed using a FTIR spectroscope (JASCO Model FT/IT 660 Plus series).

#### Results

Electron microscopy

The Tagish Lake meteorite is made up of loosely formed aggregates, making it one of the most friable carbonaceous chondrites found on Earth. High resolution transmission and scanning electron microscopy reveals its complex structure (Figs 1-3). The aggregates are composed of plaquettes or chunks of crystallized minerals, hexagonal bodies and chondrules of globular structure with variable sizes, all of which are embedded in a matrix of fine granules and fibril-like inclusions. Imaging analysis of 90-100 nm thick sections cut from a 1×2 mm<sup>2</sup> fragment shows mineral chunks having irregular shapes with sizes ranging from 1 to 10 µm (Figs 1(a) and (b)), many displaying concentric rings (Fig. 1(c)) and layers of crystallized structures (Fig. 1(b)). Chunks of minerals are partially embedded in the matrix of the parent body (Fig. 1(e)). The hexagonal bodies (0.4–2.0 µm in diameter) appear electron black, have no internal structure and are clustered in large groups (Figs 1(d) and (f)), often loosely attached to the granular matrix of mineral-rich carbonates. Many of these bodies have lost their original hexagonal shape to become almost spherical (Figs 2(a) and (c)).

Chondrules with diameters ranging from 3 to 6 µm are either clustered in groups (Fig. 3(a)) or individually attached to the matrix (Figs 3(b) and (c)). However, a large population of them is covered with granules (100-300 nm in diameter) on their surface, making it appear rough and irregular (Figs 3(a)–(c)). Many similar granules also form large clumps in the chondrule-free zones (arrows in Fig. 3(a)). All of these granules show an internal structure consisting of a rim (or wall) with an average thickness of 20-40 nm and a larger core (Figs 2(d) and (e)). While numerous granules have a high electron-dense core, many others also show a hollow interior with their bodies partially embedded into the matrix (Fig. 3(e)). Lateral diffusion of the probably volatile minerals can be seen in many large granules (Fig. 2(f)). The matrix of the parent body appears to be made up of tiny grains with sizes ranging from 5 to 100 nm in diameter and a network of fibril-like materials (Fig. 3(f)), into which are embedded plaquettes of minerals, hexagonal bodies of metal, chondrules and granules of smaller sizes. Chemical biosignatures found in acid-dissolved samples by Pizzarello et al. (2001), and the microstructure analysis of Hoover et al. (2003), support the speculation that the 5-100 nm grains have a biological origin, probably similar to the nanobacteria claimed to be present in the Mars meteorite ALH84001 (McKay et al. 1996). The indication from our work is that the parent body of the Tagish Lake meteorite underwent intense aqueous alterations

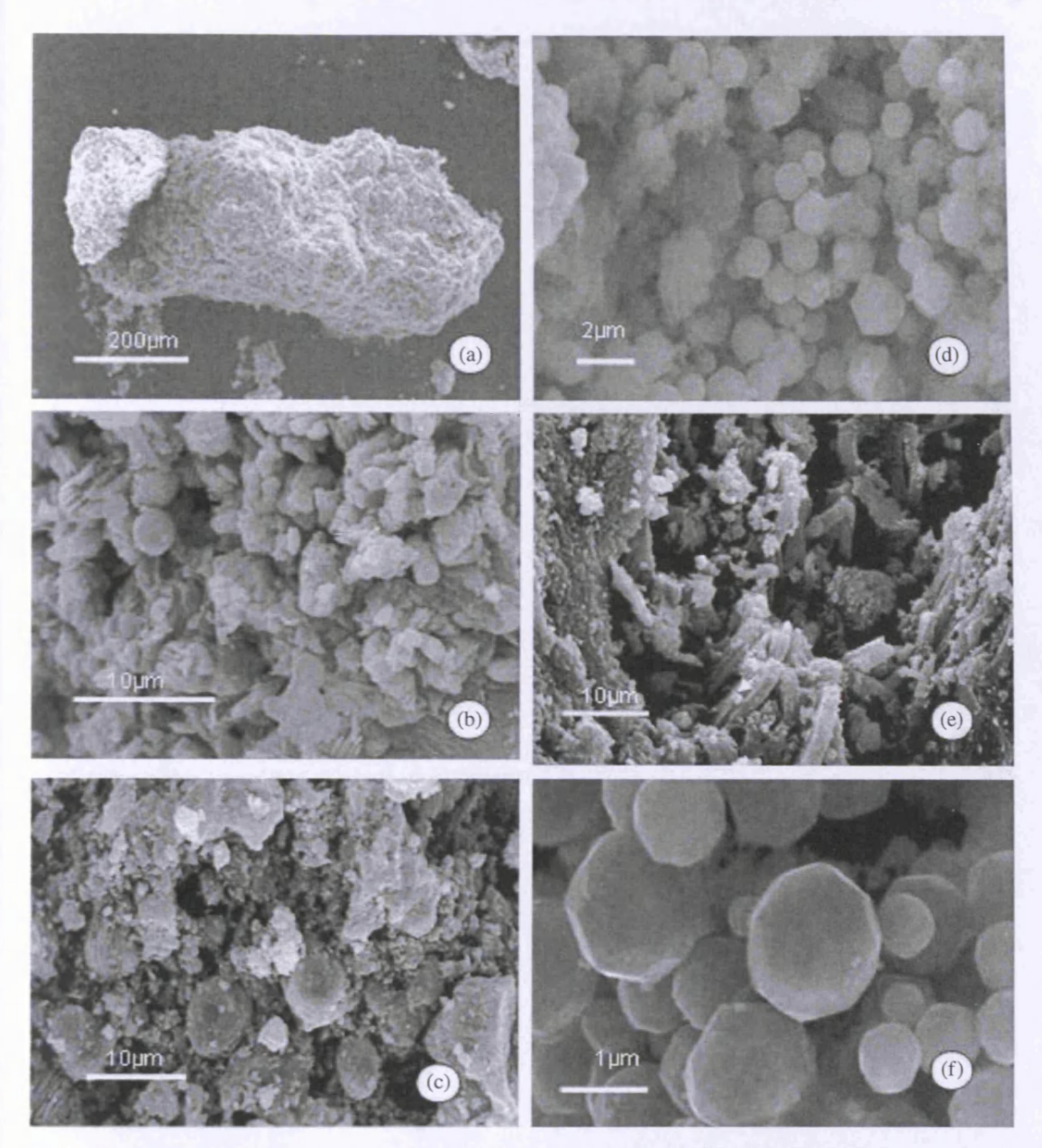


Fig. 1. Scanning electron microscopy images of Tagish Lake. (a) A fragment of Tagish Lake. (b) Plaquettes of crystallized minerals. (c) Chunks of minerals showing a concentric and layered structure. (d) A group of hexagonal bodies, some of which appear almost spherical. (e) Plaquettes of crystallized minerals partially integrated into the matrix. (f) High magnification of hexagonal bodies showing a smooth surface, suggestive of metal alloys.

in places consistent with the presence of liquid water at some stage of its history (Figs 3(d) and (e)).

#### 3.2 X-ray microanalysis

Plaquettes or chunks of crystallized minerals are mainly composed of carbon, oxygen, iron, magnesium and silicon (Fig. 4 and Table 1). Other elements, such as aluminium, sulfur, calcium, chromium and nickel, are also detected, but their relative weight (0.2–1.6 wt%) is much less significant. The hexagonal bodies contain high concentrations of iron, zinc and nickel, but a low amount of carbon, manganese, sulfur and chromium (Fig. 4 and Table 1). Traces (<1 wt%)

of magnesium, silicon, phosphorus, calcium and aluminium are also detected in these bodies.

Chondrules with a smooth surface are generally rich in carbon, oxygen, iron, magnesium and silicon, but significantly low in sulfur, nickel, calcium, aluminium, phosphorus, manganese and zinc (Fig. 4 and Table 1). The chondrules with granules on their surface are comparable to those with a smooth surface in terms of their chemical composition (Fig. 4 and Table 1). These granules have variable sizes (100–300 nm), mostly with an electron-dense core, and contain a high level of carbon, silicon, magnesium, iron, nickel, sulfur, phosphorus, manganese and zinc. Many of them also

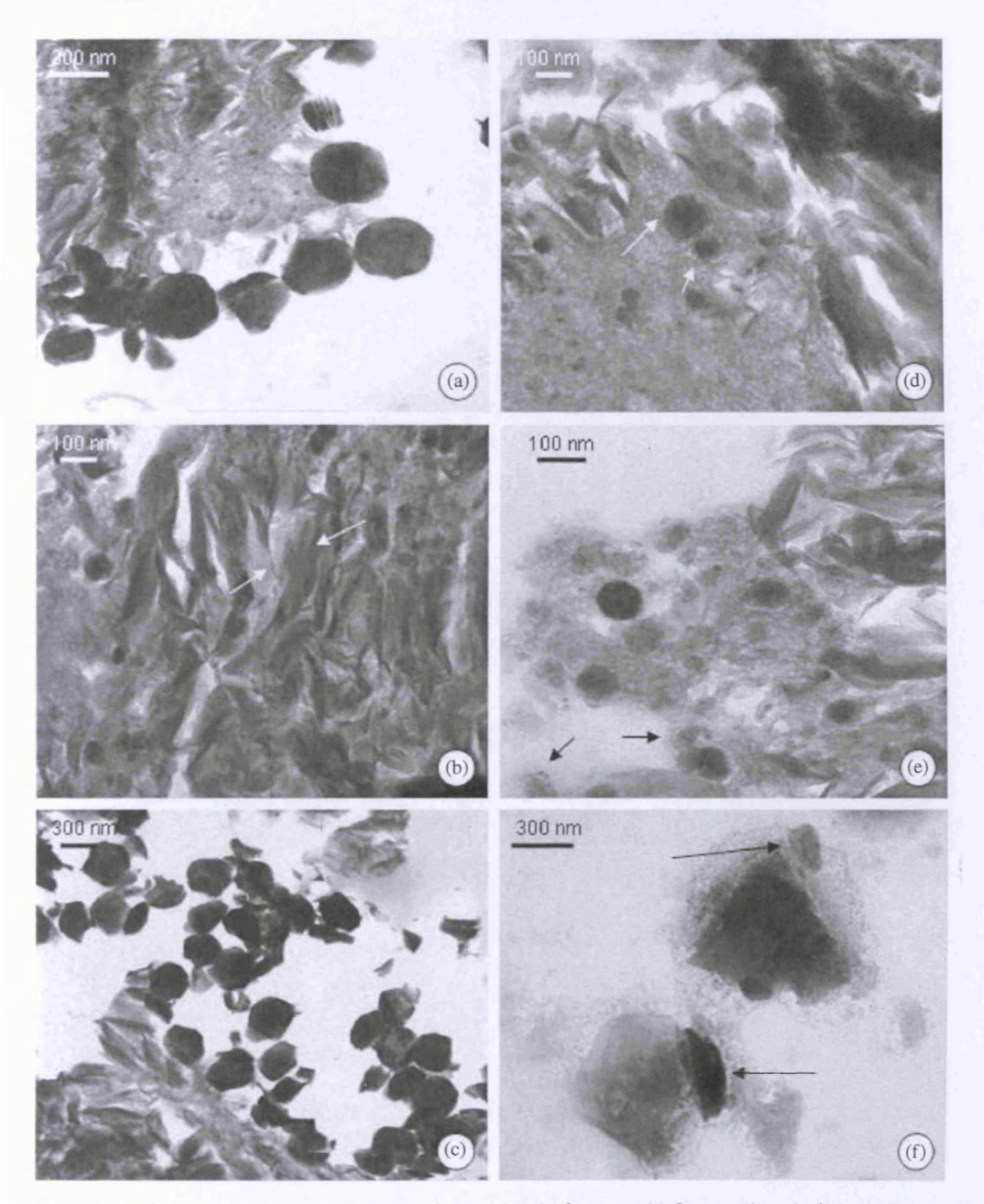


Fig. 2. Transmission electron microscopy images of a Tagish Lake fragment. (a) Cross-section of a fragment showing black hexagonal bodies partially attached to the granular matrix of the parent body. (b) Plaquettes of minerals (arrows) embedded into the matrix of the parent body. (c) A group of metal alloys, some showing their hexagonal structure and many others becoming almost spherical. (d) A partial view of the matrix of the parent body showing granules of variable sizes and fibril-like materials, onto which plaquettes of minerals are attached; the arrows show granules with an electron dense core. (e) Plaquettes of crystallized minerals partially integrated into the altered matrix; the arrows show granules with an electron dense core. (f) Diffusion of minerals as a result of hydrothermal reaction; the arrows show diffused minerals.

form clusters in the chondrule-free regions, and basically have the same chemical composition as those on the chondrules (Fig. 4 and Table 1). A large population of these granules is also integrated into the matrix of the parent body; those with a hollow core show a reduced amount of silicon,

magnesium, nickel and iron, but are rich in carbon and sulfur elements, mostly confined to the wall (Fig. 4 and Table 1). The possibility of microfossils cannot be ruled out from our work, but further research is needed to resolve this important issue.

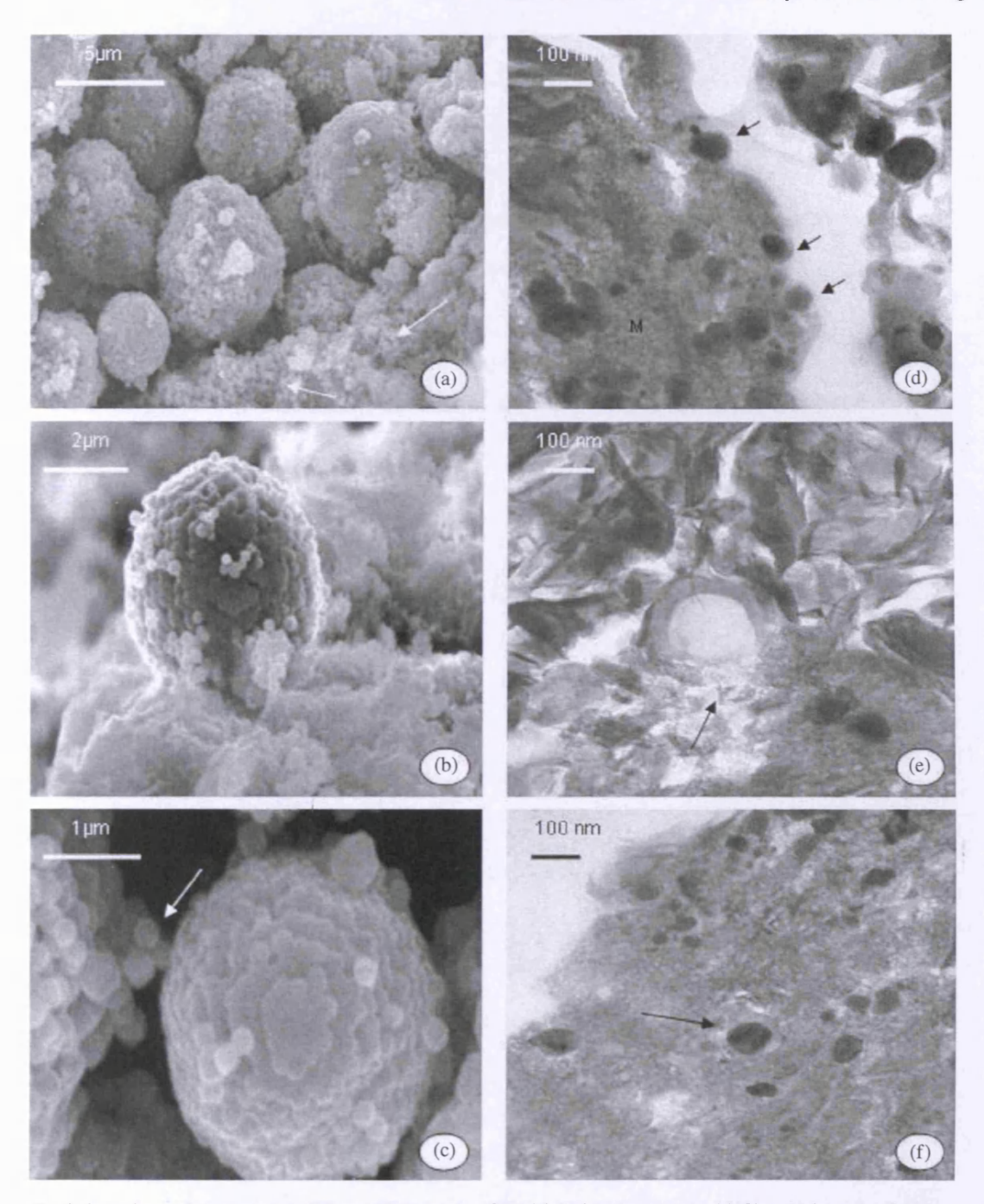


Fig. 3. Scanning and transmission electron micrographs of Tagish Lake components. (a) Chondrules covered with granules; the arrows show granules in the chondrule-free area. (b) A chondrule partially embedded in the parent body. (c) A high-magnification scanning electron micrograph showing a chondrule covered with granules; the arrow shows isolated granules. (d) Granules showing a wall (arrows) and an electron dense core. (e) A hollow chondrule partially embedded in the parent body; the arrow shows leakage of materials into the parent body. (f) The arrow shows a granule in the parent body.

The grains and fibril-like materials that make up the matrix of the Tagish Lake meteorite contain high concentrations of carbon, oxygen and sulfur. A significant amount of iron, silicon, magnesium and nickel is also detected in the matrix, together with traces of calcium, aluminium, manganese, sodium, zinc and chromium (Fig. 4 and Table 1). Again our results are generally consistent with the biological

interpretations offered by Hoover et al. (2003) and Hoover (2009).

#### FTIR spectroscopy

The FTIR spectrum displays five features centred at 6.1, 6.9, 9.8 and  $11.3\,\mu m$  (Fig. 5). The 2.9 feature is indicative of the presence of water. The 9.8  $\mu m$  band is characteristic of

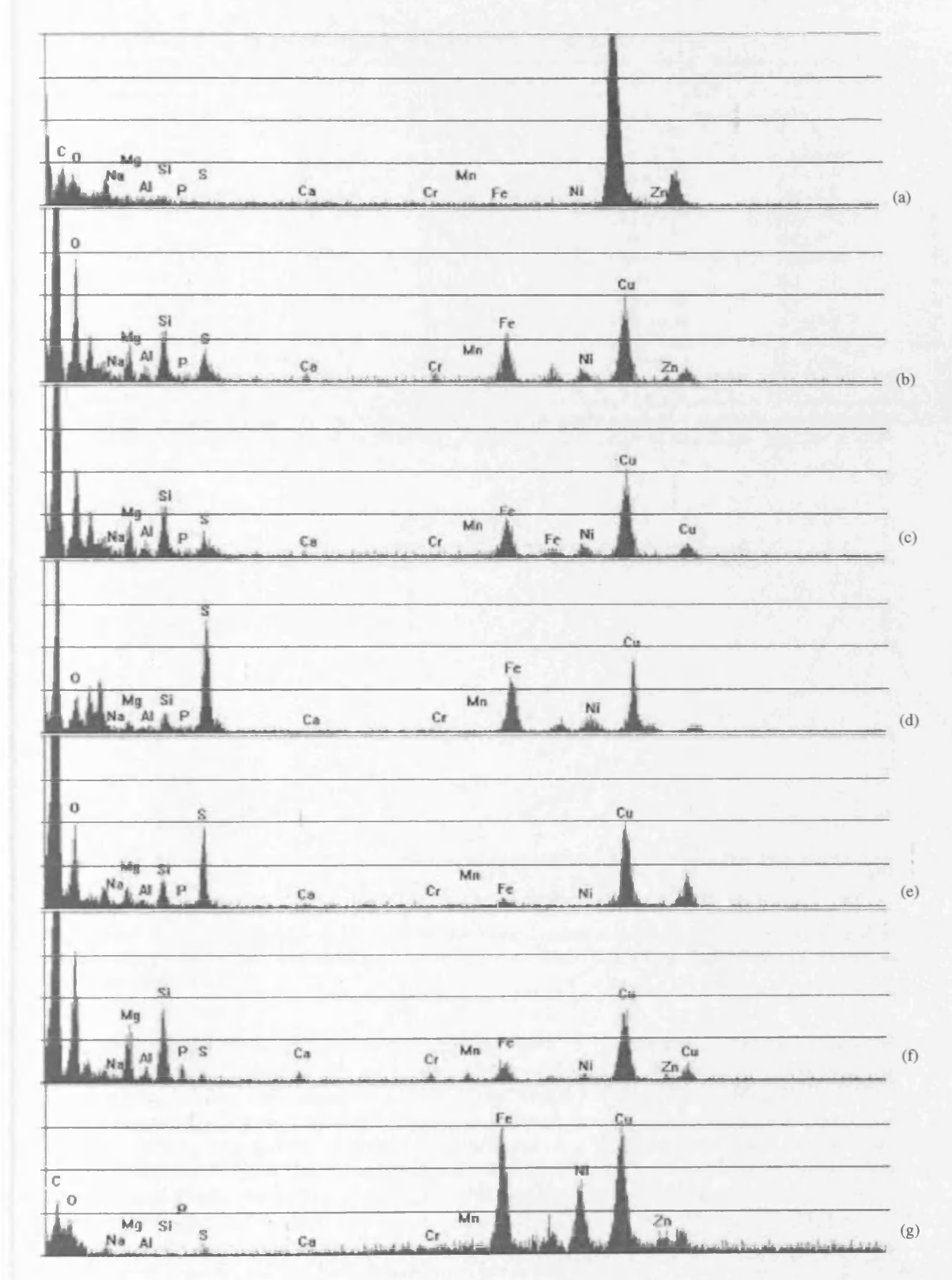


Fig. 4. X-ray spectra of chemical elements in the Tagish Lake meteorite. (a) Background of film-coated copper grid. (b) Matrix of parent body. (c) Mineral chunk. (d) Non-hollow granule. (e) Hollow granule. (f) Chondrule. (g) Hexagonal body.

silicates and shows the highest intensity of absorption. The less intense peaks at 6.1 and  $11.3\,\mu m$  correspond to the aromatic nature of carbon, whereas that at  $6.9\,\mu m$  is related to the aliphatic carbon.

#### Discussion

The Tagish Lake meteorite is composed of minerals loosely intergrown in the granular matrix of a carbonaceous parent

		<del>-</del>	<del>-</del>			
$\mathrm{Fe_2O_3}$	$35.3 \pm 2.8$	$1.0 \pm 0.1$	$4.1 \pm 0.3$	$1.2 \pm 0.06$	$2.1 \pm 0.2$	2
NiO	$18.4 \pm 1.09$	$0.1 \pm 0.04$	$0.6 \pm 0.04$	$0.1 \pm 0.04$	$0.1 \pm 0.05$	0
CuO**	$31.1 \pm 2.2$	$25.1 \pm 1.8$	$29.2 \pm 1.6$	$30.5 \pm 2.1$	$34.9 \pm 2.2$	35
ZnC	$5.2 \pm 0.42$	$0.1 \pm 0.05$	$0.5 \pm 0.04$	$0.2 \pm 0.04$	0.0	0

Values  $\pm$  SD (standard deviations), which were obtained from nanoprobe analysis of randomly selected materials, are measurements. \*\* CuO represents the copper grid used to mount thin sections of the Tagish Lake sample.

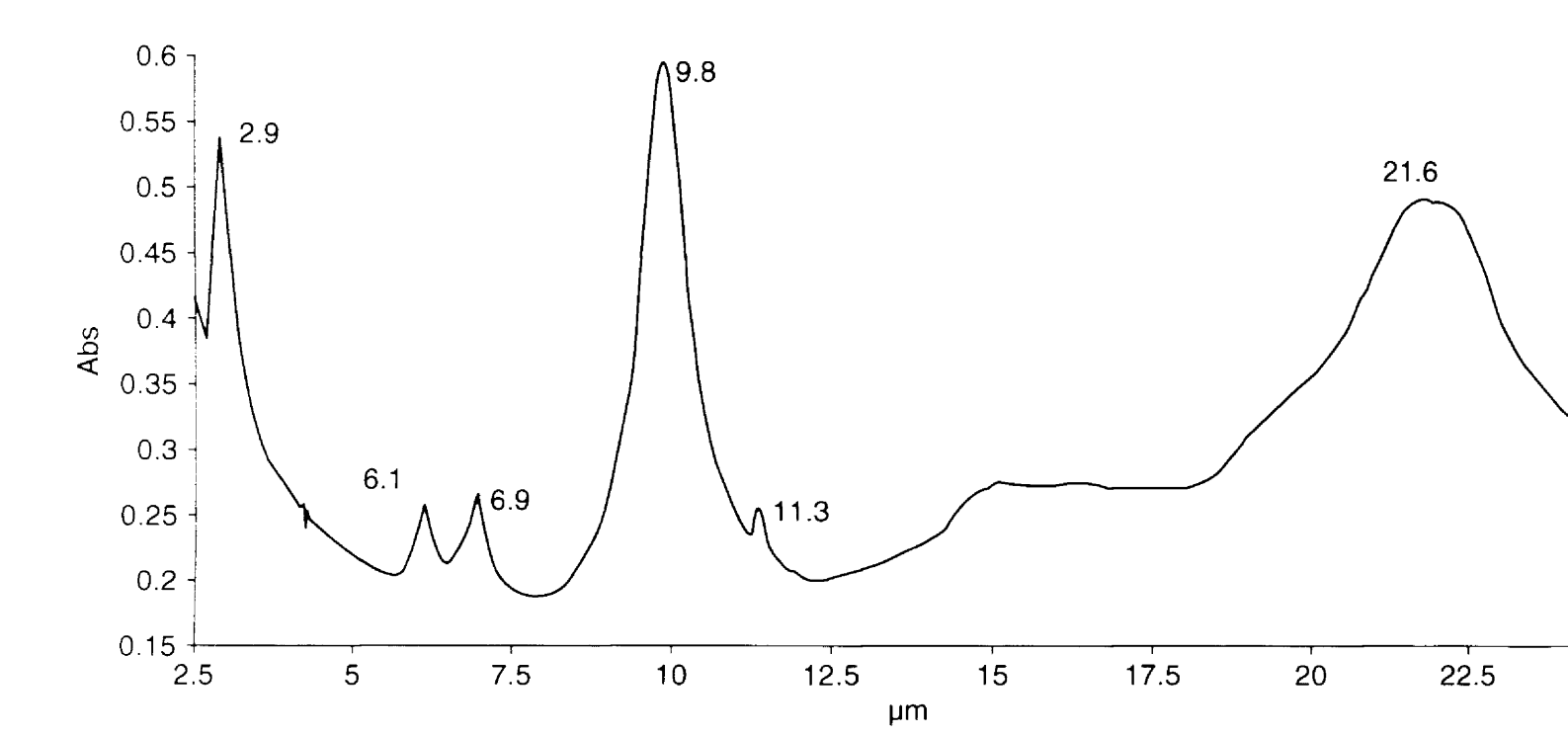


Fig. 5. FTIR spectrum showing the characteristic bands of the aromatic carbon centred at 6.1 and 11.3 μm (Cataldo & A peak at 6.9 μm is attributed to the aliphatic carbon (Papoular *et al.* 1993). The band at 2.9 μm confirms the presence (Al-Mufti 1985).

body. Most of the hexagonal bodies are bound to each other, suggesting that this formation has taken place before the bodies were integrated into the matrix. Many of the hexagonal bodies within the groups have become almost spherical, this evidence indicating that they may have been subjected to grinding collisions in space. Containing high concentrations of iron, zinc and nickel but having no distinguishable internal structure, these bodies are most likely to be metal alloys. The occasional detection in minute quantity of carbon, magnesium, silicon, sulfur, calcium and aluminium is consistent with biological activity and microbial replication in an aqueous medium within the parent body (Wickramasinghe *et al.* 2009).

Chondrules in general appear to have a smooth surface, and are rich in carbonates, iron, silicon and magnesium, but also contain smaller amounts of sulfur, calcium and aluminium. This mineralogy suggests that the chondrules are not

comprised of the same materials as the although both appear similar in size. T feature of the chondrules is the appear of granules on their surface (Fig. 3). A suggested that such granules form by the interstellar grains on larger planetissime the outer regions of the protoplanetary consider this unlikely (McSween 1989). To of organic interstellar grains span a wide metric- to micrometre-sized particles and in the granule layers found in Fig. 3. Mai are also found in clusters in the chondrungesting that the accumulation took place body at some stage.

Although most granules appear intact, structural and chemical alterations in actions they reached Earth. The granules co

an exterior wall and a core. The apparent changes in structure can be seen on the surface and the inside of the granules. A cross-section of the affected granules reveals partial degradation of their wall through which materials appear to leak profusely from the inside into the matrix, eventually leaving the granules with a hollow core. This would be consistent with the dehydration and freeze-drying of a biological culture. Breakdown of the wall and subsequent release of minerals are shown in Fig. 2. These structural characteristics expressed by the affected granules are associated with the matrix of the parent body, and confirm that hydrothermal alteration has occurred, resulting in mass fractionation. Lateral diffusion of the interior materials through the wall, followed by a massive loss of materials, is suggestive of hydrothermal reactions taking place in the parent body. The transformation from the non-hollow to hollow granules gives an indication that the core, which is rich in carbonates and water-bearing minerals, is very susceptible to hydrothermal conditions. The hydrous minerals in the meteorite are similar to terrestrial clay, and are believed to be the products of lowtemperature aqueous alterations of pre-existing anhydrous minerals in asteroids (Llorca 2004). The hydrated mineralogy of Tagish Lake and its richness in carbonaceous matter are reminiscent of the expected characteristics of D-type asteroids, which are situated in the outer part of the Kuiper Belt (Hiroi et al. 2001; Grady et al. 2002). The Tagish Lake meteorite also shows characteristics strikingly similar to the Mars meteorite ALH84001 (McKay et al. 1996).

Mineral chunks, including those with concentric structures, are mainly composed of C-O-Fe-Mg-Si elements; their predominance in Tagish Lake reflects that the chondrite is rich in minerals and metals, probably MgSiO<sub>3</sub>. The formation of concentric rings and layers of crystallized minerals suggests that these materials have been subjected to a cycle of high temperature and rapid cooling processes. Another unique composition of Tagish Lake is that it contains high concentrations of iron-magnesium rich carbonates, but an unusually low amount of high-temperature nebular elements, such as calcium and aluminium, reflecting that these elements are probably altered to form Mg-Fe rich serpentine. These compositional characteristics are also consistent with those of extinct comets including P- and D-type asteroids (Bell *et al.* 1989).

The X-ray nanoprobe analysis of the granules shows that they are rich in carbon, silicon, magnesium, iron and sulfur, and that most of the carbon, oxygen and sulfur is concentrated in the wall, indicating the existence in these granules of insoluble macromolecular organic material with the general formula C<sub>100</sub>H<sub>60</sub>N<sub>7</sub>O<sub>12</sub>S<sub>2</sub> (Hayatsu & Anders 1981). The presence of organic compounds in Tagish Lake is further confirmed by the results obtained from the infrared spectroscopic analysis. The 6.1, 6.9 and 11.3 μm features of the absorption waveband are all linked to organic/biological species. Those at 6.1 and 11.3 μm are characteristic of aromatic carbon (Cataldo & Keheyan 2003), whereas that at 6.9 μm is linked to aliphatic character (Papoular et al. 1993). These features match the emission bands of

several astronomical objects, in particular the unidentified bands and the protoplanetary nebulae spectrum (Hudgins & Allamandola 1997; Rauf & Wickramasinghe 2009; Wickramasinghe et al. 2009).

The present work confirms early observations that a high proportion of carbon in Tagish Lake derives from organic species (Brown et al. 2000) and that the organic material occurs as sub-micrometre, hollow globules (Nakamura et al. 2002; Nakamura et al. 2006). As reported by Pizzarello et al. (2001) and Busemann et al. (2006), over 99 % of total organic carbon makes up the insoluble macromolecular group, and only ~100 parts per million constitutes the soluble compounds. The unusually low concentration of soluble organic compounds may be attributed to low-temperature chemical oxidation as proposed by Cody & Alexander (2005). It is generally accepted that organic matter in meteorites is introduced into the asteroid belt from interstellar space through radial turbulent mixing in the protoplanetary disk (Wooden et al. 2005). However, their assembly into monodisperse particles resembling nanobacteria and micrococi invites an alternative interpretation in terms of biological activity within aqueous niches of a parent body.

Our microscopic and analytical data reveal that materials with sizes larger than 350 nm are vulnerable to solar hydrothermal reactions, whereas the majority of smaller granules appear unscathed despite severe aqueous alterations on the parent body (Fig. 2). These granules (<350 nm in diameter) are rich in carbon, oxygen and sulfur, the important elements that compose the macromolecular organic material, and such evidence suggests that these granules may be the carriers of large organic species. Here, we report the presence of structural and chemical imprints in Tagish Lake, which are reminiscent of the characteristics of P- and D-type asteroids in the outer belt.

#### References

Al-Mufti, S.A.R. (1985). Laboratory studies relating to a bacterial model of interstellar grains, *PhD thesis*, University College Cardiff, UK.

Bell, J.F., Davis, D.R., Hartmann, W.K. & Gaffey, M.J. (1989). In Asteroids II, Univ. Arizona Press, Tucson, Arizona, USA 921-945.

Busemann, H., Young, A.F., Alexander, C.M.O'D., Hoppe, P., Mukhopadhyay, S. & Nittler, L.R. (2006). Science 312, 727.

Cataldo, F. & Keheyan, Y. (2003). Int. J. Astrobiology 2(1), 41–50.

Claus, G. & Nagy, B. (1961). Nature 192, 594.

Brown, P.G. et al. (2000). Science 290, 320.

Cody, G.D. & Alexander, C.M.O'D. (2005). Geochim. Cosmochim. Acta 69, 1085.

Garvie, L.A.J. & Buseck, P.R. (2006). Lunar Planet. Sci. 37, Abstract 1455. Grady, M.M., Verchovsky, A.B., Franchi, I.A., Wright, I.P., & Pillinger, C.T. (2002). Meteoritics & Planet. Sci. 37, 713-735.

Hayatsu, R. & Anders, E. (1981). Top. Curr. Chem. 99, 1-37.

Hiroi, T., Zolensky, M.E. & Pieters, C.M. (2001). Science 293, 2234.

Hoover, R.B. (2009). Proc. SPIE, 7441, doi: 10.1117/12.832643.

Hoover, R.B., Jerman, G., Rozanov, A.Y. & Davies, P.C.W. (2003). *Proc. SPIE* **4859**, 15–31.

Hoyle, F. & Wickramasinghe, N.C. (2000). Astronomical Origins of Life. Kluwer Academic Publishers, Dordrect, The Netherlands.

Hoyle, F. & Wickramasinghe, N.C. (1982). Proofs that Life is Cosmic. Mem Inst Fund Studies, Sri Lanka (http://www.astrobiology.cf.ac.uk/proofs...pdf)

- Hudgins, D.M. and Allamandola, L.J. (1997). J. Phys. Chem. A, 101(19), 3472-3477
- Llorca, J. (2004). Int. Microbiol. 7, 239-248.
- Martins, Z., Botta, O., Fogel, M.L., Sephton, M.A., Glavin, D.P., Watson, J.S., Dworkin, J.P., Schwartz, A.W. & Ehrenfreund, P. (2008). *Earth Planetary Sci.* 270, 130-136.
- McKay, D.S., Gibson Jr., E.K., Thomas-Keprta, K.L., Vali, H., Romanek, C.S., Clemett, S.J., Chillier, X.D.F., Maechling C.R. & Zare R.N. (1996). Science 273, 924–930.
- McSween, H. Jr. (1989). Meteorite and their parent planets. Cambridge University Press, Cambridge, UK.
- Nakamura, K., Messenger, S., Keller, L.P., Clemett, S.J. and Zolensky, M.E. (2006). Science 314, 1439.

- Nakamura, K., Zolensky, M.E., Tomita, S., Nakashima, S. and Tomeoka, K. (2002). *Int. J. Astrobiology* 1, 179.
- Papoular, R., Ellis, K., Guillois, O., Reynaud, C., & Nenner, I. (1993).
  J. Chem. Soc. Farady Trans., 89(13), 2289-2295.
- Pizzarello, S., Huang, Y., Becker, L., Poreda, R.J., Nieman, R.A., Copper, G. and Williams, M. (2001). Science 293, 2234.
- Rauf, K. & Wickramasinghe, C. (2009). Int. J. Astrobiology 8, 1-6.
- Wickramasinghe, J., Wickramasinghe, C. & Napier, W.M. (2009). Comets and the Origin of Life. World Scientific Publishing Co., Singapore.
- Wooden, D.H., Harker, D.E. and Brearley, A.J. (2005). ASP Conf. Ser. 341, 774.
- Zolensky M.E., Nakamura K., Gounelle M., Mikouchi T., Kasama T., Tachikawa O., & Tonui E. (2002). *Meteoritics Planet. Sci.* 37, 737-762.

# Study of putative microfossils in space dust from the stratosphere

### Kani Rauf<sup>1</sup>, Anthony Hann<sup>2</sup>, Max Wallis<sup>1</sup> and Chandra Wickramasinghe<sup>3</sup>

<sup>1</sup>Cardiff Centre for Astrobiology, Cardiff University, Cardiff CF10 3DY, UK <sup>2</sup>School of Biosciences, Cardiff University, Cardiff CF10 3US, UK <sup>3</sup>24 Llwynypia Road, Lisvane, Cardiff CF14 0SY e-mail: ncwick@googlemail.com

Abstract: Interplanetary dust particles (IDPs) were recovered from the stratosphere by a cryosampler flown below a balloon flying at altitudes of 20–41 km. The present study uses high-resolution scanning electron microscopy (SEM) and ultraviolet-visible (UV-Vis) spectrophotometry to examine fresh samples collected at 38–41 km. The SEM observations confirm the presence of 7–32 µm sized clusters of coccoidal (0.4–1.3 µm in diameter) and rod-shaped (0.6–2.5 µm in length) objects as components of the IDP complex. Many single globules (1.6–9.0 µm in diameter) are also observed, some of which exhibit a rough surface with filamentous features of variable lengths. The spectrophotometry of the particles in aggregate reveals a prominent peak centred at 216 nm, which is remarkably similar to that of diatoms and close to the UV astronomical feature of 217.5 nm that has been identified as the spectral characteristic of aromatic hydrocarbons. The evidence presented here suggests that the stratospheric particles are IDPs comprising an assortment of materials among which are included microfossil-like features in variable sizes and forms, such as coccoids, rods and filaments.

Received 25 February 2010, accepted 6 April 2010

Key words: astrobiology, electron microscopy, microfossil-like features, stratospheric air particles, ultraviolet-visible spectrophotometry.

#### Introduction

Tens of tons of interplanetary dust particles are believed to enter Earth's atmosphere daily, most of which vaporize (Rietmeijer 2004). However, small particles with sizes below 40 µm remain largely intact and can be recovered from the stratosphere (Brownlee 1985; Maurette *et al.* 1991). These have become known as interplanetary dust particles (IDPs) and have distinctive compositions (similar to carbonaceous and stony meteorites) and morphologies. The larger and denser particles show signs of melting and would be depleted in volatile components.

The theory of cometary panspermia proposes that grains in space consist of a mixture of complex organics and that their inclusion in many hundred billions of comets leads to the transition from prebiotic matter into primitive bacterial cells (Wickramasinghe 1974; Hoyle & Wickramasinghe 1976; Hoyle & Wickramasinghe 1977; Wickramasinghe et al. 1977). It has been suggested that pre-existing viable bacterial cells derived from interstellar space may have been present in comets in the primitive Solar System. This proposal is based on the following evidence: (1) the extinction properties of interstellar dust match precisely the expected behaviour of freezedried bacteria. (Hoyle & Wickramasinghe 1979); (2) the infrared (IR) absorption by dust in the 2.9–3.9 µm waveband

for the galactic centre source GC-IRS7 has a distinctly bacterial signature (Hoyle *et al.* 1982; Rauf & Wickramasinghe 2010); and (3) the 217.5 nm (2175 Å) ultraviolet (UV) extinction is better explained by an ensemble of biological aromatics than by spherical graphite grains (Hoyle & Wickramasinghe 1991; Rauf & Wickramasinghe 2010). Other astronomical evidence, such as the diffuse IR bands, the complex organic composition of cometary dust and the extended red emission in the red rectangle, also serve to corroborate this proposal. However, the suggestion that the universe is replete with cosmic life is slow to gain wide acceptance.

In the early years of the space age, attempts were made to probe the upper atmosphere for the presence of microorganisms. The National Aeronautics and Space Administration (NASA)-supported balloon program (Bruch 1967) and Soviet rocket experiments (Lysenko 1979) made attempts to show direct evidence for the presence of extraterrestrial microorganisms in the upper atmosphere, but the results were judged to be inconclusive due to the primitive nature of the sterilization procedures. In recent years, improved methodologies have been developed for the identification of microorganisms and stringent protocols applied to almost eliminate contamination from sampling and laboratory processes (Smibert & Kreig 1994; Lopez-Amoros et al. 1995; Lal et al. 1996; Narlikar et al. 1998).

#### K. Rauf et al.

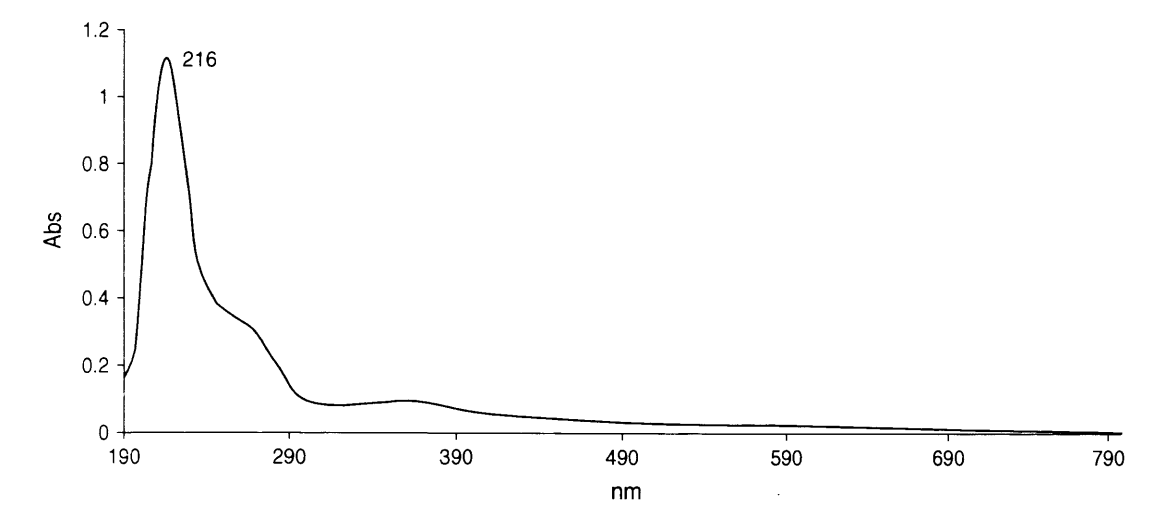


Fig. 1. UV-Vis spectrum of stratospheric air samples showing a prominent feature located at 216 nm and shoulder at 260 nm.

Claims to find viable microorganisms in the upper stratosphere have met with much scepticism. A common criticism concerns terrestrial contamination from sample handling and laboratory processes. In recognition of this criticism, stringent procedures have been used in the present investigation to prevent possible contamination during sample preparation. Experience at Cardiff with scanning electron microscopy (SEM) gives us high confidence in distinguishing contaminant particles from IDP-like cluster particles, while elemental composition identified via the energy dispersive spectroscopy (EDAX) facility adds confirmation (Miyake 2009). The current investigation uses high-resolution environmental SEM and ultraviolet-visible (UV-Vis) spectrophotometry to examine in detail some microdust samples collected at 38–41 km altitude.

#### Materials and methods

#### Collection of stratospheric air samples

The stratospheric air samples were collected at altitudes between 30 and 41 km using a cryosampler attached to a balloon according to the procedure as described in detail by Narlikar et al. (2003). The cryosampler was made of stainless steel and fitted with 16 probes. The whole assembly was electron-beam welded and electron plated. The cryosampler in pre-testing was found to be capable of withstanding temperatures between -246 °C and 140 °C. Before use, the interior components (probes and manifolds) were cleaned with acetone and thoroughly washed in de-mineralized water, steam baked and heated with an IR lamp to 140 °C. During the balloon ascent, the probe inlet was closed via a metallic valve. The inlet was opened and closed via radio signal from ground. The air samples were passed through cellulose acetate filters (0.2 and 0.45 µm pore sizes) as described by Harris et al. (2001). Due to the limited availability of samples, the present study examined only the 0.45 µm pore membranes.

#### UV- Vis spectrophotometry

The filter containing stratospheric particles was placed in a glass vial containing de-mineralized water. The particles were removed by sonication for 15 min and centrifuged at 14 000 rpm for 30 min. The resulting pellet was resuspended in cyclohexane (1 ml) for 30 min, and the mixture centrifuged at 14 000 rpm for 10 min. The clear supernatant was transferred to the UV-Vis spectrophotometer (JASCO V-570 UV/VIS/NIR spectrophotometer) for analysis.

#### Scanning electron microscopy

Millipore filters (0.45  $\mu m$  pore size) carrying the samples were cut into pieces (12 mm  $\times$  12 mm) with a sharp razor blade, attached with sticky carbon tape onto metal stubs and gold coated. This sample preparation was conducted in a clean double-filtered air chamber. The samples were examined using a high-resolution environmental scanning electron microscope (Philips XL 30-ESEM) operated at 25–30 kV. Filter membranes containing no stratospheric samples were used as controls, being mounted and examined by SEM in exactly the same way.

#### Results

UV-Vis spectroscopy of stratospheric air samples

The UV-Vis spectrophotometric analysis of cyclohexanedissolved samples produced a prominent peak centred at 216 nm, close to the 217.5 nm UV astronomical feature (Fig. 1).

Scanning electron microscopy of stratospheric air samples

SEM of the membrane revealed numerous IDPs comprising clusters of submicron grains. These IDPs are sized between 7 and 32  $\mu$ m across (Figs 2 and 3) and comprise coccoidal grains with some embedded rod or tubular objects (Fig. 2(a)). The sizes of the coccoids are between 0.4 and 1.3  $\mu$ m in diameter, whereas the rods vary from 0.6 to 2.5  $\mu$ m in length

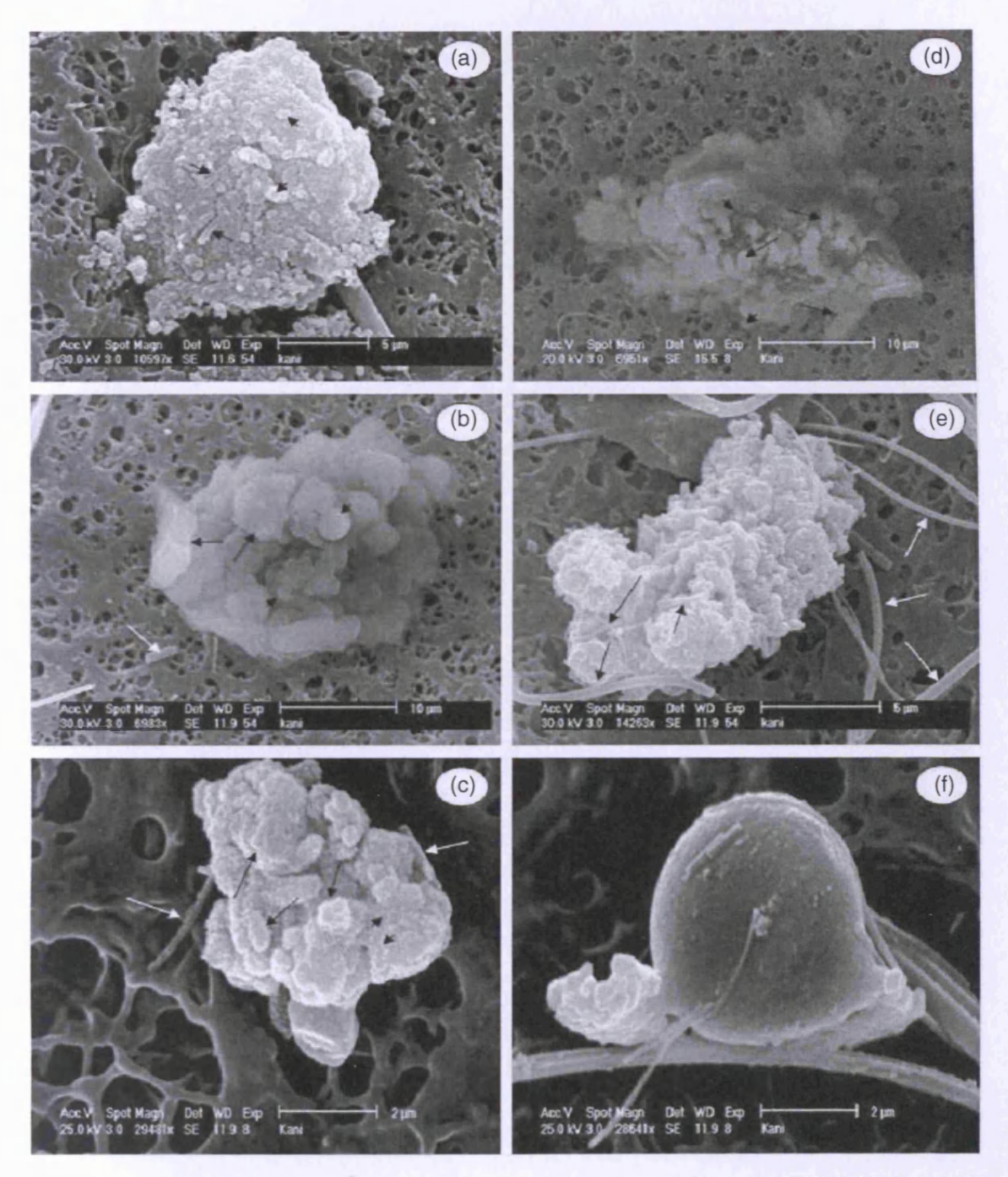


Fig. 2. Scanning electron micrographs of stratospheric air samples on 0.45 μm cellulose acetate filter. (a) A 20 μm sized clump formed by spherical particles (0.4–1.3 μm in diameter) as shown by short black arrows and rod-shaped particles (0.6–2.5 μm in length) as shown by long black arrows. (b) A 28 μm cluster of materials showing variable shapes from spherical (1.5–4.0 μm in diameter) as shown by short black arrows to irregular shaped objects (4.0–9.0 μm across) as shown by long black arrows; a few isolated filamentous or tubular objects can be occasionally seen (white arrow). (c) A 7.0 μm sized clump formed by small aggregates (0.6–3.0 μm) as shown by long black arrows; these aggregates are covered with granules (40–200 nm) as shown by short black arrows; the white arrows show filamentous or tubular objects. (d) A 32 μm clump formed by rod-shaped (2.0–5.0 μm in length) objects as shown by long black arrows and spherical features (0.4–2.0 μm) as shown by short black arrows. (e) A 16 μm clump formed by aggregates (2.5–4.5 μm across); these aggregates are composed of smaller granules (40–300 nm) and filamentous features of variable thickness (90–500 nm) as shown by long black arrows. (f) A 7.0 μm globule with a rough surface structure covered with tiny granules and rod-shaped features. The detached filaments may be contaminants (e), but not the embedded rods.

(Fig. 2(a)). Many globules with sizes ranging from 1.6 to 9  $\mu$ m can also be observed in places (Figs 2(f), 3(a), (d), (e) and (f)), some of which show a surface covered with small granules

(40–300 nm in diameter) (Fig. 2(f)) and filamentous features (Fig. 3(f)). None of the above features were found on the filter membranes used as controls.

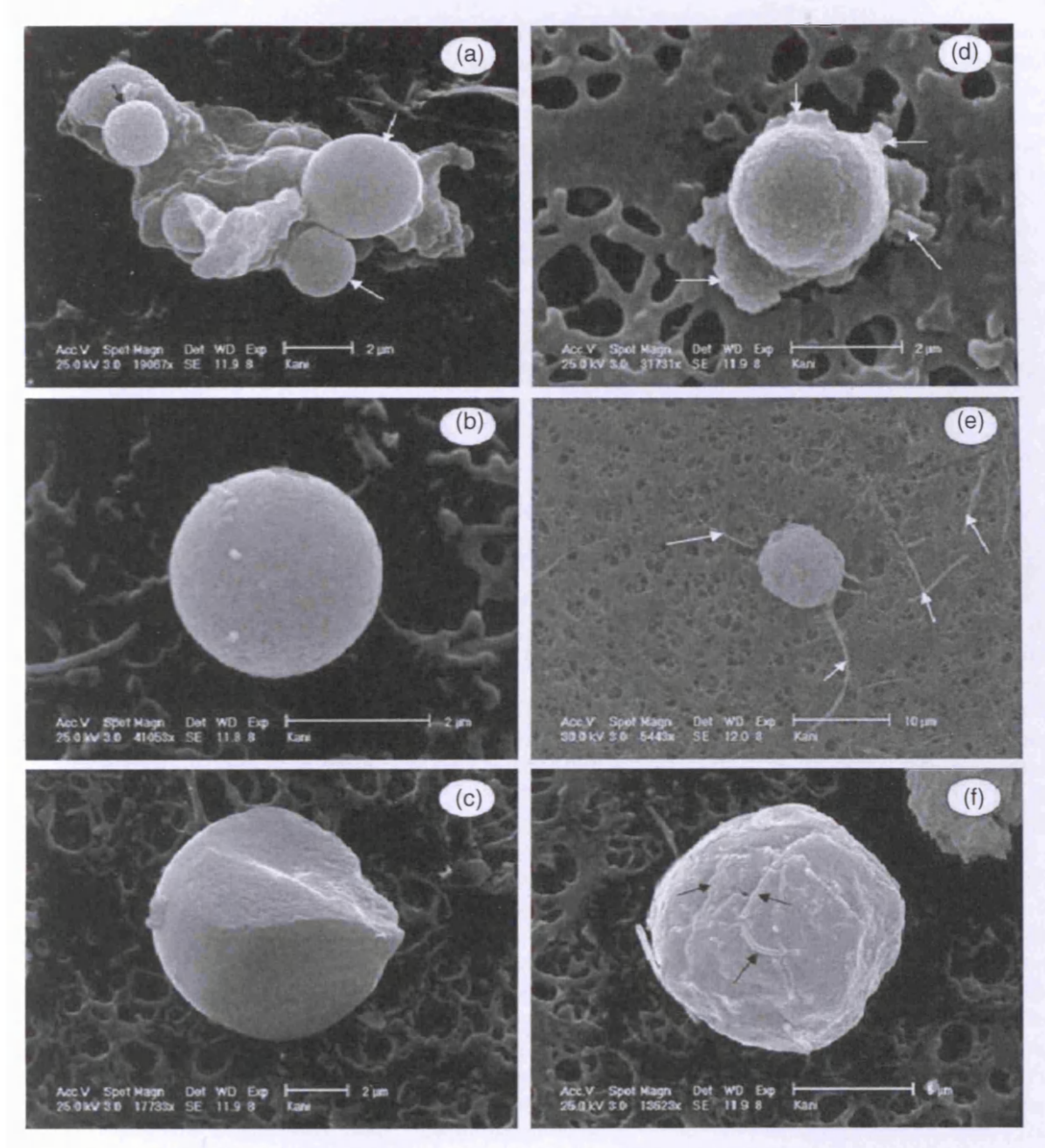


Fig. 3. Scanning electron micrograph of stratospheric air particles. (a) A 12 μm sized clump showing globules of variable sizes arranging from 2.0 to 3.3 μm (as shown by white arrows); some globules showing a rough surface are sized between 1.6 and 1.8 μm (as shown by a black arrow); the white arrows show globules that have a smooth surface. (b) A 3 μm globule showing a rough surface structure. (c) A partially broken 9 μm globule showing its internal structure. (d) A 3 μm globule showing its coccoidal shape and rough surface structure; extracellular materials can be seen attached to the globule as shown by white arrows. (e) A 9 μm sized globule showing extra cellular filaments (arrows). (f) A 11 μm sized globule showing its rough surface covered with filamentous objects of variable lengths (as shown by arrows).

#### Discussion

Many particles of interplanetary origin were successfully collected on airborne plates coated with oil, flown at altitudes of 18–20 km (Hudson *et al.* 1981; McKeegan *et al.* 1985) and at higher altitudes in the stratosphere (Messenger 2000). These particles are largely fragments of comets and asteroids, but some components have been recently identified as predating the Solar System ('pre-solar grains').

The present study using UV-Vis spectrophotometry shows the spectrum of the stratospheric samples containing only a single prominent peak centred at 216 nm, which is close to the 217.5 nm astronomical UV feature (Fig. 1). This astronomical UV feature was first observed in the spectrum of interstellar dust by Stecher (1965). According to Hoyle & Wickramasinghe (1962, 1969) and Stecher & Donn (1965), the 217.5 nm extinction bump is attributable to small spheres of graphite. However, Hoyle & Wickramasinghe (1977)

later proposed the alternative molecular explanation of the 217.5 nm absorption; they argued that the requirement of graphite, which has a planar lattice structure to be in the form of small spheres in interstellar medium (ISM), appears scarcely relevant, and instead suggested the involvement of aromatic organic molecules. The feature has since been found along every galactic line of sight (Bradley et al. 1992; Draine & Malhotra 1993; Mathis 1993; Sandford 1996; Bradley et al. 1999). Many astronomers attribute this feature to very small grains of carbon, possibly of aromatic and/or impure graphite (Draine & Malhotra 1993; Mathis 1993; Sandford 1996). The carrier of the feature was proposed to be chondritic porous IDPs (CP-IDPs), since they have high carbon content (Thomas et al. 1993) and contain inorganic carbon, including hydrogenated aliphatic and aromatic compounds (Clemett et al. 1993; Flynn et al. 1999; Brownlee et al. 2000).

Several laboratory models proposed for the carrier of the 217.5 nm feature are dehydrogenated and hydrogenated amorphous carbons, coals and polycyclic aromatic hydrocarbons (PAHs). However, none of these single compounds is generally accepted as the perfect model (Li & Greenberg 2003). It has been argued that the huge variation ( $\pm 12\%$ ) with line of sight in the width and extinction bands is indicative of a large chemical dispersion in the Galaxy (Fitzpatick & Massa 2007). It has been suggested that the interstellar grain population also includes a substantial amount of ultra-small grains with PAH composition (Muthumariappan et al. 2008). Since PAHs have strong absorptions in the wide region (2000–2500 nm), the expected carrier of the 217.5 nm feature could be a mixture of PAHs, and the observed variation in the width of the feature may be attributed to differences in the PAH mixture (Muthumariappan et al. 2008). These observations seem to imply that in addition to the 217.5 nm extinction carrier, other dust components also exist in the ISM. including a population of amorphous silicate dust, aromatic hydrocarbons. PAH molecules and aliphatic hydrocarbons. Attempts to construct an average UV spectrum from 115 aromatic biomolecules also led to a synthetic 217.5 nm band (Wickramasinghe et al. 1989). Chen et al. (2008) have reported that buckyonions exhibit a peak close to the 217.5 nm extinction feature, but a mixture of silicate-graphite-PAHbuckyonions produces a feature that shows an almost perfect fit with the interstellar bump centred at 217.5 nm. Recently, Rauf & Wickramasinghe (2010) have demonstrated that an ensemble of bio-degraded materials produced a feature centred precisely at 217.5 nm. Based on the early observations as mentioned above, the feature (216 nm) of the stratospheric air particles centred near 217.5 nm is likely to be organic in nature and interplanetary in origin.

The present study using a high-resolution environmental scanning electron microscope reveals the presence of 7–32  $\mu$ m sized clusters of ovoids (0.4–1.3  $\mu$ m in diameter) intermixed with elongated features (0.6–2.5  $\mu$ m in length) (Fig. 2(a)). Other materials that were also found include globules (1.6–9  $\mu$ m in diameter), some of which appear to have a granular surface structure (Figs 2(d) and (f)). Some of these globules display structural characteristics of bacteria, such as

coccoids showing an apparent cell division with extracellular materials (Fig. 3(d)) and flagella (Fig. 3(e)). The ovoid features as shown in Fig. 2(a) appear similar in size and shape to nanobacteria found in travertine and limestone (Folk 1993) and in Pleistocene ground water (McBride et al. 1994). The above features may possibly be regarded as products of terrestrial contamination from sample handling and laboratory processing. However, none of these were observed on the membranes used as controls, thus suggesting an endogenous origin. The discovery of macrosized clusters of coccoids by the present study confirms the observations made by Harris et al. (2001) and Wainwright et al. (2003, 2004a). Furthermore, the long filamentous features as shown in Figs 2(e) and 3(e) appear similar in structural characteristics to microfossils that have been found embedded in some carbonaceous meteorites, such as Orgueil and Murchison (Hoover 2009). Miyake (2009) and Miyake et al. (2009) ascribed these clusters to aggregates of IDPs rich in carbon and found that the rods are siliceous, suggesting that they are fragments of diatoms. Both diatoms and bacteria display an absorbance feature near 220 nm (2200 Å), similar to the observed UV spectral properties of interstellar grains, thus supporting the concept of a cosmic microbiological system in which these microorganisms might exist on comets (Hoover et al. 1999).

Although the present data obtained from the morphological and UV spectral analyses of stratospheric particles suggest that materials of biological origin are likely to be present in the samples, it may be argued that not all of the observed particles are of the same nature. The ovoid and elongated features could be the products of partial dissolution of the carbonate which is abundant in CP-IDPs, and have been reported to be similar to bacterially induced carbonate precipitation (Buczynsik & Chefetz 1991; McKay et al. 1996). A study made by Wainwright et al. (2004a) using secondary ion mass spectrometry (SIMS) has demonstrated that several clusters of bacteria-like particles found in the same stratospheric air samples are not biological, and thus pointed out that the SEM-based observation in itself cannot be used as evidence for the presence of bacteria in the stratosphere.

The early claim (Imshenetsky et al. 1978) to have detected and isolated a wide range of common bacteria and fungi via rocket probes to heights of 48-77 km is beset with contamination objections. The recent studies using cryosamplers attached to balloons flying at altitudes of 20-41 km have largely overcome that problem (Harris et al. 2001; Narlikar et al. 2003; Wainwright et al. 2004b). The microorganisms recovered from the stratosphere include bacteria-like particles (Harris et al. 2001; Narlikar et al. 2003; Wainwright et al. 2004b), two bacteria (B. simplex and S. pasteuri) and one fungus (Engvodontium album) (Wainwright et al. 2003), P. Stutzeri (Narlikar et al. 2003) and species of Penicillium and two bacteria (B. luciferensis and B. sphaericus (Griffin 2004). While most microorganisms appear unlikely to survive under harsh stratospheric conditions with low temperature and strong UV radiation, some microorganisms utilize protective strategies, such as clumping, forming thick cell walls, carbonizing outer layers and embedding in carbonaceous

dust (Narlikar et al. 2003; Wainwright et al. 2006). Furthermore, microorganisms can survive quite extreme conditions of temperature, pressure and even radiation (Hoyle & Wickramasinghe 2000). Secker et al. (1994) have shown that a carbonaceous coating of a few microns thickness of bacterial cells provides a protective shield against radiation. Microorganisms, such as spore-forming Bacilli (B. Simplex, Sarcina lutea) (Whisler 1940) and clump-forming bacteria (B. Subtilis and Staphylococcus aureus) (Horneck 1998; Darling 2001), are relatively resistant to radiation. The pigmented microbes in the mesosphere discovered by Imshenetsky (1946) led him to propose that UV resistance is given by protective pigments (melanins and carotinoids) and suggests natural selection for these pigments.

Terrestrial dust particles are generally confined to the troposphere below 12-17 km. because the stratosphere lacks large-scale turbulence, being highly stratified. However, lofting mechanisms may exist (Wainwright et al. 2006) e.g. blue lightening strikes (Pasko et al. 2002) and gravitophotophoresis (Rohatschek 1996). The powerful volcanic eruption of Mt Pinatubo in the Philippines of 15 June, 1991 was reported to eject materials up to 32 km (Grant et al. 1994). Imshenetsky et al. (1978) claimed that microorganisms were registered in a great number in the mesosphere during dust storms as compared to the absence of strong winds, but this is consistent with contaminants collected in flight through the troposphere. Terminal speeds for settling through the atmosphere are higher for larger sizes (and mean density). Moreover, lofting mechanisms are likely to discriminate in favour of smaller sizes, yet our recovered IDP-like particles show no statistical weighting to μm sizes. The >10 μm clusters we found, with relatively few smaller than this, imply there is no stochastic mechanism kicking a spectrum of sizes

The absence of a plausible explanation for lofting our  $7{\text -}32~\mu m$  clusters through the stratosphere to 40 km altitude adds weight to our identifying these materials as IDPs, and particularly carbonaceous IDPs (Miyake 2009). Although the detection in the samples of microfossil-like materials, such as coccoids, rods and filaments, suggests a biological origin, and the UV spectral data is consistent with this biological identification, more substantive evidence is needed to confirm this identification.

#### References

Bradley, J.P., Humecki, H.J. & Germani, M.S. (1992). Ap. J. 394, 643–651.
Bradley, J.P., Keller, L.P., Snow, T.P., Hanner, M.S., Flynn, G.J., Gezo, J.C., Clemett, S.J., Brownlee, D.E. & Bowey, J.E. (1999). Science 285(5434), 1716–1718.

Brownlee, D.E. (1985). Science 13, 147.

Brownlee, D.E., Joswiak, D.J., Bradley, J.P., Gezo, J.C. & Hill, H.G.M. (2000). *Lunar Planet. Sci.* XXXI, 1921–1922.

Bruch. C.W. (1967). Microbes in the upper atmosphere and beyond. In *Proc. Airborne Microbes, Society for General Microbiology Symposium*,
17. pp. 345–373. ed. Gregory, P.H. & Monteith, J.L. Cambridge University Press, Cambridge.

Buczynsik. C. & Chafetz, H.S. (1991). J. Sediment. Res. 61(2), 226-233.

Chen, J., Li, M., Li, A. & Wang, Y. (2008) On buckyonions as a carrier of the 2175 A interstellar extinction feature. In *Proc. Organic Matter in Space IAU Symposium No. 251*, pp. 71–72.

Clemett, S., Maechling, C., Zare, R., Swan, P. & Walker, R. (1993). *Science* **262**(5134), 721–725.

Darling, D. (2001). Life Everywhere. Basic Books, New York.

Draine, B.T. & Malhotra, S. (1993). Astrophys. J. 414, 632.

Fitzpatrick, E.L. & Massa, D. (2007). Ap. J. 663, 320-341.

Flynn, G.J., Keller, L.P., Jacobsen, C., Wirick, S. & Miller, M.A. (1999). Organic carbon in interplanetary dust particles. In *Proc. Bioastronomy* 99: A New Era in Bioastronomy, 6th Bioastronomy Meeting. Kohala Coast, Hawaii-E34.

Folk, R.L. (1993). J. Sediment. Res. 63(5), 990-999.

Grant, W.B. et al. (1994). J. Geophys. Res. 99(D4), 8197-8211.

Griffin, D.W. (2004). Aerobiologia 20, 135-140.

Harris, M.J., Wickramasinghe, N.C., Lloyd, D., Narlikar, J.V., Rajaratnam, P., Turner, M.P., Al-Mufti, S., Wallis, M.K. & Hoyle, F. (2001). Proc. SPIE 4495, 192-198.

Hoover, R.B. (2009). Proc. SPIE 7441, 1-19.

Hoover, R.B., Hoyle, F., Wickramasinghe, N.C., Hoover, M.J. & Al-Mufti, S. (1999). Astrophys Space Sci. 268, 197.

Horneck, G. (1998). Adv. Space Res. 22(3), 317-326.

Hoyle, F. & Wickramasinghe, N.C. (1962). Mon. Not. Roy. Astron. Soc. 124(5), 417–433.

Hoyle, F. & Wickramasinghe, N.C. (1969). Nature 223(5205), 459-462.

Hoyle, F. & Wickramasinghe, N.C. (1976). Nature 264, 45.

Hoyle, F. & Wickramasinghe, N.C. (1977). Nature 270, 323.

Hoyle, F & Wickramasinghe, N.C (1979). Astrophys. Space Sci. 66, 77–90.

Hoyle, F. & Wickramasinghe, N.C. (1991). The Theory of Cosmic Grains, p. 307. Kluwer Academic Press, Dordrecht.

Hoyle, F. & Wickramasinghe, N.C. (2000). Astronomical Origins of Life. Kluwer Academic Publishers, Dordrect.

Hoyle, F., Wickramasinghe, N.C. & Al-Mufti, S. (1982). Astrophys. Space Sci. 86(2), 341–344.

Hudson, B., Flynn, G.J., Fraundorf, P., Hohenberg, C.M. & Shirck, J. (1981). Science 211, 383-386.

Imshenetsky, A.A. (1946). Mikrobiologiya 15, 422.

Imshenetsky, A.A., Lysenko, S.V. & Kazakov, G.A. (1978). Appl. Environ. Microbiol. 35, 1-5.

Lal. S., Archarya, Y.B., Patra, P.K., Rajaratnam, P., Subbarya, B.H. & Venkataramani, S. (1996). Ind. J. Radio Space Phys. 25, 1-7.

Li, A. & Greenberg, J.M. (2003). Solid State Astrochem 120, 37-84.

Lopez-Amoros, R., Mason, D.J. & Lloyd, D. (1995). J. Microbiol. Meth. 22, 165.

Lysenko, S.V. (1979). Mikrobiologiia 48, 1066-1074 (in Russian).

Mathis, J.S. (1993). Rep. Prog. Phys. 56, 605-652.

Maurette, M., Olinger, C., Michel-Levy, C., Kurat, G., Pourchet, M., Braudstatter, M. & Bourot-Denise, M. (1991). *Nature* 351, 44–47.

McBride, E.F., Picard, M.D. & Folk, R.L. (1994). J. Sediment. Res. 64(3a), 535-540.

McKay, D.S., Gibson Jr., E.K., Thomas-Keprta, K.L., Vali, H., Romanek, S., Clemett, S.J., Chillier, X.D.F., Maechling, C.R. & Zare, R.N. (1996). Science 273(5277), 924–930.

McKeegan, K.D., Walker, R.M. & Zinner, E. (1985). Geochem. Cosmochem. Acta 49, 1971–1987.

Messenger, S. (2000). Nature 404, 968-971.

Miyake, N. (2009). Laboratory studies of stratospheric dust – relevance to the theory of panspermia, *PhD Thesis*, Cardiff University.

Miyake, M., Wallis, M.K. & Wickramasinghe, N.C. (2009). Discovery in space Micro-dust: Siliceous fragments supporting the diatom hypothesis. *EPSC abstract*, vol. 4, EPSC2009-468.

Muthumariappan, C., Maheswar, G., Eswaraiah, C. & Pandey, A.K. (2008). A study of 2175<sup>3</sup>A absorption feature with TAUVEX: An Indo-Israeli UV mission. *Organic Matter in Space, Proc. IAU Symposium No. 251*.

Narlikar, J.V., Ramadurai, S., Bhargava, P., Damle, S.V., Wickramasinghe, N.C., Lloyd, D., Hoyle, F. & Wallis, D.H. (1998).

Proc. SPIE Conf. on Instruments, Methods and Mission for Astrobiology 3441, 301.

Narlikar, J.V. et al. (2003). Astrophys. Space Sci. 285(2), 555-562.

Pasko, V.P., Stanley, M.A., Mathews, J.D., Inan, U.S. & Wood, T.G. (2002). Nature 416, 152-154.

Rauf, K. & Wickramasingh C. (2010). Int. J. Astrobiol. 9(1), 29-34.

Rietmeijer, F.J.M. (2004). Adv. Space Res. 33(9), 1475-1480.

Rohatschek, H. (1996). J. Aerosol. Sci. 27, 467-475.

Sandford, S.A. (1996). Meteoritics Planet. Sci. 31, 44.

Secker, J., Wesson, P.S. & Lepock, J.R. (1994). Astrophys. Space Sci. 329, 1.

Smibert, R.M. & Kreis, N.R. (1994). Methods for General and Molecular Bacteriology. In ed. Gerherdt, P., Murray, R.G.E., Wood, W.R. & Kreig, N.R. Am. Soc. Microbiol., 603.

Stecher T.P. (1965). Astrophys. J. 142, 1683.

Stecher, T.P. & Donn, B. (1965). Ap. J. 142, 1681.

Thomas, K.L., Blanford, G.E., Keller, L.P., Klock, W. & McKay, D.S. (1993). Geochim. Cosmochim. Acta 57, 1551-1566.

Wainwright, M., Alharbi, S. & Wickramasinghe, N.C. (2006). Int. J. Astrobiol. 5(1), 13-15.

Wainwright, M., Weber, P.K., Smith, J.B., Hutcheon, I.D., Klyce, B., Wickramasinghe, N.C., Narlikar, J.V. & Rajaratnam, P. (2004a). Aerobiologia 20, 237-240.

Wainwright, M., Wickramasinghe, N.C., Narlikar, J.V. & Rajaratnam, P. (2003). FEMS Microbiol. Lett. 218, 161-165.

Wainwright, M., Wickramasinghe, N.C., Narlikar, J.V., Rajaratnam, P. & Perkins, J. (2004b). *Int. J. Astrobiol.* 3(1), 13–15.

Whisler, B.A. (1940). Iowa State Coll. J. Sci. 14, 215-231.

Wickramasinghe, N.C. (1974). Nature 252, 462.

Wickramasinghe, N.C., Brooks, J. & Shaw, G. (1977). Nature 269, 674.

Wickramasinghe, N.C., Hoyle, F. & Al-Jubory, T. (1989). Astrophys. Space Sci. 158, 135–140.

## Microstructural investigation of the Carancas meteorite

## Kani Rauf<sup>1</sup>, Anthony Hann<sup>2</sup>, Chandra Wickramasinghe<sup>3</sup> and Barry E. DiGregorio<sup>1</sup>

<sup>1</sup>Cardiff Centre for Astrobiology, Cardiff University, Cardiff CF10 3DY, UK e-mail: kanidawan@ yahoo.com

<sup>2</sup>School of Biosciences, Cardiff University, Cardiff CF10 3US, UK

Abstract: Particles in the Carancas meteorite were examined by electron microscopy (transmission electron microscopy/scanning electron microscopy), energy dispersive analysis of X-rays (EDAX) and Fourier Transform Infrared spectroscopy. Scanning electron microscopical observations reveal that the particles of variable sizes have a stony appearance. Many of these particles show fractures in places, thus confirming an ealier observation that the meteorite was subjected to a high-velocity impact. The outer rim of many aggregates displays a mud crack-like texture. At high magifications, this texture shows ovoid and elongated features, which appear similar to microfossils found in other meteorites.

As revealed by both scanning and transmission electron microscopy, some particles show three clearly marked zones, distinguishable by their differences in electron density and texture: a light zone, a dark zone and an intermediate zone. The EDAX analysis of these particles shows that the light zone is composed of silicates rich in Fe, Ni and S (the elements of troilite and pentlandite). The dark zone contains high concentrations of Mg and Si (the major elements of high-temperature minerals, such as forsterite, Mg2SiO<sub>4</sub> and enstatite, MgSiO<sub>3</sub>) intermixed with carbonates and traces of Al, Ca and Na. The intermediate zone also contains high-temperature minerals and Fe-Ni rich silicates.

The Carancas meteorite produces an infrared waveband showing prominent features of some carbonate species, amorphous and crystalline silicates, and olivine groups. Hydrated silicates and hydroxyl groups are less abundant, as shown by the presence of small humps between 2.5 and  $8.0 \, \mu m$ .

The abundance of high-temperature minerals and iron-rich metal confirms an earlier observation that the meteorite is an ordinary H4/5 chondrite. Some particles in the Carancas meteorite are found to have structural and chemical characteristics similar to those of the 81P/Wild 2 comet.

Received 10 August 2010, accepted 7 October 2010

Key words: 81P/Wild 2 comet, Carancas meteorite, energy dispersive analysis of X-rays, Fourier Transform Infrared spectroscopy, H4/5 chondrite, scanning electron microscopy, transmission electron microscopy.

#### Introduction

The Carancas meteorite fell on 15 September 2007 approximately 10 km south of Desanguadoro, near Lake Titicaca. Peru. The impact excavated a crater having an overall diameter of 13.5 m, a 7.5 m central hole, 1 m high ejecta rim and a shallow (0.6 m deep) groundwater pond (del Prado et al. 2008). The estimated timing of the fall was recorded at approximately 11:45 AM (local time) (16:45 UT) (Macedo & Macharé 2007), but later claimed to be 11:40 AM (16:40:14.1 UT) (Tancredi et al. 2009). The meteorite was thought to travel from east to west, and the angle at which the meteorite entered the atmosphere was estimated to be between 45 and 60 degrees from the horizontal (Tancredi et al. 2009). According to the initial report (Macedo & Macharé 2007), the locals claimed that a luminous object was seen about 1 km

from the Earth's surface before a strong explosion lasting 15 minutes was heard. The fireball consisted of a head with strong bright light and a white smoky tail. The locals also reported that immediately after the explosion, a massive cloud of dust was seen followed by a 'sulphurous' smell from the site and groundwater evaporation. Neither explosion nor 'rained down' debris was reported to take place in the sky, suggesting that the meteorite remained intact on entering the atmosphere. According to the media reports, many local witnesses became ill and several of them had to be hospitalized after they came into contact with the glowing rocks (Tancredi et al. 2009). The symptoms of the illness have been reported to include headache, dermal injuries, dizziness, nausea and vomiting. Arsenic vapour from the contaminated water in the crater was thought to be responsible for the outbreak of the sickness.

<sup>&</sup>lt;sup>3</sup>24 Llwynypia Road, Lisvane, Cardiff CF14 0SY, UK

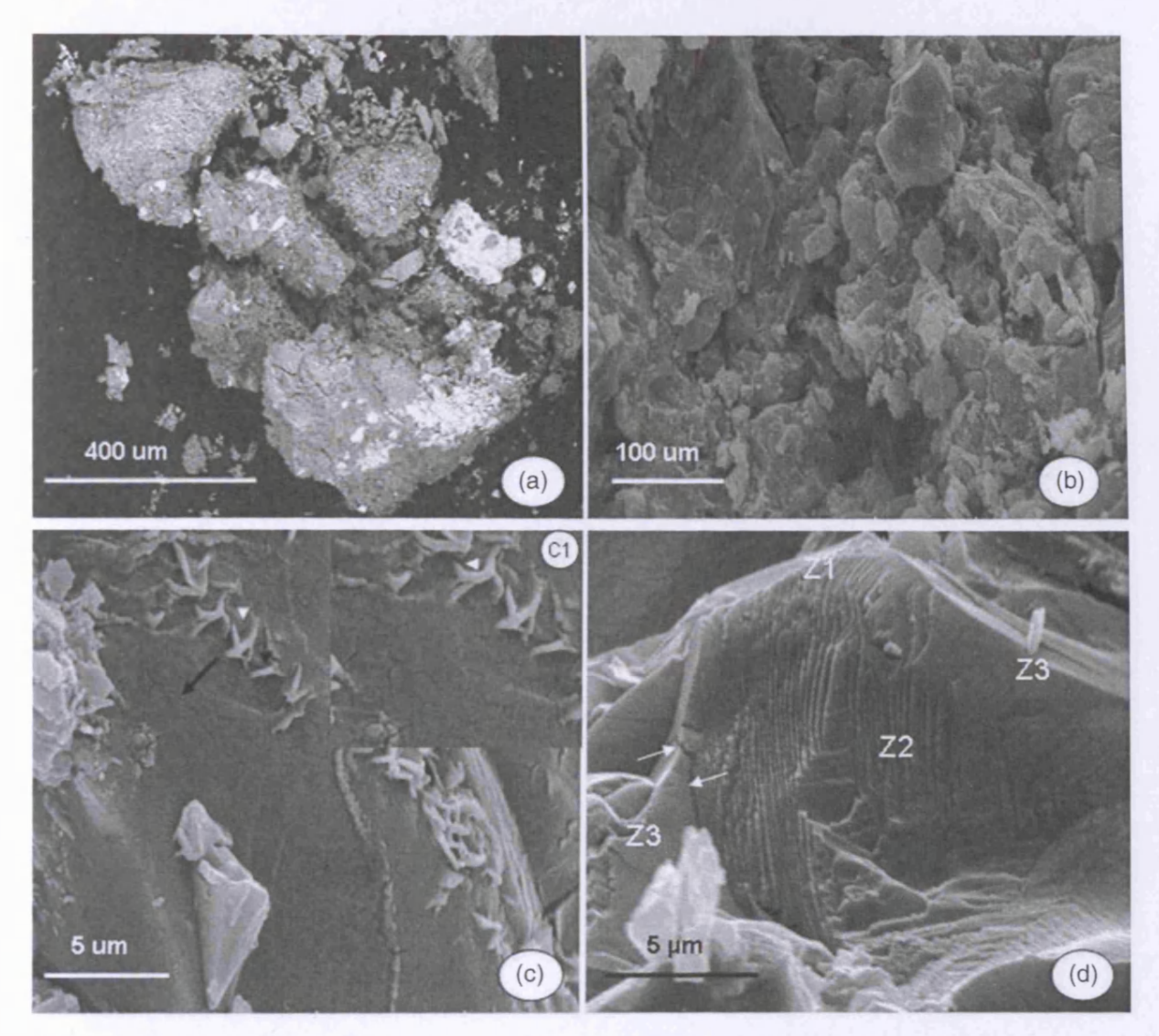


Fig. 1. Scanning electron micrographs of the Carancas meteorite. (a) Carancas particles. (b) A general view of the central region of the particle showing minerals in various forms and sizes. (c) A partial view of the peripheral region of the particle showing a mud crack-like texture; streaks of fusion crusts on the surface (arrow head); the inset (C1) shows an enlarged picture of the mud crack-like structure. (d) Aparticle showing three clearly delineated regions: a light zone (Z1) shows a layered structure; a darker zone (Z2) at the centre displays a pronounced radiating texture; an intermediate zone (Z3) is distinguishable by its smooth surface structure where cracks can be seen as shown by the arrows.

The mineralogical analysis of the fragments indicate that the meteorite is a chondrite composed of fine-grained materials with light grey coloration, rich in iron particles, pyroxene, olivine and kamacite (Macedo & Macharé 2007; Tancredi et al. 2009). Other minerals, such as forsterite, enstatite and troilite, have also been detected in the fragments (del Prado et al. 2008). The Carancas meteorite has been proposed to be an ordinary H4/5 chondrite (del Prado et al. 2008; Tancredi et al. 2008, 2009). The meteorite was found to survive the atmosphere entry without major fragmentation (Le Pichon et al. 2008). The trajectory of its fall has recently been reviewed by Tancredi et al. (2009); they have suggested that the crater was formed as a result of a hypervelocity impact. Earlier reports have presented several transmitted light optical images of the fragments (Macedo & Macharé 2007;

Harris et al. 2008; Tancredi et al. 2009). However, so far there has been little information on the microstructural characteristics and elemental composition of the particles that formed the Carancas fragments.

#### Materials and methods

Collection and preparation of Carancas samples for analysis
The samples were donated by Dr. Barry E. DiGregorio to Prof.
Wickramasinghe at the Cardiff Centre for Astrobiology.
They were collected from the surrounding creater soil and transferred into sterile bags, which were then immediately sealed before being transported to UK laboratories for analysis. Handling and subsequent processing of the samples were conducted in a double air-filtered chamber. The Carancas

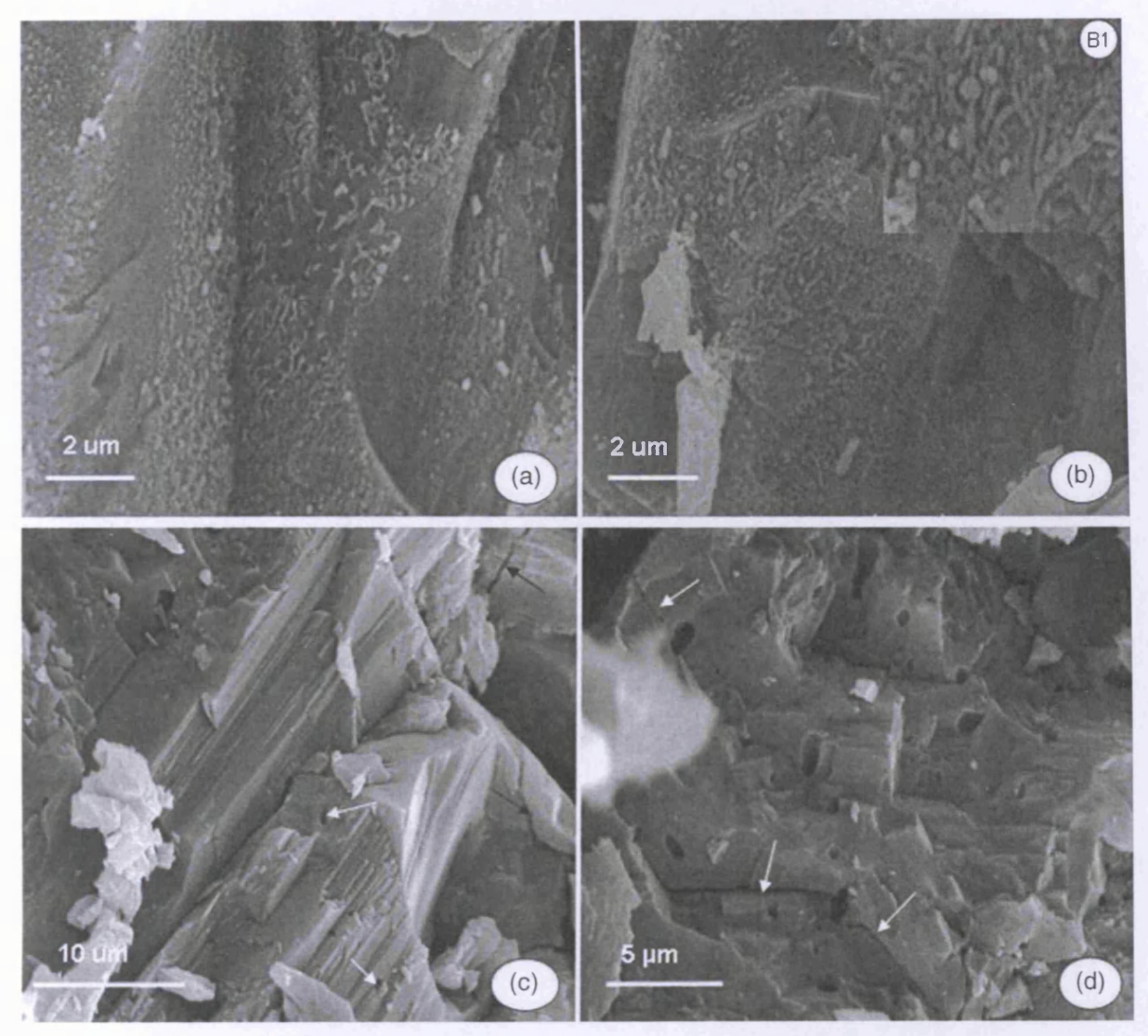


Fig. 2. SEM micrographs of the Carancas particles. (a) A high-magnification electron micrograph of the peripheral region of a particle: ovoid and elongated features are apparent. (b) An electron micrograph of the same region as (a); the inset (B1) illustrates the close-up of microfossil-like features. (c) An electron micrograph of the layered texture showing cracks (black arrows) and cavities (white arrows). (d) An electron micrograph of the central region of a particle showing fractures (arrows) and numerous cavities.

fragment was cut open using a sterile scalpel and its peripheral layer carefully removed with sterile pointed forceps. The remaining part of the sample was taken for analyses.

#### Scanning electron microscopy

The Carancas samples were mounted onto a metal stub using a piece of carbon double-sided sticky tape, and coated with gold in an Emscope sputter coater. The samples were examined using a Philips scanning electron microscope (SEM) XL 20 operated at 20 kV accelerating voltage.

#### Transmission electron microscopy

Particles taken from the internal part of the Carancas fragment were embedded in LR White resin (London Resin Co. Ltd, UK) at 55 °C for 48 hours, and the resulting polymerized resin blocks were cut into thin sections (100 nm thick) using a

diamond knife on a Reichert E ultracut microtome (Reichert-Jung, Austria). The thin sections were collected on pioloform-coated copper grids and examined using a Philips EM 208.

#### Energy dispersive analysis of X-rays analysis

A Philips CM12 transmission electron microscope (TEM), fitted with an energy dispersive analysis of X-rays (EDAX) system (EM-400 Detecting Unit, EDAX, UK), was used to analyse the thin sections. The following operating conditions were maintained constantly throughout the analyses: electron beam size (20 nm), condenser aperture (30  $\mu$ m), magnification (13 000×) and analysis live time (200 cps). During the analyses, the electron beam was focused onto the regions of interest, and a total of 25 similar measurements were randomly taken for each region. Both qualitative and quantitative analyses were performed using a 'Genesis' software.

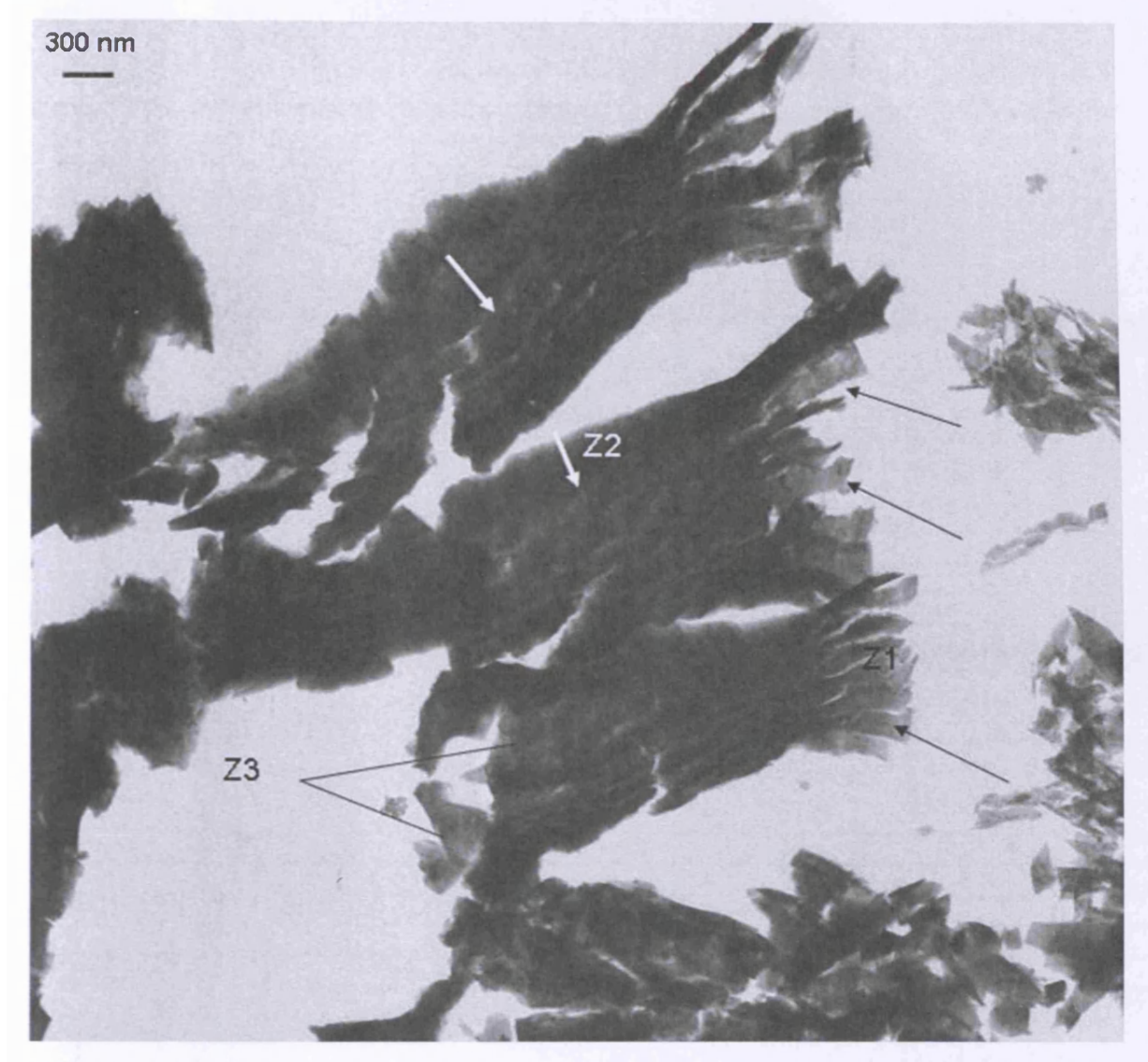


Fig. 3. A transmission electron micrograph of particles in the well-embedded resin section. Three large particles appear to have a similar structure. Each particle shows three clearly defined zones: a light zone (Z1) (dark arrows), a darker zone (Z2) (white arrows) and an intermediate zone (Z3).

#### Fourier Transform Infrared spectroscopy

The samples (0.15 mg) were prepared in KBr powder (20 mg). The mixture was transferred into a small blending mill (SPECAC mill<sup>TM</sup>) for grinding, and into the Evacuable Pellet Dies (SPECAC Ltd) under a pressure of 10 tons cm<sup>-2</sup> to make a KBr disc. The KBr embedded sample was analysed using a Fourier Transform Infrared (FTIR) spectrometer (JASCO Model FT/IR-660 Plus series).

#### Results

#### Scanning electron microscopy

The Carancas particles are mostly minerals having variable sizes and shapes (Figs 1(a) and (b)). The most common features include conchoidal, cuboidal and irregularly shaped

Table 1. Relative concentrations (wt%) of major elements that make up the three regions of the particle

Element	Z1	Z2	Z3
CO	38.4±2.1	37.8 ± 2.8	$36.3 \pm 3.2$
Na <sub>2</sub> O	0.0	$1.2 \pm 0.05$	0.0
MgO	$2.1 \pm 0.08$	$12.2 \pm 0.6$	$10.8 \pm 0.9$
$Al_2O_3$	$0.1 \pm 0.05$	$0.9 \pm 0.08$	0.0
SiO <sub>2</sub>	$1.8 \pm 0.15$	$19.8 \pm 0.9$	$13.8 \pm 1.2$
$SO_3$	$9.0 \pm 0.9$	$1.7 \pm 0.12$	$6.2 \pm 0.2$
CaO	0.0	$0.5 \pm 0.03$	0.0
Fe <sub>2</sub> O <sub>3</sub>	$35.2 \pm 3.8$	$25.9 \pm 2.3$	$22.9 \pm 2.5$
NiO	$13.4 \pm 1.68$	0.0	$10.0 \pm 1.4$

Values±standard deviations (SDs) represent the average of 25 measurements. The data are computed by the 'Genesis' thin section software, which calculates the weight percentages of the elements based on the known concentrations of the standard samples.

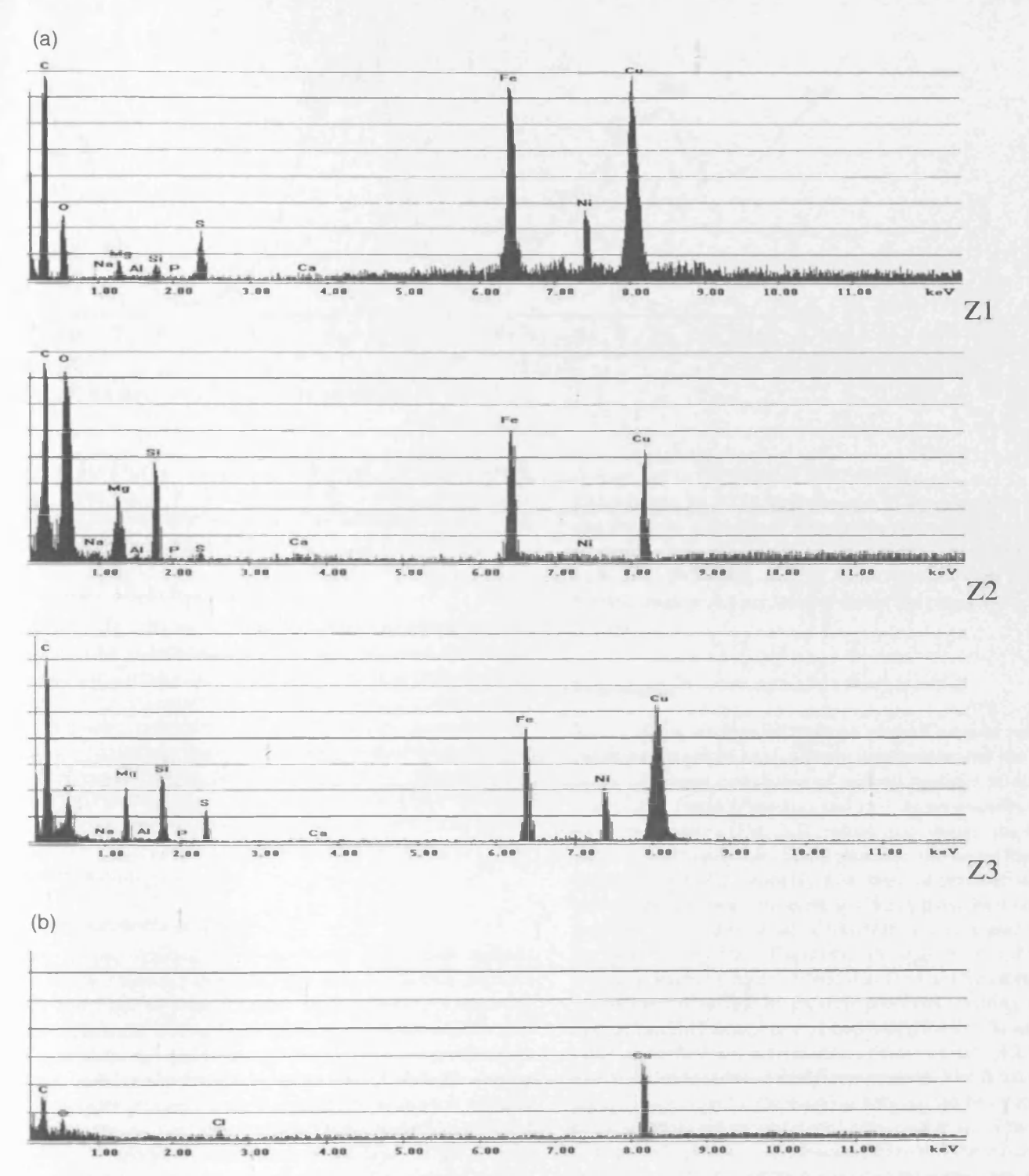


Fig. 4. X-ray spectra obtained from the analyses of a thin section. (a) The X-ray intensity of the elements detected is variable depending on the zones. Carbon, iron, sulphur and magnesium are detected in Z1, Z2 and Z3. Nickel is found only in Z1 and Z3. The presence of sodium and calcium is confined to Z2. The copper peak represents the element from the copper grid used for mounting thin sections. (b) A background area in the same section containing no sample. The X-ray intensity of carbon and chlorine is negligible.

bodies (Fig. 1(b)). The surface of some individual particles displays a mud crack-like texture. At high magnifications, this texture contains ovoid and rod-shaped objects, which are similar to microfossils of terrestrial origin (Figs 2(a) and (b)).

A large number of particles have crusts on their surface (Fig. 1(c)), whereas many others show fractures (Fig. 2(d)) and cavities (Figs 2(c) and (d)). Some particles exhibit three zones, distinguishable by their differences in both electron

#### K. Rauf et al.

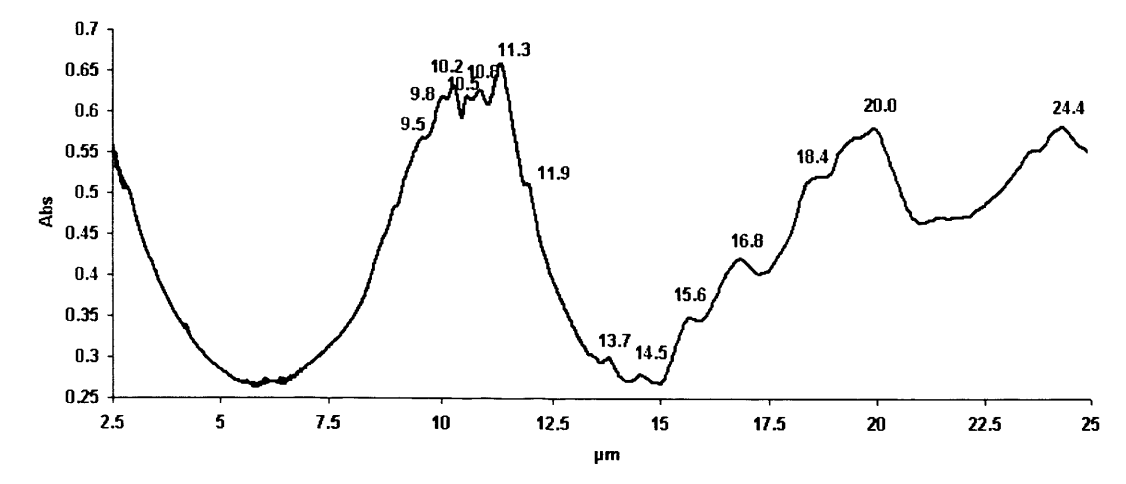


Fig. 5. FTIR spectrum of the Carancas meteorite.

opacity and texture: a light zone showing a layered or sheetlike structure, a darker zone at the centre displaying a pronounced radiating pattern and an intermediate zone with a smooth texture (Fig. 1(d)).

#### Transmission electron microscopy

Most of the sections cut from the resin-embedded particles were brittle and damaged by the electron beam bombardement. The ultrastructual observations of these sections reveal the presence of numerous holes, indicating that the samples were poorly embedded. As shown in Fig. 3, some well-embedded particles show three zones, distinguishable by their differences in electron density and structural characteristics: (i) a light zone displays a layered or thin sheet-like structure; (ii) a darker region shows aligned 'chatter pits'; and (iii) an intermediate zone has a surface structure that appears to be rather smooth.

#### X-Ray nanoprobe analysis

The results obtained from the X-ray nanoprobe analysis of the thin sections show that the resin-embedded particles are composed of three different regions, distinguishable by the differences not only in structural characteristics but also in chemical composition (Table 1). For convenience, they are labelled in the present study as Z1, Z2 and Z3. During the analyses, attempts were also made to determine whether arsenic element (As) was present in the sample. As Fig. 4 shows, the spectra do not reveal the presence of the characteristic X-ray emission peak of arsenic (As) element, which should normally be located at 10.5 KeV energy. The chemical composition of Z1 is similar to that of Z3, but the former contains less magnesium and silicon than the latter. The amounts of major elements in Z1, such as sulphur, iron and nickel, are much higher than those in Z2 and Z3. On the other hand, the chemical composition of Z2 is unique, since it contains no nickel, but is rich in magnesium and silicon as compared to Z1 and Z3. Traces of sodium and calcium are detected in Z2, but they are not present in Z1 and Z3.

#### Fourier Transform Infrared spectroscopy

The analysis by FTIR spectroscopy of the Carancas grains embedded in KBr shows a spectrum containing a series of absorption features located at 9.5, 9.8, 10.2, 10.5, 10.8, 11.3, 11.9, 13.7, 14.5, 15.6, 16.8, 18.4, 20.0 and 24.4  $\mu$ m (Fig. 5). Several small peaks are located within the range 2–3  $\mu$ m and 6–7  $\mu$ m.

#### **Discussion**

The scanning electron microscopy of the Carancas particles indicates that they have a stony appearance and are composed of a large population of mineral particles in variable shapes and forms (Figs 1(a) and (b)). Some particles show numerous cavities (Fig. 2(d)), which may suggest the occurrence of a steam phase. Many particles also show fractures (Figs 2(c) and (d)), probably as a result of the impact brecciation. Furthermore, the surface of many particles is covered in places with crusts, most of which show fusion melt along the fissures (Fig. 1(c)). These findings support an earlier observation made by Miura (2008) that the Carancas meteorite was subjected to two major step processes: melting in the atmosphere and steaming after impacting Earth. The melting process resulted in the formation of fusion crusts rich in Fe and Si and melt flakes of Fe-Ni composition. The steam phase occured as a result of the reaction between the hot meteorite metal and cold groundwater at the excavation site. Fractured or broken fragments were discovered around the crater, suggesting that the Carancas meteorite fragmented on impact with Earth. The impact velocity on the ground was estimated at between 3 and 6 km s<sup>-1</sup> (Tancredi et al. 2009).

Some particles show a mud crack-like texture intermixed with ovoid and elongated features, which appear similar to microfossils of terrestrial origin (Figs 2(a) and (b)). These features have also been found in Martian meteorite ALH84001 (McKay et al. 1996) and in other carbonaceous chondrites (Hoover et al. 2003; Hoover 2009). The origin of these objects is, however, uncertain and remains to be properly determined. One possible explanation is that the mud crack-like

structure may originate from the terrestrial contamination. It is possible that some of the fragments were exposed to the terrestrial muddy water or wet ground at the excavation site. This explanation is further supported by the observation that the Carancas fall was immediately followed by a massive cloud of dust and groundwater evaporation from the impact crater (Macedo & Macharé 2007; del Prado *et al.* 2008; Miura 2008; Schultz *et al.* 2008).

Concerning the ovoid and elongated features, an explanation could be offered that these may be the broken products of carbonate crystallization, since they appear similar to the bundles of carbonate crystal precipitation induced by bacteria, as suggested by Buczynski & Chafetz (1991) and McKay et al. (1996).

The FTIR analysis of grains in the Carancas meteorite reveals a waveband stretching from 2.5 to 25 μm showing infrared (IR) absorption peaks centred at 9.5, 9.9 and 10.2 μm, whose characteristics are of amorphous (9.5 μm) and crystalline (9.9 and 10.2 µm) silicates (Knacke & Kraetschmer 1980). The presence of many bands around 10 µm may be indicative of the band shift from amorphous to crystalline silicates, and this shift may result from the annealing of amorphous silicates at high temperatures. This process is believed to take place in the hot inner region of the solar nebular (Bockelée-Morvan et al. 2002). Amorphous silicates are found in abundance in interstellar medium (Zolensky 2006) and interplanetary dust particles (IDPs) (Molster & Kemper 2005), whereas crystalline silicates are predominant in primitive meteorites (Nuth et al. 2005; Busemann et al. 2006). On the other hand, the C1 and C2 chondrites are rich (50-60%) in hydrated silicates, which show a sharp absorption at 2.71 µm in the Orgueil and Murchison meteorites (Knacke & Kraetschmer 1980). Furthermore, the carbonaceous chondrites have been shown to display strong absorptions at 6.1 and 6.8 µm (Knacke & Kraetschmer 1980). Recently, Rauf et al. (2010) have detected these absorption features in the Tagish Lake meteorite. The 6.1 µm feature is known to be related to water absorption in many clay minerals (Farmer 1974), whereas the  $6.9 \, \mu m$  is caused by carbonate minerals (Knacke & Kraetschmer 1980). Unlike these carbonaceous chondrites, the Carancas meteorite shows considerably weaker absorptions in the IR range 2.5-4.0 μm and 5.0-7.0 μm (Fig. 5). The occurrence of such small humps indicates that hydrated silicates (probably phyllosilicate minerals), hydroxyl (OH) groups and carbonates are less common. There is no evidence of aliphatic functioning groups, as confirmed by the absence of a 3.4 µm peak. However, aromatic hydrocarbons may be present in the Carancas meteorite, as shown by the presence of a band centred at 11.3 µm, which is known to be the absorption feature of aromatic hydrocarbons in many astronomical objects (Cataldo & Keheyan 2003; Rauf & Wickramasinghe 2010; Rauf et al. 2010), including comets and 81P/Wild 2 in particular (Sandford 2008). The IR bands observed in the 10-20 µm region may be due to the presence of the olivine group (Saikia & Parthasarathy 2009).

Attempts to section the resin-impregnated particles were met with little success. Most of the sections showed

perforations and became brittle, suggesting that the particles were poorly enibedded. However, there are some small particles or grains that were reasonably well preserved. As shown in Figs 1(d) and 3 and Table 1, these grains are composed of three phases distinguishable not only by the differences in their electron density and texture, but also their chemical composition. The light zone (Z1), showing a mica sheet-like structure, is composed of sulphide minerals rich in Fe and Ni. In contrast, the darker region (Z2) displays a spectacular pattern of 'chattering pits', rich in Mg and Si (the major elements of high-temperature minerals, such as forsterite Mg<sub>2</sub>SiO<sub>4</sub> and enstatite MgSiO<sub>3</sub>). The richness of chemical elements, such as Mg, Si, and Fe, in Z2 also suggests the existence of olivine and pyroxene. The third zone (Z3), showing a rather smooth surface structure, is composed of crystalline silicates rich in Mg. Fe and Si (the major elements of olivine and pyroxene). The X-ray microanalysis also confirms that there is no evidence for the presence of the arsenic element (Fig. 4 and Table 1), thus ruling out the claim that the illness experienced by the locals in Carancas was arsenic related.

The results obtained from the elemental analysis, electron microscopy and FTIR spectroscopy suggest that the chemical composition of some particles in the Carancas meteorite is similar to that of particles of the 81P/Wild 2 comet, where both amorphous and crystalline silicates are present in abundance (Keller 2006; Zolensky 2006). The 8 µm terminal particle (known as Sitara) of this comet is composed of bright regions of sulphides rich in iron and nickle, a central grey region of enstatite marked by aligned 'chatter pits' and a smooth grey region rich in crystalline Mg-silicates (Brownlee et al. 2006).

Using FTIR spectroscopy, EDAX analysis and electron microscopy to analyse the Carancas particles, the current investigation presents the following findings: (1) the meteorite is composed of a large population of minerals that are abundant in space; (2) it is rich in chemical elements that are composed of olivine, pyroxene and high-temperature minerals, such as fosterite and enstatite; (3) the richness of these minerals and iron metal support the early proposal that the meteorite is an ordinary H4/5 chondrite (del Prado et al. 2008; Tancredi et al. 2008, 2009); (4) some particles show structural characteristics and chemical composition of minerals similar to the 81P/Wild 2 comet; and (5) the ovoid and elongated features look like microfossils found in other meteorites, many of which resemble bacterial microfossils of terrestrial origin.

#### References

Bockelée-Morvan, D., Gautier, D., Hersant, F., Huré, J.-M. & Robert, F. (2002). Astron. Astrophys. 384, 1107-1118.

Brownlee, D. et al. (2006). Science 314, 1711-1716.

Buczynski, C. & Chafetz, H.S. (1991). J. Sediment. Petrol. 61, 226-233.

Busemann, H., Young, A.F., Alexander, C.M.O'D., Hoppe, P., Mukhopadhyay, S. & Nittler, L.R. (2006). Science 312, 727-730.

Cataldo, F. & Keheyan, Y. (2003). Int. J. Astrobiol. 2(1), 41-50.

del Prado, H.N. et al. (2008). The meteorite fall in Carancas, Lake Titicaca region, southern Peru: first results. In Proc. 39th Lunar and Planetary Science Conf., League City, Texas. LPI Contribution No. 1391, p. 2555.

- Farmer, V.C. (1974). The Infrared Spectra of Minerals. Monograph 4, p. 539. Mineralogical Society, London.
- Harris, R.S., Schultz, P.H., Tancredi, G. & Ishitsuka, J. (2008). Petrology of ejecta from the Carancas (Peru) crater: Insights into the dynamics of an 'unusual' impact event. In Asteroids, Comets, Meteors, LPI Contribution. No. 1405, p. 8302.
- Hoover, R.B. (2009). Microfossils in carbonaceous meteorites [abstract]. *Proc. SPIE* **7441**, doi: 10.1117/12.832643.
- Hoover, R.B., Jerman, G., Rozanov, A.Y. & Davies, P.C.W. (2003).Biomarkers and Microfossils in the Murchison, Rainbow, and Tagish Lake meteorites. *Proc. SPIE* 4859, 15–31.
- Keller, L.P. (2006). Science 314, 1728-1731.
- Knacke, R.F. & Kraetschmer, W. (1980). Astronom. Astrophys. 92(3), 281–288.
- Le Pichon, A., Antier, K., Cansi, Y., Hernandez, B., Minaya, E., Burgoa, B., Drob, D., Evers, L.G. & Vaubaillon, J. (2008). Meteorit. Planet. Sci. 43, 1797-1809.
- Macedo, L.F. & Macharé, J.O. (2007) The Carancas meteorite fall, 15 September 2007. Official INGEMMET initial report.
- McKay, D.S., Gibson, E.K., Thomas-Keptra, K.L., Vali, H., Romanek, C.S., Clemett, S.J., Chillier, X.D.F., Maechling, C.R. & Zare, R.N. (1996). Science 273(5277), 924–930.
- Miura, Y. (2008). Multiple explosions during cratering at Carancas meteorite hit in Peru. Earth Sci.. Graduate School of Sci. &

- Eng., Yamaguchi University, Yoshida 1677-1, Yamaguchi. 753-8512, Japan.
- Molster, F. & Kemper, C. (2005). Space Sci. Rev. 119(1-4), 3-28.
- Nuth, J. A. Jr. III, Brearley, A.J. & Scott, E.R.D. (2005). Microcrystals and amorphous materials in comets and primitive meteorites: keys to understanding processes in the early solar system. In *Chondrites and the Protoplanetary Disk*, ASP Conference Series, 341, pp. 675-700.
- Rauf, K., Hann, A. & Wickramasinghe, C. (2010). Int. J. Astrobiol. 9(1), 35-43
- Rauf, K. & Wickramasinghe, C. (2010). Int. J. Astrobiol. 9(1), 29-34.
- Saikia, B. J. & Parthasarathy, G. (2009) Spectroscopic investigation of Mahadevpur H4/5 ordinary chondrites. Goldschmidt Conference Abstracts.
- Sandford, S.A. (2008). Organics in the samples returned from comet 81P/Wild 2 by the Stardust Spacecraft. In Organic Matter in Space, Proc. IAU Symposium, 251, pp. 299–307.
- Schultz, P.H., Harris, R.S., Tancredi, G. & Ishitsuka, J. (2008). Implications of the Carancas meteorite impact. *Lunar and Planetary Science*, #2409 abstract.
- Tancredi, G. et al. (2008). What do we know about the Carancas-Desaguadero' fireball, meteorite and impact crater? Lunar and Planetary Science, #1216 abstract.
- Tancredi, G. et al. (2009). Meteorit. Planet. Sci. 44(12), 1967–1984. Zolensky, M.E. (2006). Science 314, 1735–1739.